

2014

Cosmogenic dating of fluvial terraces in the Sorbas Basin, SE Spain

Ilott, Samantha

<http://hdl.handle.net/10026.1/3015>

<http://dx.doi.org/10.24382/4035>

Plymouth University

All content in PEARL is protected by copyright law. Author manuscripts are made available in accordance with publisher policies. Please cite only the published version using the details provided on the item record or document. In the absence of an open licence (e.g. Creative Commons), permissions for further reuse of content should be sought from the publisher or author.

This copy of the thesis has been supplied on condition that anyone who consults it is understood to recognise that its copyright rests with its author and that no quotation from the thesis and no information derived from it may be published without the author's prior consent.

**Cosmogenic dating of fluvial terraces in the Sorbas
basin, SE Spain**

by

Samantha Helen Ilott

A thesis submitted to the University of Plymouth
in partial fulfilment for the degree of

DOCTOR OF PHILOSOPHY

School of Geography, Earth and Environmental Sciences
Faculty of Science and Environment

November 2013

Cosmogenic dating of fluvial terraces in the Sorbas basin, SE Spain

Samantha Helen Illott

Long term fluvial incision spanning the Late Cenozoic is recorded in many fluvial systems around the world by terrace landform sequences. The incision manifests itself as inset sequences of river terraces which form terrace staircases. The timing of the onset of incision and the rate incision then proceeds at is poorly constrained due to the difficulties in dating river terraces.

This study applies the technique of cosmogenic exposure dating to a fluvial staircase, for the first time, in the Sorbas Basin, SE Spain. Cosmogenic exposure dating allows the timing of abandonment of the fluvial terraces to be calculated therefore recording periods of incision. Cosmogenic exposure dating and the profile method offer a viable way to date Early and Middle Pleistocene terrace deposits. Combined exposure and burial age's approaches using paired isotopes allow for insights into terrace aggradation and fluvial incision timing.

The fluvial deposits in the Sorbas Basin record 1.0 Ma of incision by the Río Aguas. The timing of aggradation and incision in the Sorbas basin has been linked to both tectonics and climate cycles. Terrace aggradation took place in glacial and interglacial periods. The abandonment of terrace surfaces occurred both at warming transitions and in interglacial periods.

New uplift rates calculated for the Pleistocene fluvial system suggest that tectonic activity in the Sorbas Basin has been episodic. The south margin and centre of the Sorbas Basin has uplifted at a faster rate than the northern margin impacting on the rates of incision taking place in the fluvial systems. Overall tectonic uplift has increased the fluvial system sensitivity to climatic variations.

Contents

Abstract	i
Contents	ii
List of Figures	vii
List of Tables	x
List of Equations	xii
Acknowledgments	xiii
Author's declaration	xiv
Chapter 1 Introduction	1
1.1 Introduction	1
1.2 Aims and objectives	3
1.3 The Sorbas Basin	4
1.4 Fluvial terraces	8
1.5 Climate and tectonics	9
1.5.1 Timing of terrace formation in the Sorbas Basin	13
1.5.2 Fluvial response to tectonics in SE Spain- River capture	16
1.6 Establishing an accurate chronology	18
1.7 Summary	21
Chapter 2 Study area geology and geomorphology	23
2.1 Introduction	23
2.2 Location	23
2.3 Basin Formation	24
2.4 Basin infilling	29
2.4.1 Burdigalian/Serravallian/Tortonian	31
2.4.2 Messinian basin fill	32
2.4.3 Late Miocene/Pliocene/Pleistocene basin fill	33
2.5 Fluvial system development	35
2.6 Proto Aguas/Feos terrace stratigraphy	39
2.7 Landscape development	42
2.7.1 Canyons	42
2.7.2 Badlands	43
2.7.3 Scarplands	44
2.7.4 Gypsum Plateau and Karst	44
2.8 Summary	46

Chapter 3	Methodology	49
	3.1 Introduction	49
	3.2 Philosophical approach	50
	3.3 General approach	51
	3.4 Morphological mapping	52
	3.5 Terrace height diagrams and valley cross sections	54
	3.6 Sedimentary analysis	55
	3.6.1 Facies analysis	55
	3.6.2 Clast counts	57
	3.6.3 Logs and sketches	59
	3.6.4 Palaeocurrent analysis	61
	3.6.5 Palaeohydrological analysis	61
	3.7 Dating fluvial terraces	64
	3.7.1 Soil profiles & pedogenic calcretes	66
	3.7.2 Cosmogenic dating	69
Chapter 4	Cosmogenic methodology	71
	4.1 Introduction	71
	4.2 Cosmogenic exposure dating	72
	4.3 The depth concentration profile method	75
	4.3.1 Theoretical background	76
	4.3.2 Burial dating	81
	4.4 Selection of sample locations	81
	4.4.1 Criteria for sample site selection	83
	4.5 Sample site selection	86
	4.5.1 Sample site GS	86
	4.5.2 Terrace A	89
	4.5.3 Sample site GTB	89
	4.5.4 Sample site CB	90
	4.5.5 Sample site TBP	93
	4.5.6 Sample site G3	93
	4.5.7 Sample site TCF	98
	4.5.8 Sample site MTC	98
	4.6 The sampling methodology	102
	4.7 Lab methodology	104
	4.8 Chlorine 36 dating	108
	4.8.1 Landsliding in the Sorbas Basin	108
	4.8.2 The Maleguica landslide	110
	4.8.3 Sample site selection	111
	4.8.4 Sampling methodology	111
	4.8.5 Laboratory method	112
	4.9 Neon dating	115
	4.9.1 Sample site	115
	4.9.2 Sampling method	116
	4.9.3 Laboratory method	117

	4.1 Summary	117
Chapter 5	The Proto Aguas/Féos fluvial archive	119
	5.1 Introduction	119
	5.2 Pre Terrace A erosion surface	119
	5.2.1 Type locality summary	121
	5.2.2 Interpretation	125
	5.3 Terrace B	126
	5.3.1 Type section summary	126
	5.3.2 Interpretation of sequence	131
	5.4 Terrace C deposits	132
	5.4.1 Terrace C type section sedimentology	132
	5.4.2 Interpretation	139
	5.5 Analysis of the palaeohydrological data	140
	5.5.1 Palaeoflood results	141
	5.5.2 Discussion of palaeohydrology data	148
	5.6 Chapter summary	151
Chapter 6	Río Jauto fluvial system	153
	6.1 Introduction	153
	6.2 The Río Jauto	153
	6.3 Level 1 Terraces	157
	6.3.1 Type locality	157
	6.4 Level 2 Terraces	162
	6.4.1 Type locality	162
	6.5 Level 3 Terraces	165
	6.5.1 Type locality	166
	6.6 Level 4 Terraces	170
	6.6.1 Type locality	171
	6.7 Palaeohydrology analysis	177
	6.7.1 Palaeoflood results	178
	6.7.1.1 Level 1	178
	6.7.1.2 Level 2	178
	6.7.1.3 Level 3	179
	6.7.1.4 Level 4	180
	6.7.2 Discussion of palaeohydrology data	181
	6.8 Development of the Río Jauto drainage system	183
	6.8.1 development of the river course	184
	6.8.2 Los Castaños valley	186
	6.9 Establishing a chronological framework	187
	6.10 Summary	190
Chapter 7	Cosmogenic exposure dating results	193
	7.1 Introduction	193
	7.2 Calculating exposure ages	193

	7.2.1 Calculation of production and attenuation lengths	194
	7.2.2 Modelling of data	195
	7.2.3 Chi-squared minimization method	198
7.3	Concentration profile results	200
	7.3.1 GS sample site (Pre Terrace A erosion surface)	200
	7.3.1.1 AMS data	200
	7.3.1.2 Concentration profile age	201
	7.3.2 GTB sample site (Terrace B)	205
	7.3.2.1 AMS data	205
	7.3.2.2 Concentration profile Age	205
	7.3.2.3 Burial age	206
	7.3.3 CB sample site (Terrace B)	207
	7.3.3.1 AMS data	207
	7.3.3.2 Concentration profile Age	208
	7.3.3.3 Burial age	209
	7.3.4 TBP sample site (Terrace B)	209
	7.3.4.1 AMS data	209
	7.3.4.2 Concentration profile Age	211
	7.3.4.3 Burial age	214
	7.3.5 G3 sample site (Terrace C)	214
	7.3.5.1 AMS data	214
	7.3.5.2 Concentration profile Age	214
	7.3.5.3 Burial age	215
	7.3.6 TCF sample site (Terrace C)	215
	7.3.6.1 AMS data	215
	7.3.6.2 Concentration profile Age	217
	7.3.6.3 Burial age	218
	7.3.7 MTC sample site (Terrace C)	218
	7.3.7.1 AMS data	218
	7.3.7.2 Concentration profile Age	219
	7.3.7.3 Burial age	222
7.4	Causes of anomalies in cosmogenic nuclide profiles	222
7.5	Chlorine 36 dating results	225
7.6	Neon dating results	226
7.7	Discussion of results	227
7.8	Summary	230
Chapter 8	Controls on incision in the Sorbas Basin	233
8.1	Introduction	233
8.2	When did incision start in the Sorbas Basin?	233
8.3	Climate and tectonic controls on terrace formation	237
8.4	Tectonic uplift	243
	8.4.1 Published uplift rates	245
	8.4.2 Terrace spacing and uplift rates	246
	8.4.3 Discussion	250

8.5	Lithological controls on terrace formation in the Río Jauto	256
8.6	Palaeoflood estimates for the Pleistocene deposits	258
8.7	Landslides: The keep up vs. Catch up model	262
8.8	Palaeoenvironmental model of terrace formation	265
8.9	Summary	268
Chapter 9	Conclusions	271
9.1	Conclusions: Cosmogenic exposure dating	271
9.2	Conclusions: Timing of fluvial incision	273
9.3	River capture	273
9.4	Timeline creation	275
9.5	Key conclusions	275
Appendix 1	Sedimentary data for the cosmogenic sample sites	279
A.1.1	Sedimentary log for the C.B sample site	280
A1.2	Clast assemblage data for C.B	281
A1.3	Sedimentary photo sketch for the C.B sample site	282
A1.4	Sedimentary log for the T.B.P sample site	283
A1.5	Clast assemblage data for the T.B.P sample site	284
A1.6	Photo sketch of the T.B.P sample site	285
A1.7	Sedimentary log from the M.T.C site	286
A1.8	Clast assemblage data for the M.T.C. sample trench	287
Appendix 2	DEM data for the Sorbas basin	289
A2.1	DEM data for the Sorbas basin	290
Appendix 3	Geological maps of the Sorbas Basin	291
A3.1	Geological maps of the Sorbas Basin	292
A3.2	Geological maps of the Río Jauto	293
Appendix 4	Palaeohydrology data for the Río Jauto	295
A4.1	Palaeohydrological data for the Río Jauto fluvial system	296
Appendix 5	Calculation data for cosmogenic exposure dating	299
A5.1	Data table for cosmogenic exposure dating	300
Appendix 6	Tectonic uplift calculations	305
A6.1	Uplift calculations	306
	References	309

List of Figures

Chapter 1		
Figure 1.1	Location of the Sorbas basin	5
Figure 1.2	Map of the main fluvial systems	6
Figure 1.3	Simplified sedimentary log-Sorbas basin	7
Figure 1.4	Schematic basin topographic profile-Sorbas basin	7
Chapter 2		
Figure 2.1	Location of Neogene sedimentary basins	24
Figure 2.2	Location of the plate boundary	25
Figure 2.3	Log of sedimentary basin infill	30
Figure 2.4	The main fluvial systems of the Plio/Pleistocene	35
Figure 2.5	Early Plio/Pleistocene drainage systems	35
Figure 2.6	River capture event	37
Figure 2.7	Location map of Sorbas basin	41
Figure 2.8	Long profile of Río Aguas	41
Figure 2.9	Features of landscape development	47
Chapter 3		
Figure 3.1	Symbols used for sedimentary logs	60
Chapter 4		
Figure 4.1	Cosmogenic rays diagram	73
Figure 4.2	Concentration profile of cosmogenic nuclides	78
Figure 4.3	Diagram showing inheritance of cosmogenic nuclides	79
Figure 4.4	Location map of sample sites	83
Figure 4.5	Photo of Góchar surface sample site	87
Figure 4.6	Location map of Góchar sample site	89
Figure 4.7	Location map of GTB sample site	91
Figure 4.8	Location map of C.B sample site	92
Figure 4.9	Location map of T.B.P sample site	95
Figure 4.10	Location map of G3 sample site	96
Figure 4.11	Map of fault in G3 terrace	97
Figure 4.12	Location map of T.C.F sample site	100
Figure 4.13	Location map of M.T.C sample site	101
Figure 4.14	Photo of a sample methodology	102
Figure 4.15	Schematic overview of laboratory methodology	105
Figure 4.16	Process of Anion exchange chromatography	107
Figure 4.17	Location map of Maleguica landslide	110
Figure 4.18	Location map of Maleguica sample site	112
Figure 4.19	Schematic overview of chlorine analysis	113
Figure 4.20	Location map of Río Jauto erosion surface	116

Chapter 5

Figure 5.1	The Góchar surface	120
Figure 5.2	Sedimentary log for Pre Terrace A type locality	122
Figure 5.3	Provenance data for Pre Terrace A erosion surface	123
Figure 5.4	Photo sketch of the Pre Terrace A type section	124
Figure 5.5	Photos of the Pre Terrace A type locality	125
Figure 5.6	Provenance data for Terrace B type section	127
Figure 5.7	Sedimentary log for Terrace B type locality	129
Figure 5.8	Photo sketch of the Terrace B type section	130
Figure 5.9	Provenance data for Terrace C type section	133
Figure 5.10	Sedimentary log for type locality G3	134
Figure 5.11	Photo sketch of the Terrace C type section	136
Figure 5.12	Photo and sketch of faulted sediments	138
Figure 5.13	Sketch log of the T.C.F terrace deposit	140
Figure 5.14	Map showing the reaches of the Río Agaus	142

Chapter 6

Figure 6.1	Long profile of the Río Jauto	155
Figure 6.2	Profile of the Río Jauto with associated terrace levels	156
Figure 6.3	Map of type locality for Level 1 deposits	158
Figure 6.4	Photos showing Level 1 palaeovalleys	159
Figure 6.5	Photo sketch of the Level 1 type locality	160
Figure 6.6	Provenance data for Level 1	161
Figure 6.7	Map of type locality for Level 2 deposits	163
Figure 6.8	Photo sketch of the Level 2 type locality	164
Figure 6.9	Provenance data for Level 2	165
Figure 6.10	Map of type locality for Level 3 deposits	166
Figure 6.11	Provenance data for Level 3	168
Figure 6.12	Photo sketch of the Level 3 type locality	168
Figure 6.13	Sedimentary log of the Level 3 type section	169
Figure 6.14	Provenance data for Level 4	172
Figure 6.15	Location map for the Level 4 type section	174
Figure 6.16	Photo sketch of the Level 4 type locality	175
Figure 6.17	Sedimentary log of the Level 4 type section	177
Figure 6.18	Ariel image of the Level 1 palaeovalleys	179
Figure 6.19	Loma Orandona ridge	184
Figure 6.20	Los Castaños river valley	185
Figure 6.21	Clast assemblage data; Río Jauto	186

Chapter 7

Figure 7.1	Example of simple and complex exposure models	195
Figure 7.2	Expected concentration profiles	197
Figure 7.3	Graph of ^{10}Be data for G.S sample site	201
Figure 7.4	Graph of ^{26}Al data for G.S sample site	201

Figure 7.5	Modelled ages for G.S ¹⁰Be data,	202
Figure 7.6	Modelled erosion rate for G.S sample site	203
Figure 7.7	Probability data for G.S sample site	203
Figure 7.8	Banana plot for G.S ¹⁰be data	204
Figure 7.9	Graph showing the expected age of the G.S sample site	205
Figure 7.10	¹⁰Be data for GTB sample site	206
Figure 7.11	Modelled ages for the GTB ¹⁰Be data	206
Figure 7.12	¹⁰Be data for the C.B sample site	207
Figure 7.13	²⁶Al data for the C.B sample site	208
Figure 7.14	Single exposure model for the C.B ¹⁰Be data	208
Figure 7.15	Single exposure model for the C.B ²⁶Al data	209
Figure 7.16	¹⁰Be data for the TBP sample site	210
Figure 7.17	²⁶Al data for the TBP sample site	210
Figure 7.18	Single exposure model for the TBP ¹⁰Be data	212
Figure 7.19	Single exposure model for the TBP ²⁶Al data	212
Figure 7.20	Complex exposure model for the TBP ¹⁰Be data	213
Figure 7.21	Complex exposure model for the TBP ²⁶Al data	213
Figure 7.22	¹⁰Be data for the G3 sample site	214
Figure 7.23	Single exposure model for the G3 ¹⁰Be data	215
Figure 7.24	¹⁰Be data for the TCF sample site	216
Figure 7.25	²⁶Al data for the TCF sample site	216
Figure 7.26	Single exposure model for the TCF ¹⁰Be data	217
Figure 7.27	Single exposure model for the TCF ²⁶Al data	217
Figure 7.28	¹⁰Be data for the MTC sample site	218
Figure 7.29	²⁶Al data for the MTC sample site	219
Figure 7.30	Single exposure model for the MTC ¹⁰Be data	220
Figure 7.31	Single exposure model for the MTC ²⁶Al data	221
Figure 7.32	Complex exposure model for the MTC ¹⁰Be data	221
Figure 7.33	Complex exposure model for the MTC ²⁶Al data	222
Figure 7.34	Terrace stratigraphy of the Proto Aguas/Féos	228

Chapter 8

Figure 8.1	New chronological framework for the Proto Aguas/féos	234
Figure 8.2	Sedimentary log for the Plio/Pleistocene stratigraphy	235
Figure 8.3	Stratigraphical position of the quaternary terrace sequences	238
Figure 8.4	Bridgland & Westaway (2008) model of terrace formation	240
Figure 8.5	Uplift rates for the Río Aguas	248
Figure 8.6	Uplift rates for the Río Jauto	249
Figure 8.7	Lithological controls on terrace formation in the Río Jauto	255
Figure 8.8	Isotope curves from 150 ka to 75 ka	261
Figure 8.9	Pollen data for the Sorbas basin	264

Figure 8.10	Model of terrace formation	267
Chapter 9		
Figure 9.1	Diagram of tectonic, climatic and chronological data	277

List of Tables

Chapter 2

Table 2.1	Description of metamorphic basement	26
Table 2.2	Uplift rates for the Sorbas Basin	29
Table 2.3	Chronological, soil and calcrete data	40

Chapter 3

Table 3.1	List of maps used within the study	53
Table 3.2	Lithofacies codes	57
Table 3.3	Calculation method for palaeohydrological analysis	65
Table 3.4	Geochrometric dating techniques	66
Table 3.5	Classification of pedogenic calcretes	68

Chapter 4

Table 4.1	Cosmogenic isotopes	74
------------------	----------------------------	-----------

Chapter 5

Table 5.1	Palaeohydrology data for the Proto Aguas/Feos	147
Table 5.2	Average palaeohydrology data	148

Chapter 6

Table 6.1	Palaeohydrology data for the Río Jauto	182
------------------	---	------------

Table 6.2	Palaeoflood data for the Río Jauto	182
Table 6.3	Soil data for the Ríos Aguas and Jauto	190
Chapter 7		
Table 7.1	Sample of output data from AMS	194
Table 7.2	Cosmogenic nuclide data for chlorine dating	225
Table 7.3	Cosmogenic exposure dating results	227
Table 7.4	Database of terrace formation in the Río Aguas	229
Chapter 8		
Table 8.1	Time averaged uplift rates for the Neogene basins	243
Table 8.2	Published uplift rates for the Sorbas Basin	244
Table 8.3	Terrace spacing and time gaps for terrace deposits	245
Table 8.4	Calculated uplift rates for the Ríos Aguas & Jauto	250
Table 8.5	Calculated uplift rates for the Río Aguas	252
Table 8.6	Maximum flood discharge, Río Jauto	255
Table 8.7	Maximum flood discharge, Sorbas Basin	256
Table 8.8	Climatic conditions during a climate cycle	267

List of Equations

Chapter 7

Equation 7.1	Chi squared equation	196
Equation 7.2	Exposure age calculation	197
equation 7.3	quality factor calculation	197

Acknowledgements

Firstly I would like to thank my supervisors Dr. Martin Stokes and Dr. Anne Mather for their help, advice, support and supervision during my time in Plymouth.

For all his help, advice and assistance preparing samples for cosmogenic isotope analysis, I would especially like to thank Mr Allan Davidson at the SEURC laboratories in East Kilbride. My thanks also go to Dr. Angel Rhodés for all his help on the mathematical and statistical modelling methods used during this thesis.

I would like to thank NERC for funding my PhD and the British Sedimentary Research Group for providing funding for fieldwork. I would also like to thank Lindy Walsh and Debbie at Urra for looking after me during my fieldwork season and a big thanks to all the universities and colleges who allowed me to join their groups for evening meals. A big thank you goes to my field assistants Miss Amanda Owen and Dr. Tim Kearsey who help out on various trips to Spain. Thanks also go to my office mates Nikita and Martha for all their support and entertainment during long hours in the office.

Finally I would like to thank my family for their support and interest throughout this project. Last but not least, I would like to thank Tim for his tolerance of me over the past year whilst I was writing up and for taking me out to go cycling, climbing and into the mountains when I needed to regain perspective.

Author's Declaration

At no time during the registration for the degree of Doctor of Philosophy has the author been registered for any other university award without prior agreement of the graduate committee.

Work submitted for this research degree at the Plymouth University has not formed part of any other degree either at Plymouth University or any other establishment.

This study was financed with the aid of a studentship from the Natural Environment Research council. Cosmogenic isotope analysis was funded by NERC and carried out at the SUERC laboratories in East Kilbride. Fieldwork was sponsored by NERC and The Steve Farrell Memorial Fund from the British Sedimentological Research Group (2009) awarded to S. Illott.

Relevant scientific seminars and conferences were regularly attended at which work was often presented and external initiations were visited for consultation purposes.

Presentations and conferences attended:

International Union for Quaternary Research Congress Bern (July 2011)

British Society for Geomorphology Annual Conference, Liverpool (June 2011)

British Sedimentary Research Group Annual Meeting, Southampton (Dec 2010)

7th Fluvial Archives Group Biennial Meeting, Portugal (Sept 2010)

British Sedimentary Research Group Annual Meeting, Liverpool (Dec 2008)

Word count of main body of thesis: 56786 words

Signed S. I. Lott

Dated 23/04/2014

Chapter 1: Introduction

1.1 Introduction

Long term fluvial incision spanning the Late Cenozoic is recorded in many fluvial systems around the world by terrace landform sequences (Bridgland & Westaway, 2008). The incision manifests itself as inset sequences of river terraces which form terrace staircases. Fluvial terraces are the former floodplains of a fluvial system that have been isolated by incision (Stokes *et al.*, 2012a). The fluvial terraces are present as topographically flat or very gently dipping surfaces that grade in a downstream direction. There are two types of fluvial terraces; strath terraces and fill terraces. Strath terraces are fluvial deposits that consist of an erosional bedrock surfaces with a thin cover of fluvial gravels (Leopold *et al.*, 1964). They are typical of upland and mountain settings undergoing tectonic uplift (Starkel, 2003). Fill terraces refer to river terraces that developed within channel and floodplain sediments. Fill terraces are developed by and often record complex incision and aggradation patterns (Lewin & Gibbard., 2010). Fill terraces are commonly formed in the distal reaches of large rivers where tectonic activity is typically lower (Starkel, 2003).

The timing of the onset of incision and the rate at which incision then proceeds is poorly constrained. Although there are numerous studies showing successful dating of Late Pleistocene to Holocene fluvial terrace deposits (Bridgland *et al.*, 2007; Gábris & Nádor, 2007; Tyráček & Havlíček, 2009), the dating of fluvial terraces resulting from events in the Plio/Pleistocene remains challenging due to the fragmentary nature of the terrace deposits (Stokes *et al.*, 2012a), lack of suitable material for dating and the age range limitations of the more commonly used absolute dating techniques (e.g. radiocarbon dating (40-50 ka), U-series dating (~350 ka) and OSL dating (~200 ka)).

Chapter 1: Introduction

Cosmogenic exposure dating is a relatively new and rapidly developing technique that appears to address many of the problems presented when trying to date Plio/Pleistocene fluvial landscapes. Cosmogenic dating uses the concentration of cosmogenic nuclides present in a deposit to calculate an exposure age and, where paired isotopes are analysed, a burial age.

In this study, the profile dating method of cosmogenic exposure dating is applied to a top basin fill surface, and the fluvial terraces inset into it, in order to document long term fluvial incision in the Sorbas Basin, SE Spain. Cosmogenic exposure dating allows the timing of abandonment of the fluvial terraces to be calculated therefore recording periods of incision. The Sorbas Basin has been chosen as an ideal location for this project because it comprises an inset sequence of terraces spanning from the Early Pleistocene to the Holocene cut into a Pliocene/early Pleistocene sedimentary basin fill record. A basic chronological framework is in place for the Plio/Pleistocene terrace deposits of the Río Aguas fluvial system with a more detailed chronology available for the Late Pleistocene/Holocene terraces based primarily upon U-series dating of pedogenic carbonates of soils that cap the river terraces (Kelly *et al.*, 2000; Candy *et al.*, 2004, 2005). This existing chronology serves as a check that the cosmogenic exposure dating technique applied by this study is producing valid dates.

Whilst the development of the Río Aguas is well understood (e.g. Harvey & Wells., 1987; Mather, 1991; Mather, 2000; Stokes *et al.*, 2002) the Río Jauto is a relatively unstudied tributary system to the Río Aguas (Harvey, 2007). A detailed examination of its terrace record provides the opportunity to add to the regional fluvial landscape development story and to enhance the understanding of the spatial and temporal patterns of drainage development and its controlling factors (tectonics, climate etc.). By studying the fluvial terraces within the Jauto system, an exploration of how the Río Jauto evolved

Chapter 1: Introduction

can be made. Also the impact of the headward incision by the Lower Aguas on the Río Jauto system can be investigated.

This study aims to contribute to the ongoing debate concerning fluvial landscape evolution and also demonstrate the application of cosmogenic exposure dating to river terraces in order to better understand the spatial and temporal patterns of Late Cenozoic landscape development.

1.2 Aims and objectives

The principle aim of this project is to apply a developing chronological technique, the cosmogenic profiling method, to fluvial terraces in a system that has undergone base level lowering linked to differential tectonic uplift and drainage network reorganisation via a basin-scale capture event. The cosmogenic exposure dating method is applied to calculate exposure ages for the abandonment of fluvial terraces by incision. Burial ages are calculated for deposits, where paired isotopes have been collected, to provide a maximum age for the surface sediments. The resultant geochronological database is used to quantify spatial and temporal patterns of fluvial system incision. Both mega scale (10^6 - 7) and macro scale (10^4 - 5) patterns are investigated. The timing and pattern of long term fluvial incision is driven by regional tectonics uplift. Shorter term incision patterns are driven by river capture related drainage network reorganisations and climate related sediment supply. This research addresses the following questions:

- 1) Can cosmogenic dating techniques be used to explore fluvial landforms (^{10}Be & ^{26}Al on fluvial terraces and ^{21}Ne on fluvial straths) and landscape developments (^{36}Cl dating of landslides)?

Chapter 1: Introduction

- 2) How do cosmogenic profile results compare with previously used chronological methods (e.g. U-series of pedogenic calcretes used to date river terraces in the Río Aguas)?
- 3) When did incision start in the Sorbas Basin? Is it synchronous with other basins in the Iberian Peninsula and does the dating of a long term fluvial record provide information about long term regional tectonic uplift rates and patterns?
- 4) Does cosmogenic exposure dating of river terrace landforms provide any insights into the relationships of the timings between terrace formation (fluvial aggradation), abandonment and river downcutting (fluvial incision) and glacial/interglacial climate cycles?
- 5) Can a formal stratigraphy be constructed for the Río Jauto fluvial archive? Can a relative stratigraphy be created for the Río Jauto using stratigraphic information and sedimentology data?
- 6) Can a localised model be created to represent the evolution of the Río Jauto fluvial system using depositional and environmental data collected in the field?
- 7) Can the application of palaeohydrology equations on field data be used to identify the magnitude of flood events in the Sorbas Basin? Do the terrace deposits of the Río Jauto and Aguas show any variability? Is there a climatic link?

1.3 The Sorbas Basin

The Sorbas Basin is a small east-west orientated sedimentary basin formed in the Betic Cordilleras and is located in the Almería province, SE Spain (Figure 1.1). The basin,

Chapter 1: Introduction

which is bordered by the Sierra de Los Filabres/Bédar to the north and the Sierra Alhamilla/ Cabrera to the south (Chapter 2), is one of a number of sedimentary basins which have formed within the Trans-Alboran shear zone, a zone of sinistral movement located in the Internal Zone of the Betic Cordilleras (Larouzière *et al.*, 1988).

The Río Aguas forms the main axial drainage of the Sorbas Basin with a drainage area of 550 km² (Figure 2.1). The Río Aguas is sourced in the Sierra de los Filabres and flows in a centripetal pattern towards the centre of the Sorbas Basin where it then becomes a strike orientated drainage following a weak band of Tortonian marls (Abad Member, Chozas Formation). The river course is also influenced by the structural geology of the area following a mountain front fault zone (Sanz De Galdeano, 1987).

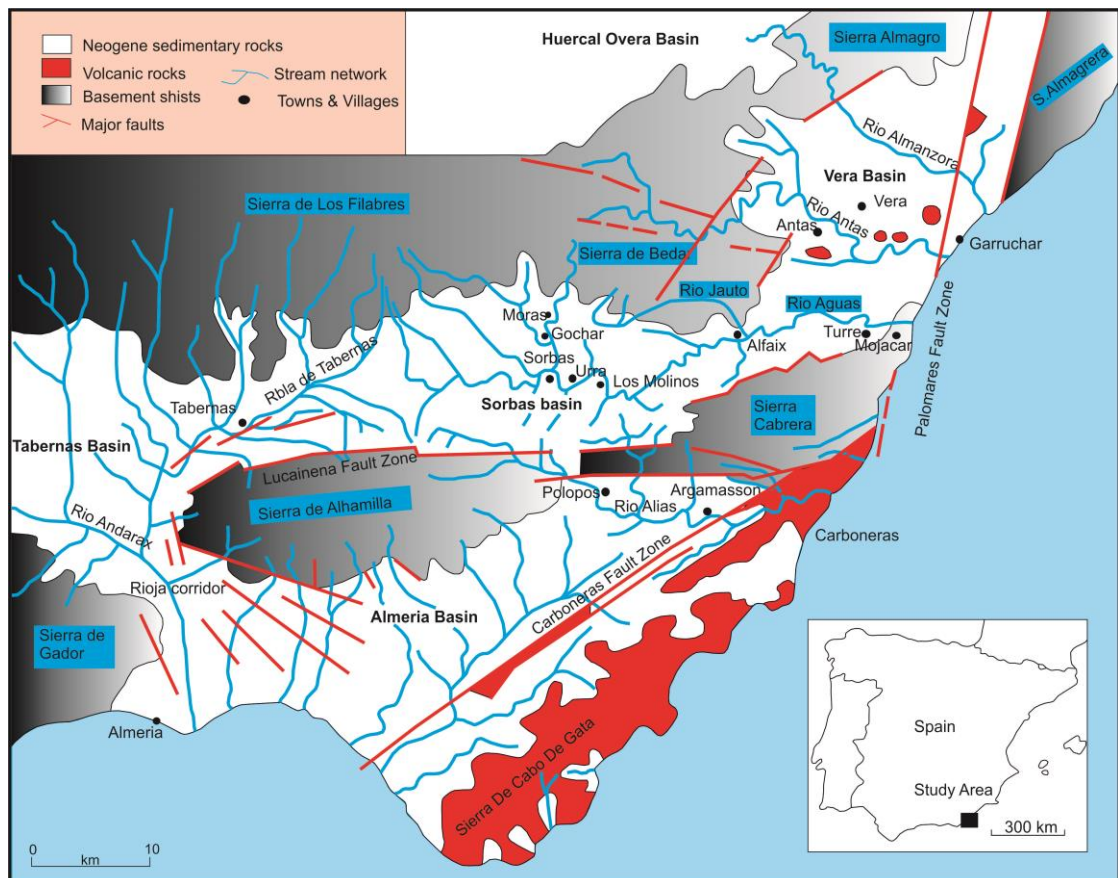


Figure 1.1: Location map for the Sorbas Basin, showing the surrounding Neogene basins and the main drainage systems in the basin (Río Aguas and Río Jauto). Modified after Harvey (2007).

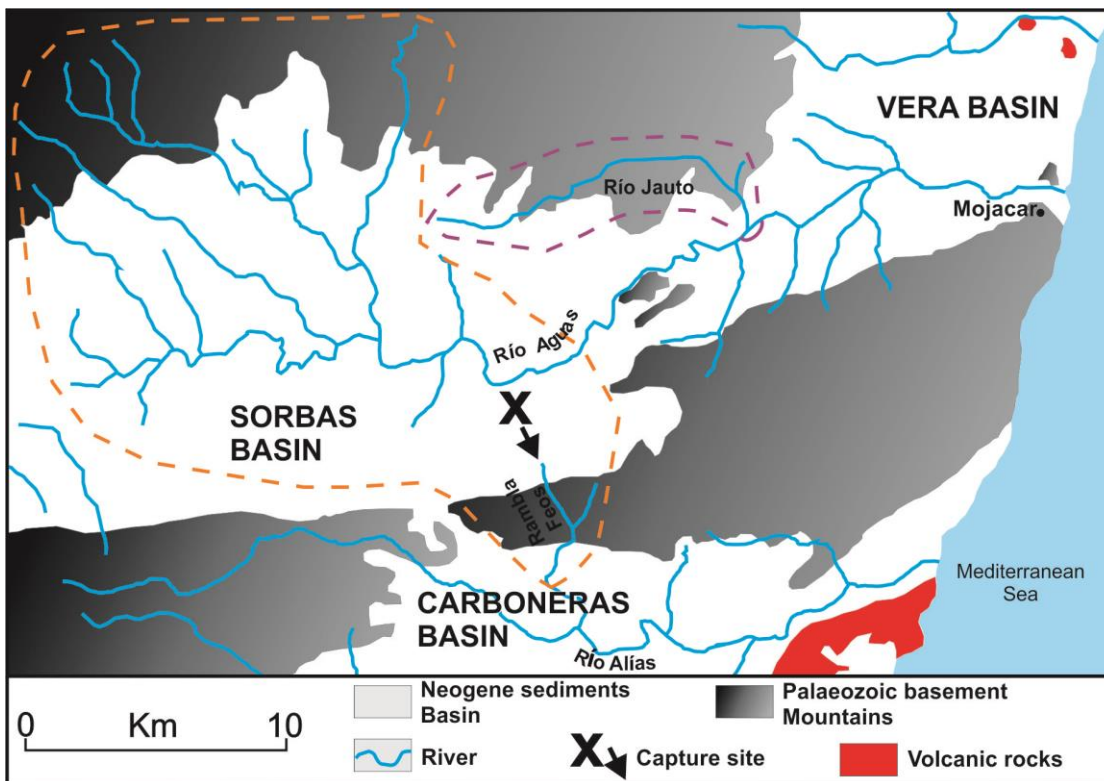


Figure 1.2: Map of the Sorbas Basin showing the main fluvial systems; The Río Aguas (outlined in orange) and the Río Jauto (outlined in purple). Modified after Harvey (2007).

The lower part of the Río Aguas drainage is also sourced from the Sierra Cabrera and the southern part of the Vera Basin. The Río Aguas drains east through the Vera Basin entering the Mediterranean Sea at the town of Mojácar Playa. The Río Aguas system is highly incised in its middle (~107 m) and lower reaches (~230m) caused by a significant base level drop due to headwards erosion driven by differential uplift within the Betic Cordilleras (Harvey, 1987). The incision history of the Río Aguas is recorded in a series of river terraces incised into the sedimentary basin infill of the Sorbas Basin (Figure 1.1). The river terraces consist of coarse clastic fluvial gravels (Harvey & Wells, 1987). The terrace deposits have a clear and well preserved morphological expression represented by five major levels (labelled A [oldest] to E [youngest] after Harvey & Wells, 1987) which are inset into a top basin fill surface, the Góchar surface, (Figure 1.1 and 1.2) representing some ~160 m of Quaternary and possibly Pliocene incision.

Chapter 1: Introduction

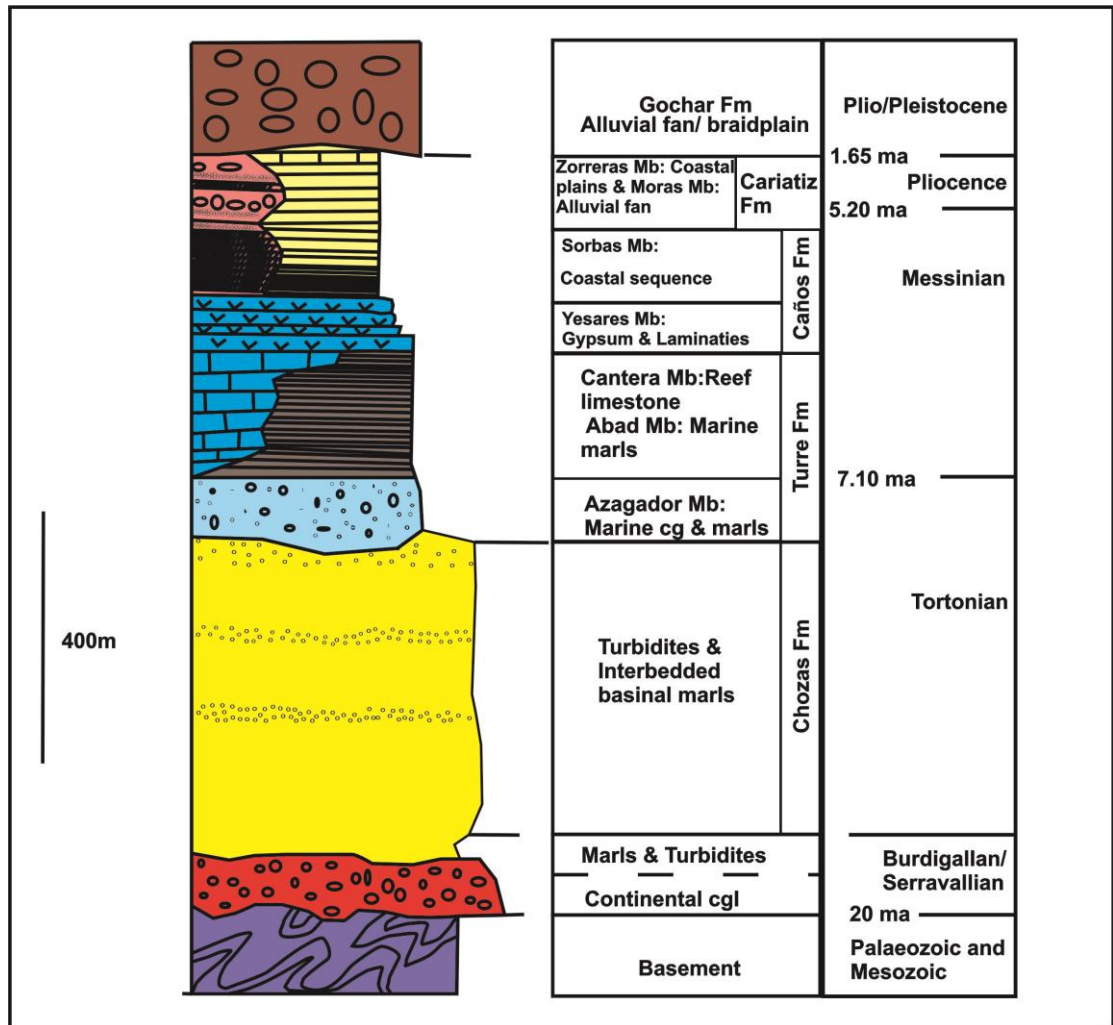


Figure 1.3: Simplified composite stratigraphic log of the sedimentary infill of the Sorbas Basin, SE Spain (after Mather, 1991).

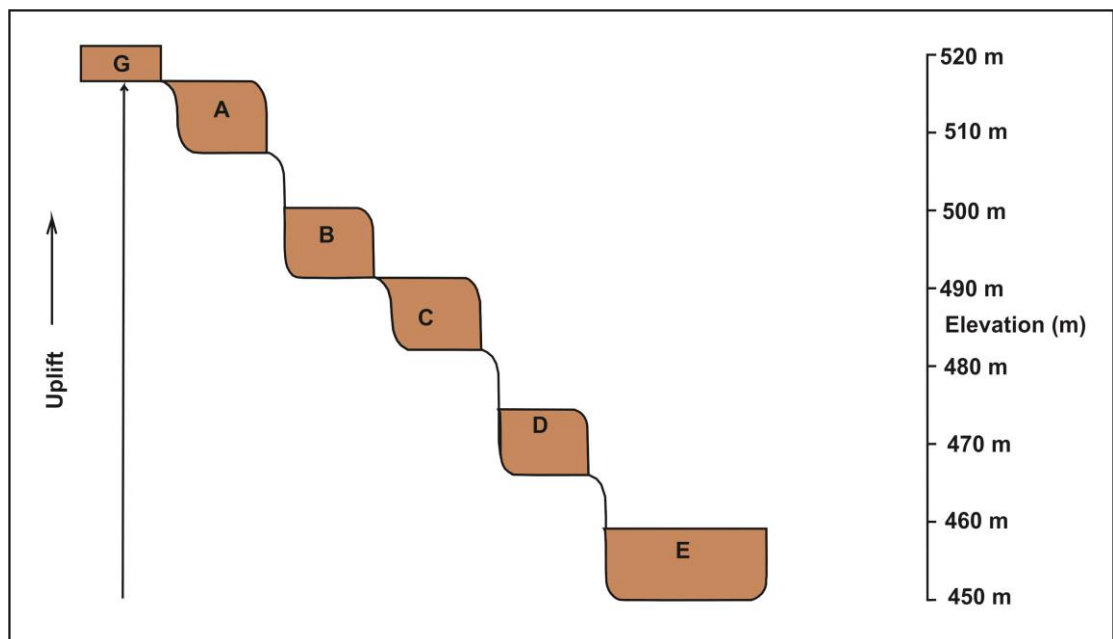


Figure 1.4: Schematic basin topographic profile showing the top basin fill (Góchar surface -G) and the inset terrace levels present in the Río Aguas system (after Harvey, 2007).

Chapter 1: Introduction

The Río Jauto (Figure 1.2) forms a major tributary of the Río Aguas flowing eastwards along the northern edge of the Sorbas Basin from its source in the Sierra de los Filabres. The Jauto is 12 km in length with a drainage area of 22 km². The Jauto drains the foothills of the Sierra de los Filabres and the Sierra Bédar collecting numerous north-south flowing systems along its course. The course of the Jauto is marked by a number of gorge sections, which cut through basement highs, and wide open valleys formed in softer geology. The Río Jauto is a major tributary to the Río Aguas and it joins the larger system at the village of Alfaix. Terrace deposits consisting of fluvial gravels and sandy lenses are also present along wide open valleys of the Río Jauto but are not present in the gorge sections.

1.4 Fluvial terraces

River terraces can be seen in most river systems around the world (Bridgland *et al.*, 2007). River terraces are the former floodplains that have been isolated from the river system via incision (Stokes *et al.*, 2012a). The terraces form via aggradation of channel and floodplain sediments which is then followed by incision of the valley floor preserving the terrace sediments along the valley sides (Lewin & Gibbard, 2010; Stokes *et al.*, 2012a). The terraces are expressed as topographically flat or very gently dipping surfaces that grade in a downstream direction (Bridgland & Westaway., 2008).

Two main types of river terraces are present in the Sorbas Basin; strath terraces and fill terraces (section 1.1). The Early-Mid Pleistocene fluvial terraces in the Sorbas Basin are strath terraces whilst the younger Late Pleistocene terraces in the Urrea area (Figure 1.1) could be considered as fill terraces.

Chapter 1: Introduction

Terrace deposits in the Sorbas Basin form inset sequences of fluvial terraces referred to as terrace flights or staircases (Figure 1.4). Terrace staircases are present in many river systems throughout the world recording tectonic and climate cycles over long periods of time (10^5 - 10^6) (Bridgland & Westaway, 2008; Lewin & Gibbard, 2010; Westaway *et al.*, 2009; Stokes *et al.*, 2012a). To form a terrace staircase there must be a period of sustained base level lowering.

The base level of a fluvial system is the point below which a river cannot erode. The ultimate base level of a river is the sea (Leopold & Bull, 1979; Bull, 2009). Changes in base level lead to disequilibrium in the long profile of the river system and cause the river to modify its length or width either through incision or aggradation.

The base level of a river can be changed tectonically, climatically or locally affected by lithological variations related to rock strength. Tectonically induced base-level modifications are driven by changes in surface gradient. Tectonic changes of the base-level can be either regional (i.e. regional uplift) or local (faulting) in nature. Changes in sea-level will shorten or lengthen a river modifying channel gradients. Sea-level fluctuations are driven by temperature changes via climatic cycles leading to base-level lowering (in glacial periods) and base level rising (in interglacial periods).

1.5 Climate and tectonics

Tectonics and climate are key controls on a fluvial system development. They operate over different timescales with climatic cycles occurring on shorter timescale than tectonics. Climate can fluctuate at all timescales from decades to tens of millions of years (Bull, 1991). It is the longer term fluctuations (10^4 a⁻¹) in climate from glacial to interglacial conditions that can modify a rivers base-level (Twidale, 2004). Tectonics

Chapter 1: Introduction

operate over geological timescales (millions of years) (Gibbard and Lewin, 2009). The following text describes the way that climate and tectonics control fluvial system behaviour.

Climate and climate cycles have a direct impact upon fluvial systems (Bull, 2009). Shifts in climate can lead to geomorphic thresholds being crossed resulting in changes in fluvial system behaviour. Climate controls discharge and flood regimes in a fluvial system. It also modifies other geomorphic thresholds, for example discharge and flood regimes, changes in vegetation due to an increase or decrease in precipitation impacts on slope stability which in turn regulates the amount of sediment available to a river system (Bull, 1991). Climate also modifies the in situ processes of weathering and can therefore increase the amount of sediment available to be supplied to a river (Bull, 1991). Another way that climate can modify fluvial system behaviour is through sea-level fluctuations as a result of temperature change and modification to polar ice volumes. Falling sea-levels as a result of climate cooling would lead to incision as the base level fell whilst sea level rise during an interglacial period would create a base-level rise leading to aggradation in the river systems. These responses are typically focused on distal reaches of the fluvial system but will depend upon the gradient of the river system and the morphology of the coastal shelf (Blum & Tornquist, 2000). In areas where there is a steeper gradient coastline with a narrow shelf and a pronounced shelf break the impact of the base-level on the fluvial system is lessened and in some cases the fluvial system becomes disconnected from the sea-level (Vis *et al.*, 2008; Meikle, 2009). It is suggested that this is the case in the Río Aguas system as there is a very narrow shelf in this area with the continental slope break being only 2.5 km from the coastline (Schulte *et al.*, 2008; Meikle, 2009). At Alfaix (Figure 1.1), a major knickpoint, 20 m high, occurs in the long profile of the Río Aguas. The knickpoint formed in resistant calarenites, which is present 12 km upstream from the coast, is

Chapter 1: Introduction

probably the landward limit of glacio-eustatic influence on the Río Aguas system (Schulte, 2004; Schulte *et al.*, 2004). The resistant calarenites would limit the ability of the river to respond to a base-level change because the river would be unable to change the angle of the valley bottom slope quickly.

The interaction between the modern floodplain and the floodplain surface from the last glacial maximum is located 4 km upstream from the coastline. This suggests that the upstream extent of the coastal onlap is small (Schulte *et al.*, 2008). Sea-level is therefore not considered as a major driver of fluvial incision in the Sorbas Basin because of its inland distance away from the coast and also because the resistant nature of the rock in the Alfaix area limits the ability of the river to respond to any sea level change (Schulte *et al.*, 2004).

The sensitivity of river systems to climate means that climate is a driving force of terrace aggradation and incision. Correlation to the Milankovitch 100 ka glacial to interglacial climate cycles has been noted by many researchers (e.g. Bridgland & Westaway, 2008). Although the Sorbas Basin was beyond the reach of Quaternary glaciations that occurred in the Sierra Nevada, around 100 km to the northwest, the climate changes related to the glaciations still had an impact on the Mediterranean region. Pollen data indicates that the climate during interglacials was warm and dry whilst in the glacial periods it was cold and dry with steppe vegetation covering the slopes (Tzedakis, 2009).

The classical models of terrace formation proposed that fluvial incision occurred in the interglacials whilst fluvial aggradation took place during glacial periods (Gibbard & Lewin, 2002; Vandenburg, 2003 and refs therein). The glacial periods are characterised by periods of valley slope instability due to limited vegetation cover leading to increased soil erosion and sediment supply to the valley floor. This promotes fluvial

Chapter 1: Introduction

aggradation. Incision dominated during interglacials because vegetation cover stabilises the valley sides reducing sediment supply to the valley floors (Vandenburge, 2008).

More recent studies of fluvial archives indicate that fluvial aggradation and incision may have taken place during glacial to interglacial transitional periods (Bridgland & Westaway, 2008 and refs therein; Vandenburge, 2008).

The transitional periods between glacial and interglacial periods are suggested to be the point at which fluvial systems aggrade valley bottoms due to the deterioration of the climate leading to thresholds being crossed (Bull, 2009; Starkel, 2003). During cold to warm transitions slopes will have limited vegetation cover, having not recovered from the glacial conditions, meaning that large amounts of sediment will be available to transport to the river systems. An increase in rainfall will lead to mass movement processes on the slopes delivering sediment to the rivers which have limited stream power. As vegetation recovers with the warming of the climate sediment supply will decrease due to the increasing root mass. The increase in rainfall means that the river begins to incise and isolate the river terraces in the landscape (Olszak, 2011).

Bridgland & Westaway (2008) present a model for terrace formation in response to climatic forcing which evokes incision during transitional periods. Three theories are presented 1) downcutting at warming transitions 2) downcutting at warming and cooling transitions and 3) downcutting only at cooling transitions. Chapter 8 examines these climate cycle models in more detail and presents a model for terrace formation in the Sorbas Basin.

Tectonics act over geologically long periods of time (millions of years) and can influence the land surface by changing surface gradients over a range of spatial scales leading to drainage initiation, incision and drainage network expansion. Regional base-level lowering can be attributed to the variability (both spatial and temporal) of tectonic

Chapter 1: Introduction

uplift rates (Starkel, 2003). The rate of tectonic uplift of an area depends upon the proximity of the area to a plate boundary and the type of plate boundary. In areas that are being tectonically uplifted due to a compressive plate boundary setting the rates of uplift tend to be high leading to larger base-level falls creating steep gradients causing rivers to modify the course via incision. In such areas, the vertical altitudinal spacing between individual terrace levels tends to be wider (Starkel, 2003).

Areas which are less tectonically active due to being located in continental interiors tend to be characterised by lower uplift rates and smaller base-level changes (Bridgland & Westaway, 2008). In uplift limited areas terrace formation tends to be less common, with complex fill terrace architectures and morphologies or strath terraces where the altitudinal spacing between terraces is generally small (Starkel, 2003).

It is clear that tectonics should be a fundamental driver of long term sustained base-level lowering. Whilst sea level fall could produce a base level fall to allow fluvial systems to incise, in the Quaternary the sea level fluctuated between lows of 120 m to 160 m and a high of + 6 m. Sea level fluctuations do not provide the sustained base level fall to allow terrace staircase formation (Stokes et al., 2012a). However, climate plays an important part in terrace formation as climate fluctuations are required for the variations in sediment supply to the fluvial systems. It is therefore suggested that the terraces form primarily as a result of the interplay between longer term tectonics and shorter term climatic fluctuations (Bridgland & Westaway, 2008).

1.5.1 Timing of terrace formation in the Sorbas Basin

Previous research on the terrace landforms in the Sorbas Basin seems to indicate a link between climate and terrace formation in the Río Aguas system (Harvey & Wells, 1987;

Chapter 1: Introduction

Kelly *et al.*, 2000; Schulte, 2002; Candy *et al.*, 2004; 2005; Schulte *et al.*, 2008). Kelly *et al.*, (2000) produced the first absolute dates for the terrace deposits of the Río Aguas using U/Th dating techniques on pedogenic calcretes capping the terrace surfaces.

Pedogenic calcretes form by leaching of carbonate by downwards percolation of rain and precipitation of carbonate in the vadose zone of soils (Alonso-Zarza, 2003). The calcretes form in soils and their age therefore represent the floodplain abandonment and terrace formation by incision. The results of the research indicated that the deposition of the C and D2 terrace deposits are probably related to the beginning and the end of the last glaciations (Level C-68-104 ka [MIS 6], terrace D2 8 ka [MIS 2]).

Work by both Schulte (2002) (using ^{14}C , IRSL and U/Th radiometric dating) and Candy *et al.*, (2004) (U/Th on pedogenic calcretes) focuses on the younger terrace deposits (the terrace D deposits). The results presented in Table 1.1 indicate that terrace D was isolated between 12.12 ± 0.46 ka and 8.43 ± 60 ka. These results agree with earlier research by Kelly *et al.*, (2000) that the aggradation of terrace D is linked to the Last Glacial Maximum (LGM). Candy *et al.*, (2004) suggests that during the Late Quaternary the Río Aguas was highly sensitive to climate change with phases of aggradation corresponding well to glacial events whilst incision occurs at interglacial periods.

Terrace Level	Candy et al, 2004	Schulte (2002)
	Age (ka)	
D3	8.69 +/- 0.46*	8430 +/- 60^
D2	9.67 +/- 0.82 *	n/a
D1	12.14 +/- 0.37*	9640 +/- 60^

Table 1.1: Minimum ages for the terrace D deposits of the Río Aguas (* based on U/Th, ^ based on ^{14}C).

Chapter 1: Introduction

Candy *et al.*, (2005) produced the first set of dates for the older Late Pleistocene deposits of the Río Aguas system with U/Th dates provided for the surfaces of terrace levels A through to D3. The U-series dates indicate that the terrace A had finished aggrading by 304 +/- 26 ka and terrace B by 207 +/- 11 ka. The terrace A date is at the maximum extent of the accuracy of the U-series methodology and work by Candy *et al.*, (2004) suggests that within the Sorbas Basin stage V calcretes may require between 70-120 ka to form meaning that the terrace A landform is likely to have been progressively isolated within the landscape for at least 400 ka (Candy *et al.*, 2005).

U- series dates obtained for terrace C and D suggest that incision occurred at transition periods and therefore indicate that the aggradation of the deposits correspond to the beginning of the glacial periods (Candy *et al.*, 2005) with terrace C being related to OIS 6 and terrace D to OIS 2 (Schulte *et al.*, 2008). The picture of the timing of terrace formation in the Sorbas Basin is complicated by ongoing active tectonic uplift (Chapter 2; section 2.3) and by basin-scale river captures (Section 1.5.2), both of which result in base-level lowering and incision in the Sorbas Basin.

There are several problems with applying U-series dating to pedogenic calcretes. The quality and morphology of calcretes evolve over time (Kelly *et al.*, 2000) as demonstrated by the Machette classification of calcrete development (Chapter 3). This means that the mature calcretes capping the Río Aguas river terraces contain multiple carbonate phases with a large range of ages. Only taking one sample is therefore unlikely to provide a correct date for the terrace landform. Whilst this can be mitigated by testing multiple isochron dates, the derived ages will be average minimum ages for the terrace surface.

Another problem with applying U-series dating techniques to the older terrace deposits in the Sorbas Basin (Góchar surface and terrace A) is that the expected dates for the

Chapter 1: Introduction

deposits are at or over the maximum extent for the methodology (~ 350 ka Walker, 2005). This means that there are large error bars on the dates, particularly the ages for terrace A. Dating the Góchar surface using this method is impossible as the surface is believed to be over 1 Ma, well beyond the maximum extent for the U-series dating methodology.

There is also a time lag between the end of aggradation and the formation of calcretes, as indicated by Candy *et al.*, (2004). U-series techniques date soil formation which is a function of climate. A way to overcome this problem is to date the terrace surface sediments themselves and one chronological method that does this is cosmogenic dating (Section 1.6). This research attempts to obtain dates for the older Plio/Pleistocene deposits present in the Río Aguas system (i.e. the Góchar surface through to terrace C). Cosmogenic dating is going to be applied to try and provide a clearer picture of the timing of terrace aggradation and incision for the Plio/Pleistocene deposits in the Sorbas Basin.

1.5.2 Fluvial response to tectonics in SE Spain-River capture

In the Iberian Peninsula tectonics are believed to be a key driver on drainage evolution due to the close proximity of the plate boundary between the colliding African and European plates (Pérez-Peña *et al.*, 2010). Numerous studies have taken place on river systems in SE Spain (Harvey & Wells, 1987; Stokes, 1997; Stokes & Mather 2003; Maher, 2006; Blum, 2009; Meikle, 2009). Harvey & Wells (1987) noted that river systems in the eastern area of the Betic Cordilleras show discordance with geological structures. In areas which are tectonically active, the river systems tend to exhibit a series of characteristics due to the changing base level. The base-level changes occur as a result of landscape changes caused by the tectonic uplift. Rivers in tectonically active

Chapter 1: Introduction

areas tend to display aggressive headwards erosion over steepened topographic gradients (Schumm *et al.*, 2002). The systems also show aggressive incision as a result of the accelerated uplift which leads to drainage rearrangement; via river capture or stream piracy, integration and network expansion (Mather & Harvey, 1995 etc.).

As a river begins to erode and incise headwards, the drainage network is expanded, leading to an increase in drainage density. As expansion occurs, interactions between streams can take place and river capture can occur. River capture takes place when a more actively eroding river captures the headwaters of a less actively eroding river (Bishop, 1995). A base-level drop takes place which leads to a wave of incision to be initiated which propagates upstream through the captured system (Stokes *et al.*, 2002; Mather *et al.*, 2002; Garcia *et al.*, 2004).

The Río Aguas, the main axial drainage of the Sorbas Basin, displays characteristics of a river system that has been affected by tectonic uplift; headward erosion, incision and drainage rearrangement via river capture leading to landscape instability (Harvey & Wells, 1987; Mather, 1991; 2000; Stokes *et al.*, 2002; Maher, 2004; Hart, 2008; Maher *et al.*, 2007; Whitfield & Harvey, 2012). The ancestral drainage of the modern Río Aguas system is the Proto Aguas/Feos. The Proto Aguas/Feos formed in the Plio/Pleistocene and began to incise into the basin sediments creating a series of fluvial terraces (Mather, 1991; Mather and Harvey, 1995). The fluvial terrace record indicates that a major basin scale river capture event has taken place with the Lower Aguas rerouting the southwards flowing Proto Aguas/Feos eastward into the neighbouring Vera Basin (Figure 1.1) (Harvey & Wells., 1987; Mather *et al.*, 2002; Stokes & Mather., 2003; Maher, 2005; Maher *et al.*, 2007; Harvey, 2007; Maher & Harvey, 2008). The capture event led to widespread incision (~90 m), valley side destabilisation (leading to landsliding), badland formation and karst formation (Harvey & Wells, 1987; Harvey,

Chapter 1: Introduction

2007; Mather *et al.*, 2002; Calaforra & Pulido-Bosch., 2003; Stokes & Mather, 2003; Hart, 2008). The capture event is described further in Chapter 2.

1.6 Establishing an accurate chronology

An accurate chronology for terrace staircases is important as it enables the timescale of fluvial landscape development to be established. This in turn allows for a more detailed insight into fluvial landscape controlling factors (tectonics, climate etc.). A number of different methods have been developed to date river terraces (Radiocarbon, Optically Stimulated Luminescence [OSL], Electronic Spin Resonance [ESR] etc.) and accurate ages for younger terraces have been achieved (Bridgland & Westaway, 2008). Dating older river terraces, especially those deposited during the Middle Pleistocene and earlier, can be challenging due to the fragmentary and limited nature of the deposits.

There is often limited organic material in river terraces meaning radiocarbon dating is normally not possible, especially in semi-arid or arid settings. Older fluvial landforms are also difficult to date because they are outside of the accurate limit of most methods with Optically Stimulated Luminescence (OSL), the main absolute method applied to fluvial deposits, have an upper time limit of 200 ka (Walker, 2005). Whilst the development of new OSL techniques using feldspar are starting to push the limits of the methodology back to more accurate older ages (Buylaert *et al.*, 2012) other issues with applying the technique to river terraces exist. OSL dating involves assessing how long quartz and feldspar sand grains have been buried in a terrace deposits by determining how much time has passed since the grains were last exposed to daylight. In some cases grains can get bleached and this affects the signal that the quartz gives off. Bleaching of the quartz is a common problem in samples from terraces in SE Spain (Maher, 2007; Meikle, 2008). U-series dating is another method which has regularly been applied to

Chapter 1: Introduction

terrace deposits, especially in south east Spain (Kelly *et al.*, 2000; Schulte, 2002; Candy *et al.*, 2004; 2005). However, as discussed previously the use of this method on older terraces is restricted by age range. Other dating methods for older terrace deposits include ESR dating and K-Ar/ Ar-Ar dating. K-Ar/Ar-Ar dating does however depend on the river terraces being buried by or incising through volcanic deposit (Walker, 2005) which is not the case for the fluvial landscape in SE Spain.

ESR dating has been used to date Pliocene and Pleistocene fluvial deposits (Wenzen, 1991; Cordier *et al.*, 2012). ESR dating measures the amount of paramagnetic centres of quartz grains present in a sample in order to determine how long a terrace has been exposed (Grün, 1989; Cordier *et al.*, 2012). A recent study by Cordier *et al.*, (2012) applied ESR dating to Pliocene and Pleistocene deposits producing dates ranging from 1.2 Ma to 340 Ka. In SE Spain, ESR dating has been used to date the oldest fluvial deposits in the Vera basin to 2.3 Ma- 1.4 Ma. The Cordier *et al.*, (2012) study highlighted the large error bars on dates produced using the ESR dating technique on older fluvial deposits.

A recently developed method that has started to become utilised for dating terrace deposits is cosmogenic dating which has developed as Accelerated Mass Spectrometry (AMS) techniques have improved leading to increased capabilities to measure smaller concentrations of nuclides (Gosse & Phillips, 2001; Watchman & Twidale, 2002; Duani, 2010). Cosmogenic dating involves measuring the concentration of cosmogenic nuclides present in quartz, a material which is abundant in terrace deposits (Gosse & Phillips, 2001; Watchman & Twidale, 2002). Cosmogenic dating overcomes many of the issues raised by other chronological methods as it utilises quartz which is abundant in fluvial deposits. The accurate range of this method has been pushed back to 5 million years, due to improved understanding of methods for modelling the datasets, producing

Chapter 1: Introduction

adequate coverage to the time range expected to be spanned by the Río Aguas river terrace.

Cosmogenic dating involves measuring the concentration of cosmogenic nuclides that are present in a landform or rock outcrop (Gosse & Phillips, 2001). Cosmogenic nuclides are produced by cosmic rays impacting on target minerals (e.g. quartz) in the landform. Cosmic rays are sourced from the sun and also from super nova explosions that occur in and beyond the Milky Way (Gosse & Phillips, 2001). The rays consist of high energy particles which interact with atoms of target elements when they impact on rocks in the Earth's surface (Friedlander, 1989) (Chapter 4). Cosmogenic dating can be used to calculate both an exposure age of a deposit and erosion rates. To date, cosmogenic exposure dating has mainly been used to date bedrock exposure by glacial erosion (Rinterknecht *et al.*, 2012; Glasser *et al.*, 2012), landsliding (Ballantyne & Stone, 2009; Ballantyne & Stone, 2013) and volcanic events (Fenton & Niedermann, 2012; Fenton *et al.*, 2013). Dating of depositional landforms by cosmogenic dating is less common although with the development of the concentration profile methodology by Anderson *et al.*, (1996) this area of research is beginning to be developed and more widely applied.

In this study the concentration of Beryllium 10 (^{10}Be) and Aluminium 26 (^{26}Al) (both produced from quartz) found in the surface sediments of river terrace deposits is measured to ascertain when the terrace landform was abandoned. The concentration profile sampling method is used to collect multiple samples through the terrace deposits to date the exposure of the terrace (Chapter 4).

Chapter 1: Introduction

1.7 Summary

This chapter has introduced the main aims and themes of this research. The research methods used to investigate the aims of the research are presented in the Methodology chapter (Chapter 3), the geological history of the area in Chapter 2, the sedimentology and palaeohydrology of the Sorbas Basin drainage are described in Chapter 5 & 6. Cosmogenic exposure dating is discussed in Chapter 4 with a background of the development of the concentration profile method presented. The cosmogenic exposure dating results are presented in Chapter 7. The role of tectonics and climate on terrace formation are also discussed in Chapter 8. A terrace model for the Rio Aguas deposits is also presented. Conclusions are then provided in Chapter 9.

Chapter 2: Study area geology and geomorphology

2.1 Introduction

This chapter provides an overview of the geological and geomorphological settings in which fluvial system development has occurred within the study area region. The geological and geomorphological development of the study area is presented in stratigraphic order. The tectonic setting and development of the Neogene basins are considered, as these components have a direct impact on the fluvial systems.

Descriptions of the metamorphic basement rocks and sedimentary basin infill are provided as these form the basis of provenance data used to understand the source area and sediment routing patterns of the evolving fluvial systems. The underlying bedrock geology of an evolving fluvial system also exerts a passive influence often controlling the course that a river takes in terms of rock strength and structure. Finally, the initiation of the primary fluvial systems of the Sorbas Basin (The Góchar Formation) and the deposits of the current fluvial system are introduced.

2.2 Location

The Sorbas Basin is one of a series of east-west orientated Neogene basins, formed by a series of folds and isolated by a series of strike slip faults, developed in the Internal Zone of the Betic Cordillera in south east Spain (Sanz de Galdeano *et al*, 2010) (Figure 2.1). The Sorbas Basin is located near the city of Almería and is surrounded by a series of basement highs. Figure 2.1 illustrates how the Sorbas Basin is bounded by the Sierra de los Filabres to the north and by the Sierra Cabrera/Alhamilla to the south. The boundaries to the west, with the Tabernas Basin, and to the east, with the Vera Basin, are not well defined topographically by basement highs. The hydrological boundary between the Sorbas and Tabernas Basins are very clear with fluvial systems flowing to the east into the Sorbas Basin on one side of the divide and west into the Tabernas Basin

on the opposite side of the divide. There is also a clear geological divide between the basins marked by a lack of continuity of stratigraphic units between adjoining basins (Mather *et al.*, 2001).

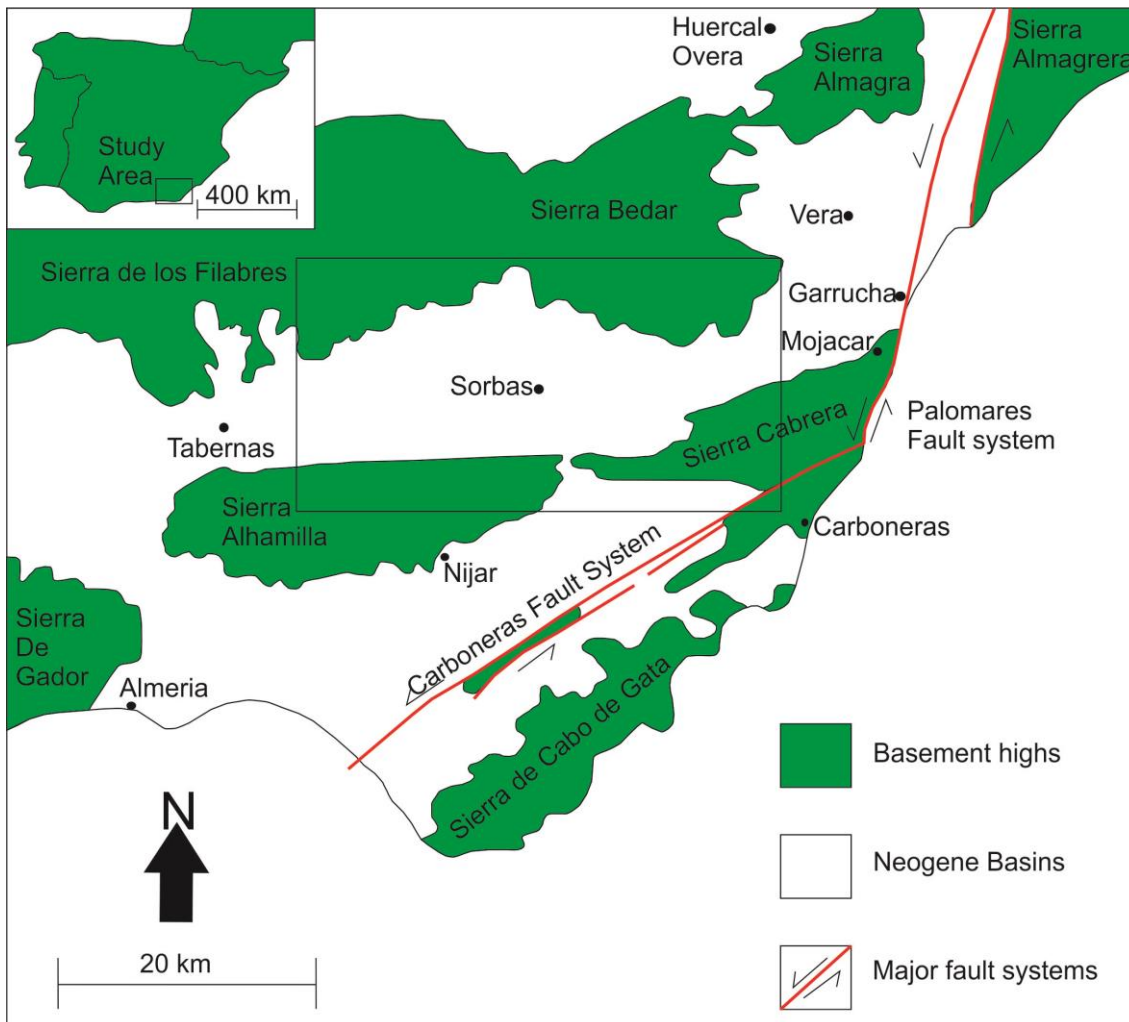


Figure 2.1 Map showing the locations of the Neogene sedimentary basins that surround the Sorbas Basin. The basement highs are shown in green and the Neogene basins is white. The major fault systems present in the Almería Province are also marked in red (Modified from Griffiths *et al.*, 2005).

2.3 Basin Formation

The current form of the Betic Cordilleras in the Almería region is a series of isolated blocks of basement (Sierras) between which sedimentary basins have formed (Figure 2.1). The sedimentary basins are formed by narrow troughs (20 x 10 km) that were created alongside the strike slip faults. They are strongly subsiding basins with a

symmetrical synclinal north south cross section (Cloetingh *et al.*, 1992; Galdeano *et al.*, 2010) and are filled with Neogene sediments.

The Betic Cordilleras formed as a result of continental collision between the African and European plates as the Tethys Ocean closed. The collision between the continental plates is a function of differential spreading along the mid-Atlantic ridge (Mather, 2009). The present day position of the plate boundary runs along the northern coast of Africa through the Gibraltar Arc in an east-west direction (Zitellini *et al.*, 2009) (Figure 2.2). The collision of the African and Iberian plates began in the early Mesozoic and led to the uplift of the Betic Cordilleras which are part of an Alpine orogenic belt (the Betic Rifian system) that stretches round the straits of Gibraltar (Smith & Woodcock, 1982; Larouzière *et al.*, 1988; Tubía *et al.*, 1992; Biermann, 1995; Pla-Pueyo *et al.*, 2009).

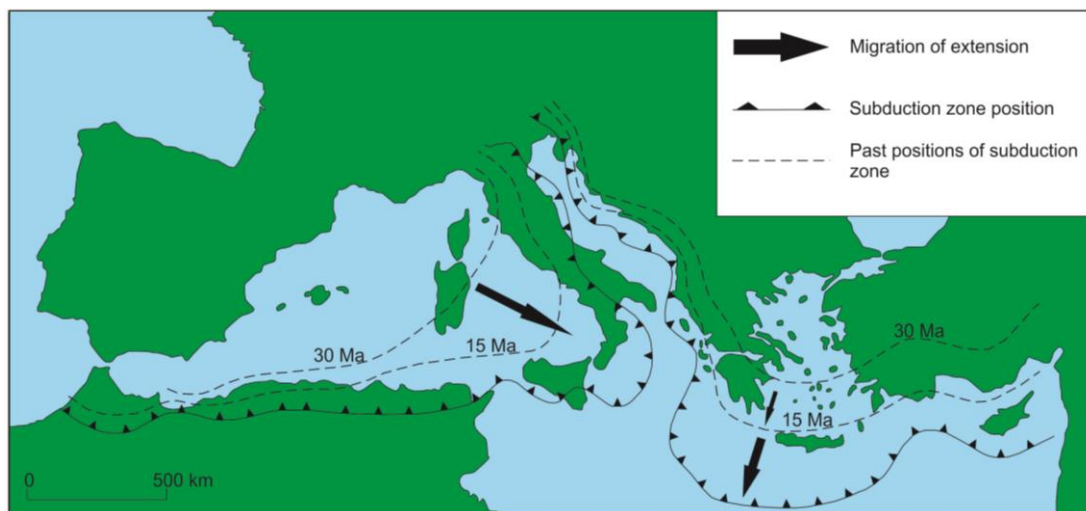


Figure 2.2: Location of the plate boundary between the African and European plates. The diagram shows the present and the past locations of the subduction zone (Mather, 2009).

The Betic Cordilleras are divided into two parts, the External Zone and the Internal Zone (Egeler & Simon, 1969; Ruiz-Constán *et al.*, 2009; Pedrera *et al.*, 2009; Pérez-Peña *et al.*, 2010), each distinguished on the basis of lithological, tectonic and palaeogeographic properties (Fallot, 1984; Sanz De Galdeano, 1990). The Neogene sedimentary basins are present in the Internal Zone of the Betics (Pedrera *et al.*, 2009; Pérez-Peña *et al.*, 2010).

The Internal Zone of the Betic Cordilleras consists of a series of metamorphic nappe structures, which were thrust on top of the External Zone during the Oligocene to the Earliest Miocene, and forms the southern part of the range (Weijermars, 1991; Huibregtse *et al.*, 1998). The nappe units of the Internal Zone, termed the Nevado-Filábride, Alpujárride and Maláguide Complexes, are part of the Tethys ocean subduction closure complex and were formed in the Upper Cretaceous.

The three complexes, summarised in Table 2.1, can be distinguished on the basis of relative age, phase of deformation and degree of metamorphism. The Maláguide complex displays the lowest grade of metamorphism and the Nevado-Filábride complex the highest grade of metamorphism (Weijermars, 1991) (Table 2.1). The basement lithology in the Sorbas Basin is dominated by the Alpujárride and Nevado-Filábride complex. A description of these units is given below as they provide the main sediment supply from basement rocks to the Rio Aguas and Jauto and are therefore important for source area determination using clast identification.

Complex name	Age	Metamorphic grade	Lithologies
Maláguide complex	Triassic-early Tertiary	Low	Mica schist, sandstones and limestones
Alpujárride complex	Permo-Triassic	Low-Medium	Harzburgite, eclogite, metagranite, granulite, gneiss, migmatite, mica schist, phyllite, quartzite, limestones, mudstones and dolostones
Nevado-Filábride complex	Palaeozoic-Triassic	Medium-High	Mica schist quartzite, mafic, ultramafic rocks, marble and carbonates

Table 2.1: Stratigraphic relationships of the basement units along with metamorphic status (after Egeler & Simon, 1969). Metamorphic information after Sanz De Galdeano & Vera, 1992).

- 1) Nevado Filábride Complex (after Egeler, 1963):- This complex is the lowest and therefore the oldest of the nappes within the metamorphic basement. Outcrops occur in the Sierra De Los Filábride, Sierra Alhamilla and the Sierra Nevado. The main lithologies include schists (mica and graphite bearing), quartzites, marbles and carbonates (Weijermars, 1991).

- 2) Alpujárride Complex (after Van Bemmelen, 1927):- The complex outcrops in the Sierra Alhamilla and consists of Triassic carbonate rocks, which have been subjected to low grade metamorphism, phyllites, quartzites and black greenschist facies.

- 3) Maláguide Complex (after Blumenthal, 1927):- The Maláguide Complex is characterised by graphite-bearing schists, carbonates, sandstones, shales and conglomerates which have been subjected to either no metamorphism or very low grade metamorphism (Weijermars, 1991). The rocks outcrop outside the Almeria Province in the Sierra Espuña (Murcia) and the Sierra De Las Estancias (Malaga) (Gomez-Pugnaire, 2001). They range in age from Silurian to Oligocene with a pre Permian basement and a Triassic -Tertiary cover (Hodgson, 2002).

During the Early to Mid-Miocene there was a switch to compressive tectonics regime due to the on-going collision of the African and Iberian plates leading to the final emplacement of the nappes within the Internal Zone (Weijermars *et al.*, 1985; Sanz de Galdeano *et al.*, 2010). The direction of compression was N-S to NNW-SSE and this led

to the formation of the Trans-Alboran Shear Zone (Larouzière *et al.*, 1988; Zeck, 2004; Rutter, Faulkner & Burgess, 2012).

The Neogene basins of SE Spain, such as the Sorbas, Vera and Carboneras basins, are formed in the Trans-Alboran Shear Zone which developed in the Late Miocene and is still active today. The Trans-Alboran Shear Zone is an area of left-lateral faults which is 70 km wide and runs over an area of 250 km from Alicante in the North to Almeria in the south (Larouzière *et al.*, 1988; Rutter *et al.*, 2012, Faulkner & Burgess, 2012). The different displacement of the strike slip faults split the nappe complexes of the Internal Zone into individual blocks of the basement leading to the creation of sedimentary basins (Larouzière *et al.*, 1988; Keller *et al.*, 1995). The Neogene basins formed in three ways; firstly, in the late Tertiary strike-slip tectonics took place along a NE-SW trending major fault zone that was sinistral in nature (Montenat *et al.*, 1987; Montenat & Ott d'Estevou, 1999). Secondly east-west trending dextral strike slip faults developed (Sanz de Galdeano, 1989; Sanz de Galdeano & Vera, 1992; Stapel *et al.*, 1996). Finally there was north-south extension which was associated with orogenic collapse (Vissers *et al.*, 1995) that led to the creation of a series of half grabens.

The on-going collision of Africa and Europe is uplifting the Betic Cordilleras with the main axis of the Sierra Alhamilla and Cabrera being uplifted. The uplift of the Betic Cordilleras is being facilitated through movements of reverse and strike slip faults with a normal component of vertical uplift (Giménez *et al.*, 2000). Table 2.2 presents a summary of proposed uplifted rates for the Neogene basins of southern Spain, along with references, whilst figure 2.1 shows the location of the Neogene sedimentary basins. The values in the table show the variability of the uplift rates with the Sorbas Basin being uplifted quicker than the neighbouring Vera Basin at a rate of 0.07 ka^{-1} compared to values of 0.02 ka^{-1} in the Vera Basin. The area to the north of the Sorbas Basin (The

Almanzora corridor) is undergoing uplift at a rate of 0.015 ka^{-1} . In the Almeria Basin lower rates are recorded (0.04 m/ka^{-1}). These uplift rates have been calculated assuming a constant rate of uplift rather than episodic uplift. However, a constant rate of tectonic uplift and therefore base level fall would not account for the amount of incision that has occurred in the Betic Cordilleras.

The differential uplift recorded by the values in Table 2.2 has had a significant effect on the regional fluvial systems leading to river capture events and drainage rearrangement (Harvey & Wells, 1987; Mather, 1991; Stokes, 1997; Hart 2004; Garcia *et al.*, 2004; Maher, 2005).

Basin	Author	Method	Time averaged uplift rate
Vera	Stokes & Mather, (2003).	Pliocene shoreline	0.02 m Ka^{-1}
Vera	Stokes, (1997).	Pliocene shoreline	0.015 m Ka^{-1}
Huércal-Overa	Stokes & Mather, (2003).	Pliocene shoreline	0.05 m Ka^{-1}
Eastern Vera	Booth-Rea et al., (2004).	Pliocene shoreline	0.05 m Ka^{-1}
Almeria	Zazo et al., (2003).	MIS 5e Raised beaches	0.04 m Ka^{-1}
Cope	Zazo et al., (2003).	MIS 5e Raised beaches	0.023 m Ka^{-1}
Sorbas	Braga et al., (2003).	Tortonian shoreline	0.07 m Ka^{-1}

Table 2.2: Uplift rates for the Neogene basins, SE Spain.

2.4 Basin Infilling

This section discusses the sedimentary infill of the Sorbas Basin (Figure 2.3; Appendix 2a). The nomenclature and lithostratigraphy used for the sedimentary basin fill will follow that used by Mather (1991) and Stokes (1997) which is based on the work of Ruegg (1964) and Völk & Rondell (1964). The sedimentary basin infill ranges in age

from the Burdigalian to the Quaternary (22 Ma and younger). The rocks record three major transgression/regression cycles that took place during the Serravallian-Tortonian, the Messinian and the Pliocene. The transgression/regression cycles occurred as global sea levels fluctuated. The sediments also record the progressive isolation of the Neogene basins from each other as the tectonic evolution of the Betic Cordilleras progressed and basement blocks became uplifted. The final part of this section covers the evolution of the regional drainage systems and the formation of a terrace staircase.

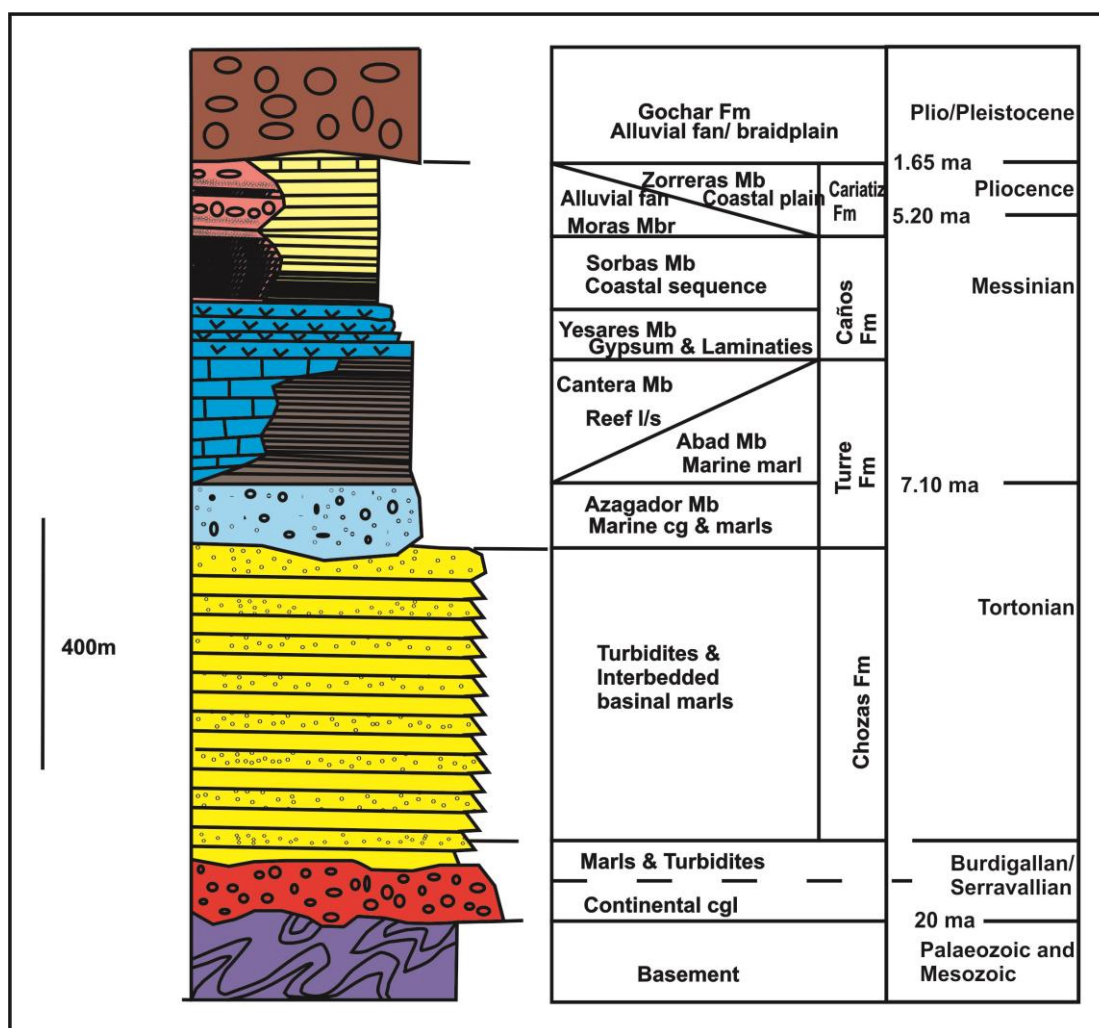


Figure 2.3: Log show the sedimentary infill present in the Sorbas Basin (after Mather, 1991).

2.4.1 Burdigalian/Serravallian/Tortonian

The older Neogene sediments are dominated by Alpujarride-derived sediments with no material being sourced from the Nevado-Filábride nappe (Volk, 1967a,b). This indicates that the Nevado-Filábride nappe was not unroofed during this time. The early stage basin infill (Burdigalian/Serravallian/Tortonian) records the first major marine transgression which occurred in the Serravallian to the Tortonian. This period also includes the tectonic uplift of early forms of the Sierra Alhamilla/Cabrera.

The marine transgression is recorded by the Chozas Formation. The sediments recording the sea level rise are preserved in the southern margin of the Sorbas Basin along the northern flank of the Sierra Cabrera. The Chozas Formation can be split into an upper and lower sequence separated by an angular discordance (Ott d'Estevou, 1980; Mather, 1991). The upper sequence (Upper Tortonian) is best preserved in the Sorbas Basin and comprises turbidites and intercalated marls that have been derived from the north (Weijermars et al., 1985).

During the Late Tortonian early forms of the Sierra Alhamilla and Cabrera mountains were uplifted when a switch in tectonic regime occurred (Weijermars *et al.*, 1985).

Regional compression replaced the extensional tectonics that formed the basins leading to the Tortonian sediments becoming strongly folded. Compression directions of N-S to NNW/SSE led to the uplift of the Sierra Alhamilla/ Cabrera with the northern boundary faults of the mountains becoming reversed (Weijermars *et al.*, 1985; Sanz de Galdeano *et al.*, 2010).

Towards the end of the Tortonian/ Early Messinian NE-SW trending basement faults led to the separation of the Tabernas, Sorbas and Vera Basins. The increasing isolation of the basins is recorded by an unconformity between the Tortonian and Messinian

sediments that is more pronounced in the Sorbas Basin infill than in the Vera Basin infill.

2.4.2 Messinian basin fill

A second marine transgression occurred during the Late Tortonian –Messinian when the sedimentary basins were completely open to the sea. The Tabernas, Sorbas, Carboneras and Vera Basins were all still connected at this time (Ott d'Estevou, 1980). The marine conditions are first recorded by the shallow marine reefs of the Azagador Member (Turre Formation) which indicate that the climate was temperate (Martín & Braga, 2001). The maximum flooding of the basins, marking the peak of the transgression, occurred in the Early Messinian with 120 m of marine marls (Abad Member marls) being deposited (Weijermars, 1985). The foraminifera in the marls indicate that the water depth reached a maximum of 100-300 m (Troelstra *et al.*, 1980, Baggeley, 2000). Whilst deep water sedimentation occurred in the southern area of the Sorbas and Vera Basins, shallow water sedimentation was occurring at the margins with limestone reefs (Cantera Member) developing along the basement highs (Braga *et al.*, 2003). Figure 2.3 shows the palaeogeography of the Neogene basins during this period. Reefs began to form in the more central parts of the basin as the sea level began to fall gradually after peaking. Reef formation gave way to the deposition of gypsum in the centre of the Sorbas Basin as the Messinian Salinity Crisis (Hsü *et al.*, 1972; Bache *et al.*, 2012) took place leading to the deposition of 130 m of evaporates (Yesares Member, Caños Formation) in response to a lowering of the water depth to between 10 and 100 m during this period (Dronkert, 1976; Pagnier, 1976). The shallow water depths are also recorded in the sedimentary structures of the Yesares Member with a lack of wave ripples or desiccation cracks indicating that the gypsum was deposited below the wave base (Krijgsman *et al.*, 2001).

The marine connection became restricted to the Sorbas Basin during the deposition of the Sorbas Member (Caños Formation) which marked the re-flooding of the basin following the Messinian Salinity crisis. The Sorbas Basin was connected to the sea via the Vera and Tabernas basins during the early Messinian but this connection was restricted by a sill which forced the main connection basin to become the Carboneras basin to the south (Braga & Martín, 1997; Martín *et al.*, 1999; Martín & Braga, 2001). This restriction of the basin marked the beginning of the transition to continental conditions (Krijgsman *et al.*, 2001) which occurred first in the Sorbas Basin and then in the neighbouring Vera Basin.

2.4.3 Late Miocene/Pliocene/Pleistocene basin fill

During the Late Miocene/Pliocene the Neogene basins switched from marine conditions to become fully terrestrial. In the Sorbas Basin this switch is recorded by the Cariatiz and Góchar Formation. The sediments preserved in the Sorbas Basin record first a coastal plain with alluvial fans prograding from the basin margins (The Zorreras and Moras Members respectively of the Cariatiz Formation [after Mather, 1991]). This was followed by the development of fluvial systems (Góchar Formation). Magnetic Stratigraphy of the Zorreras Member represents the only formal age control on the sedimentary infill of the Sorbas Basin. Research by Martín-Suárez *et al* (2000) indicates that the Zorreras Member spans the Miocene-Pliocene boundary. It has been suggested by Mather (1991) that during the deposition of the Cariatiz Formation the Pliocene sea was in the south in the Carboneras/Almería Basin. A marine connection was maintained in the south of the Sorbas Basin by a restricted opening in the Sierra Alhamilla/Cabrera. The Cariatiz Formation contains three distinctive marker beds; two light coloured/white carbonate beds and one yellow bioturbated sandstone bed (Mather, 1991). The beds are

laterally extensive and can be traced easily over substantial parts of the central area of the Sorbas Basin. The carbonate marker beds were deposited in lacustrine conditions that developed across the basin reflecting the low gradient of the coastal plain. The lakes would have been unstratified, fairly shallow and probably connected to the open sea in the south (Mather, 1991). The top of the Cariatiz Formation is marked by a yellow basin-wide marine unit (Marine Band [Mather, 1991]) which is Pliocene in age (Ott d'Estevou, 1980). The fauna present in the Marine Band indicate that the basin was linked to more open marine conditions in the south and probably represents global sea level rise recorded at this time (Haq *et al.*, 1988).

The final stage of basin fill in the Sorbas Basin is the fully terrestrial Góchar formation. The Góchar Formation, a series of conglomeratic and sandstone deposits, represents the initiation of fluvial systems within the Sorbas Basin and is the ancestral drainage of the current Río Aguas drainage system (Mather, 1993a). Sedimentological, palaeocurrent and clast assemblage evidence has shown that the Góchar Formation was deposited by four systems (Figure 2.4 & 2.5); two feeder systems from the northern margin of the Sorbas Basin (Góchar and Marchalico systems), one from the South margin (Mocatán system) and a fourth axial drainage (Los Lobos system) which drained into the Carboneras basin to the south where it fed a small marine delta fan (Mather, 1991., Mather, 1993b., Mather & Stokes.,2001). These systems are described fully by Mather (1991; 1993) and Mather et al (2001).

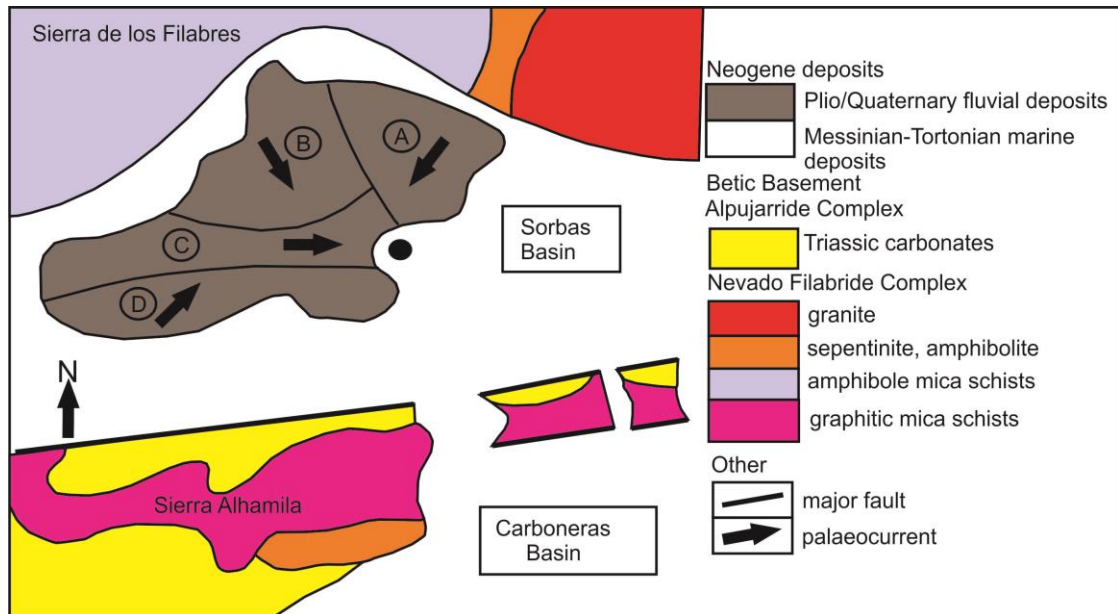


Figure 2.4: The main fluvial systems of the Plio Pleistocene (after Mather 1991) as preserved by the Góchar Formation within the Sorbas Basin; A) Marchalico system B) Góchar system C) Los Lobos system D) Mocatán system (modified after Mather, 1993a)



Figure 2.5: Early Plio/Pleistocene drainage system in the Sorbas Basin was in the form of alluvial fans and a main axial system which drained into the Carboneras basin in the South (modified after Mather & Stokes, 2001).

2.5 Fluvial system development

During the Late Pliocene/Early Pleistocene there was a switch from deposition to incision due to increasing uplift. The switch to incision led to the superimposition of secondary consequence drainage over the former Late Pliocene/Early Pleistocene basin topography. The Vera Basin became a receiver for drainage systems originating from outside the basin. There were three major fluvial systems developed; the Almanzora, Antas and Lower Aguas.

Chapter 2 Study area geology and geomorphology

In the Sorbas Basin the first incisional fluvial system to develop into the top basin fill was the Proto Aguas/ Feos (Harvey & Wells, 1987). This system consisted of a main drainage system that exited the basin to the south in a gap between the Sierra Alhamilla and the Sierra Cabrera. The Proto Aguas /Feos flowed into the main drainage of the Carboneras basin the Rio Alias which developed as a strike orientated drainage system (Harvey & Wells, 1987; Maher, 2005; Maher *et al.*, 2007; Maher & Harvey, 2008; Whitfield & Harvey, 2012).

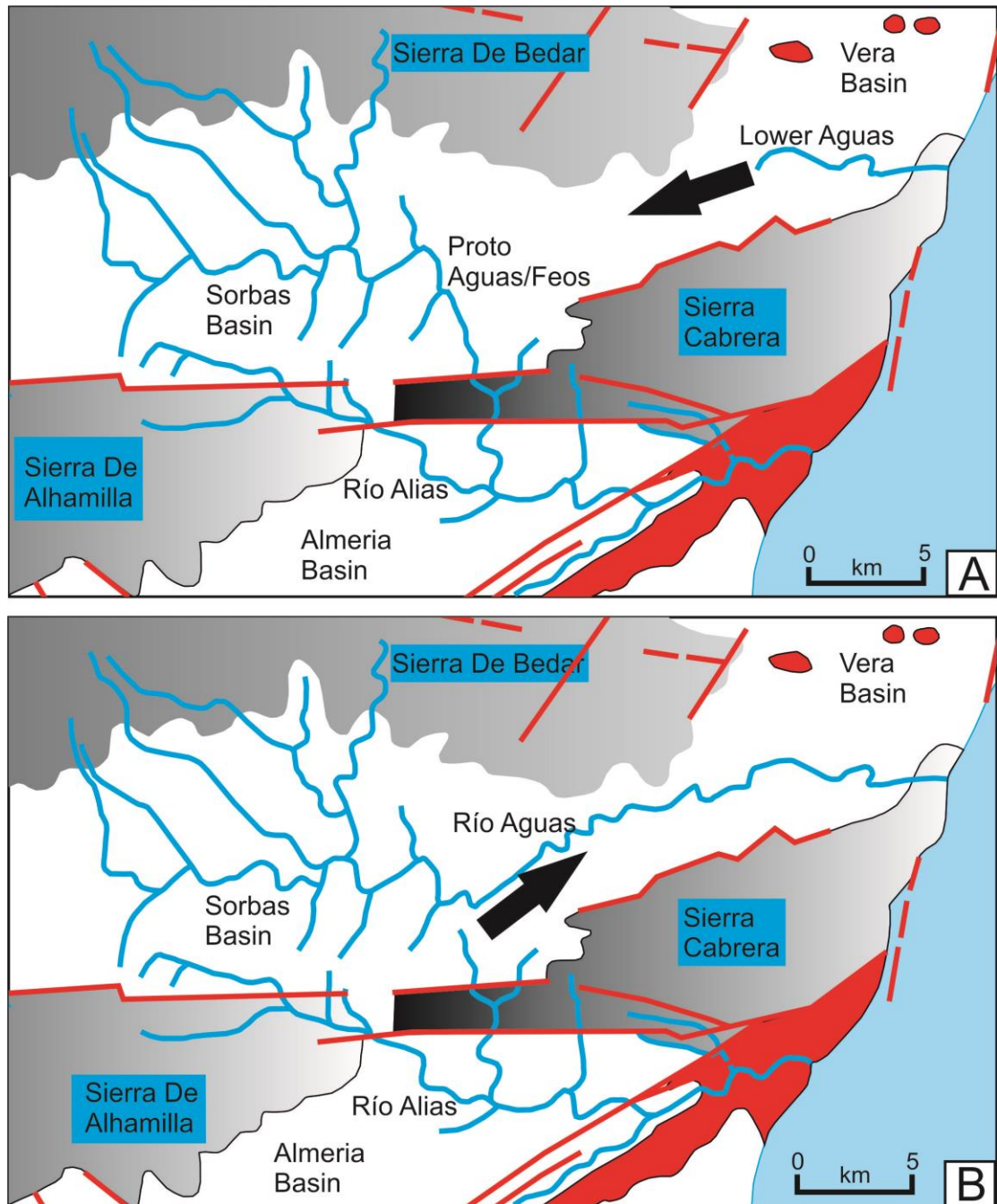


Figure 2.6: River capture event where the headwaters of the Proto Aguas/Feos were captured by the Lower Aguas (adapted from Harvey, 2007).

Differential uplift of the Betic Cordilleras continued into the Pleistocene leading to drainage rearrangement and river capture (Chapter 1). Interaction between the Vera, Sorbas and Carboneras drainage systems occurred when the Lower Aguas, a westerly headcutting strike orientated drainage system, captured the headwaters of the Proto Aguas/Foes rerouting 73% of the Sorbas Basin drainage away from the Río Alias and into the Vera Basin (Harvey & Wells, 1987; Mather, 1991; Mather, 1993a; Stokes &

Mather, 2003). This capture event is recorded in the terrace deposits aggraded by the Río Aguas. Differential uplift between the Sorbas and Vera Basins (80 M ma^{-1} for Sorbas, $11\text{-}21 \text{ M ma}^{-1}$ for Vera (Mather, 1991; Mather & Harvey, 1995; Stokes, 1997)) created a sharp gradient between the two basins allowing the Lower Aguas to erode headwards (Stokes, 2008). The local geology, a band of weak marls (Abad Member, Turre Formation), enabled the strike orientated Lower Aguas to erode aggressively headwards and capture the headwaters of the Proto Aguas/Feos. The diversion of the headwaters led to an increase in the catchment area by 225 km^2 (a 50% increase) rerouting 73% of the original Sorbas Basin drainage into the Vera Basin leaving the beheaded Rambla de los Feos with a modern drainage area of 50 km^2 (Mather, 2000; Stokes *et al.*, 2002). The capture event led to a 90 m base level drop at the capture site and created a wave of incision that propagated 20 Km upstream of the capture site. Incision into the top basin fill surface has occurred to a depth of 180 m near the centre of the Sorbas Basin and decreases upstream to a depth of 90 m at Sorbas town (Harvey *et al.*, 1995; Mather, 2000; Stokes *et al.*, 2002). Stokes *et al.* (2002) have calculated that at least 0.86 km^3 of sediments has been removed from the capture area with surface lowering accounting for 1.29 km^3 of sediment removed. The amount of incision within the Río Aguas catchment has increased since capture occurred with the average amount of incision in the Upper Aguas valley being 40 m pre capture and 59 m post capture (Stokes *et al.*, 2002). This indicates that there are higher rates of incision occurring post capture than occurred pre capture (Stokes *et al.*, 2002). The incision has destabilised the valley sides leading to landsliding with mass movement ranging in size from a few tens of m^3 to a few million m^3 (Hart & Griffiths, 1999; Hart, 2004) (e.g. Maleguica landslide, Sorbas town). The river capture related incision has also impacted on landscape development in numerous ways including karst formation, canyon development, badlands creation and scarplands (section 2.7).

2.6 Proto Aguas/Feos terrace stratigraphy

River terrace preserving fluvial sediments deposited by the Proto Aguas/feos system are present in the Sorbas Basin. The Proto Aguas-Feos deposited three major river terrace levels (named A [oldest]-C [youngest]) before the capture event diverted the headwaters of the fluvial system into the Lower Aguas river system. The fluvial terraces are inset into the top basin fill surface, the Góchar surface, formed by the topographic expression of the Góchar Formation. The river terraces can be traced from the Sorbas Basin through the Feos valley into the Almeria basin (Harvey & Wells, 1987) (Figure 2.6).

The terraces consist of stratified coarse clastic fluvial gravel sequences with sandstone lens. The deposits can be up to 20m in thickness with an average clast size of 10-20cm which often display imbrication. The terraces are capped by carbonate accumulating red soils, with well-developed Bt horizons, that are up to two metre thick. (Harvey *et al.*, 1995) The terraces are also typically capped by a pedogenic calcrete with cemented horizons and nodules growing within the sediments (See Chapter 4 for explanation of Munsell data and calcretes). Table 2.3 displays data relating to the age and the level of soil and calcrete development for the terrace deposits and it indicates that the level of soil and calcrete development is dependent on the age of the terrace deposit. The older terrace levels have more extensive soil and calcrete development with terrace A deposits contain type IV calcretes and soils with 2.5 YR hues. Soils with 2.5 YR hues also cap terrace B deposits which generally contain type III-IV calcretes. Terrace level C deposits contain less well developed soils and calcretes with type II-II calcretes presents (Harvey & Wells, 1987; Harvey *et al.*, 1995; Candy *et al.*, 2004; 2005). The soils which cap terrace C deposits normally display a hue of 5 YR (Harvey & Wells, 1987; Harvey *et al.*, 1995). Terrace D deposits contain the least well developed soils out of the Pleistocene deposits with type I-II calcretes and 7.5-10 YR hues in the soils. U-series

dating of the calcretes that form within the soils indicate that the terrace A sediments were deposited about 400 ka, the terrace B deposits around 300 ka and the terrace C deposits around 70-100 ka (Candy *et al.*, 2004; 2005).

Terrace	U-series	Soil	Calcrete development	Soil Hues
Góchar Surface	No date	Plio/Pleistocene	IV	2.5 yr
A	224-380 ka	700 ka-1.6 ma	IV	2.5 yr
B	145-207 ka	Mid Pleistocene	IV-III	2.5 yr
C	68-104 ka	> 100 ka	II-III	5 yr
D	9-31 ka	80 ka?	I-II	7.5 yr
E	2310±80/-90	n/a	0	10 yr

Table 2.3: Chronological, calcrete and soil data for the fluvial terraces present in the Sorbas Basin. U-series data from Candy et al (2004; 2005); Soil data from Harvey & Wells, 1987; Harvey *et al* (1995).

Figures 2.7 shows the geography of the Sorbas Basin and 2.8 show the extent of the terrace deposits that occur along the course of the Río Aguas. The five terrace levels can be traced from the upstream source streams to the wind gap just south of Los Molinos where they can then be traced along a transverse reach through a wind gap along which the Rambla de los Feos flows (Figure 2.8). The traceability and palaeoflow direction of the terraces along the path of the Rambla de los Feos indicates that the Proto Aguas/Feos used to exit the Sorbas Basin to the south into the Carboneras basin as opposed to its current exit point to the east (Harvey & Wells, 1987). The spacing between the terrace levels increases downstream and also increases rapidly between terrace levels C and D (Harvey, 2007).

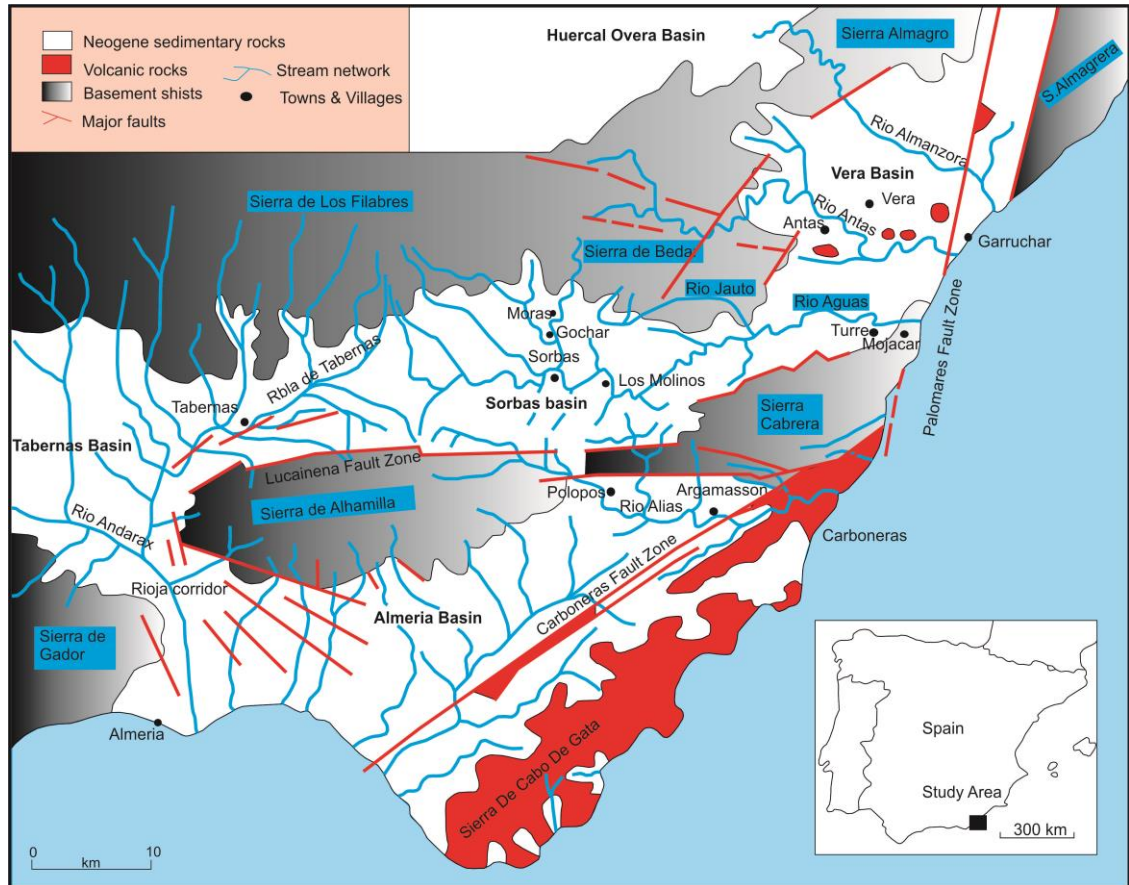


Figure 2.7: Location map showing the Sorbas Basin, the surrounding Neogene basins and the extent of the Rio Aguas catchment area (Harvey, 2007).

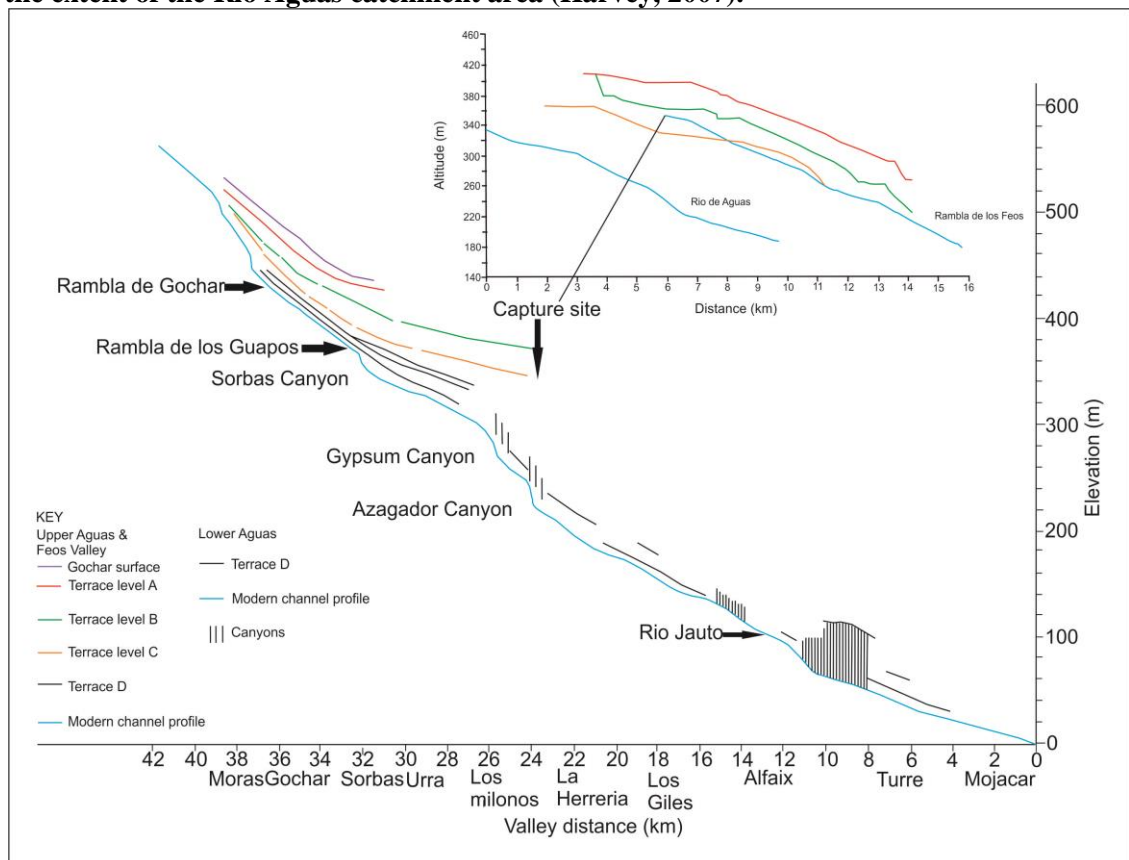


Figure 2.8 showing the full Aguas long profile down to Mojácar and the long profile of the Feos Valley with terraces A-C (Modified after Harvey, 2007).

2.7 Landscape development

The landscape of the Sorbas Basin is dominated by erosion with deposition restricted to valleys (river terraces) and mountain fronts (alluvial fans). The erosional landscape represents the regional tectonic uplift patterns, the local geology and the Quaternary climate. The main control on landscape development in the Sorbas Basin is base level lowering via river capture. Erosion in the Sorbas Basin is recorded by scarplands, canyons, badlands and gypsum karst.

2.7.1 Canyons

In areas where rapid vertical incision coincides with areas of more resistant rock, deep canyons and incised valleys have developed. Canyons occur in uplifted mountains where rivers have superimposed/antecedent transverse reaches. Examples of canyon formation in the Sorbas Basin occur in the Río Jauto (where the river crosses the Sierra de Bédar) (Figure 2.9 a&c). In the centre of the Sorbas Basin where more resistant rocks within the basin fill sequence outcrop canyons have also formed. Examples of canyons in the centre of the basin are where the Río Aguas and the Rambla de Sorbas cuts through the Azagador limestones or the Sorbas Member sandstones.

Incised valleys in the form of abandoned meander loops are also present in the Sorbas Basin (Harvey, 2001; 2007). The incised valleys and abandoned meander loops are present in the headwaters at Moras and around the area of Sorbas town. The town of Sorbas itself is built on a knoll isolated by an abandoned meander. There are also a number of abandoned meanders near Urra along the Barranco de Hueli (Harvey, 2001; 2007).

2.7.2 Badlands and deeply dissected landscapes

Badlands, areas of extensive gullying, form where rapid incision along occurs in the areas of outcrops of weaker rocks. Along with selective weathering and erosion of soft rock, incision in these areas produces deeply dissected erosional landscapes characterised by gullies and badlands (Calvo-Cases et al., 1991; Harvey, 2001; Mather, 2009). Many of the Neogene sedimentary basins in SE Spain contain examples of badlands with the badlands in Tabernas Basin being considered by some the most spectacular in Europe (Harvey, 2001).

In the Sorbas Basin, there are two main areas of badlands. The first area, located between Los Molinos and La Huelga, is named the Gypsum Escarpment badlands (Hart, 2009). The badlands in this area occur along a reach of the Río Aguas that cuts through the Yesares Member gypsum and have formed within the calcareous mudstones of the Abad Member. The badlands extend northwards to the village of Los Castaños and eastwards into the Vera Basin (Figure 2.9e).

The second area of badlands occurred in the Plio/Pleistocene sediments of the Barranco de Mocatán. The Mocatán badlands occur within mudstones, sands and silts of the Zorreras and Góchar Formations. In some places the Zorreras Member is highly erosive and susceptible to piping and other dissolution features forming badlands topography. The badlands areas surrounding Barranco de Mocatán have been studied by numerous researchers (Spivey, 1997; Alexander *et al.*, 1999; Faulkner *et al.*, 2000; 2003; Chilton *et al.*, 2008) who have investigated the geochemical and ecological aspects of badlands morphology and weathering. The processes operating in badlands areas reflect interactions between geological, topographic and climatic factors.

2.7.3 Scarplands

Scarplands form where erosion has coincided with alternating strong and weak rocks with the resistant bands forming ridges or escarpments. The main resistant lithologies that form scarps in the Sorbas Basin are limestones of the Azagador Member, reef limestones of the Cantera Member and gypsum of the Yesares Member.

Scarplands present on the southern margin of the Sorbas Basin are formed in the Azagador Member (limestone) and the Cantera Member (Martín & Braga, 2001). The reef limestones of the Cantera Member also form a ridge on the northern margin of the Sorbas Basin in the Cariatiz area. Yesares Member gypsum forms escarpments in the Los Molinos area and spread in a northern direction towards Los Castaños (Figure 2.9g).

2.7.4 Gypsum Plateau and Karst

The Yesares gypsum plateau, which constrains some exceptional examples of gypsum karst morphology, has been documented by Calaforra and Pulido-Bosch (1997; 2003). The Sorbas Basin has an area of 12 km² of gypsum karst which is ~120 m thick with selenitic gypsum intervals of up to 20 m (Calaforra & Pulido Bosch, 2003). The gypsum is interbedded with calcareous mudstones that strongly control the hydraulic flow through the gypsum and the karstification processes occurring. Karst features that are present in the Sorbas Basin gypsum plateau include solution and collapse dolines, karren landforms and interstratification karst (Figure 2.9 b&f).

There is only a small number of solution and collapse dolines in the Sorbas gypsum. The collapse dolines are created by the breakdown of gypsiferous material once layers of calcareous mudstones have been eroded away. This process has been described by

Calaforra & Pulido Bosch (1997) as a special phenomenon that occurs in the gypsum karst of Sorbas.

Karren landforms are widely present in the outcrop however; they are generally affected by the texture of gypsiferous material which is controlled by gypsum crystallography. The greatest gypsum solution is observed through the exfoliation planes and on the selenitic twins. Crystal faces are the least affected by solution processes (Calaforra & Pulido Bosch, 1997).

The most important karst feature present in the Yesares Member is the interstratification karst which has developed as a result of the presence of calcareous mudstone that is interbedded with the gypsum (Calaforra & Pulido Bosch, 2003). Cave passages have been observed to have developed along the interstratification planes (between the mudstones and the gypsum) and are related to the hydrological development of the gypsum aquifer (Calaforra & Pulido Bosch, 2003).

Calaforra & Pulido Bosch's (2003) paper proposed a model for gypsum karst evolution suggesting that during the initial stages of karst formation the Yesares Member acted as a multilayer aquifer under semi-confined conditions. During this period the gypsum would dissolve along fractures and any mudstone present would also dissolve to produce small proto conduits. As the piezometric level fell, erosion of the calcareous mudstone dominated as conditions changes from phreatic conditions to vadose conditions. This led to the development of the interstratifications karst (Calaforra & Pulido Bosch, 2003). In the area around the river capture site (near Los Molinos) the gypsum is underlain by mudstones leading to the formation of a prominent scarp slope escarpment undercut by distinctive badlands topography (Figure 2.9g).

2.8 Summary

River system development is controlled by underlying geology, the tectonic and structural setting of a region and climatic cycles. The aim of this chapter was to describe the geological setting of the Sorbas Basin including the tectonic and structural setting. The lithologies underlying the river valleys were described as they insert a local control over the course of the river systems. The impact of differential uplift on the fluvial systems has been described and the geomorphic consequences discussed. The chapter provides the tectonic background to uplift rates that will be further discussed in Chapter 8 as well as introducing the river terrace staircases. The river terrace deposits are described in more detail in Chapters 5 and 6. The next chapter (Chapter 3) presents the research methodology for this project.

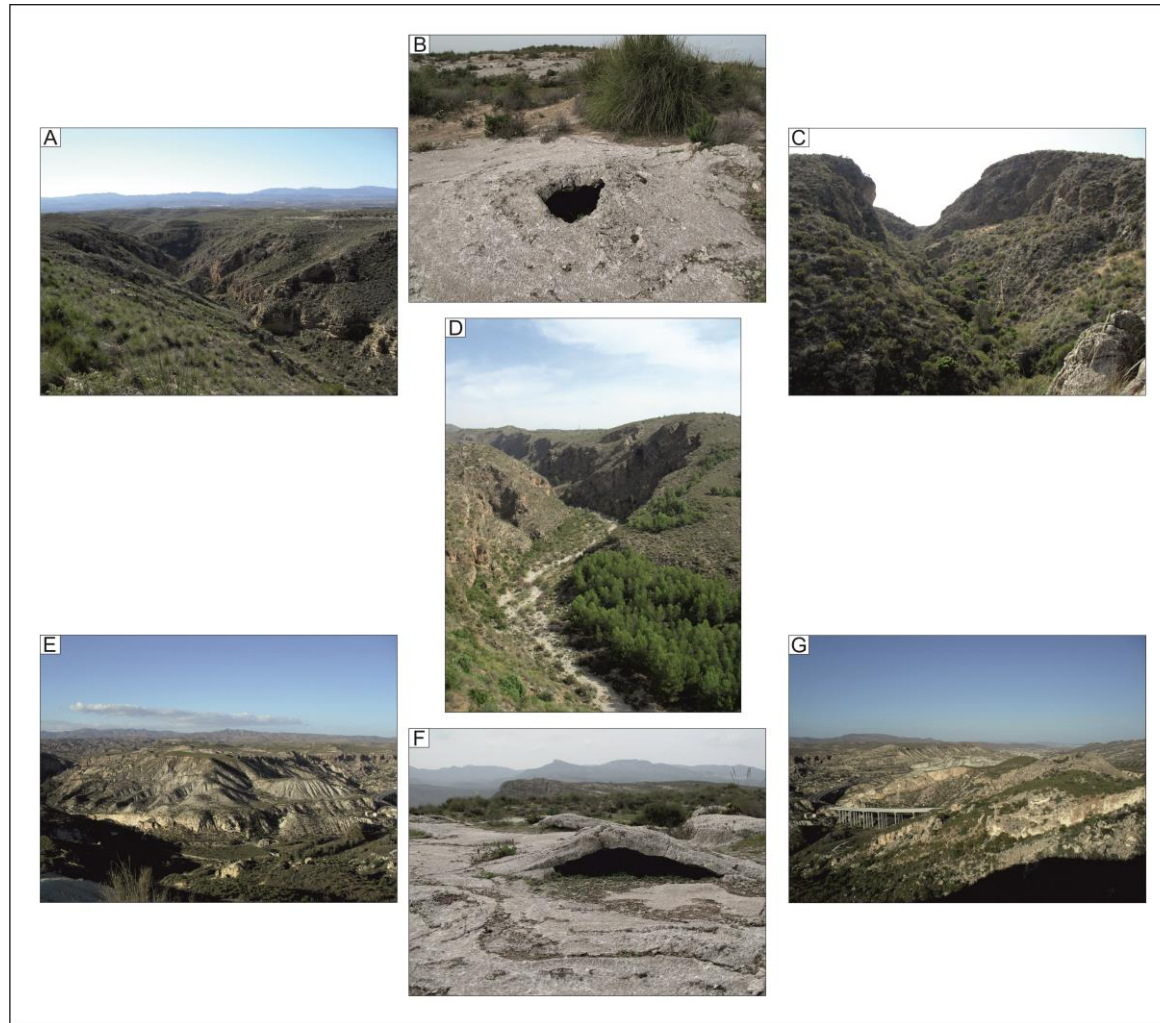


Figure 2.9: Landscape development features present in the Sorbas basin: A) Cariatiz Gorge, Río Jauto B) Karst features C) & D) Lower Gorge, Río Juato E) Badlands development, Los Molinos F) Karst features, Gypsum plateau G) Gypsum Plateau, Los Molinos.

Chapter 3: Research Methodology

3.1 Introduction

In order to investigate spatial and temporal long-term fluvial incision patterns within the Río Aguas and Jauto catchments in the Sorbas Basin, field, laboratory (cosmogenic exposure dating), sedimentological and morphological methodologies have been employed. A total of 18 weeks of field data collection was undertaken with two major field seasons in March 2009, March/ June 2010 and one final field season undertaken in February 2011. Sampling for cosmogenic dating was undertaken in March 2009 and March/ April 2010. Field data collected included stratigraphical and sedimentary data which has been described and interpreted using facies analysis which enabled depositional and environmental information for the sedimentary successions to be assembled. Palaeohydrological calculations have been applied to field data to estimate the magnitude of floods responsible for sediment transport and deposition during valley aggradation. These data were then grouped to produce localised palaeoenvironmental models for different temporal stages of fluvial system evolution. By testing the models using extrinsic variables a terrace staircase model was developed. Terrace height diagrams and valley cross sections have been constructed to enable quantification of incision amounts, rates and volumes of sediment removal in the system.

This chapter describes the philosophical and general approach to the data collection, analysis and interpretation. The chapter address methods used to achieve the following aims of this thesis introduced in Chapter 1:

- What impact did the wave of incision have on the stability of the catchment slopes? Is landsliding related to the wave of incision or later climatic events?

Chapter 3: Research Methodology

- Can a formal stratigraphy be constructed for the Río Jauto fluvial archive?
Can a relative stratigraphy be created for the Río Jauto using stratigraphic information and sedimentology data?
- Can a localised palaeoenvironmental model be created to represent the evolution of the Río Jauto fluvial system using depositional and environmental data collected in the field?
- Can the application of palaeohydrology equations on field data be used to identify the magnitude of flood events in the Sorbas Basin? Do the terrace deposits of the Río Jauto and Aguas show any variability? Is there a climatic link?

3.2 Philosophical approach

There are two types of philosophical approaches to geomorphic problems; inductive or deductive approaches (Trochim, 2006). An inductive approach involves hypothesis testing by creating a model and then collecting the data to prove or disprove the model. Deductive reasoning involves the collection and interpretation of data from which a research hypothesis is developed without any prior theories. An inductive approach could be potentially misleading and could lead to bias of data with important data missed due to its irrelevance to the selective hypothesis. Due to this potential problem this study has been undertaken using a deductive approach with field data collected and working hypotheses constructed and refined. This approach has been used successfully on other similar topics in SE Spain (e.g. Mather, 1991; Stokes, 1997; Meikle, 2009).

Chapter 3: Research Methodology

3.3 General approach

The initial approach to this project was to focus on a known entity in terms of fluvial terraces (the Río Aguas). There is an existing spatial and temporal framework developed for the Río Aguas (Harvey & Wells, 1987; Harvey *et al.*, 1995; Schulte, 2001) with absolute dates for the terrace system (Candy *et al.*, 2004 (a, b); Candy *et al.*, 2005; Schulte, 2001; Schulte *et al.*, 2008). Reconnaissance mapping and surveying using existing terrace maps were undertaken to ensure that the mapping of previous researchers (Harvey & Wells, 1987; Harvey, 1995; Harvey, 2007) was fit for purpose. A Garmin eTrex Legend HCx GPS was also used to record accurately (with a 10 m error) the edges of the terraces by recording x and y co-ordinates. The major aim of the mapping in the Río Aguas system was to locate terrace sites which were suitable for cosmogenic dating. Site selection for cosmogenic sampling needs to fulfil a series of special site specific criteria (man-made section, minimal/negligible erosion of terrace landforms etc.) which are outlined in Chapter 5. Once suitable sites were located samples for the profile technique were collected from six sites. Data were then analysed in terms of relationships with climate and tectonics.

The project then focused on a fluvial system that is relatively unknown in terms of its terrace record (the Río Jauto) with the specific aim of creating a terrace formation model for this system. The river terraces present in the Río Jauto catchment were mapped and classified on the basis of visual continuity creating a stratigraphic framework. The outcomes from the Jauto research were then compared to the Río Aguas system data to compare the development of the two systems. The data from the Sorbas basin was then compared against regional data for SE Spain to see whether there is a regional control on terrace formation.

Chapter 3: Research Methodology

3.4 Morphological mapping

Morphological mapping is used to locate, interpret and represent the landforms present in an area according to their morphology (Knight *et al.*, 2011). The maps record both the extent of the landforms and the material within the landforms. Morphological mapping involves two main stages; firstly to map the morphological features that are present in an area and secondly to interpret the mapped features with respect to their origin and spatial relationships (Knight *et al.*, 2011). Terraces can be mapped and classified on the basis of visual continuity. Terrace deposits were located in the field by looking for flat gravel surfaces that contain fluvial rounded quartz clasts often topped with red soils and pedogenic calcretes. The base of the terrace deposits is located by looking for the contact with the fluvial gravels and the underlying basement or basin fill geology. The edges of the terraces were located by looking for changes in the surface sediment (e.g. the discontinuation of quartz clasts and end of red soil discolouration) and also by looking for breaks/changes of slope. In the Jauto system, terrace deposits rarely have well developed soils and therefore terraces were located primarily by searching for gravel deposits, quartz clasts and changes in surface topography. River terraces are often relatively simple to map due to their distinctive sedimentology compared to the underlying bedrock geology but it can be more challenging to differentiate between different generations of terrace deposits (i.e. identify different terrace levels). The best way to distinguish between levels is to accurately measure the surface elevation of the terraces above the modern stream bed (Knight *et al.*, 2011). The terraces were mapped using 1:25,000 and 1:10,000 topographic base maps (see table 3.1 for details of maps used). A handheld GPS was used to map the edges of the terrace (see above) and the data was uploaded into ArcMap 10 to create digital maps.

Chapter 3: Research Methodology

Map District	Map name	Topographic sheet number	Source
Sorbas	Sorbas	1031-I	1.25,000- Instituto Geográfico Nacional
	Turre	1031-II	
	Polopos	1031-III	
Vera	Lubrín	1014-III	
Sorbas	Sorbas	1031	1:10,000 MOPU
Almeria	Almería-Gurrucha	84-85	IGME Mapa Geologico de España 1:250000

Table 3.1: List of maps used within the study published in 2002.

Once terrace deposits were located, their heights above the modern stream were recorded using a Lasertech TruPluse 360 laser measurement tool. The terrace heights were surveyed from the base of the modern stream-bed level to the base of the terrace gravel deposits. The base of the terrace deposits were defined by their contact with the underlying geology. This method enables the accuracy of the measurement to be increased because the error caused by erosion taking place on top of or burial of the terrace by slope material will be minimised. Since the terraces analysed in this study were dominated by strath forms, measurements to the base was possible in all instances. An average of three height readings were taken per terrace section to account for changes in the height downstream from the initial point of deposition and to allow for accurate plotting on height range diagrams. The terrace sediments were then examined and described. The sedimentological characteristics of the terraces were described enabling the sedimentary processes to be interpreted and therefore the fluvial palaeoenvironment during aggradation to be determined. The palaeoenvironmental information for different terrace levels was then used to reconstruct the development of the river system through time.

Within the Jauto catchment individual terrace deposits have been grouped and correlated according to sedimentary characteristics, terrace base heights and degree of soil development (section 3.7.1). A type section was then identified per terrace level

Chapter 3: Research Methodology

(*sensu* the American Stratigraphical Code (1983); Meikle *et al.*, 2010). This approach is normally adopted by geologists for geological sections (e.g. basin fill sequences); however, in this study it introduces increased scientific rigor when defining and using geomorphic criteria (Meikle *et al.*, 2010). Data from numerous sections for each terrace level is presented to demonstrate regional validity of correlations between terrace deposits. The characteristics of each terrace level (sedimentary details (section 3.5), clast assemblage (section 3.6.2), palaeocurrent indicators (section 3.6.4)) are recorded and used to infer the sedimentary processes and palaeoenvironment during aggradation.

For the cosmogenic sample sites in the Río Aguas, the above mapping methodology was followed to spatially locate the terrace deposits. Once mapping was complete the samples of quartz clasts were collected following the methodology presented in Chapter 4 for ease of reference.

3.5 Terrace height diagrams and valley cross sections

Terrace height-range diagrams and valley cross sections are used to express stratigraphic relationships and to quantify fluvial incision amounts and volumes of valley erosion by the incising fluvial system. They can also be used to identify knick points in fluvial systems. Terrace height diagrams were plotted using a longitudinal profile of the modern river channel and the heights of the base of the terrace deposits above the modern river channel. Along with the age control from the cosmogenic data these data can be used to produce a minimum rate of river incision and erosion.

In the Río Jauto catchment, where no absolute age data exists, this method can be used to produce a minimum rate of river incision and erosion based on estimated ages of the

Chapter 3: Research Methodology

terrace levels by correlation of soils developed on the terrace surfaces and their relationships to the adjacent Río Aguas system.

Valley cross sections have a two-fold purpose; they can be used to locate the position of terraces and they can be used to establish the relationship between the bedrock geology, its structure and the terrace landform. Valley cross sections were plotted from the 1:10,000 base maps and the geology was superimposed onto the cross sections to identify where the local valley shape could be influenced by local geology.

3.6 Sedimentary analysis

Sedimentary analysis of terrace deposits included general descriptions of clast size, clast type, sedimentary structures, palaeocurrent indicators, soil types and pedogenic calcretes formations were recorded. Sedimentary facies were then identified which were then grouped to allow for environmental interpretation.

3.6.1 Facies Analysis

Facies analysis involved the detailed description of a sedimentary rock unit which has followed by the interpretation of the depositional processes and environment of deposition. Facies are defined as “the sum total of all primary characteristics of a sedimentary rock from which the environment of deposition may be induced” (Walther, 1894). The original concept of facies in the stratigraphical sense was first introduced by Gressly (1838). Reading (2004, p.19) further defined a sedimentary facies as “a distinctive rock that formed under certain conditions of sedimentation, reflecting a particular process, set of conditions or environment, colour, bedding composition,

Chapter 3: Research Methodology

texture, fossils and sedimentary structures can all be used to distinguish one facies from another.”. This study involves the researching of fluvial terraces which contain little or no biological material and therefore lithofacies (where emphasis is placed on the characteristics of rocks) are applied (Reading, 2004).

Individual facies can then be grouped together into facies associations. Facies associations are defined as “comprising sediments, generally deposited in the same broad environment in which there are several different depositional processes operating distinct sub-environments or fluctuations in depositional conditions” Tucker (1996).

Miall’s (1996) lithofacies code system has been applied for the conglomeratic deposits of the Ríos Aguas and Jauto fluvial systems (Table 3.2) (Mather, 1991; Stokes, 1997; Meikle, 2009). The lithofacies code is used as a descriptor in facies analysis and not as a direct interpretation of the environment of deposition in isolation.

Chapter 3: Research Methodology

Code	Lithofacies	Sedimentary structure
Gms	Gravel boulder conglomerates, poorly sorted, matrix supported	Generally none, occasional weak clast imbrication & vertical orientation of clasts
Gm	Gravel-cobble conglomerate, moderately sorted, clast supported	Massive/weakly bedded, weak clast imbrication
Gh	Gravel-pebble conglomerate, well sorted, clast supported	Horizontal bedding, well imbricated
Gl	Gravel-pebble conglomerate, well sorted, clast supported	Low angle cross bedding
Gt	Gravel conglomerate, well sorted, clast supported	Trough cross bedding
Gp	Gravel conglomerate, well sorted, clast supported	Planar cross beds
Sl	Sand, moderate/well sorted, fine-coarse	Massive
Sp	Sand, moderate/well sorted, fine-coarse	Horizontal lamination
Sm	Sand, moderate/well sorted, very fine to very coarse, sometimes pebbly	Low angle cross bedding
Sh	Sand, moderate/well sorted, medium to coarse, sometimes pebbly	Planar cross beds
Fm	Silt-mud	Massive

Table 3.2: Table which summaries the lithofacies codes, textural and sedimentary characteristics (Miall, 1996) that have been used during this study (modified from Stokes, 1997).

3.6.2 Clast counts

Clast counts can be used to provide a range of sedimentary information such as lithological content of rudaceous components and average clast size. The clast content of a terrace can sometimes be used to determine the provenance of a terrace deposit and then therefore be used to reconstruct the palaeo drainage/ palaeo-environment of a

Chapter 3: Research Methodology

fluvial system (Collins *et al.*, 1998). This method has been successfully used in SE Spain region by several researchers (Harvey & Wells, 1987; Mather, 1991, 1993a, 2000; Stokes, 1997; Stokes & Mather, 2003; Maher, 2006; Meikle, 2009) to trace the provenance of terraces due to the distinct and diverse lithological variations within the basements nappes along with their well known distributions (Chapter 2). A problem with clast provenance data is whether the clasts have been reworked from previous deposits. Clast size can be used to distinguish between first and second cycle conglomerates. Clast size also provides important information about source areas. The size of a clast is depended on lithology, breakdown and distance from the source area. Clast counts followed a method of the clast counting techniques outlined in Bridgland (1986).

Where a clast count was undertaken a set amount of clasts (300) per terrace section, of greater than 2 cm were collected, counted and measured. Clasts of smaller than 2 cm were not counted as smaller clast sizes made lithological identification in the field difficult. For terrace deposits which were highly cemented, such as the level 2 deposits of the Río Jauto system, 100 clasts were counted following the methods of Mather (1991) and Stokes (1997). The size and lithology of the clasts were recorded (see above). To prevent recounting of a clast chalk was used to mark the recorded clasts. Clasts that could be linked to a specific source area were grouped together into an assemblage. Any clast which could not be assigned a specific source area due to the widespread nature of the lithology type, such as quartz, was grouped separately according to lithology.

In the Jauto system; clast counts were undertaken on all terrace sections. This provided greater understanding of the geomorphic context of the terrace deposits. For the Aguas

Chapter 3: Research Methodology

terraces it also permits checking for any mixing and/or faulting of the terrace deposit that would make the section unsuitable for cosmogenic dating.

3.6.3 Logs and sketches

Vertical sedimentary logging took place in the field with logs drawn in a field notebook and measured using a tape measure. Vertical logging of sections along with sketches illustrates the vertical and lateral relationships within terrace sequences. The vertical and horizontal distances of all sections from their base were recorded using a Truepulse 360 laser range finder. Digitisation of the logs and field sketches was undertaken using CoralDraw X5 software using the standard symbols in Figure 3.1. The logs were used to record the composition and texture of the terrace deposit along with the sedimentary structures and the bed geometry. Sediment grain size was measured using a grainsize comparator and described using the Udden-Wentworth scale. The sedimentology in each section was analysed using facies association using the method featured in section 3.6.1.

- **Composition:** constitute clasts which compose a terrace.
- **Colour:** Primary and secondary colours are described. Primary colour refers to the original colour of the sediment upon deposition; Secondary colour is produced by weathering, during pedogenesis or by secondary mineral enrichment processes. Soil colours are recorded by the standard notation from a Munsell soil colour chart (hue/colour/chroma) and any calcrete present are described using the classification of Machette (1985) (Section 3.7.1).
- **Textural characteristics:** Refers to the size, shape and arrangement of the clasts including roundness and sorting. Sorting refers to the packing of the grains and

Chapter 3: Research Methodology

size of the grains with descriptions ranging from poorly sorted to well sorted.

The roundness of the clasts relates to the shape of the grains and is described as either angular or round with a series of sub categories in between (Jones, 1999).

- Sedimentary structures: Identified from differences in textural characteristics with commonly observed structures being stratification and biogenic structures.
- Bed thickness and maximum clast size: Bed thickness is an important factor for representing the flow depth of flood events with thick beds possibly reflecting larger magnitude events whilst thin beds reflect common background sedimentation. For the maximum clast size; the averages of the long axis of the ten largest clasts are measured. This can give an idea of the discharge of the flood events responsible for the deposition of the sediment.
- Geometry of sedimentary bodies: The geometry of sedimentary bodies helps to define the river plan form type. Sedimentary bodies include ribbons, sheets, fingers or lenses (Friend *et al.*, 1979).

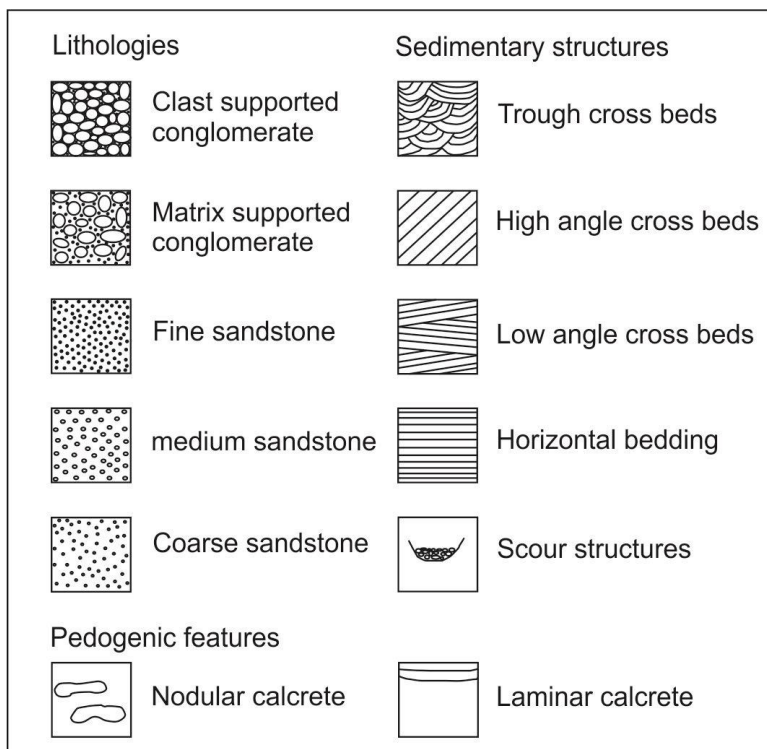


Figure 3.1: Symbols used in the logging of sediments in the Río Aguas and Jauto catchments adapted from Stokes (1997).

Chapter 3: Research Methodology

In the Aguas system, only terraces which were sampled for cosmogenic dating were logged and sketched to allow for a detailed understanding of the geomorphic context. All terrace gravel exposures located in the Jauto were logged and sketched in order to create a detailed sedimentary picture of the Jauto system. This would enable a palaeoenvironmental model of the evolution of individual terrace deposits.

3.6.4 Palaeocurrent analysis

The palaeoflow direction of the terrace deposits can be determined by analysis of cross-stratification and clast imbrication. Palaeocurrent analysis enables the sediment transport direction to be established during flood events. Palaeocurrent analysis involves measuring imbricated clasts within the terrace units which were located during logging and sketching of the deposit. More than 25 clasts were collected to provide a statistical viable sample and the A axis were measured using a compass clinometer. Selected clasts were greater than 4 cm in size. Larger clasts provide an accurate picture of channel direction at times of higher flow stages when the whole channel is utilised by the water flow (Tucker, 2003). Collected data were plotted onto rose diagrams as unidirectional data and displayed against graphic logs drawn using the CorelDraw programme to enable spatial and temporal patterns of palaeocurrents to be established.

3.6.5 Palaeohydrological Analysis

Palaeohydrological reconstruction is the science of reconstructing flood events in the geological past using techniques that have no involved direct measurement or observation of the flood event (Stokes *et al.*, 2012b). The techniques involves applying physical mathematical principles to terrace deposits in order to calculate past water

Chapter 3: Research Methodology

flows and associated sedimentary transport (Baker, 2008). In this study palaeohydrological reconstruction methods have been applied to suitable terrace sediments in both the Río Aguas and Jauto catchments.

Palaeohydrological studies have rarely been undertaken on fluvial terraces (although example studies can be found in the following papers; Leopold & Millar, 1954, Baker 1974, Dawson & Gardiner, 1987, Benito *et al.*, 2010 and Stokes *et al.*, 2012b) possibly due to difficulties in locating suitable sites. In order to reconstruct the magnitude of flood events that were responsible for the transport and deposition of sediment during valley floor aggradation a number of criteria must be fulfilled (Stokes *et al.*, 2012b). Firstly, sediments deposited by flood events must be clearly identifiable within the terrace deposit. In order to fulfil the first criterion, good preservation of terrace sediments is vital so that sedimentological and geomorphological features can be identified. An understanding of the age of the deposits is also important because this allows the timing of the aggradation of the terrace to be discussed in terms of climatic cycles (for example high magnitude floods being linked to known periods of high precipitation). Lastly, an understanding of the magnitude of floods occurring in a system is useful to place the palaeohydrological reconstruction results in context, to see if past events were smaller or larger than monitored events, although this is not always possible due to lack of records.

There are two main methods of palaeohydrological reconstruction: one based on flow competence and the other on flow regime theory. The flow competence method is based on Clark (1996) and Costa (1983) and involves estimating the flood flow velocity needed to entrain the maximum clast size observed, typically using boulders. The flow regime theory is based on the reconstruction of hydraulic geometry of the palaeo-channel/valley in which sediment aggradation was occurring. In this study the method

Chapter 3: Research Methodology

of flow competence has been applied. The flow competence method involves identifying the largest clast (typically a boulder) within a terrace outcrop. The triaxial dimensions of the boulder are then measured and inputted into the equation described in Table 3.3. Other data input parameters include the relict channel width, channel slope, a channel roughness value and the lithology of the measured clast. The slope of the channel has been measured using the dip of the base of the terrace deposit. The relict channel width is estimated by measuring from the edge of the terrace deposit furthest from the channel to the corresponding edge of the terrace on the opposite side of the stream or to the opposite valley side if in a confined valley. All channel width measurements were taken using the TruPulse. Valley widths were also checked against a review of abandoned meanders, several of which can both found in both the Aguas and Jauto systems for different terrace levels (Harvey, 2007).

An issue with using the largest boulder present in a terrace deposit to determine flood events is firstly proving that the boulders are not in situ (i.e. an outcrop of local rock) and secondly that the boulder have not been deposited in the deposit by mass movement processes (Stokes *et al.*, 2012b). In order to solve these problems only boulders that display evidence of having been transported by fluvial processes are measured. This means that only boulders that have rounded edges, rather than sharp corners and are clearly within the terrace deposit are selected for sampling. Where possible a boulder that was not made of immediately local geology was used for measurement purposes. Such a boulder will clearly have been transported in order to be deposited in the terrace deposit and is not a local geological outcrop. The axis measurements of the boulders might also be underestimated because the boulders are embedded within the outcrop meaning that one axis of the boulder is not fully exposed.

Chapter 3: Research Methodology

Other problems with applying this method to terrace deposits include whether the boulder selected was the biggest clast that could have been moved by the flow or was the biggest available clast to be moved (Mather & Hartley, 2005). If it was the biggest available clast to be moved, the method could be underestimating the size of the floods that occurred.

3.7 Dating fluvial terraces

The difficulties of dating river terraces in a terrace staircase are well documented (Bridgland & Maddy, 2002). These difficulties relate to the lack of datable material within the terrace sediments and also due to the ages of the landforms being beyond the maximum age limit of the most suitable absolute dating techniques. Table 3.4 provides a summary of the different dating techniques that have been applied to fluvial terraces in South East Spain and lists the problems associated with that technique. Two of the main, most regularly used, techniques are U-series dating and OSL dating (Candy *et al.*, 2004a, b; 2005; Maher, 2004; Meikle, 2009). However, the limitations of applying U-series and OSL dating to the deposits in south east Spain mean that the U-series/ OSL dating provide a minimum age for older deposits that are > 150 ka. Ages produced by the OSL method may also be underestimating the ages of the deposit due to bleaching although OSL dating does date the sediments themselves and therefore provides a better context for when the sediments were aggrading. U series dating provides a minimum age estimate for the deposit as the method is undertaken on calcretes in the terraces which develop once the soil is stable. There is believed to be a time lag of at least 1,000 years for stage II calcretes with mature calcretes believed to develop over a much longer timescale (Candy *et al.*, 2005).

Chapter 3: Research Methodology

Property	Formula	Example calculation
A – boulder major axis (m) B – boulder major axis (m) C – boulder major axis (m) σ – boulder’s density (kg/m ³) w – channel width (m) β – bed slope angle (radians/degrees)	Basic concepts: ρ – fluid density = 1,150 kg/m ³ μ – coefficient of sliding for a cubic boulder = 0.675 μ – coefficient of sliding for a round boulder = 0.225 g – acceleration due to gravity (9.81 m/s ²)	A = 0.5m B = 1.0m C = 0.75m σ = 2,700 kg/m ³ β = 0.052 radians (3 degrees) w = 10m
Nominal diameter of boulder (D)	$D = (A B C)^{0.33}$	$D = (A \times B \times C)^{0.33} = 0.721\text{m}$
Mass of a cubic boulder (M _B)	$M_B = \sigma D^3$	$M_B = 1,013\text{kg}$
Mass of a spherical boulder (M _B)	$M_B = \sigma [(\pi/6) D^3]$	$M_B = 530\text{kg}$
Resisting force in Newtons (F _R)	$F_R = M_B [(\sigma - \rho)/\sigma] g \{ [\cos \beta] \mu - [\sin \beta] \}$	$F_R = 3545$ for a cubic boulder $F_R = 515$ for a round boulder
The critical force is the minimum force that can be applied to the boulder in the direction of stream flow that will initiate movement (F _C)	Set $F_C = F_R$ (i.e. the critical force is assumed to be equal to the resisting force)	
The drag force is dependent on the flow conditions and the shape of the boulder (F _D). Its and is a function of the lift (C _L) and drag (C _D) coefficients of the boulder	$F_D = (C_D F_C)/(C_L + C_D)$ C _L = 0.178 for the cubic boulder and 0.20 for the round boulder C _D = 1.18 for the cubic boulder and 0.20 for the round boulder	$F_D = 3081$ Newtons for the cubic boulder and 257 Newtons for the round boulder
The critical velocity (V _C) is equivalent to the competent bottom velocity at a height of about 1/3 of a particle diameter above the bed at the condition of incipient movement (m/s)	$V_C = \{2[(F_D / C_D)/\rho] / A_B\}^{0.5}$ A _B = cross sectional area of the boulder	A _B = 0.52m ² for a cubic boulder and 0.408m ² for a round boulder V _C = 2.95m/s for a cubic boulder and 2.34m/s for a round boulder The average V _C = 2.65m/s for both forms
The average velocity of stream flow, V _{avg} , is 1.2 x V _C (Costa, 1983)	$V_{avg} = 1.2 V_C$	$V_C = 3.18\text{m/s}$
Mannings roughness coefficient, ‘n’, as a function of channel slope (in degrees)	$n = 0.295 (\tan \beta)^{0.377}$	n = 0.0971
Mean flow depth: for channel flows with high width to depth ratio hydraulic radius is approximately equal to mean flow depth, i.e. d = R (m), and Manning’s equation can be used to calculate mean flow depth	$d = \{[(V_{avg} n) / (\tan \beta)^{0.5}]^{0.5}\}^3$	d = 1.56m
Discharge, Q (m ³ /s)	$Q = w d V_{avg}$,	$Q = (20 \times 2.99 \times 4.98) = 50 \text{ m}^3/\text{s}$

Table 3.3: Table showing the calculation method for flood flow estimation based on maximum boulder size method of Clark (1996). The example calculation uses data from the terrace level C of the Río Aguas catchment.

Chapter 3: Research Methodology

Dating Method	Study	Optimum Timescale	Problems with applying technique to fluvial terraces
OSL	Maher, 2004; Mickle, 2008; Candy <i>et al.</i> , 2005	~90 ka	Bleaching of grains, dosage rate
U-series	Candy <i>et al.</i> , 2004; 2005	~90 ka	Contamination, diagenetic issues
Radiocarbon	Harvey & Wells, 1987	~50 ka	Limited organic material for dating due to dryland setting
Cosmogenic	This study	>1 ma	Inheritance

Table 3.4: A summary of the dating methods which have been applied to the fluvial terraces in south east Spain and the associated problems with applying the methods to terrace deposits.

3.7.1 Soil profiles & pedogenic calcretes

Soils on river terraces can be used to provide information on the fluvial systems as relative age indicators, and indirectly climate (Harvey *et al.*, 1995; Candy *et al.*, 2005), for a number of reasons. Firstly, the similarity of the origin of the terraces over a large area means that the method of soil development should be similar on all the terrace surfaces. This is based on the assumption that terrace incision and isolation within the landscape occurs at more or less the same time. This may not apply to landscapes where time transgressive incision is taking place due to a wave of incision and isolation of the individual terraces may have occurred at different times. Second, the geomorphic expression of the terraces allowed for quick soil development with little inheritance of former soils and thirdly once the terrace surfaces have been abandoned they are isolated from further deposition resulting in simple age related soil profile development (Harvey *et al.*, 1995).

For terrace deposits in the Aguas, Munsell readings and soil development measurements were taken from deposits which have been sampled for cosmogenic dating whereas in the Jauto Munsell readings were taken where soils were present. The colour of a soil can be used as a quantitative measure of the amount of pedogenic change that has taken

Chapter 3: Research Methodology

place in the parent material. Soil redness (rubification) has been identified as increasing with age and can be used as a relative age indicator (Harvey *et al.*, 1995 & references therein). Soil redness results from the oxidation of iron present in the soil. The stronger the reddening of the soils, the longer the soil has had to developed into a mature soil (Yaalon, 1997). Rubification of soils may therefore be used to relatively date soils in a similar way that calcretes are used (Harvey *et al.*, 1995; Yaalon, 1997). The redness rating index (after Harvey *et al.*, 1995) can be used to express the redness of the soil numerically. The redness rating can be calculated by multiplying the hue by the chroma divided by the value of the soil (Birkeland, 1999).

Redness rating=Hue X Chroma/Value

Where the hue of the soil is the dominating wave length range (colour), the chroma is the relative purity, intensity and strength of the hue and the value is the relative lightness of the colour as measured by the munsell colour chart. The hue is converted to a numerical value following the method of Hurst (1977) by adding the fraction 10-hue to the front of the equation however the 10 yr value is going to be represented by a value of 1 to increase the sensitivity of the lower end values (after Harvey *et al.*, 1995).

Pedogenic calcretes are the terrestrial accumulations of calcium carbonate that occur in a variety of forms from powdery, nodular, laminated to hardpans. The calcretes form in areas where the vadose and shallow phreatic ground water becomes saturated with respect to CaCO₃ (Wright & Tucker, 1991). Forming near the land surface the calcretes develop within the soil profile in several discrete horizons as sub profiles to the main soil (Wright & Tucker, 1991). The morphological forms of calcretes in the deposits are clearly controlled by time with thicker more complex forms of calcrete present on older surfaces (Alonso-Zarza, 2003). Calcretes are widespread in semi-arid to arid environments (Wright & Tucker, 1991). In the Río Aguas system it has been noted by

Chapter 3: Research Methodology

several researches that the stage of calcretes present in a terrace level is dependent on the age of the terrace; with calcretes only beginning to form once the terrace surface has been abandoned and is stable (Candy *et al.*, 2004; 2005). Terrace A (the oldest level in the Aguas system) has the greatest level of calcrete development and terrace D (the youngest) has the lowest level present. The presence of hardpan calcretes (Machette stage IV and above) on the terrace surface are a key feature that were used for the cosmogenic dating because hardpan calcretes indicate that no significant erosion has taken place. The level of calcrete development in each terrace section was recorded and categorised following the Machette (1985) scheme which is based on the morphology of the calcretes (Table 3.5). The morphological scheme recognises six stages of calcrete development with thin clast coatings representing the early stages and thick laminar calcretes the later stages.

Soils developed in gravels		
Stage	Diagnostic features	CaCO₃ distribution
I	Thin discontinuous coatings on pebbles	sparse
II	Continuous thin to thick coatings on pebbles	common coatings
III	Accumulations around clasts	continuous in matrix
IV	Thin to thick laminae capping hard pan	cemented, platy to tabular structure
V	Thick laminae	Indurated, dense, strong, platy to tabular, 1-2 cm thick
VI	Complex fabric of multiple generations of calcretes	Indurated, dense, strong, platy to tabular, >2 cm thick

Table 3.5: Classification of pedogenic calcretes based on the stages of morphological development (After Machette, 1985). This scheme was used to record the degree of calcrete development present in fluvial deposits.

Chapter 3: Research Methodology

3.7.2 Cosmogenic dating

Cosmogenic dating involves measuring the concentration of cosmogenic nuclides which are produced when cosmic rays generated by super nova explosions and stars impact with atoms knocking off particles. The resulting particles are cosmogenic nuclides which build up over time. By measuring the concentration of the nuclides within a sample, the age of the deposits can be calculated. Cosmogenic exposure dating can be used to calculate time at which the surface of a landform became exposed to the cosmic rays by sampling the surface. However, a terrace is made up of lots of individual clasts which have undergone multiple periods of transportation and burial and therefore exposure to cosmic rays, within the fluvial system leading to a build-up of residual nuclide content (inheritance). Inheritance is one of the major problems with cosmogenic dating, creating big uncertainties within the data. To overcome this problem, this study has applied the concentration profile method to the terraces to attempt to produce an age for the older landforms (Chapter 4). One advantage that cosmogenic dating has over other absolute dating methodologies is that it covers a longer time range of over 1 ma (Dunai, 2010) allowing more accurate dating of older fluvial landforms. It also provides some insight into the erosion rates in a basin. Cosmogenic exposure dating and the sampling strategies applied for this method are covered more fully in Chapter 4.

Chapter 4: Cosmogenic exposure dating methodology

4.1 Introduction

For this project in situ cosmogenic exposure dating utilising Beryllium 10 (^{10}Be) and Aluminium 26 (^{26}Al) has been applied to fluvial terraces in the Río Aguas system.

Cosmogenic dating was applied to selected terrace levels (B&C) and the top basin fill surface (the surface of the Góchar Formation) in the Sorbas Basin. Cosmogenic exposure dating has also been applied to a landslide using Chlorine 36 (^{36}Cl) dating and to a fluvial erosion surface in the Jauto catchment using Neon 21 (^{21}Ne).

Cosmogenic dating is being used to address three main points:

- 1) ^{10}Be and ^{26}Al have been used via the profile methodology to date the surfaces of fluvial terraces to address the timing of incision events. Burial dating has been applied to constrain the timing of aggradation events. The cosmogenic method can also provide more accurate dates for the older fluvial surfaces related to the Aguas system due to the extended age range of the technique.
- 2) By dating the stratigraphically older surfaces in both the Jauto and Aguas systems the timing of the switch from deposition to incision can be determined. Timing of the Jauto incision would also provide the start of a chronological framework for the Jauto system which has not yet been dated by absolute methods.
- 3) Landslides in the Aguas system have been dated to test whether they are related to the incision wave created by the capture event (chapter 5) or whether they can be linked to climatic events (e.g. Wetter phases).

Chapter 4: Cosmogenic exposure dating methodology

This chapter discusses the theoretical background of cosmogenic dating, the field sampling methodology, chemical preparation and calculation methodology for the individual isotopes used. The sample sites are also described.

4.2 Cosmogenic exposure dating

Cosmogenic dating involves measuring the concentration of cosmogenic nuclides present within a landform (Dunai, 2010). Cosmogenic nuclides are produced by cosmic rays impacting on target minerals in the landform. The rays are sourced from the sun and also from super novas that are located both within and beyond the Milky Way. Super nova explosions, which are the final stage in star evolution, are considered to be the main source for cosmic rays (Friedlander, 1989). Very high energy particles (up to 10^{20} eV) are thought to originate from outside our galaxy (Gosse & Phillips, 2001). The rays consist of high energy particles (mostly protons) which interact with the nuclei of atoms in the Earth's atmosphere. This interaction between atoms produces a secondary flux of radiation which cascades through the atmosphere via a series of spallation reactions to the Earth's surface (Figure 4.1). When the particles of the secondary flux impact rocks on the Earth's surface they interact with atoms of target element in the rocks and spallation reactions produce isotopes (Watchman & Twidale, 2002).

Spallation reactions occur when a high energy cosmic ray particle hits the nucleus of a target element and causes the target element to shatter, leading to the loss of smaller particles from the nucleus. The process of spallation continues in the target nucleus until energy dissipation leads to a fall in energy below the binding energy of the particles which make up the nucleus. The production of cosmogenic nuclides decreases with depth as attenuation of the cosmic rays occurs and ceases altogether at around 3 m below the earth's surface (Gosse & Phillips, 2001).

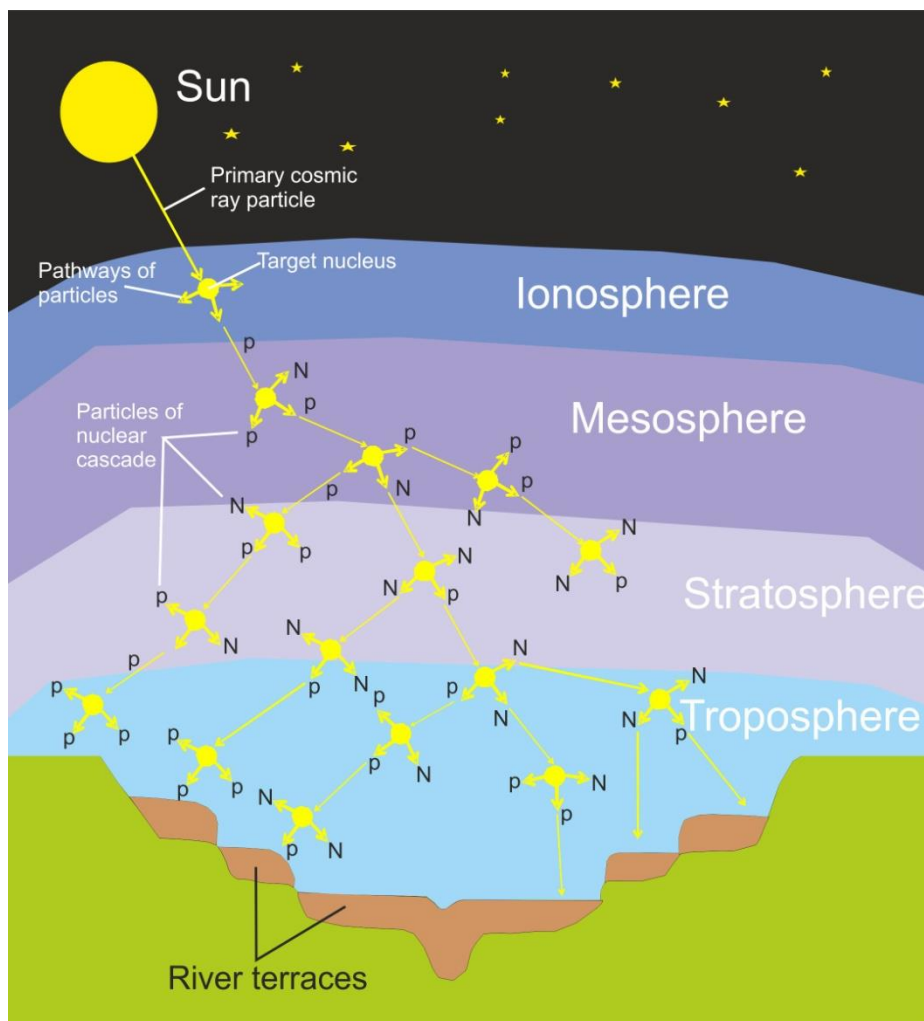


Figure 4.1: Cosmic ray travel through the earth’s atmosphere via spallation reactions to the earth’s surface where they impact on target minerals to produce cosmogenic nuclides. Green represents the surface of the earth and river terraces are shown in brown.

Any cosmogenic isotopes produced in the rock are known as ‘*in situ*’ cosmogenic isotopes whereas those isotopes produced in the atmosphere are referred to as ‘*meteoric*’ cosmogenic isotopes. Cosmogenic isotopes produced in the earth’s atmosphere rain down onto the earth’s surface and this meteoric flux needs to be taken into account during chemical preparation and/ or calculation of the cosmogenic exposure age of a landform. Some elements are created in higher quantities than others in the atmosphere and therefore calculations need to be adjusted accordingly (Watchman & Twidale, 2002). There are six cosmogenic isotopes (^3He , ^{10}Be , ^{14}C , ^{21}Ne , ^{26}Al , ^{36}Cl) which are now becoming routinely used in cosmogenic exposure dating that can be applied to a wide range of applications (see Table 4.1). Stable isotopes (^3He and ^{21}Ne) are produced

Chapter 4: Cosmogenic exposure dating methodology

constantly over time, assuming that the production rate is constant, and therefore have no theoretical upper age limit. However, cosmogenic radionuclides (^{10}Be , ^{14}C , ^{26}Al & ^{36}Cl) start to decay as soon as they are produced and can only be used to date landforms that are within the time span of 2-3 times the half-life of the cosmogenic radionuclide applied. Chlorine 36 (^{36}Cl) has been used to date the exposed backscar of the Maleguica landslide as it is formed from limestone which contains the target mineral calcite. The erosion surfaces in the Jauto fluvial system that have been sampled are formed in metamorphic rocks and have been dated with Neon 21 (^{21}Ne). Neon 21 is used to date the erosion surface as the age of the surface is unknown and therefore it may not be within the datable range of ^{10}Be . The isotopes that have been applied to fluvial terraces in this study are ^{10}Be ($t_{1/2}=1.36$ my) and ^{26}Al ($t_{1/2}=0.705$ my). ^{10}Be is used because it has the longest half-life of the cosmogenic nuclides and therefore can be used to date the older parts of the river terrace sequence, some of which could be early-middle Pleistocene.

Isotope	Half-life (yrs)	Target Mineral	Example of application	Source
^3He	stable	olivine, pyroxene, hornblende, garnet	Volcanic landform formation	Anthony, E.Y & Poths, J. 1992
^{10}Be	1.51×10^6	quartz, olivine	Fluvial terraces	Repka <i>et al.</i> , 1997
^{14}C	5.73×10^3	quartz, calcite	Landslides	Ballantyne, C., Stone J.O.H & Fifield, L.K. 1998
^{21}Ne	stable	quartz, olivine, garnet, clinopyroxene	Volcanic landform formation	Gillen <i>et al.</i> , 2010
^{26}Al	7.20×10^5	quartz	Glacial moraines	Shulmeister <i>et al.</i> , 2010
^{36}Cl	3.01×10^5	k-feldspar, plagioclase, calcite	Fault plane slip rates	Kozaci <i>et al.</i> , 2007

Table 4.1: Isotopes used in cosmogenic exposure dating, some applications of the isotopes and some examples from the literature (source: Cockburn & Summerfield, 2004; Dunai, 2010).

Chapter 4: Cosmogenic exposure dating methodology

For terrace deposits which are believed to be over 500 ka, paired isotopes are utilised because in older surfaces single isotope measurements will only produce a minimum estimate of the exposure age due to erosion reducing the concentration of nuclides in the top layers of the terrace levels. By using two nuclides, one with a shorter half-life (in this case ^{26}Al) and one with a long half-life (^{10}Be), the rate of erosion can be constrained using the nuclide with the shorter half-life and the exposure age of the landform can be determined by the nuclide with the longer half-life (Gosse & Phillips, 2001; Cockburn & Summerfield., 2004; Dunai, 2010).

Quartz is used as sampling material in this research because it is abundant in the terraces making up at least 10% of the terrace clast content. Quartz also contains abundant target nuclei for the cosmogenic nuclides used in this study (^{10}Be (oxygen) ^{26}Al (silicon)). The resistance of quartz to chemical weathering is another key reason to use quartz; it is also resistant to the meteoric nuclides meaning that they cannot dominate the quartz. The final reason to use quartz is that the rate of nuclide production of cosmogenic nuclides from quartz is well constrained (Dunai, 2010).

4.3 The depth concentration profile method

There are several methods for cosmogenic dating; the most common methods are 1) a single rock sample taken from a surface bolder or surface rock exposure (Schulmeister *et al.*, 2010; Evenstar *et al.*, 2009) 2) multiple samples taken from current fluvial channels and boulder samples from landforms (Cook *et al.*, 2009) and 3) multiple samples collected from a profile through a landform. The profiling method has been chosen for this study as the most suitable cosmogenic method to date river terraces because it can be used to constrain multiple issues. Applying cosmogenic dating to fluvial landforms is problematic as they are dynamic landforms made up of individual

Chapter 4: Cosmogenic exposure dating methodology

clasts each with separate cosmogenic exposure histories. The two biggest problems with dating terraces using cosmogenic dating are inheritance issues and mixing of the sediment during deposition. Both of these issues can be addressed by the profile method (Repka *et al.*, 1997). The next section addresses the theoretical background of the method and the assumptions which are applied when using this method.

4.3.1 Theoretical background

The profiling method involves taking multiple samples from a profile through the terrace landform which has been selected for dating. This method was pioneered by Anderson *et al.* (1996) who first applied it to Pleistocene fluvial terraces in Utah and Wyoming. The method was developed to overcome the inheritance problems which are common in fluvial settings. Inheritance is the residual cosmogenic nuclide content generated when the original clasts were first exposed then deposited before they were eroded, transported by the fluvial systems and deposited in river terraces. Figure 4.3 demonstrates how clasts in a fluvial system are first exposed to cosmic rays at point of exhumation and then gain further cosmogenic nuclides during fluvial transport and deposition.

A clast in a fluvial terrace has two components: 1) inherited cosmogenic nuclides (see above) and 2) cosmogenic nuclides that accumulated following deposition. Fluvial systems, and the sedimentation and erosion that occurs within a drainage basin are stochastic in nature, which means that clasts within a terrace have a significant and variable amount of inheritance gained by variable production rates as a clast moves through the fluvial system (Anderson *et al.*, 1996). Equation 1 can be used to represent the inheritance present in a sample, with the concentration of cosmogenic nuclides in a sample being a function of depth (z) and the age of the deposit (t).

$$N(z, t) = P(Z)/\lambda \cdot (1 - e^{-\lambda t}) + N_{im} \cdot e^{-\lambda t}$$

Equation 1

Chapter 4: Cosmogenic exposure dating methodology

Where N is the concentration of cosmogenic nuclides in a given sample, P is the surface production rate ($\text{g}^{-1}\text{a}^{-1}$), λ is the ^{10}Be decay constant and N_{im} is the amount of cosmogenic inheritance in the sample. The first part of the equation represents the expected growth in the exponential cosmogenic nuclide profile following deposition and the second part of the equation represents the decay of the inherited cosmogenic nuclides (Hancock *et al.*, 1999).

Due to differences in lithology, grain size and transport distance within a catchment area, any single clast in a terrace deposit is likely to have a significantly difference inheritance component to a neighbouring clast. This relates to the stochastic nature of fluvial transport and production rates of nuclides in a system. This increases the difficulty in dating a terrace deposit with a single sample since any age calculated by using a single clast approach would likely contain a significant amount of inheritance. Furthermore, any age generated from age calculation based on a single clast would have to be considered as a maximum age for the deposit with a large error bar.

There are two sampling methodologies which have been developed to overcome the inheritance problem. The first is to take a sample of quartz from the active river bed. This means that the nuclide concentration of the sample would have to be entirely pre-depositional and therefore be equivalent to the inheritance value. The nuclide concentration can be then used to correct the age of the sample taken from the terrace surface (Nissen *et al.*, 2009). However, this sampling methodology assumes that the material sampled in the active channel has a similar depositional history of the system that deposited the terrace. Since the Río Aguas has undergone a basin scale capture event (Chapter 2) this is unlikely to be the case. The second methodology is the concentration profile method which involves only sampling the landform and not the active channel. This method does not involve making assumptions about the previous

Chapter 4: Cosmogenic exposure dating methodology

drainage mechanism of the fluvial system but does allow for the average inheritance history of the clasts in the terraces to be determined.

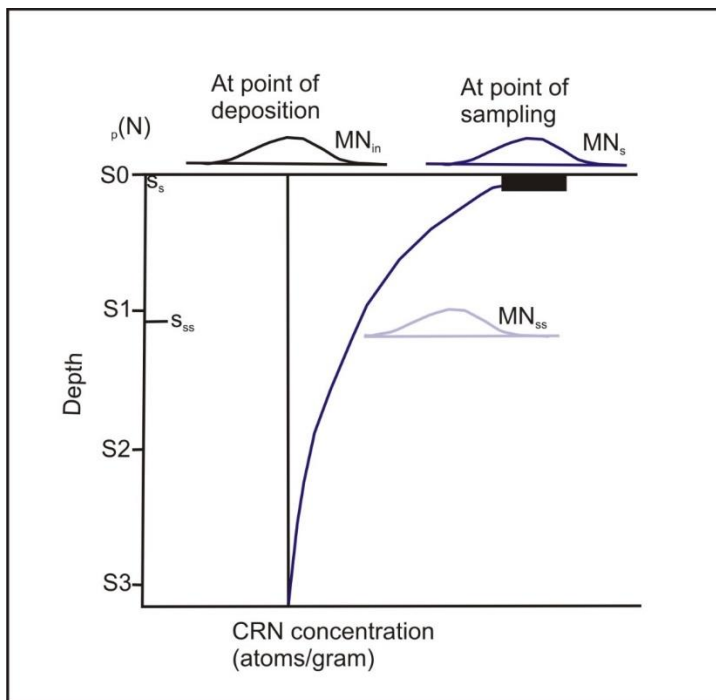


Figure 4.2: Graph showing the mean average cosmogenic nuclide concentration with depth at point of deposition and at point of sampling. Note the straight line at point of deposition compared to that at time of sampling. Modified after Hancock *et al.*, 1999.

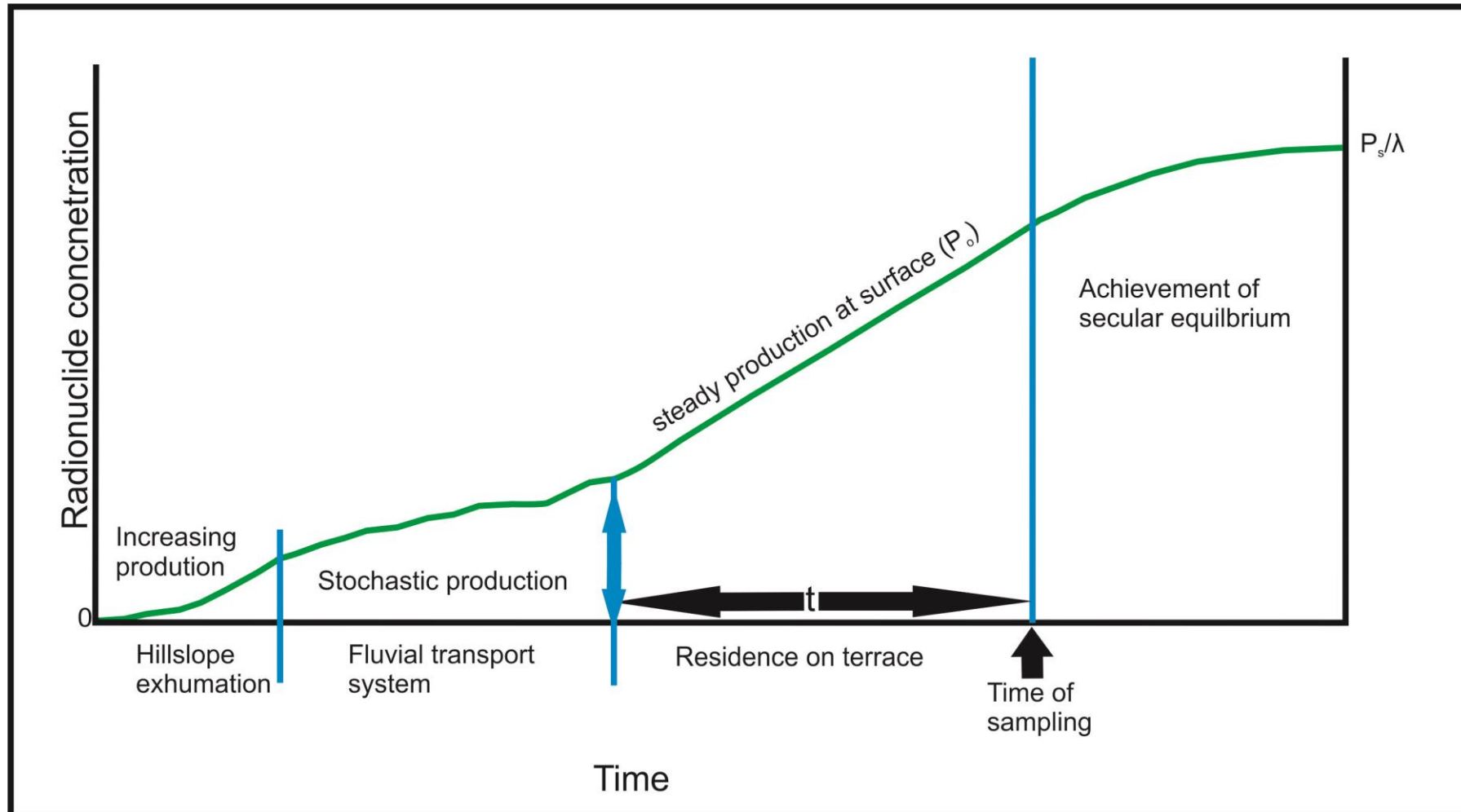


Figure 4.3: Diagram showing how quartz clasts in terraces begin to inherit cosmogenic nuclides from the point of exhumation in basement rocks through to when they are sampled. The problem of inheritance needs to be taken into consideration when using cosmogenic dating as it increases the age of the samples. The profiling method was developed to deal with this issue. Modified after Anderson *et al.*, 1996.

Chapter 4: Cosmogenic exposure dating methodology

The original profile method developed by Anderson et al (1996) involved taking one sample of multiple clasts from the surface and a second multi clast sample from the subsurface of the terrace deposit. The principle behind this was that inheritance in single clasts just deposited on a terrace is, as explained above, random but in an amalgamated sample it does not deviate with depth in the top two metres due to the attenuation length of cosmic rays. When the terrace is sampled at a later date, the surface sample will have gained cosmogenic nuclides since it was deposited whereas the lower sample will have the same or similar concentrations at the point of deposition. The difference between cosmogenic nuclide content with depth at time of deposition and at time of sampling is demonstrated by Figure 4.2. The difference in the concentration of cosmogenic nuclides between the two samples is the amount of nuclides which have accumulated since the terrace surface was deposited (Anderson *et al.*, 1996., Hancock *et al.*, 1999).

The profile method was further developed by Repka et al (1997) who used both computer modelling and field methods to indicate the optimum number of clasts to collect per amalgamated sample in order to constrain mean inheritance. Their research indicated that 25-40 clasts, greater than 5 cm in size, were sufficient numbers to constrain the mean inheritance of a sample. The size of the clast collected was deemed significant as smaller clasts may be dominated by the meteoric component and also may not withstand the chemical preparation needed for analysis (section 4.4).

Following on from Anderson et al (1997), Hancock et al (1999) went on to apply the method to fluvial terraces from the Wind River, Wyoming, developing the method to include taking multiple samples through the terraces whereas previous work had only used a surface and subsurface sample. A full cosmogenic profile through the terrace provides a better test of the assumptions which are made with this project (section 4.2)

Chapter 4: Cosmogenic exposure dating methodology

because if any assumptions made are incorrect then the mean concentration profile would not be exponential with depth (Hancock *et al.*, 1999).

4.3.2 Burial dating

Burial dating can be used to calculate the timing of burial of sediments or rock samples. The method can be used on sediments that have been buried leading to temporary or permanent shielding from cosmogenic rays. Burial dating involves measuring the ratio of ^{26}Al to ^{10}Be in the lowest sample collected via the profile method. ^{26}Al and ^{10}Be are the most commonly applied isotopes for this method because they are produced in the same quartz clast by the same cosmic ray flux over the same period of time. The production rate for ^{26}Al and ^{10}Be is largely independent from altitude and latitude. The production rate of the two cosmogenic nuclides also does not vary substantially with depth in a rock (Granger & Muzikar, 2001). Once clasts have been deposited and buried to a depth of ~ 3m, production of cosmogenic nuclides ceases (Dunai, 2010) and radioactive decay begins. The rate of radioactive decay is a known parameter and therefore can be used to calculate when the clasts were buried. The burial method provides a maximum age for the deposit and therefore acts as an upper age limit for the profile method. The burial method therefore gives an insight into when the terrace aggradation occurred whilst the profile method can be used to constrain the timing of incision into the terrace surface.

4.4 Selection of sample locations

A spatial and temporal methodology has been applied to sampling for cosmogenic exposure dating. The current chronology for the Río Aguas terraces, based on U-series dates from pedogenic calcretes, is limited to the captured system approximately 20 km upstream of the capture site. In order to increase the spatial distribution of terrace dates

Chapter 4: Cosmogenic exposure dating methodology

sample locations have been identified at fixed distances through the catchment upstream from the capture point. Originally samples were going to be taken at 0, 10 and 20 km along the catchment, however; this approach has been limited by the availability of suitable sites, particularly near the capture point. Sampling locations (see Figure 4.4) were identified at 5, 10 and 20 km upstream from the capture site.

Figure 4.5 shows the location of the seven terrace sites that have been sampled for cosmogenic dating with one site being taken from the Góchar Formation top basin fill surface, three from terrace level B and three from terrace level C. Terrace level A has not been sampled as a suitable sample site was not located. Each sample site was selected via a strict criterion (see section 4.4.1 & 4.5.2). All the terrace sections were road cuts except for two terrace C samples. The terrace C G3 sample was collected from an existing trench (possibly dug for agricultural irrigation) and the Mirador C profile was taken from a specially dug trench using a JCB/Backhoe machine.

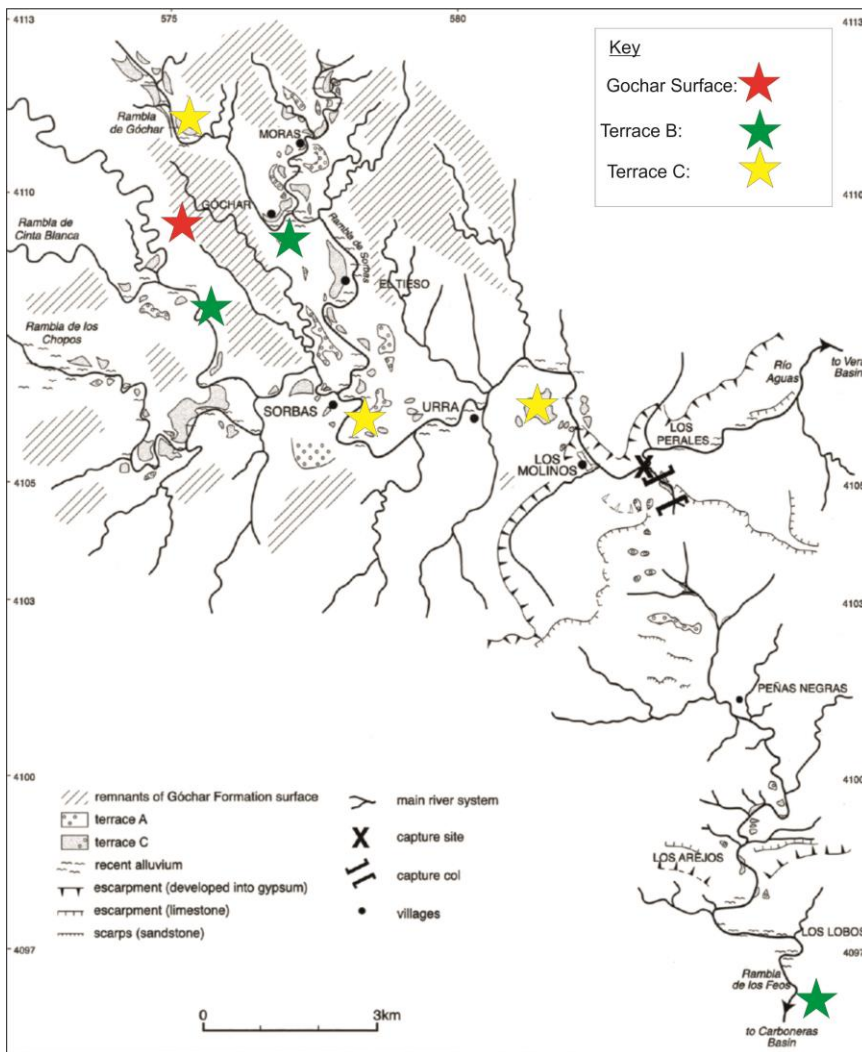


Figure 4.4: Map showing sample sites and potential sample sites in the Río Aguas catchment. Map modified from Harvey *et al.*, 1995).

4.4.1 Criteria for sample site selection

The main points to consider when selecting a site to sample using the concentration technique are: type of section, quality of the cut (deformation/ erosion), depth of section (~2.5 m), location with respect to shielding and cut of section through landform (does it cut the surface of the landform). Each of these points are going to be selected in turn and discussed with respect to their impact on the accuracy of in situ cosmogenic exposure dating.

Chapter 4: Cosmogenic exposure dating methodology

I. Type of cut

The section selected to be sampled must be a man-made section such as a road cut or a man-made trench. If a natural section was selected then the cosmogenic dating data would reflect the amount of erosion that is taking place on that surface rather than the age of the surface. By using a man-made cut such as a quarry, road cut or trenches that have been specifically excavated, this erosion element is negated.

II. Quality of cut

The quality of the section selected for sampling is one of the most important considerations when deciding which section to sample. Quality in this case refers to the amount of surface degradation and erosion which the section has been subjected too.

The ideal situation is that no surface degradation or erosion has taken place. It is particularly important that no erosion has taken place, especially off the top of the landform, because this will reduce the concentration of cosmogenic nuclides present in the surface of the landform and will therefore reduce the age produced by cosmogenic dating.

The presence of soil and hardpan calcretes were used as indicators that the terrace section had not undergone large amounts of erosion. Sedimentary structures within the terrace gravels were also checked to make sure that no mixing of the profile has taken place (e.g. by bioturbation or deformation).

Degradation, in the form of landslips and weathering, can also affect the concentration profile of ^{10}Be . If there has been a landslip it is possible that clasts have been moved out of position in the profile so that clasts that were originally deposited at or near the surface of the landform have been transported to nearer the bottom of the profile. This

Chapter 4: Cosmogenic exposure dating methodology

would cause a skew in the concentration of ^{10}Be present leading to a higher concentration of cosmogenic nuclides than would be expected at a selected level.

III. Depth of section

The depth that a section must be is dictated by the attenuation length of cosmic rays that produce cosmogenic nuclides. Attenuation length is the distance into the material that it takes the energy of the cosmic ray to drop below the energy required to produce cosmogenic nuclides (Dunne *et al.*, 1999). The attenuation length of cosmic rays is about 2 m; therefore any section sampled must be two metres in depth. If samples are collected at greater than two metres depth would lead to a measured cosmogenic nuclide concentration of consisting of inherited nuclides.

IV. Location with respect to shielding

Shielding is the blocking of cosmogenic nuclides from reaching the landsurface by topography or vegetation. Shielding vastly reduces the amount of cosmogenic nuclide that would reach a surface and would lead to a reduced amount of cosmogenic nuclides being produced in the sediment (Dunne *et al.*, 1999). This would lead to a smaller nuclide concentration with respect to the time that the sediment has been deposited leading to the generation of a younger date. To avoid shielding, sample sites should not be surrounded by large trees, heavy vegetation or have taller landforms very close by.

The landform should also be relatively flat so that self-shielding does not occur.

Surfaces should not be dipping because these would require adjustment for foreshortening effects due to the total cosmic ray flux (the amount of rays reaching the earth's surface) being less than on a flat surface (Gosse & Phillips., 2001). Tilting could also indicate that surface deformation has taken place and this can also affect the concentration profile produced by the cosmic rays due to mixing of the gravels.

V. Positioning of the section through a landform

Where a section is cut through the landform is important particularly if the timing of the abandonment of the landform is required. If the section does not cut through the top surface of the landform then the timing of abandonment will not be measured. The concentration profile would either produce an age that is far too young for the surface due to removal of terrace material containing cosmogenic nuclides or it would produce an erosion rate for the surface.

4.5 Sample site selection

The next sections of text describe the rationale behind the selection of the chosen sample sites for dating with the concentration profile method. The text includes details of the location of the sample sites as well as a description of the sites. A detailed sedimentological analysis of the sample sites is not presented in this chapter as it is undertaken in chapter 5 as part of a discussion describing the hydrological development of the Río Aguas. Sedimentary logs and sketch for the sites not covered in chapter 5 can be found in appendix 1.

4.5.1 Sample site GS (the Góchar surface sample site)

The Góchar surface type locality (Figure 4.5) is a 30 m long road cut that is located near the village of Góchar (UTM:0575756 4109450- Figure 4.6). The site consists of two exposures that run parallel to each other orientated E/W. The Góchar surface sample site is situated 520 m.a.s.l on the western valley side of the Rambla de Sorbas. A detailed description of the deposit is undertaken in Chapter 5.

The sample site for the Góchar surface was selected for a number of reasons; firstly the section has a hardpan calcrete and a soil profile present indicating that it cuts the top of the Góchar surface, secondly the section sampled has not been affected by any

Chapter 4: Cosmogenic exposure dating methodology

deformation and faulting and thirdly it is a man-made road cut of over three metres in height fulfilling the recommended parameters for choosing a suitable sample site for cosmogenic dating. Man-made cuts in the Góchar surface are limited to road cuts which reduced the number of suitable sample site. Road cuts which cut through the Góchar surface are very rare.

One of the key issues with locating a suitable section for the Góchar surface was identifying a section that had not been subjected to deformation that affects the Góchar Formation (Mather, 1991). Another problem with identifying a section for the Góchar Formation is locating a profile which cuts through the top of the basin fill surface and not a surface inset into the Góchar surface. If the sample was collected from a surface inset into the Góchar Surface then the age returned by the cosmogenic dating would be too young. This is due to the surface form of the Góchar Formation dipping at its edges. To counter this issue the selected site was chosen by limiting the search for a section to the highest point of the basin infill which is situated near the village of Góchar (Figure 4.6).



Figure 4.5: Picture of the west facing Góchar surface sample site. The 3 m long back line shows the where the concentration profile samples were collected. The location of the sample site within the Aguas catchment is shown in Figure 4.7.

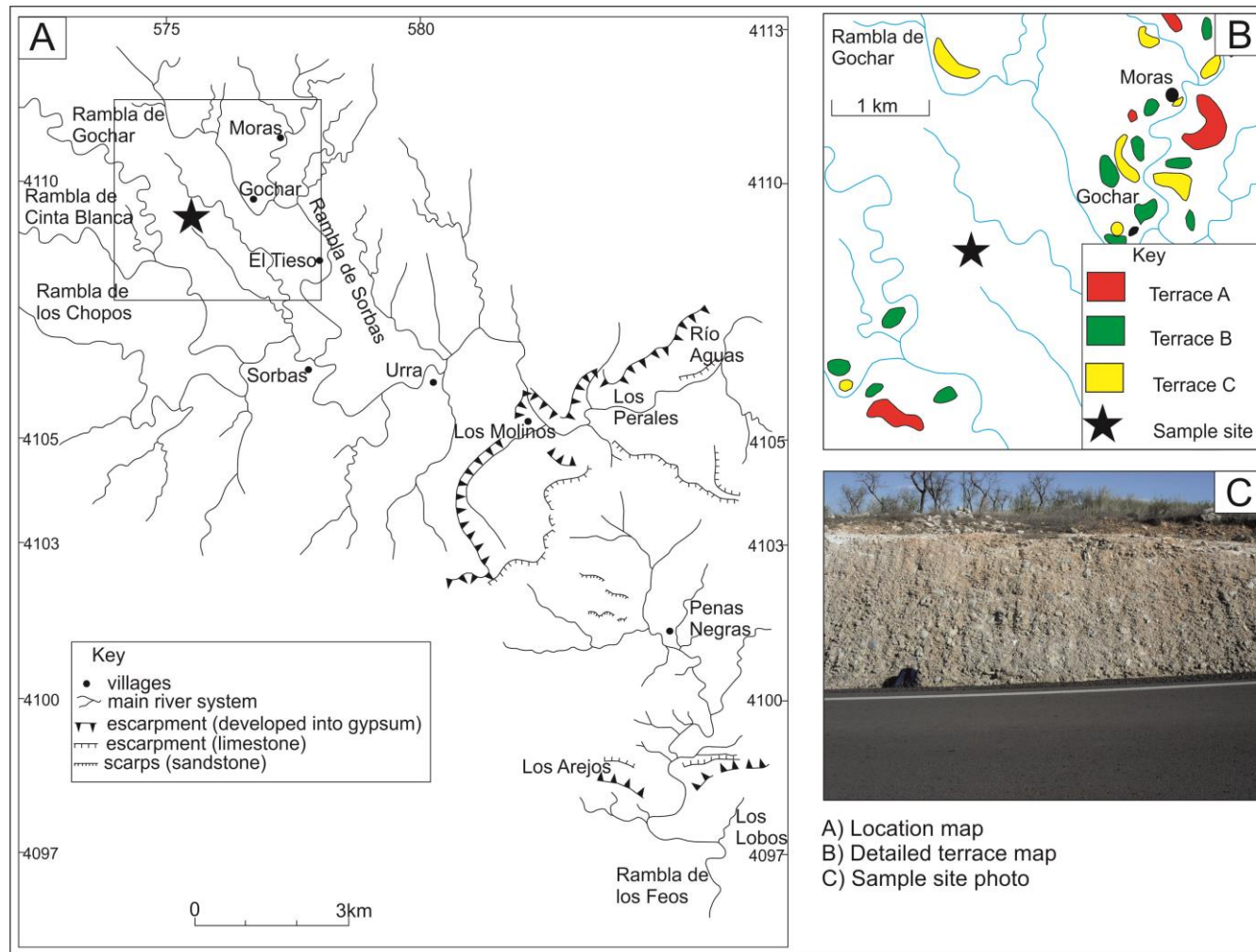


Figure 4.6: Location map for the Góchar surface sample site (UTM: 0575756: 4109450). Map modified from Harvey *et al.* (1995).

Chapter 4: Cosmogenic exposure dating methodology

4.5.2 Terrace A

There was no suitable terrace level A sites available for sampling due to no man made cuts through the deposits. Although terrace A deposits are found throughout the Proto Aguas/Feos catchment, no roads or trenches cut the deposits. Where a quarry cuts through a terrace A deposit, near Sorbas town, there is some uncertainty of whether material has been removed from the surface of the terrace. Difficulties in obtain permits to dig a trench at a suitable location due to the protective orders on the local funa and flora (see 4.5.8) meant that it was not possible to gain permission to dig a trench within the timescale of this research.

4.5.3 Sample site GTB (Terrace B)

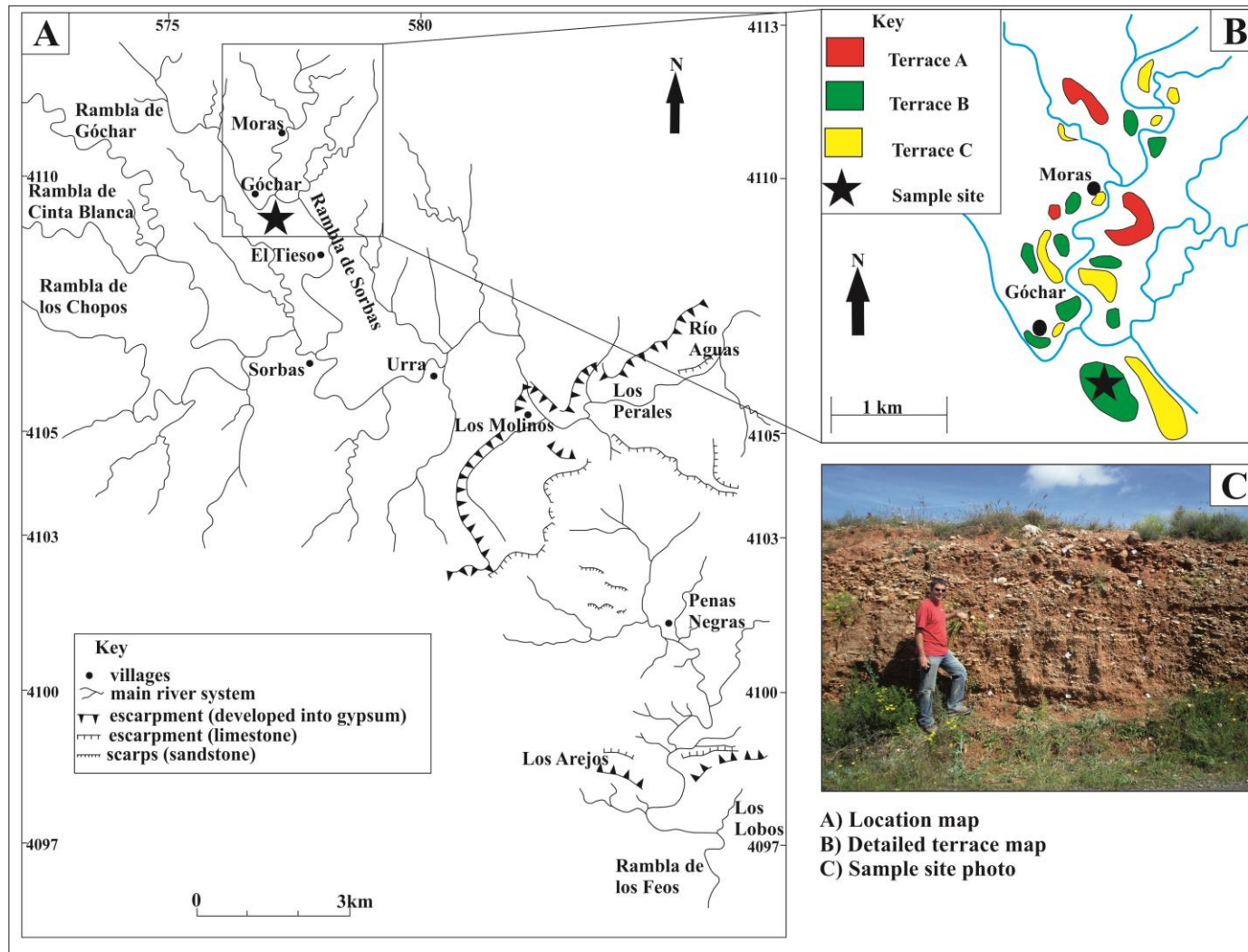
The selected section for cosmogenic dating in the upper section of the Río Aguas catchment is the GTB site. The GTB sample site is a profile through a single terrace landform located near the village of Góchar (UTM: 0577312 4109292- Figure 4.7) in the Rambla de Góchar. The terrace gravels are exposed in a road cut (~100 m long) present on the south side of the modern Rambla Góchar and the west valley side of the modern Rambla Sorbas. The selected exposure is orientated E/W with samples being collected from the western end of the deposit (Figure 4.7)

The base of the terrace is at 454 m.a.s.l (45 m above the current stream base) and forms an undulating contact with the Góchar surface below. The sample site consists of up to 5 m of fluvial gravels capped by a red soil (2.5 YR 5 (red)) which contains calcretes. There is no discernible erosion, faulting or deformation in the section and there is no shielding of the site by high topography nearby. The site was selected due to its thickness (greater than 3 m), location in the terrace (cuts through the surface) and type (man-made road cut).

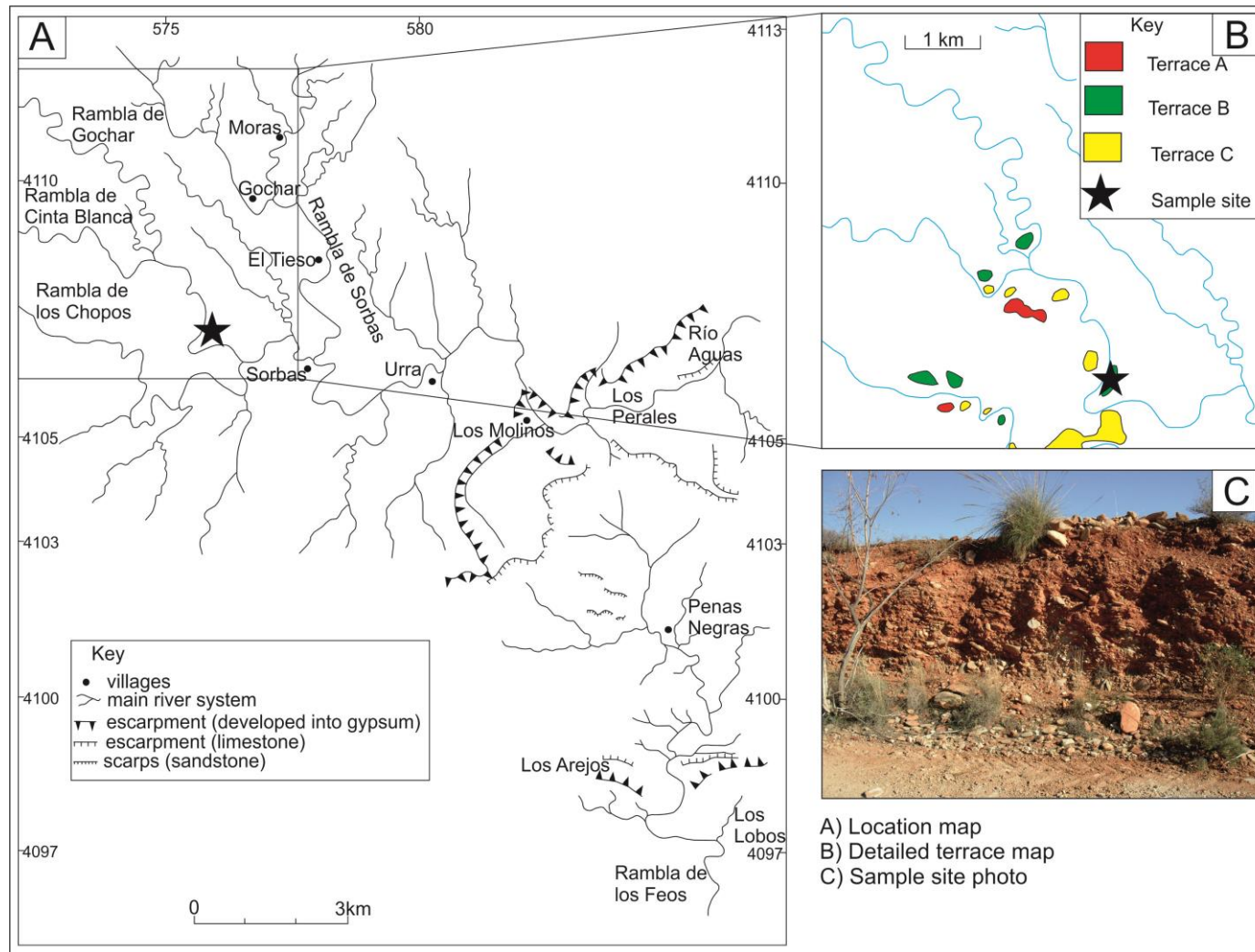
Chapter 4: Cosmogenic exposure dating methodology

4.5.4. Sample site C.B (Terrace B)

The Cinta Blanca sample site (UTM: 0575600 4108254-Figure 4.8) is a cutting made by a track in a terrace B deposit located on the north valley side of the Rambla de Cinta Blanca. The exposure at the section is a single section 200 m in length and 2.5 meters high. Samples were collected from the middle of the exposure which is orientated NW/SE. The section displays no faulting with clear continuity of sedimentary structures along the whole length of the deposit. The deposit has a clear red soil which produces a Munsell reading of 7.5 Yr 4 (red) and has type III/IV calcretes at its surface. Although ploughing takes place on the top surface of the terrace, it does not extend right to the edges of the terrace meaning that the profile section of the terrace where the quartz clasts were collected from is unlikely to have been artificially lowered or disturbed and no mixing of the profile had taken place by the agricultural activity. Although in some places large boulders that have been disturbed by ploughing have been piled up at the edge of the terrace this area was avoided when sampling the site.



4.7: Location map for the GTB sample site (UTM: 0577312: 4109292). Map modified from Harvey *et al.* (1995).



4.8: Location map of the C.B sample site UTM: 0575600: 4108254. Map modified from Harvey *et al.* (1995)

Chapter 4: Cosmogenic exposure dating methodology

4.5.5 Sample site T.B.P (Terrace B)

The Polopos sample site is a terrace B deposit which has been cut by a road producing a single exposure. The sample site (UTM: 0583950: 4095100-Figure 4.9) is located near the town of Polopos in the southern end of the Féos Valley. The NW facing section is 10 m high and 400 m in length (300 m.a.s.l). The nearest high topography is the southern Basin margin, the Sierra Cabrera, which occurs at an angle of 5° from the section. The site was carefully logged and sketched in order to pinpoint a suitable place to take the sample as there was some faulting of the section. The presence of a type III/IV calcrete on top of the deposit indicates that there has been no significant removal of terrace material. Soil present at the section produced a Munsell reading of 2.5 YR 4 (red).

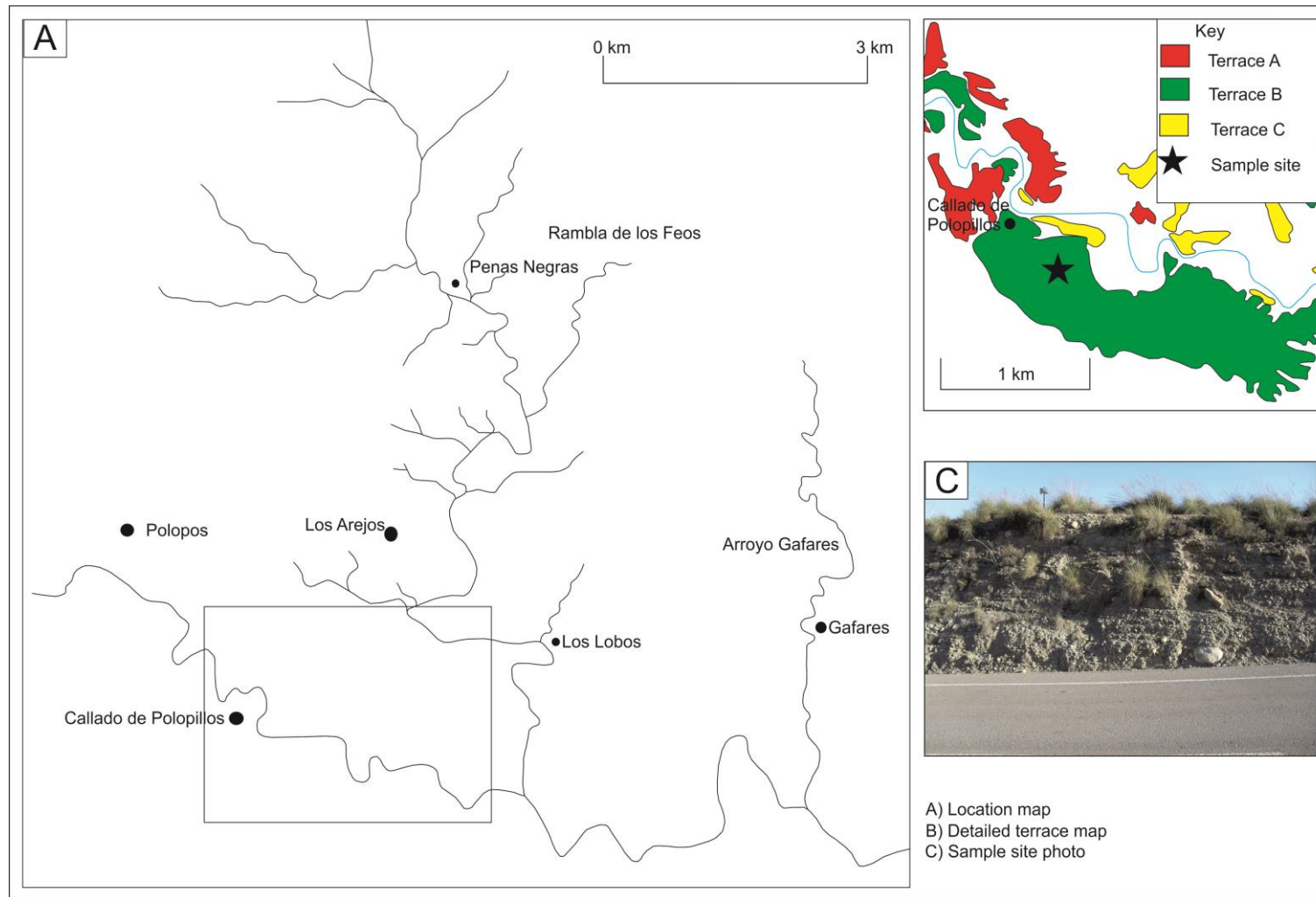
4.5.6 Sample site G3 (Terrace C)

The selected section for the upper section of the Río Aguas catchment is the G3 site (UTM: 0575574: 4111057). The level C sample site forms part of a single terrace landform developed on the northern side of the valley side of the modern Rambla de Góchar 480 m.a.s.l (Figure 4.10). The samples were collected from a profile of gravels exposed by a man-made trench in an olive grove pictured in Figure 4.10.

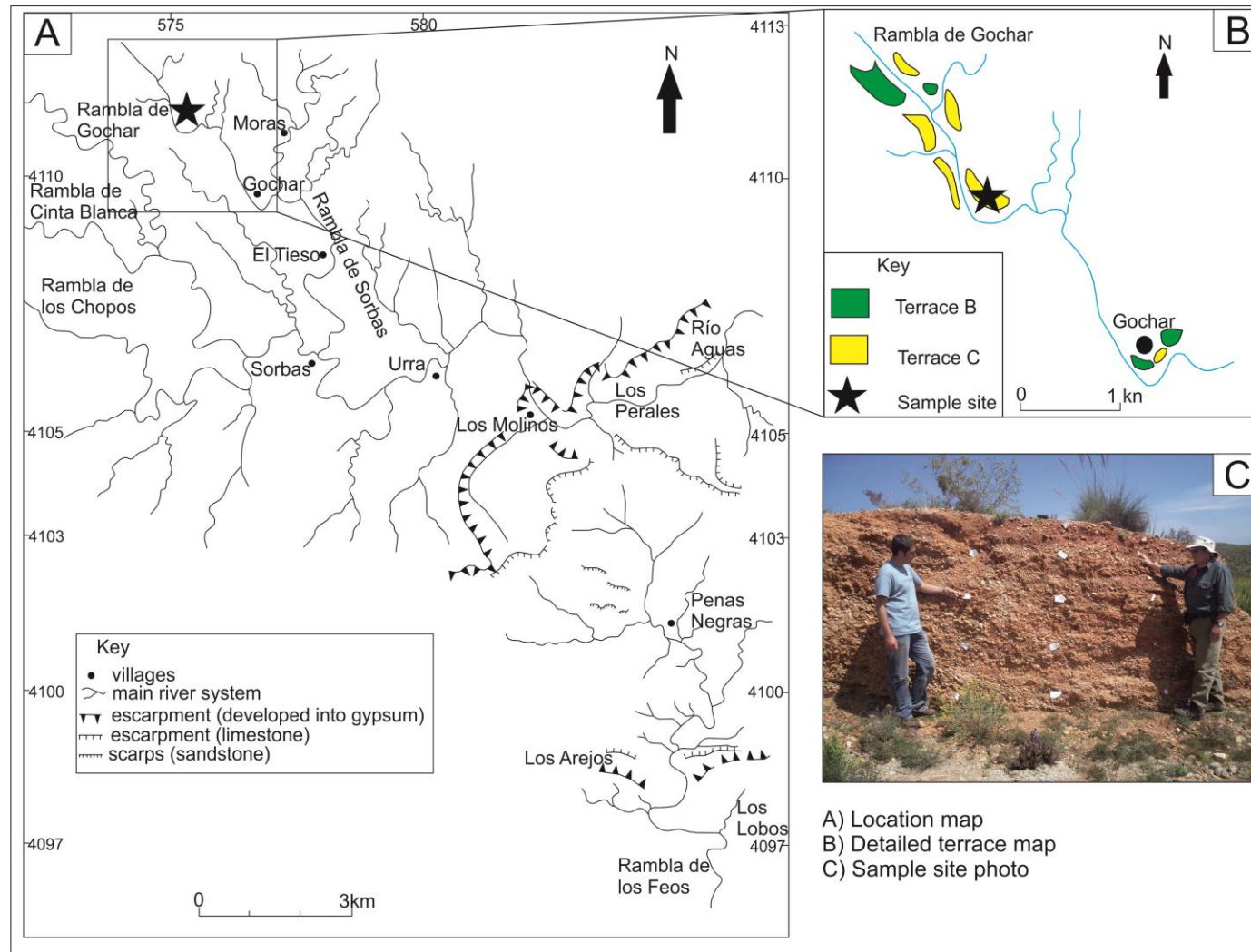
The sample site consists of 4 m of fluvial gravels capped by a red soil (2.5 YR 5 (red)) which contains calcretes (type III). There are clear sedimentary structures (cut and fill features, cross bedding etc.) which display no disruptive features that might be caused by Quaternary faulting indicating that this area of the terrace has not been affected by tectonic activity. Evidence of obvious soil erosion at the site is absent and there is a full surface calcrete present. There is limited shielding of the site by high topography. The G3 site was carefully chosen as Quaternary deformation affects parts of the terrace C deposits in that area and mixing of the cosmogenic profile due to syn-sedimentary

Chapter 4: Cosmogenic exposure dating methodology

faulting would result in a poor age control was a possibility (section 5.5.2). Figure 4.11 illustrates the extent of faulting present at the G3 sample site. The faulting is localised in nature causing a 1 metre wide section of sediments to be disrupted. The location where samples were collected from was away from the faulted zone so that no mixing of the profile would have occurred. The nature of deformation in this terrace is described in Chapter 5 (section 5.5.1).



4.9: Location map for sample site T.B.P (UTM: 0583950: 4095100). Map modified from Harvey *et al.* (1995)



4.10: Location map for the sample site G3 (UTM: 0575574: 4111057). Map modified from Harvey *et al.* (1995)

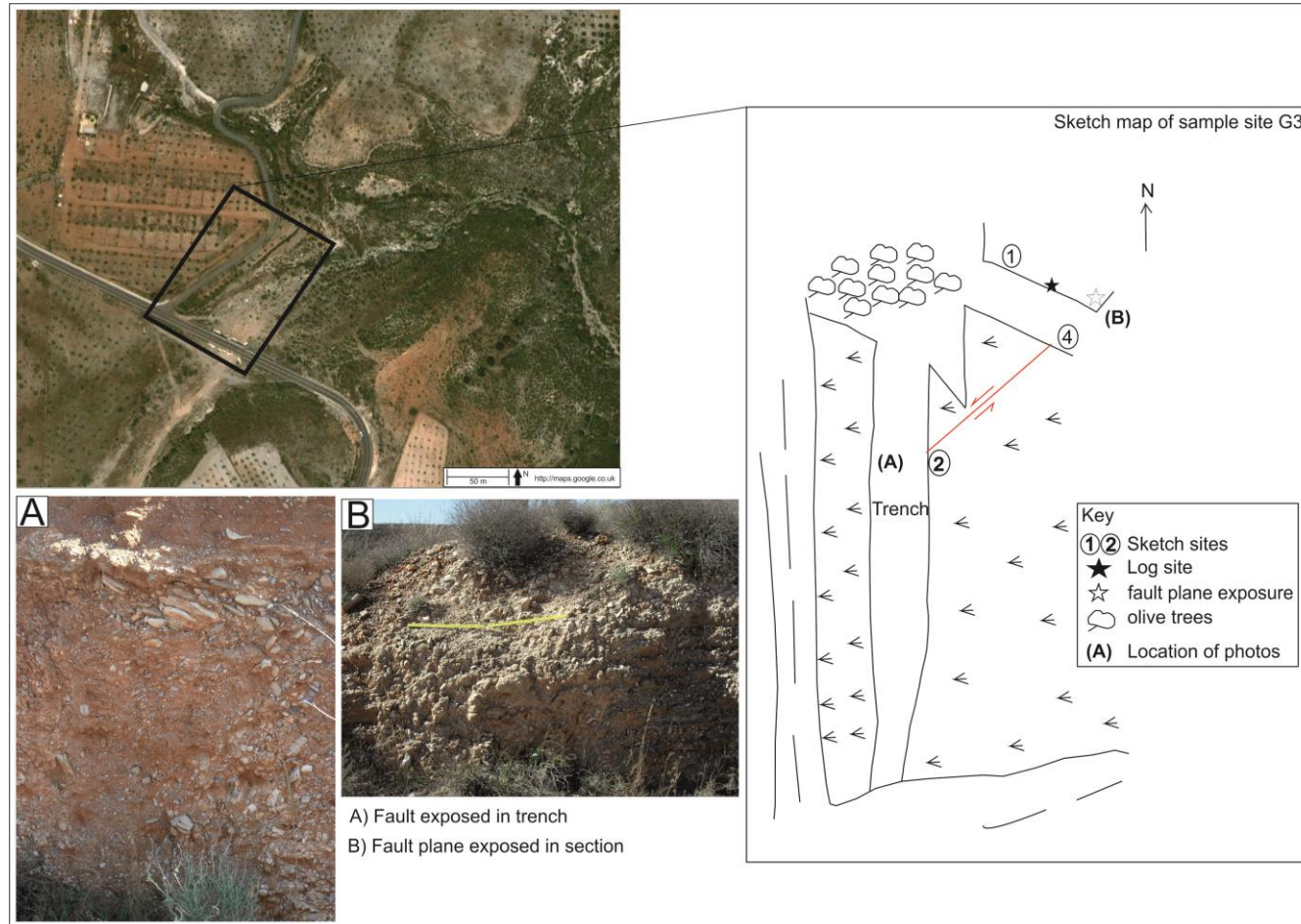


Figure 4.11: Map showing the location of the fault present in sample site G3. The cosmogenic profile was collected away from this localised deformation so that disruption of the nuclide profile would not have occurred (UTM: 0575574: 4111057). Imaged sourced from Google earth & DigitalGlobe. Permission to reproduce this image has been granted by Google Earth.

Chapter 4: Cosmogenic exposure dating methodology

4.5.7 Sample site T.C.F (Terrace C)

The forge sample site (UTM: 0578475; 4105825- Figure 4.12) is located to the east of the town of Sorbas next to an industrial site 453 m.a.s.l. The west facing profile through a terrace C deposit is situated on the eastern valley side of the modern Río Aguas. The exposure, created when a factory was built, is 20 m high and 15 m wide. There is a soil profile at the top of the terrace (5 YR 4 (red) and a 10 cm thick calcrete present (type II/III). The deposit consists of sand and gravels which display undisturbed sedimentary structures indicating no deformation or mixing of the profile. Due to the unstable nature of the deposits extra care was taken when collecting the sample to ensure no mixing of the profile occurred. Sample bags were kept closed whilst quartz clasts were selected to ensure no clasts entered the bag and only clasts which were firmly embedded into the terrace sediments were collected. This limited the possibility of mixing occurring.

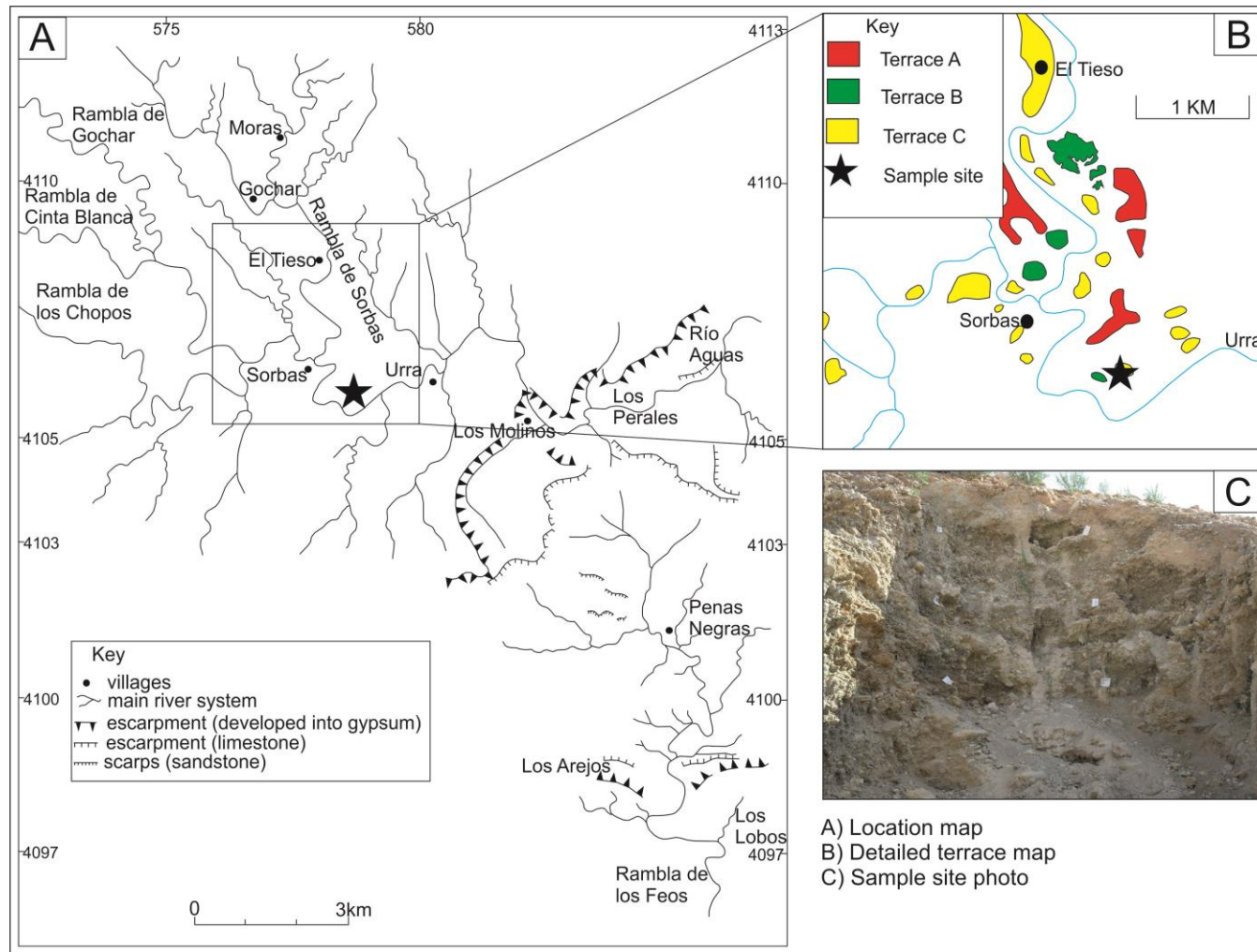
4.5.8 Sample site M.T.C (Terrace C)

The Mirador sample site is located near the Urra field centre (UTM: 0581425; 4106200- Figure 4.13) 2 km downstream from the town of Sorbas. The terrace C sample site is situated 380 m.a.s.l on the south side of the modern Río Aguas valley. The terrace deposit has no man-made sections cut through it so a trench was dug for the Mirador sample site using a mechanical digger. The area selected for the 2 m wide by 4m deep trench was located first by a process of geomorphic mapping to determine the extent of the deposit and secondly by choosing an area where quartz clasts were clearly seen at the surface along with red colouration of the ground. Natural sections cut by the Río Aguas were used to help infer the geomorphic setting of the trench along with logs and sketches taken once a section was cut. A limiting factor on the choice of where to dig the trench was protection laws for the local fauna and flora since the site was located in the Paraque Natural Karst en Yesos. An area free of protected species had to be found

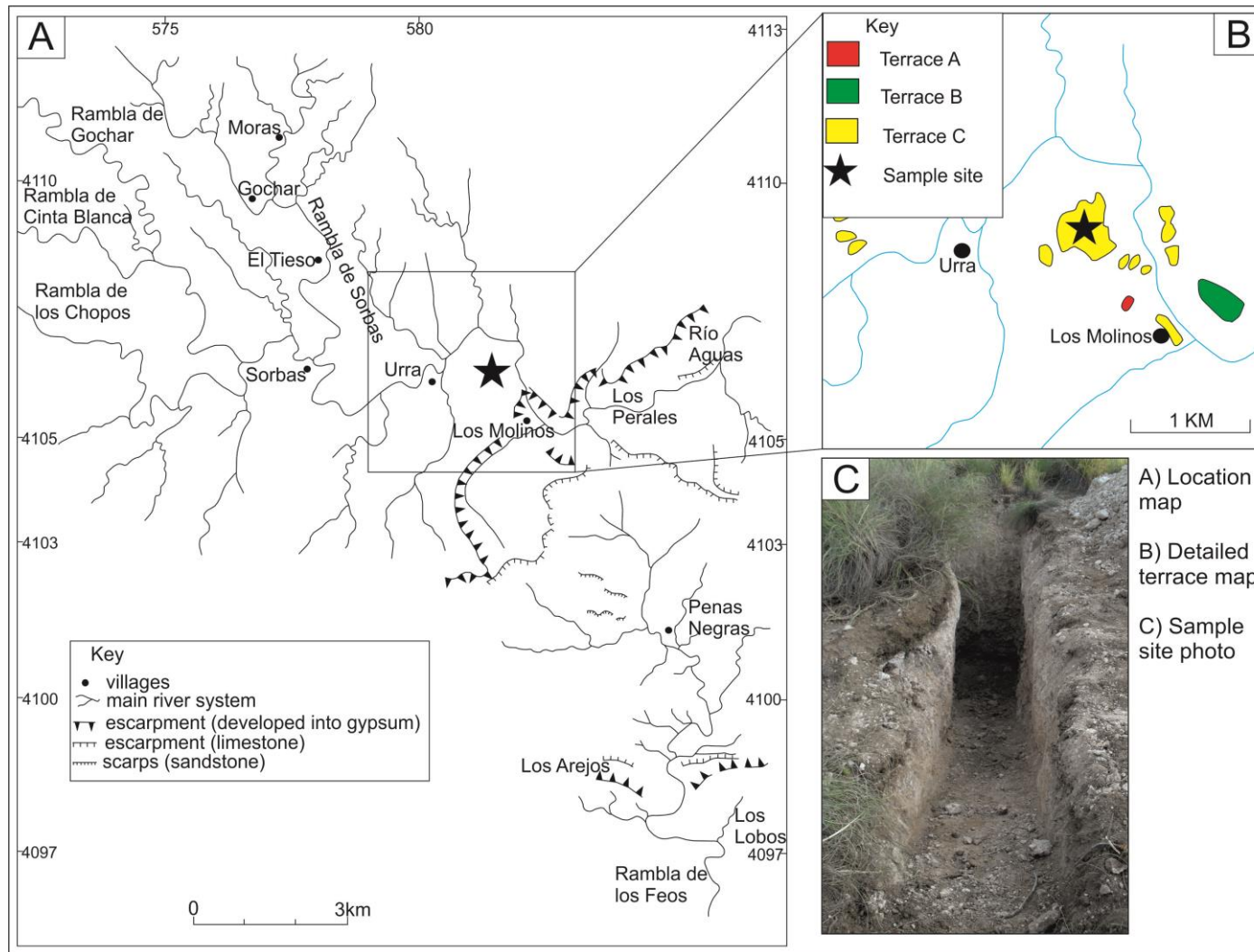
Chapter 4: Cosmogenic exposure dating methodology

and agreed following a site inspection by the Medio Ambiente. The selected site had no outward signs of deformation or faulting and no sign of tectonic activity was detected once the trench had been dug. There was a clear soil profile (5 YR 4 (red)) on top of the hardpan calcrete (type III) present indicating that there had been no removal of sediments from the top of the terrace.

Some difficulties were encountered whilst sampling the Mirador site. The gravels were very well cemented making collecting the quartz clasts difficult. This meant that fewer clasts were collected for the Mirador site compared to other terrace sample sites (although 30 clasts were collected for each level of the profile). The clasts were also significantly smaller in size than at other sites and also there was less quartz available to be collected. This could be due to the geomorphic setting of the chosen sample site (the edge of the terrace). The thickness of the hardpan calcrete at the site could also be an issue as shielding could have taken place (Rhodes *et al.*, 2010). This was accounted for in the calculation processes by introducing a shielding factor. The cemented nature of the deposit meant that carrying out a clast count was impossible due to the difficulties in ascertaining the lithology of the individual clasts. The density variation in the section was accounted for in the calculation processes by using a variable value for the density of the section (Chapter 7).



4.12: Location map for sample site T.C.F (UTM: 0578475: 4105825). Map modified from Harvey *et al.* (1995).



4.13-Location map for the M.T.C sample site (UTM: 0581425: 4106200). Map modified from Harvey *et al.* (1995).

Chapter 4: Cosmogenic exposure dating methodology

4.6 The sampling methodology

For this project the sampling methodology of Hancock et al (1999) is followed and developed. This involves taking multiple samples from numerous depths down through a profile in a terrace. The top two metres of the terrace exposure is first measured out from the surface of the terrace with every 0.5 m marked with a nail. A distance of 0.5 m is measured horizontally from the first marked point on the profile and marked with a nail. This process is repeated down the section to the right and left hand side of the profile so that five 1m interval lines are present in the profile (see Figure 4.14). The intervals are then marked clearly with a piece of paper put onto the nails stating the interval level e.g. 0 m, 0.5 m etc (see figure 4.4). This was done to ensure that samples were taken at the correct depth along the terrace profile. This also prevented samples being taken from too high above the profile line. All measurements for the profile were made with a laser range finder (Lasertech Tru-Pulse 360) and a tape measure to ensure accurate positioning of the intervals and to avoid mixing of the profile layers.



Figure 4.14: Picture of a terrace C sample site showing the marked profile for collecting the quartz clasts from the terrace profile. The bits of paper mark out 0.5 m intervals down the section with a metre width allowed for each interval level.

Chapter 4: Cosmogenic exposure dating methodology

Starting at the 2 m interval line, quartz clasts were collected for every interval level, from no more than 10 cm above and below the interval line, to ensure that there was no mixing of the vertical profile. For every interval level more than 30 clasts of greater than 5cm (long axis) in diameter were collected. The clasts need to be greater than 5 cm for two reasons; firstly so that the bulk of the nuclides in the quartz will be in situ rather than meteoric nuclides and secondly so that the clasts can stand up to the etching process which removes atmospheric contamination. Where clasts were heavily coated in carbonate cement they were brushed with dilute HCL in a bucket to remove the crust. The clasts were then washed with water to prevent further reactions. The samples were then placed into sample bags labelled with the terrace name and depth (for example a terrace B sample from Góchar for a 0.5 m sample line would be labelled as GTB 0.5 m).

Samples were collected from the bottom upwards so that mixing of the profile was prevented. Removal of clasts from a weakly cemented gravel/conglomerate can destroy the section via degradation with material falling out and burying the bottom of the section. To avoid this process the bottom of the section was sampled first. All quartz pebbles collected were firmly in the terrace surface, loose clasts were not collected as they could have fallen from higher up the terrace section and would therefore have a higher concentration of ^{10}Be .

As the nuclide content of a terrace deposit depends on the geomorphic setting of the sample site, a number of key observations need to be made in the field (Gosse & Phillips, 2001; Dunai, 2010):

- 1) The geographical orientation of the terrace
- 2) Angle of exposed section face
- 3) Angle to the highest topographic feature to the South of the exposure.

Chapter 4: Cosmogenic exposure dating methodology

The geographic orientation (longitude, latitude and direction which the terrace section is facing) affects the amount of cosmogenic rays which reach the terrace surface with higher altitude terraces being within reach of more cosmic rays than lower altitudes due to the thinning of the atmosphere (Balco *et al.*, 2008). The angle of section is an important measurement because higher elevated parts of a surface will receive a higher concentration of cosmic rays to the lower elevated surface. This is due to the cosmic rays reaching the higher parts of the terrace sooner (Gosse & Phillips, 2001; Dunai, 2010). The latitude of a site is important due to both atmospheric thinning and also the geomagnetic field which deflects the cosmic ray flux towards the poles (Lifton *et al.*, 2008). Any topographical highs that can be seen from the terrace section, and the angle at from the section to the topographical highs, need to be recorded as these can shield the terrace from cosmic rays reducing the amount of nuclides that can form in the terrace surface (Dunne *et al.*, 1999; Dunai, 2010). This would cause the concentration profile in the terrace profile to be at lower values for any given age than would be normally expected and would therefore result in an anomalously low age for the terrace surface. These readings are used to produce a production rate of cosmogenic nuclides which is used in the calculation of exposure ages for terraces.

4.7 Lab methodology

Figure 4.15 is a schematic overview of the method for preparing samples for accelerated mass spectrometry analysis (Anderson *et al.*, 1996). A more complete explanation of the steps follows in the text below.

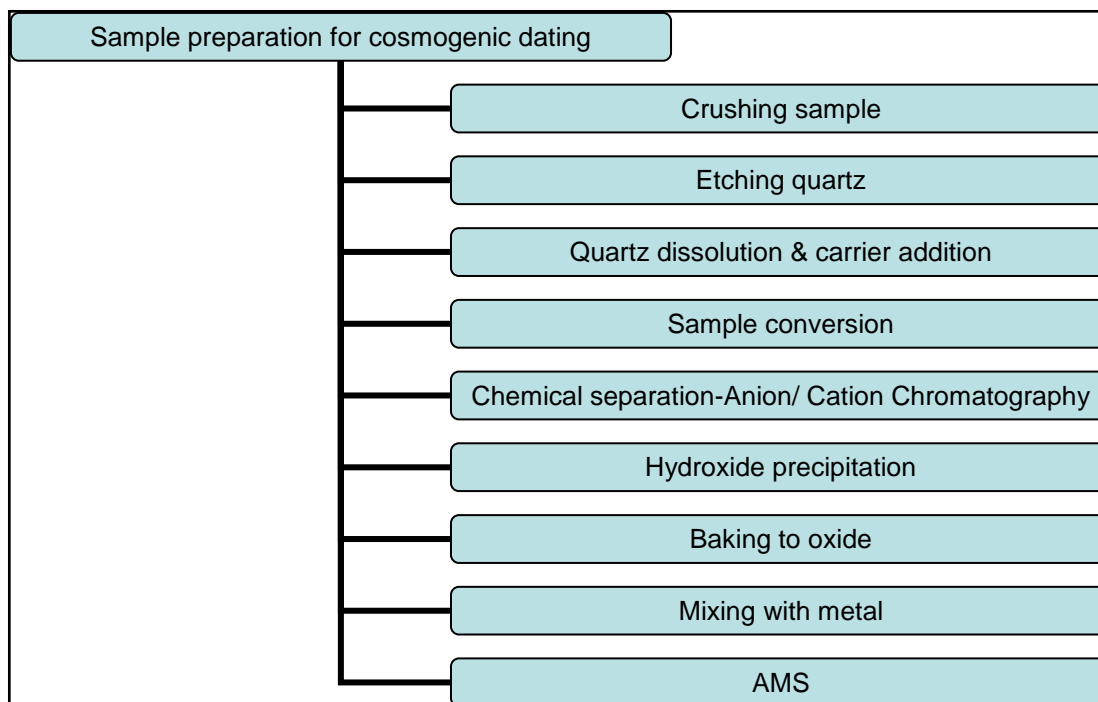


Figure 4.15: Schematic overview of the chemical preparation of quartz clasts for AMS measurements followed for this research. Method after Anderson *et al.*, (1996).

The quartz clasts were first crushed with a rock crusher and then reduced to a finer grain size with a Tema mill. The samples were then put through a series of sieves (500 μ m, 250-500 μ m & 125-250 μ m) with the 250-500 μ m fractions being retained. After sieving the samples are then put through a Franz magnetic separator to remove any magnetic minerals present in the samples. After this initial processing the samples are ready to go through an etching process.

The quartz clasts are etched to remove any atmospheric (meteoric) ^{10}Be on the surface of the quartz grains and also to remove any remaining impurities. This procedure is done by first pre etching the samples in 130 ml hexafluorosilicic acid (H_2SiF_6) and 65 ml Hydrochloric acid (HCL) for 24 hours. The pre etching process removes the easily dissolvable impurities such as carbonate and iron oxide that are found in quartz (Kohl & Nishiizumi, 1992). The main quartz etch (950 mL 15 MOhm water & 50 mL 40% specified hydrofluoric acid [HF]) then follows this and is carried out for 48 hours. This etch is usually carried out five times. The samples are then weighted to see how much

Chapter 4: Cosmogenic exposure dating methodology

of the sample has been etched, once 30% of the sample has been removed by etching, the sample is ready for further preparation, because the meteoric element is deemed to have been removed (Kohl & Nishiizumi, 1992). The etching process described above has been determined as the most effective method of eliminating unwanted impurities whilst maximising the purity and yield of the quartz (Kohl & Nishiizumi, 1992). After etching, a test for the amount of aluminium concentration is completed using a small test sample (0.4 g), the results of which indicate the purity of the quartz. If the aluminium content of a sample is less than 200 ppm, then the sample is considered to be pure and then a solution can be created from the sample. For samples which are being prepared for ^{26}Al measurements then the aluminium content must be less than 150 ppm.

Dissolution of quartz is the process of creating a solution from the solid purified quartz sample to a liquid using 20 ml of hydrofluoric acid. The sample is then gently heated (less than 120°C) to allow the liquid to evaporate to dryness. This process is repeated until all the quartz is dissolved and then carriers are added to the sample. Carrier addition is an important process with respect for ^{10}Be because the concentration of ^{10}Be in quartz is very low (~ 1 ppb). For ^{26}Al analysis, the addition of a carrier to the sample is dependent on the Al concentration of a sample and the sample masses. If the sample contains less than 1.6 mg Al/ sample, then additional aluminium would be used.

During sample conversion HF is driven off as fully as possible without allowing the formation of oxides (Al_2O_3 and BeO) which would cause incomplete re-dissolution. Once sample conversion has been completed chemical separation of the samples has to be achieved.

Chemical separation is a very important part of the preparation process because it is the process by which unwanted elements (such as Boron and titanium) are removed. Boron needs to be removed from the samples because both ^{10}Be and boron have a similar

Chapter 4: Cosmogenic exposure dating methodology

chemical composition. This causes problems when analysing the samples using AMS because the machine will not be able to separate the ^{10}Be from the boron.

Chemical separation is achieved firstly by anion exchange chromatography (Figure 4.16) and secondly by cation exchange chromatography. Anion exchange removes iron (Fe) content from the sample and cation exchange removes the boron because it does not form positive ions and therefore will pass through the negative resin whereas ^{10}Be and ^{26}Al move much more slowly through the resin.

Hydroxide precipitation is the final process for removing boron from the ^{10}Be sample. It is also the process by which magnesium is removed. The samples are then heated until they are dry and mixed with metal. The samples are mixed with metal because ^{10}Be has high electrical and thermal conductivity which can affect the AMS. Once this process is complete then the samples are ready to be analysed by AMS.

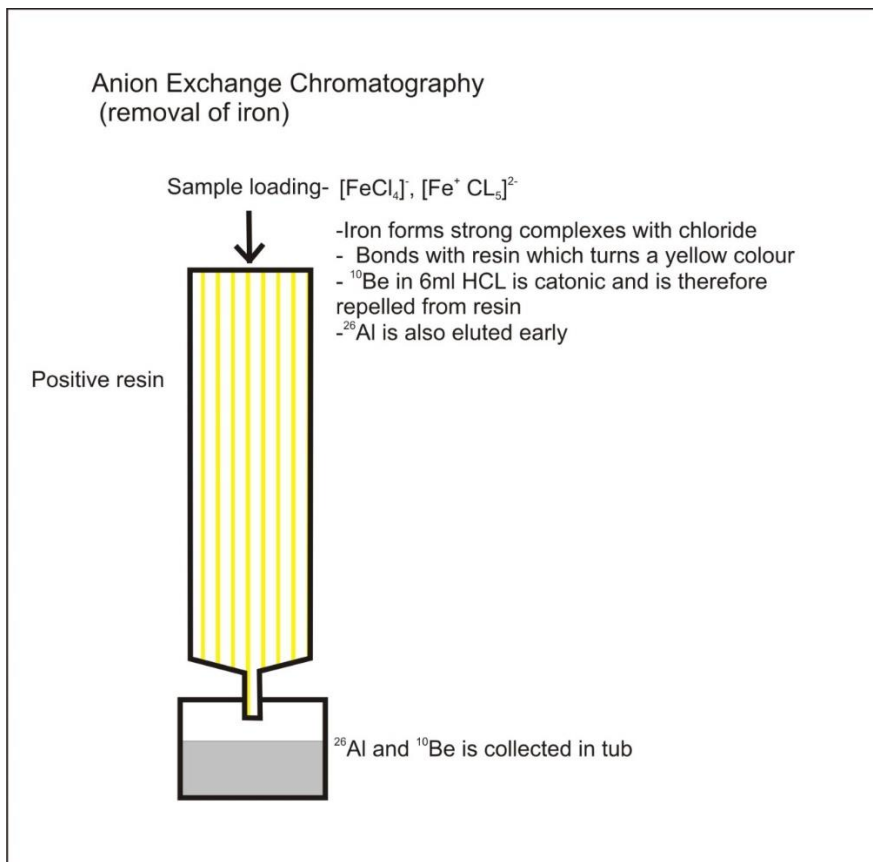


Figure 4.16: The processes of Anion exchange chromatography which is used during the chemical preparation of the samples for AMS to remove unwanted elements from the sample which may interfere with the AMS measurement.

Chapter 4: Cosmogenic exposure dating methodology

The samples were analysed in the SUERC AMS facility in East Kilbride where the concentration of either ^{10}Be or ^{26}Al was measured. For more information on how AMS works see Hellborg & Skog (2008).

4.8 Chlorine 36 dating

Chlorine 36 (half life: 301 ± 2 ka) is the only cosmogenic nuclide that is routinely used for exposure dating of carbonate rocks (Gosse & Phillips, 2001; Dunai, 2010) and is therefore now becoming regularly used for palaeoseismic studies of faulted limestone terranes (Kozaci *et al.*, 2007). This is due to the increased preservation of fault scarps in carbonate rocks (Dunai, 2010). Chlorine 36 is also used for basalts not containing He retentive phenocryst phases used for ^3He dating (Dunai, 2010). In samples with suspected complex exposure histories ^{10}Be and ^{36}Cl in feldspars can be used to constrain the exposure history. Chlorine 36 is also regularly used for dating landslides (Ballantyne *et al.*, 2009).

In this study chlorine 36 has been used to date a landslide site within the Sorbas Basin to determine when the landslide was initiated and to assess its relationship to the capture related wave of incision. Several sections of the Río Aguas system have large scale landsliding which is believed to result from the undermining of slope toes by the incising river (Hart, 2004). However, it is not clear as to whether the landslide occurs as the incision takes place or after a time lag. The following text describes where and why landslides occur in the Sorbas Basin, sampling procedures and the results of the cosmogenic dating.

4.8.1 Landslides in the Sorbas Basin

In the Sorbas Basin there are a series of individual circumstances that combine to increase the susceptibility to landsliding. Weak geology or situations where hard rock

Chapter 4: Cosmogenic exposure dating methodology

overlies soft rock (Hart., 2004) combined with the sensitivity of slopes to climatic events and the undercutting of slopes by fluvial incision relating to the tectonic uplift of the basin (Harvey & Wells, 1987; Mather, 1991; Mather *et al.*, 2002). Landscape instability can be detected in numerous places throughout the Sorbas Basin, in particular within the Sorbas-Los Molinos area where landslides, rockfalls and badland formation can be observed (Mather *et al.*, 2002). Mass movement processes dominate with over 300 landslides occurring within the Río Aguas catchment (Hart, 2004; Griffiths *et al.*, 2002; 2005) varying in size from small scale (tens of m³) to large scale (millions of m³) (Hart, 1999; 2004). The landslides generally follow the course of the Río Aguas valley and sometimes in tributaries, however, it has been noted that the landslides form clusters around the river capture site, where the Río Aguas captured the Proto Aguas /Féos, and also upstream around Sorbas Town where there has been canyon development due to increased incision (Hart, 2004; Griffiths *et al.*, 2002; Griffiths *et al.*, 2005). This indicates that the landsliding may be related to landscape instability created by the rapid incision induced by the river capture event.

Rapid incision creates instability because it leaves little time for the affected hillslopes to adjust to the steepening of gradient by toe removal. This means that the landscape becomes inherently unstable. Although it is clear that the landslides in the Río Aguas catchment must be related in some way to the wave of incision created by the capture event it is unclear as to the exact timing of failure. It is possible that the landscape reacted instantaneously (in geological terms) to the increased incision and that successive landslide slippages occurred as the incision took place. Alternatively the landslides could have occurred later on once the wave of incision had passed upstream and could be linked to subsequent climate variability, with landsliding occurring during the wetter climatic phases as is thought to be the case with the La Cumbre slide by Mather *et al* (2003) of a large inactive (fossil) landslide complex. In this study,

Chapter 4: Cosmogenic exposure dating methodology

cosmogenic dating, using chlorine 36, was applied to a landslide associated with the main capture related wave of incision (the Maleguica landslide) in order to examine the issue of timing.

4.8.2 The Maleguica landslide

The Maleguica landslide is a large scale failure covering an area of 1 km with a volume of $3.14 \times 10^6 \text{ m}^3$ (Hart, 2004). It is situated to the south east of Sorbas town (Figure 4.17; UTM: 05780 41055) on the outside of a meander bend relating to the current active channel. The landscape surrounding the landslide is deeply entrenched with some 90 m of incision below the Góchar surface creating wide (500 m) canyons.

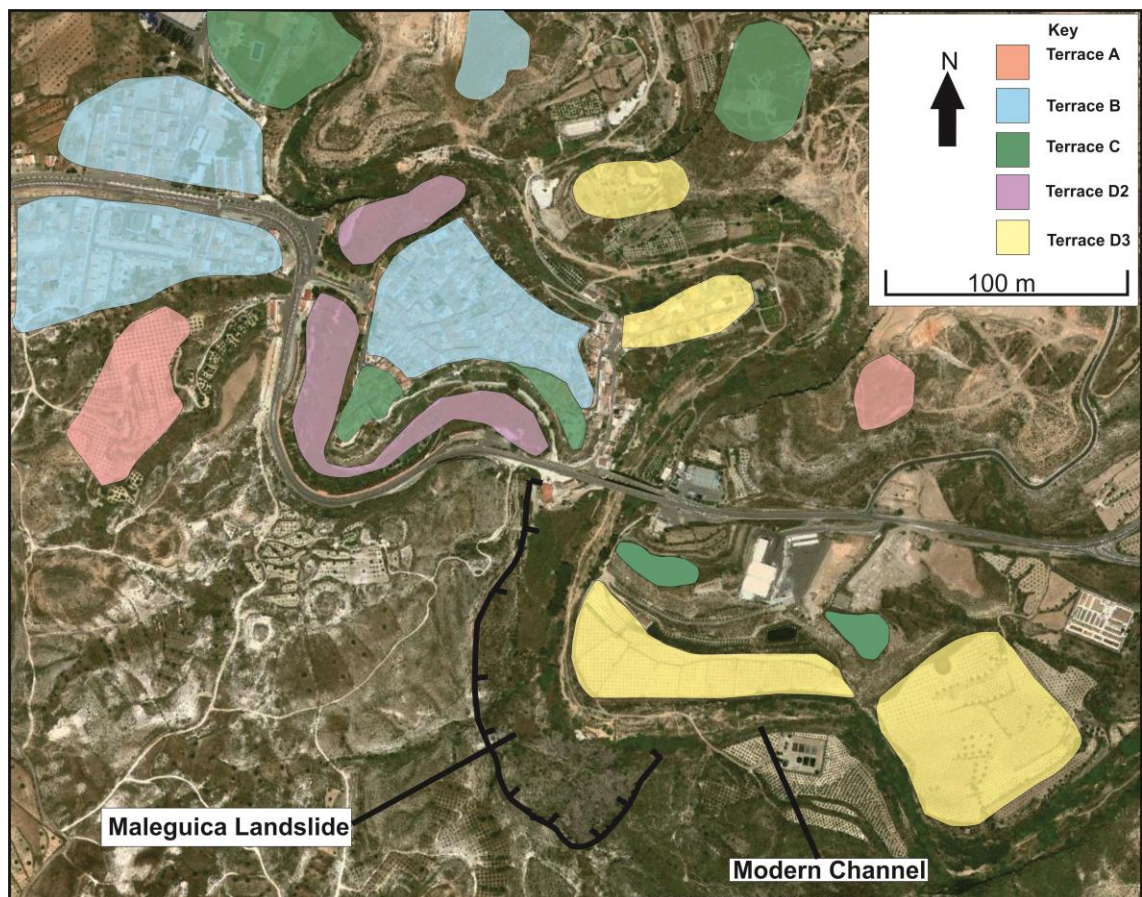


Figure 4.17: Location map for the Maleguica Landslide showing the proximity of the landslide to the modern river channel and terrace deposits. Image sourced from Google Earth & DigitalGlobe. Permission has been granted to reproduce this image by Google Earth.

Chapter 4: Cosmogenic exposure dating methodology

The failure occurs in the Sorbas Member (limestones, sandstones and calcareous mudstones) and the underlying Yesares Member (gypsum and calcareous mudstones) which dip to the N/NE into the current river channel. The failure mechanism on the Maleguica landslide is complex with several different types operating (rock falls, rock topples and non-rotational landslides) (Griffiths *et al.*, 2002; 2005; Hart, 2004). The toe of the landslide complex appears to be buried under the terrace D3 deposit, which occurs on the opposite side of the channel (Figure 5.10), giving a minimum age control of ~12 ka (Candy *et al.*, 2004). There appears to have been some sediment removal from the toe of the landslide as the current channel of the Río Aguas is entrenched into it (Hart, 2004).

4.8.3 Sample site selection

The sample site for the Maleguica landslide is located on the east side of the landslide 375 m.a.s.l (UTM: 05777946 4105847; Figure 4.18). The samples were collected from a section of exposed limestone rock that was discoloured to a dark grey/ black colour. The discolouring is caused by weathering of the rock which has been exposed for a long time period. Areas of fresh limestone outcrop were avoided as this would provide an age for the recent failure rather than the date of original/ main complex failure. The sample site was also selected due to limited shielding by the surrounding landscape.

4.8.4 Sampling methodology

Three blocks of limestone, approximately 20 cm by 20 cm were collected, with a hammer and chisel, from an area of the backscar of the landslide (Figure 4.18). The orientation, location (longitude and latitude) and height of the sample site above the sea level were all recorded. The angle of slope, orientation and angle to the highest topography were also recorded.

Chapter 4: Cosmogenic exposure dating methodology

4.8.5 Laboratory method

The landslide blocks were sent to the SUERC laboratories to be chemically prepared for analysis following the method of Stone et al. (1996) and Vincent et al. (2010). The main aim of the laboratory method is to remove isobar ^{36}S and prevent the loss of chlorine through selective volatilisation in the preparation process. High purity chemicals are used throughout the method to minimise contamination by natural sulphur and chloride containing compounds. Figure 4.19 shows the chemical processing steps involved in preparing a rock sample for ^{36}Cl analysis in an AMS. The chemical methods are further described in the next section of text.

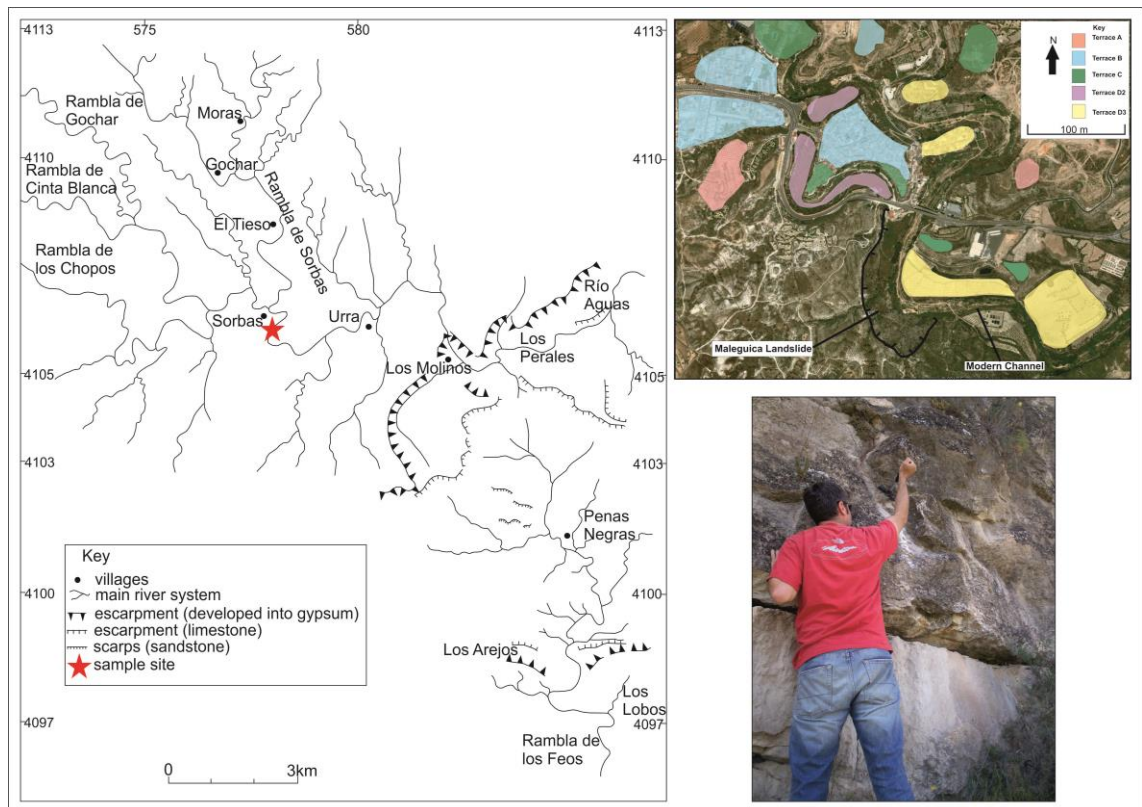


Figure 4.18: Location map and photo of the Maleguica sample site (UTM: 05777946 4105847). Image sourced from Google Earth & DigitalGlobe Permission has been granted to reproduce this image by Google Earth.

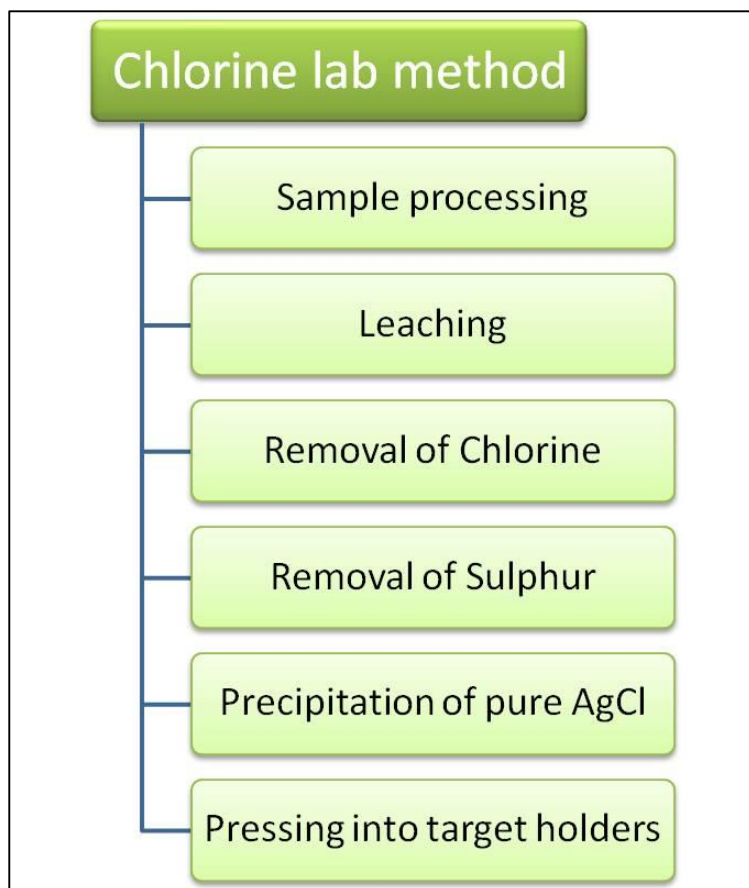


Figure 4.19: A schematic overview of the chemical methods used to prepare a rock sample for ^{36}Cl analysis. Method after Stone *et al.* (1996).

Before the samples were chemically processed, they were crushed using a rock crusher and then reduced to a finer grain size using a Tema mill. The samples were then sieved with the 250-500 fraction reserved for further processing. The AMS fraction was rinsed until no further fines could be washed out of it. The sample was then rinsed with de-ionised water and left to dry overnight. Once dry the samples were put through a Franz isodynamic magnetic mineral separator to remove grains containing very high susceptibility minerals.

The next process in the chemical methodology is to leach the samples to remove any meteoric contamination present on the surface of the grains. 20-25 g of the sample is placed in a beaker and mixed with ~100 mL MQ (ultra pure water) to wet the sample thoroughly. In a separate beaker 15 mL 2 HNO₃ and 50 mL MQ is mixed. The resultant liquid is then poured onto the rock sample and swirled gently to wet the grains. This

Chapter 4: Cosmogenic exposure dating methodology

process helps to get a slow and even dissolution of the grain surfaces. It also minimises the preferential dissolution of smaller grains (Stone *et al.*, 1996). The beaker is then covered and left to stand for 12-24 hrs. The sample is then rinsed 3-4 times with MQ and then the leaching process was repeated. After the second leaching took place the sample was rinsed thoroughly with MQ to ensure complete removal of $\text{Ca}(\text{NO}_3)_2$ and is then dried overnight in an oven at 70°C .

Sample addition takes place before dissolution to minimise the loss of ^{36}Cl . 3.5 mg of chlorine carrier is added to the samples before dissolution in 10 mL 2M HNO_3 (trace metal grade) and 13% ultrapure HF. The solution was then spun by a centrifuge to separate out chloride from the fluorides that formed during dissolution. The chloride is then removed from the sample solution by precipitation of rough AgCl from hot solution.

The next stage of chemical processing removes the sulphur from the sample by dissolution. The rough AgCl is first dissolved in 2 mL of 1:1 NH_3 and 10 mL of MQ. 1 ml of saturated $\text{Ba}(\text{NO}_3)_2$ solution is added and mixed with the NH_3 solution. The sample is then covered and left for 48 hrs in the dark. The sample is left in the dark as light causes the decomposition of the chemical compound used during this process. After being left to settle, the precipitate formed is allowed to fall to the bottom of the tube by gentle tapping the base. The sample is then centrifuged at 220 RPM for 5-10 minutes. A pipette is then used to transfer the liquid that is present beneath the meniscus to a clean polypropylene centrifuge tube. A little of the liquid is left behind in the bottom of the tub to avoid contamination by BaSO_4 (Stone *et al.*, 1996).

The sample is now processed to precipitate the final pure AgCl that is measured in the AMS. To form the pure AgCl, 2 M HNO_3 , 1 mL 10% AgNO_3 and MQ water is added to a breaker and heated on a hotplate until the volume drops to 35 mL. Once the liquid is

Chapter 4: Cosmogenic exposure dating methodology

being to boil, it is removed from the hotplate and the AgCl solution is added. MQ is used to rinse out the centrifuge tube that contained the AgCl solution and is added to the breaker. The beaker is then returned to the hotplate for 1 hour. The sample is then left to cool for 30 minutes, covered and left in a dark place for 2-4 hours to allow the AgCl to settle out.

Once cooled, the supernatant is removed without disturbing the AgCl precipitate. The AgCl precipitate is then washed into a centrifuge tube using MQ. The bottom of the centrifuge tube was then tapped to cause the precipitate to lump together. The sample is then centrifuged in order to remove any final liquid from the precipitate. The precipitate is then left in an oven overnight at 60-70°C to dry.

Finally the sample was pressed into high purity AgBr (99.9% metal basis, Alfa Aesar) 6 mm diameter Copper target holders ready for AMS analysis. The ^{36}Cl content was measured with isotope-dilution AMS at 5 MV (Wilcken et al., 2009).

4.9 Neon dating

In the Jauto catchment an erosion surface possibly equivalent to a terrace A or the Góchar surface in the Río Aguas catchment has been sampled for Neon dating. A date for this surface would provide the beginnings of an absolute chronological framework for the Jauto system to back up the relative chronology of the terrace deposits.

4.9.1 Sample site

The Neon sample site (UTM: 0583948 4111373) is located in the Río Jauto section on an erosion surface that is present upstream of Los Castaños (Figure 4.20). The site is located on top of a prominent ridge that is 419 m.a.s.l and 30 m above the modern river channel. The erosion surface is formed on an outcrop of tourmaline gneiss which is part

Chapter 4: Cosmogenic exposure dating methodology

of the metamorphic basement of the Sierra de los Filabres (Nevado-Filabride Complex).

The sample site was selected because there was limited shielding from surrounding topography and limited weathering on the selected rock outcrop.

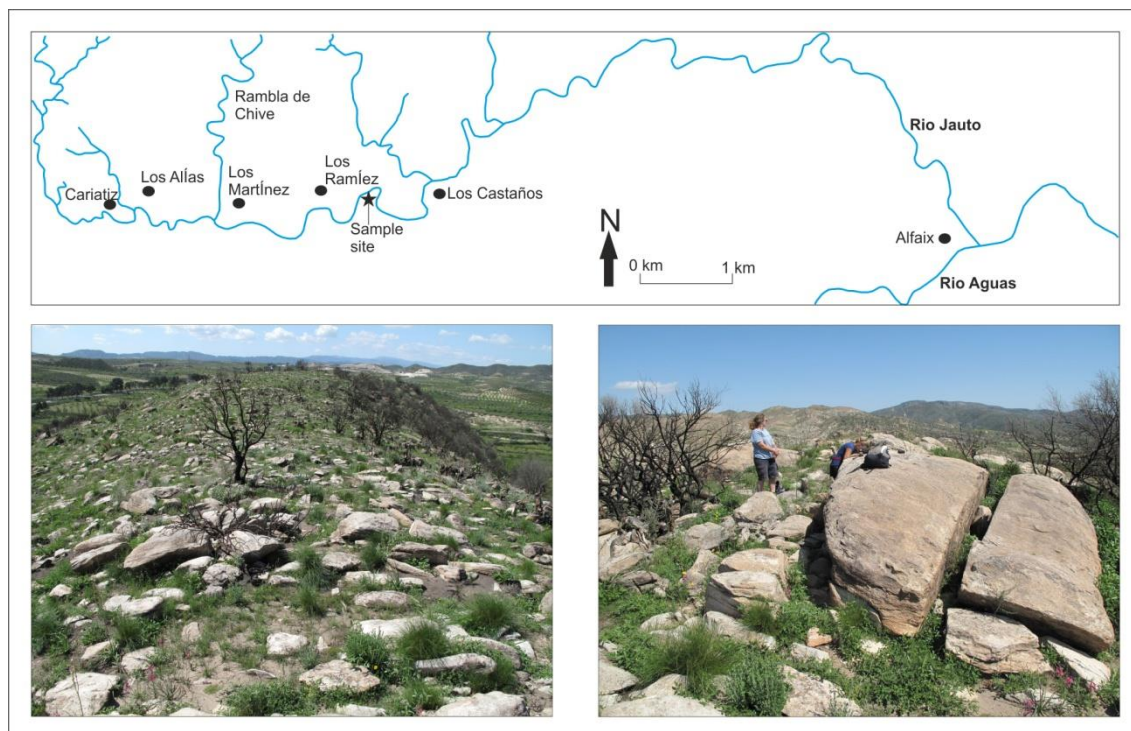


Figure 4.20: Photos and location map for the erosion surface in the Río Jauto sampled for Neon dating (UTM: 0583948 4111373).

4.9.2 Sampling method

In order to determine the concentration of cosmogenic neon within the rocks on the erosion surface two blocks of Tourmaline gneiss, greater than 20 cm in size, were collected from surface exposures on the top of the erosion surface using a hammer. The rock samples were from areas on the top surface of the rock exposure that were relatively free from weathering to prevent degradation of the samples. Angle of slope, orientation, angle to the highest topography, location (longitude and latitude) and height above sea level were all recorded.

Chapter 4: Cosmogenic exposure dating methodology

4.9.3 Laboratory method

Preparation of the sample for Neon analysis was undertaken at the SUERC laboratory in East Kilbride. The samples were first crushed in a rock crusher and then further reduced in size to a 250-500 μ m fraction. The samples were first picked under a microscope so that pure quartz grains are separated out from other minerals in the sample. The pure quartz grains are then left in Nitric acid (HNO₃) for 5 hours on a hotplate at 80°C and then leached in hydrofluoric acid (HF-2%) and HNO₃ for 24 hours at 80°C. The quartz is then rinsed thoroughly with water and afterwards further cleaned in ultra-pure acetone. 500 mg of sample are then packed into aluminium foil packets. Samples were analysed by the SUERC laboratories.

4.10 Summary

The above chapter has provided an explanation of cosmogenic dating. The main sampling methodology has been described and the theoretical background of the concentration profile sampling methodology discussed. The rationale behind the choice of sample site has been explained and the sample sites described. Chlorine and Neon dating has also been described in detail with sampling methodology, sample sites and sample preparation discussed for each cosmogenic nuclide. The methodology of statically modelling the AMS data and the results of cosmogenic dating are presented in Chapter 7.

Chapter 5: The Proto Aguas/Féos fluvial archive

5.1 Introduction

This chapter focuses on the Río Aguas and more specifically the fluvial archive relating to the Proto Aguas/Féos fluvial system, the main axial drainage for the Sorbas basin prior to the river capture event (~ 80 Ka) that created the modern Rio Aguas system (Chapter 2). The Proto Aguas/Féos was the initial drainage system that formed by incision into the top basin fill surface (the Góchar surface) as a west-east flowing drainage system. The system was sourced in the northern and southern basin margin and was then routed in an eastward direction down a weakly folded synclinal basin axis where the system exited the basin to the south through a gap in the Sierra Alhamilla/Cabrera into the Carboneras basin (Figure 2.6). A flight of river terraces are formed by the Proto Aguas/Féos consisting of four major landform levels labelled A-D (Section 2.5). This chapter is used to present the sedimentology of the river terrace deposits relating to the Proto Aguas/Féos using data collected in the field. Palaeohydrology data and tectonic data for the terrace deposits are also presented. The aim of the chapter is to provide the field context for the cosmogenic exposure dating sample sites and also to explore the magnitude of flood events taking place in the Proto Aguas/Feos fluvial system using palaeohydrology equations (chapter 3).

5.2 Pre Terrace A erosion surface

The Góchar surface marks the top of the Góchar Formation (Appendix 2) which represents the final stage of basin infilling before the switch to incision occurred (Chapter 2). The Góchar surface appears as a topographically flat surface when viewed obliquely from the basin margin settings; however in reality it forms an undulating

surface separated by river valleys (Figure 5.1). Inset into the Góchar formation are a series of river terraces and also an erosion surface which occurred prior to deposition of terrace A. The erosion surface can be seen in the DEM data for the Sorbas basin area (Appendix 2).

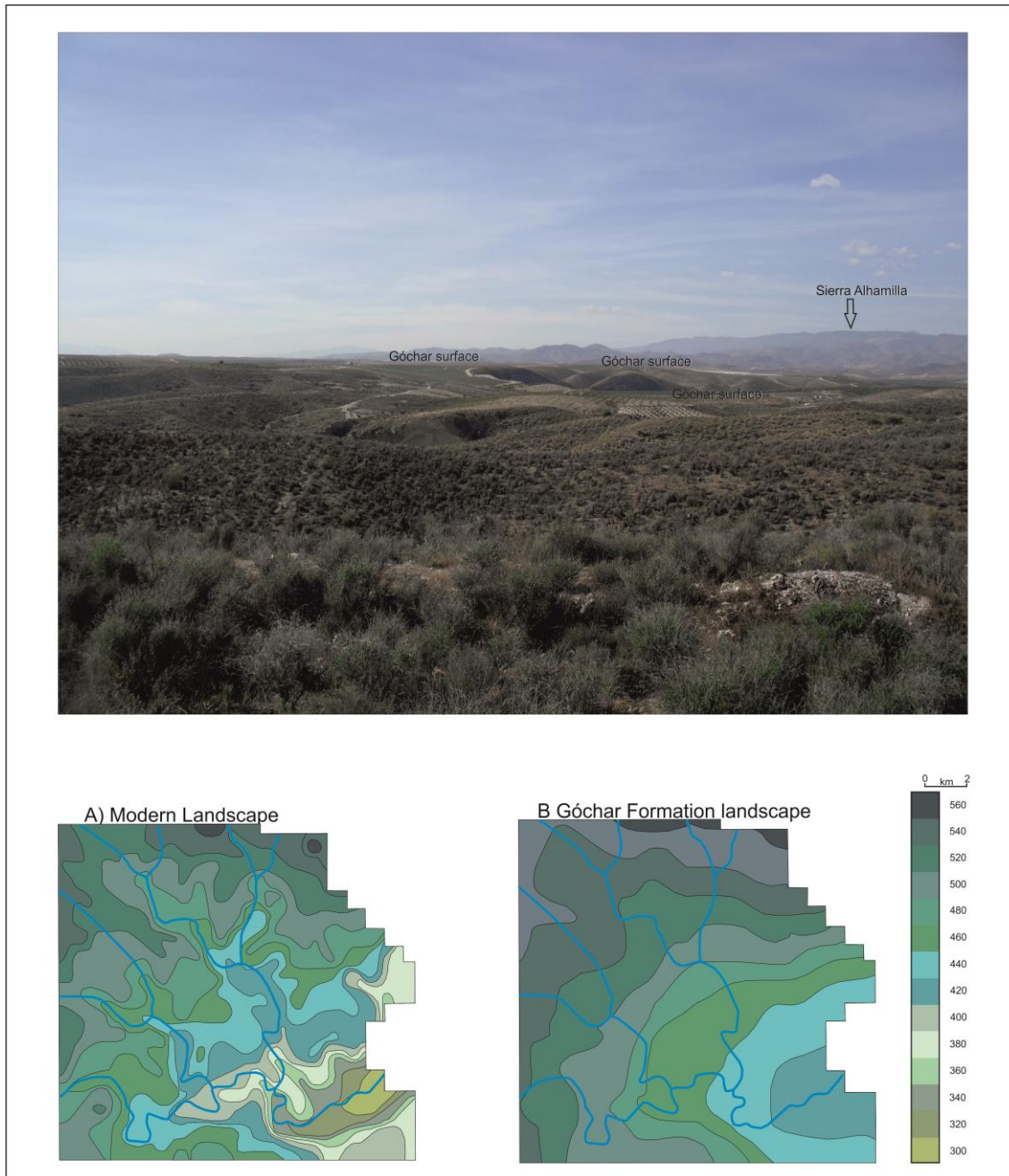


Figure 5.1: The Góchar surface: 1) View looking SW across the basin showing the Góchar Formation top basin fill surface 2) Topographic expression of the Góchar surface 3) Góchar surface pre fluvial incision (modified from Stokes *et al.*, 2002).

5.2.1 Type locality summary

The pre terrace A erosion surface type locality is a 30 m road cut that is located near the village of Góchar (UTM:0575756 4109450; Figure 4.7) at 500 m a.s.l. The site consists of two exposures that run parallel to each other orientated N/S.

The terrace sediments consist of 6 m of clast supported cobble/pebble conglomerates (Figure 5.2). The sub angular to sub rounded clasts have an average size of 7 cm ($D_{\max}=27$ cm). The sediments are poorly sorted with rare imbrication and erosive contacts. The conglomerates are highly cemented (Gm). Occasionally the gravels contain a fine sandy matrix. There are also some well sorted, clast supported pebble/gravel beds present. Provenance data, which has been collected for all the type sections (Chapter 3), is presented in Figure 5.3. The provenance of the conglomerates is characterised by clasts sourced from the basement (93%) with the source area of the clasts being from the northern basin margin (Sierra de los Filabres).

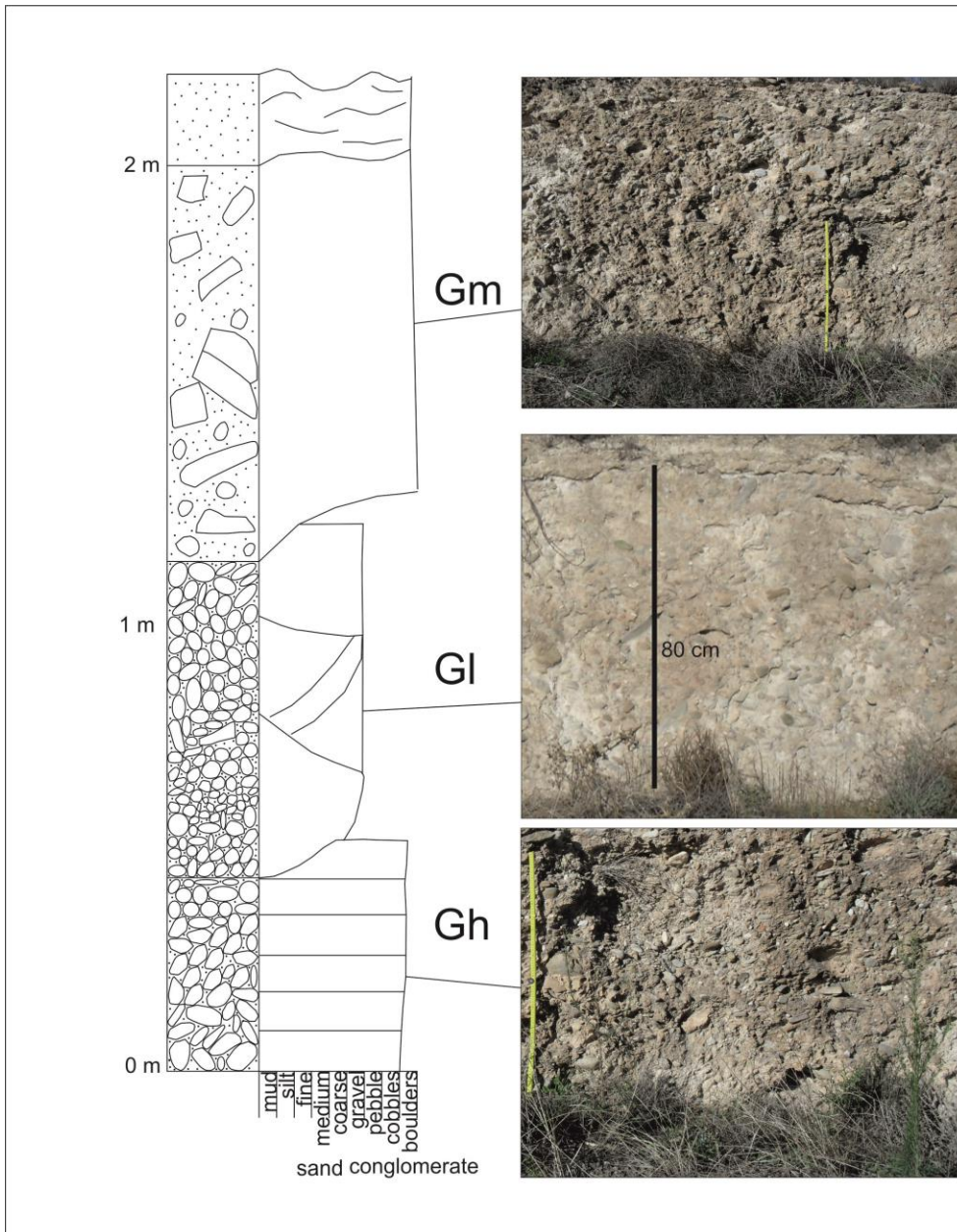


Figure 5.2: Sedimentary log for the Pre Terrace A type section.

The eastern side of the exposure is characterised by horizontally bedded clast supported cobble conglomerates (Gh) and low angled cross bedded gravel/pebble conglomerates (Gl) (Figure 5.4). The lithofacies Gh are present at the base of the section and grade upwards into the Gl lithofacies. The Gh and Gp lithofacies laterally grade into lithofacies Gl.

Lithofacies Gp comprises of high angled cross bedded gravel/cobble conglomerates. The gravel/cobble conglomerates are very well sorted and are clast supported.

Imbrication of the clasts occurs with the mean transport direction being to the north (n=10).

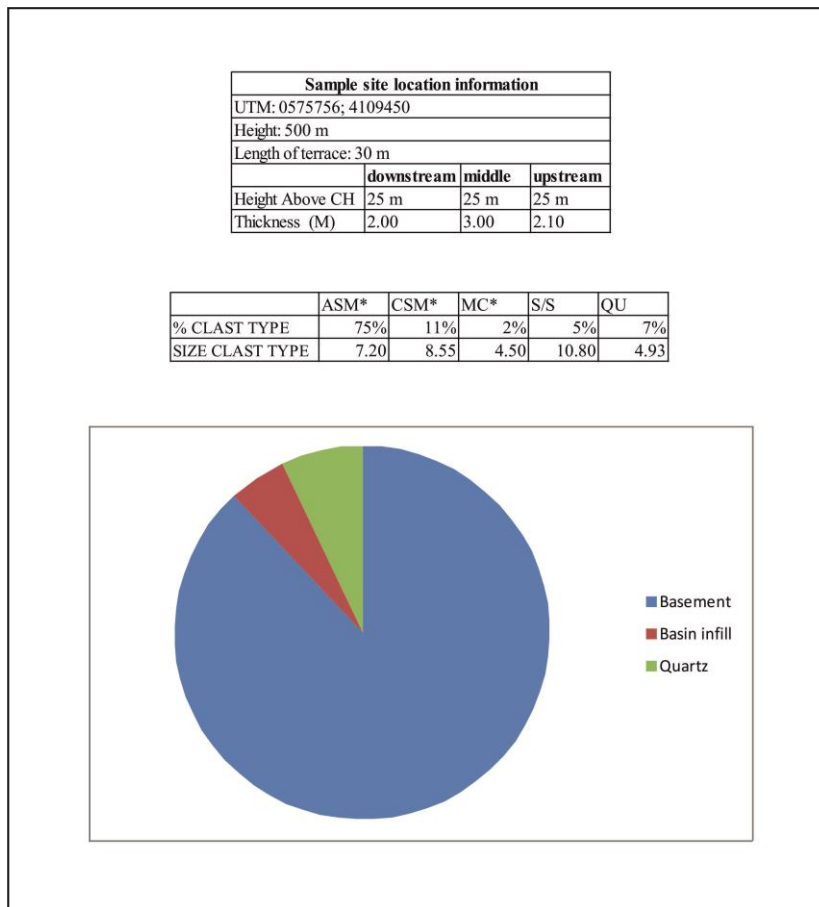


Figure 5.3: Provenance data for the Pre Terrace A erosion surface.

The western side of the deposit is dominated by very well cemented, poorly sorted, massive, clast supported cobble/pebble conglomerates which has a fine sandy matrix (Gm). The average clast size at the base of the unit is 5 cm with rare imbrication of the clasts. The massive conglomerates coarsen upwards into a clast supported cobble conglomerate ($D_{50}=15\text{cm}$). The cobble clasts are supported by pebbles and gravels infilling between the larger cobbled sized clasts.

Figure 5.5 is a series of photos of the described deposits and it illustrates the 10 cm thick stage IV laminar calcrete which forms an undulating layer at the surface of the deposit. The calcretes can be seen 30 cm below the surface in the photo. This calcrete

appears to follow an erosion surface that has formed at the surface of the gravels. A 30 cm thick dark red soil then caps the calcrete and the deposit. The soil gives an average Munsell reading of 7.5 Yr 4R.

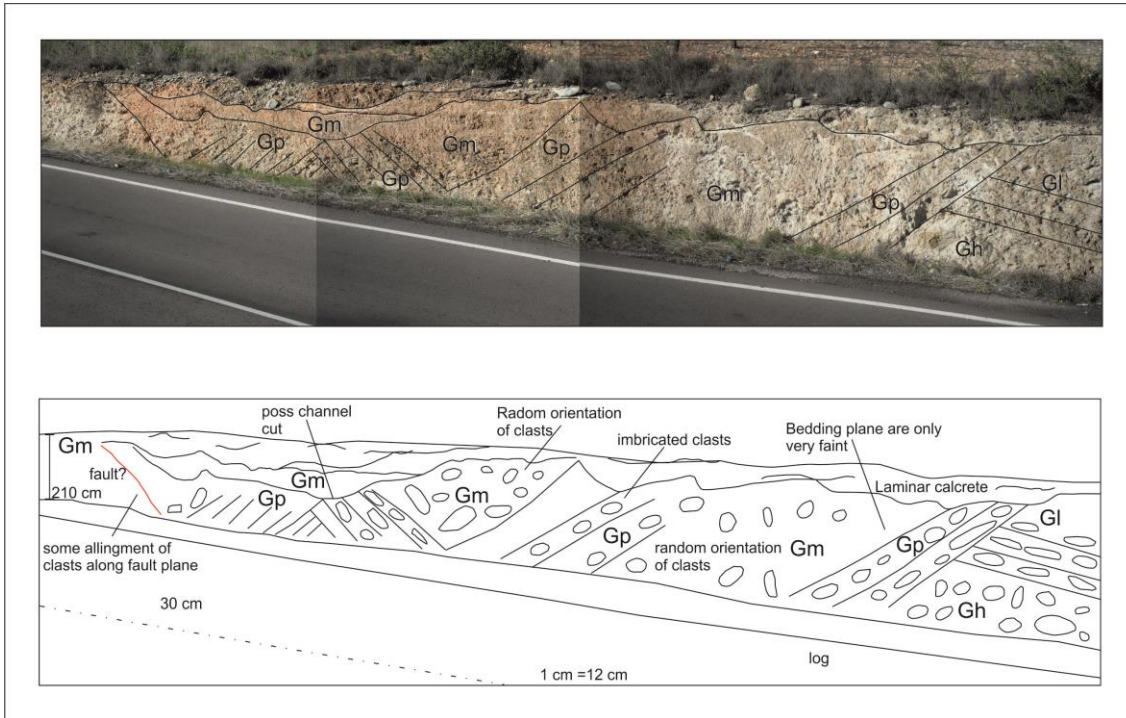


Figure 5.4: Photo sketch of the Pre Terrace A type section.



Figure 5.5: Series of photos showing the characteristics of the Pre terrace A type section.

5.2.2 Interpretation

The clast provenance data suggests that the main source of clasts was the Sierra de los Filabres. The dominance of clasts of basement origin and the lack of clasts originating from the older (Miocene) basin infill indicates that the river has not yet incised into the sedimentary infill of the Sorbas basin. This would make sense as the pre-terrace A erosion marks the first stage of basin fill incision into the sedimentary fill.

There are four facies types that can be identified from the pre-terrace A erosion surface type locality (Figure 5.4); Gm, Gh, Gp and Gl. The facies types indicate that a fluvial system, possibly braided in nature, dominated by weak longitudinal bars was forming. The massive, poorly sorted nature of the Gm facies along with the erosive contacts

suggests that they were transported by a high energy flow in thin diffuse sheets. The Gm facies were then deposited as the internal friction of the flow increases due to a drop in stream power (Miall, 1996). Both high angle (Gp) and low angle (Gp) cross stratification are present. The Gp and Gl facies suggests that lateral accretion and downstream aggradation took place possibly prograding out from a bar core formed from the Gm facies.

5.3 Terrace B

Terrace B landforms are found throughout the Sorbas basin (Appendix 1b) ranging in height from 496-380 m.a.s.l. The base of the terrace B deposits occur around 24-47 m below the bases of the terrace A deposits at a height of 22 m above the modern Río Aguas.

5.3.1 Type section summary

The terrace B type locality is a single terrace landform located near the village of Góchar (0577312 4109292- Figure 4.8) in the Rambla de Góchar. The terrace gravels are exposed in a road cut (100 m long) present on the south side of the modern Rambla de Góchar and the west valley side of the modern Rambla de Sorbas. There are two exposures of the sediments both orientated E/W with one north facing section and one south facing section. The terrace base is 43 m above the modern stream bed at a height of 454 m a.s.l.

The terrace B sections comprise of up to 5 m thick sediments with a metre scale undulating contact with the underlying Góchar Formation. The sediments are coarse

clastic gravel to cobble grade sediments with an average clast size of 6 cm ($D_{max}=22$ cm). The clasts are sub angular to sub rounded in nature and display very poor to moderate sorting. Clasts commonly show imbrication with mean transport direction to the northeast. Metamorphic basement dominates provenance with ~80% sourced from the basin margins with a limited 4% input from the basin sedimentary fill. Quartz clasts make up the other 16% of the clast assemblage (Figure 5.6).

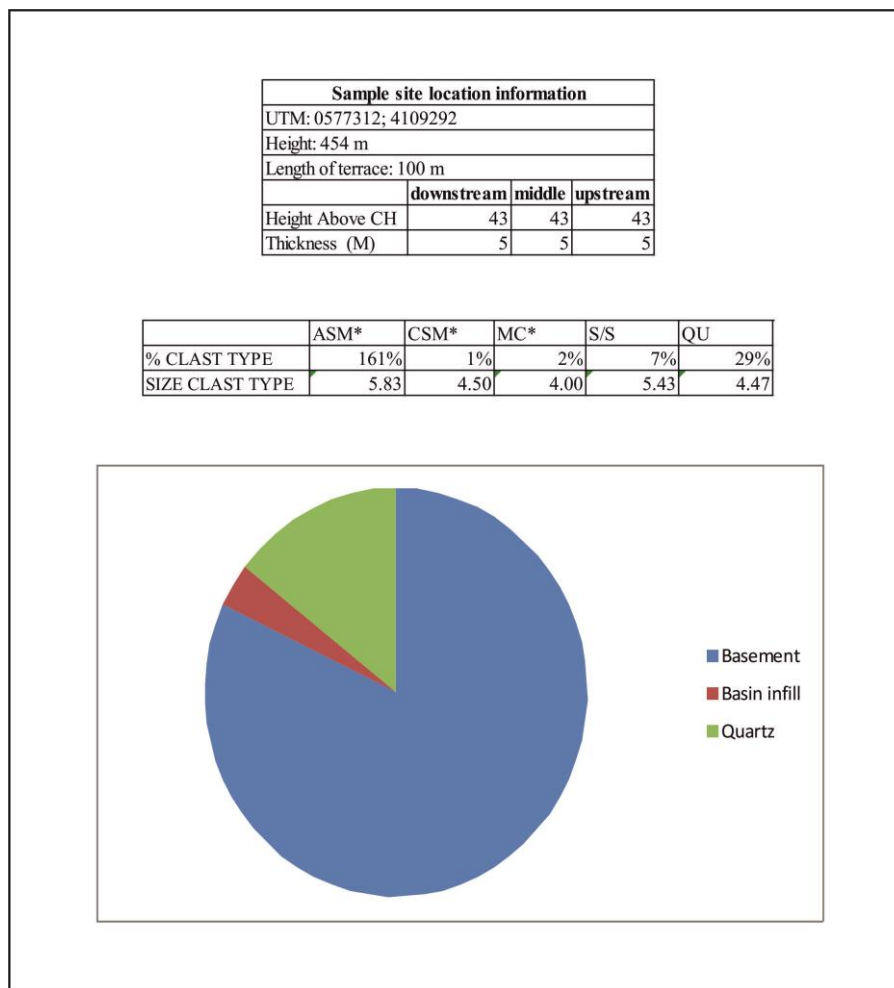


Figure 5.6: Provenance data for the Terrace B type section.

The terrace sediments consist of horizontally bedded pebble/cobble clasts (Gh facies), which are well imbricated, low angle cross bedded sediments (Gl facies) that show coarsening upwards trends and trough cross bedded gravels/pebbles (Gt facies). The

exposure can be subdivided into two distinct groups of sediments facies; group 1 characterised by Gh facies and group 2 consisting of G1 and Gt facies (Figure 5.7).

Group 1 is present on the eastern side and also on the very edge of the western side of the section. The sediments of group 1, lithofacies Gh, display coarsening upward features with beds grading from pebble clasts to cobble size clasts (Figure 5.8). The largest clasts recorded are generally found within this group ($D_{\max} = 22$ cm). The beds dip towards the north east at a very low angle (4°).

The sediments in group 2 are present towards the centre and western edge of the deposit. This group contains the lithofacies G1 and Gt. The lithofacies G1 comprise of 20 cm thick concentrated pebble and gravel beds which dip to the south (10°) (Figure 5.8). The G1 beds at the bottom of the section are more gravel dominated whereas in the middle of the section the sediments fine to pebble grade beds that are supported by a fine grained sandy matrix. The individual beds themselves show coarsening up trends that occur at a 20 cm scale.

The Gt lithofacies are also present in group 2. The trough cross bedding in the section is formed by gravel and pebbles clasts. The clasts fine upwards to sand grade material. The average clast size on the Gt lithofacies is 2 cm with the finer clasts picking out the bedding planes. The beds are on average 30 cm in thickness. The sediments are cut by numerous erosion surfaces that are concave upwards. The erosion surfaces range in size from 4 m deep to 1 m deep. The biggest erosion surface is around 4 m deep and 5 m wide. The trough cross bedding and the low angled cross bedded sediments infill the erosion surfaces. There are also lenses of very well sorted gravels present.

The base of group 2 is marked by a large erosion surface that cuts the horizontal bedding of group 1 (Figure 5.8). The sediments of group 2 have then in filled the concave erosion surface.

Towards the top of the section 10 cm of deep red fine sand grade sediments are present. The terrace sediments are capped by stage III-IV calcretes represented by nodular carbonates which are cemented together to form a hard layer across the surface of the terrace. The calcrete is then capped by a soil which recorded a Munsell reading of 2.5 YR 5R.

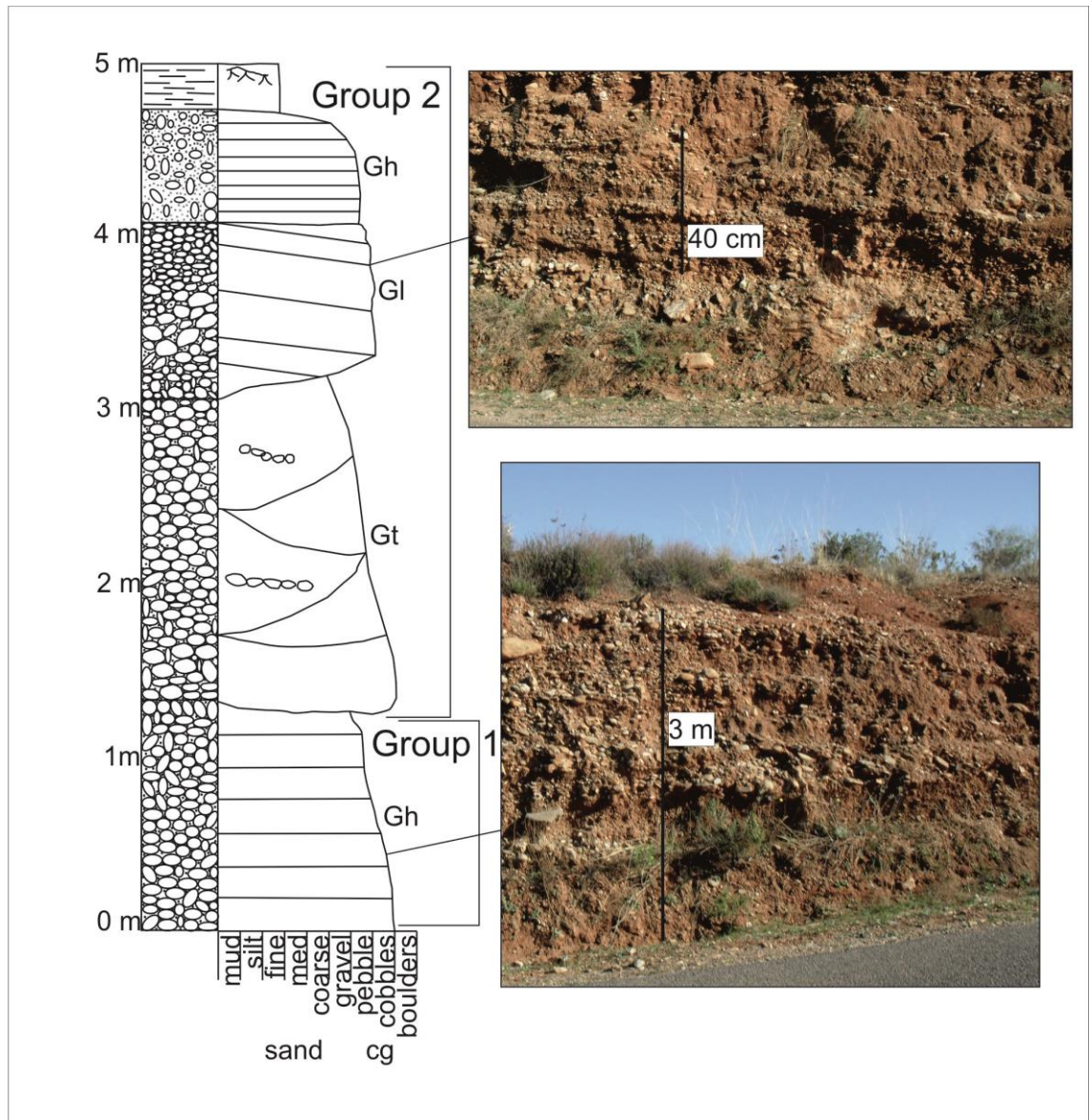


Figure 5.7: Sedimentary log of the Terrace B type section log.

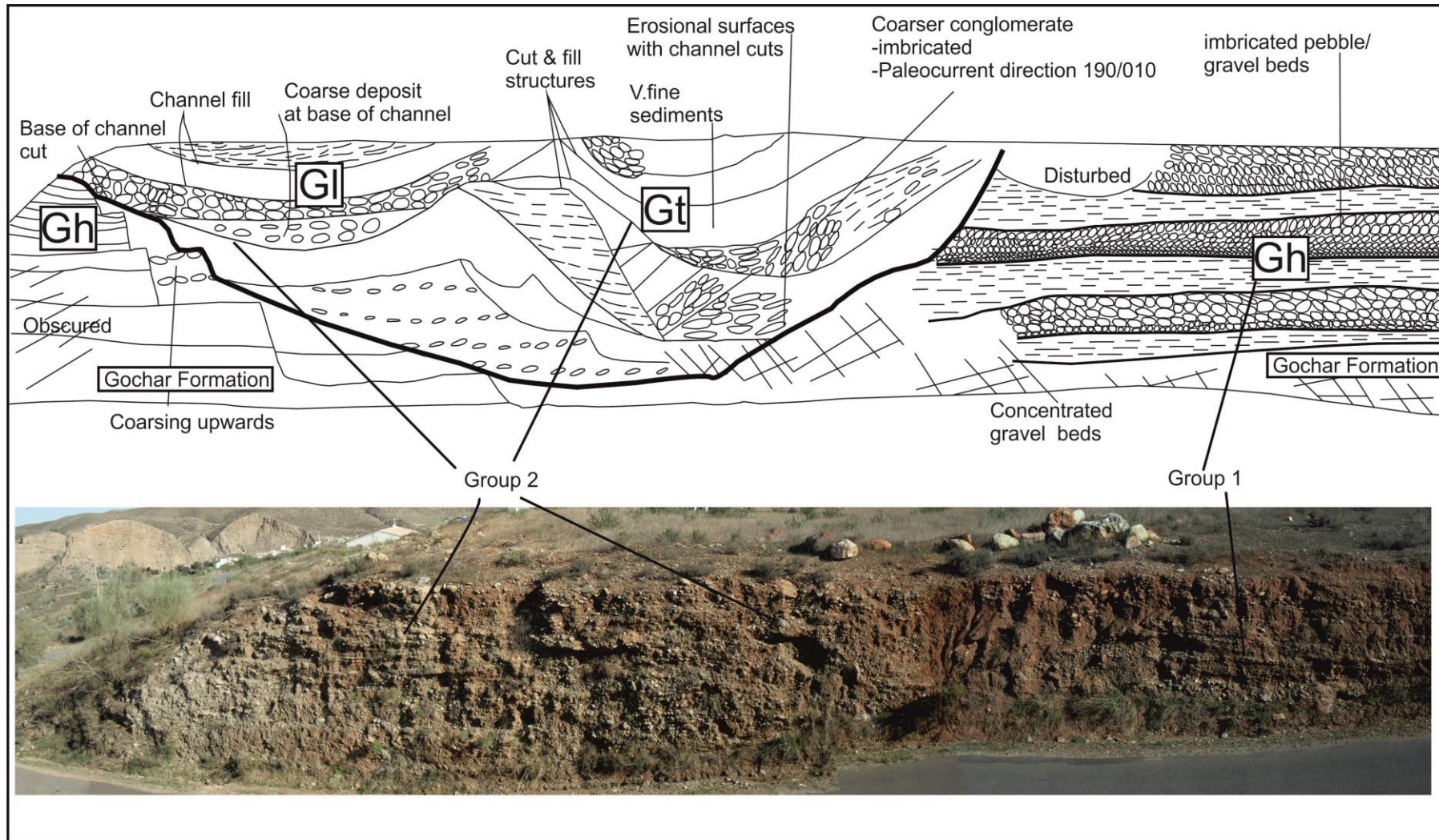


Figure 5.8: Photo sketch of the Terrace B type section showing the main sedimentary characteristics of the site.

5.3.2 Interpretation of sequence

The development of the terrace B type locality occurred in two stages. The first stage was the deposition of 5 m of horizontal bedding which make up the group1. Gh facies are deposited during episodes of high water and sediment discharge with the clasts moving as sheets (Miall, 1996). The erosional base of the terrace into the Góchar Formation sediments indicates that there were strong flows bringing sediment down the channel scouring the base of the channel. The clast-gravel rich sheets build upwards by clast addition to the top surface of the sheet to form a horizontally stratified gravel longitudinal bar. The coarsening upwards nature of the Gh facies, seen in Figure 5.8, indicates that bar migration was occurring downstream with coarser material depositing over the fine top material of the lower bar form (Miall, 1996). The flow direction indicated from palaeocurrent measurements on imbricated clasts in the section is to the south.

After bar formation a large channel developed into the bar creating a concave upwards erosion surface that marks the top of group 1 (Figure 5. 8). The channel, which is 5 m wide and 4 m depth, was in filled by Gt and Gl facies. The low angled cross bedding and trough cross bedding migrate out from the channel margins in-filling the channel.

Towards the top of the section deep red (2.5 YR 5 red) fine sand grade sediments are present possibly relating to weakening flows as the channel was abandoned. The dark red colour at the top of the section could relate to soil development.

The sediments in the terrace B type locality represent deposition by a longitudinal bar forms (Gh) possibly in a braided system. An erosive event took place with a channel being cut into the bar sediments which are then in filled by channel facies (Gt and Gl facies).

5.4 Terrace C deposits

Terrace C deposits are present across the whole catchment of the Proto Aguas/Feos. The terrace C deposits range in height from 400 to 300 m.a.s.l. They are present 10- 80 m above the present river channel.

5.4.1 Terrace C type section sedimentology

The level C type section locality (UTM: 0575574 4111057) forms part of a single terrace landform developed on the northern side of the valley side of the modern Rambla de Góchar (Figure 4.11). The terrace is exposed by a man-made trench in an olive grove which provides two sections; a north west-south east orientated one and a north-south orientated section.

Terrace gravels at this locality are up to 4 m thick with an undulating contact (~30 cm relief) with the Góchar Formation below. The sediments are medium grained gravels and range from sub angular to rounded in shape. The average clast size of the deposit is 4 cm. Large cobbles are frequently found in the deposit ($D_{max}= 14$ cm). The terrace gravels coarsen upwards. Coarse clasts often mark the base of the cross bedded sections. Clasts are rarely imbricated. Where imbrication occurs the mean transport direction is to the southwest (n=10).

The gravels are moderately sorted with finer clasts (small pebbles and sand grains) infilling around the larger clasts. The provenance of the clasts is characterised by metamorphic basement lithologies (schists, metacarbonates) sourced from the northern basin margin (Sierra de los Filabres) (Figure 5.10).

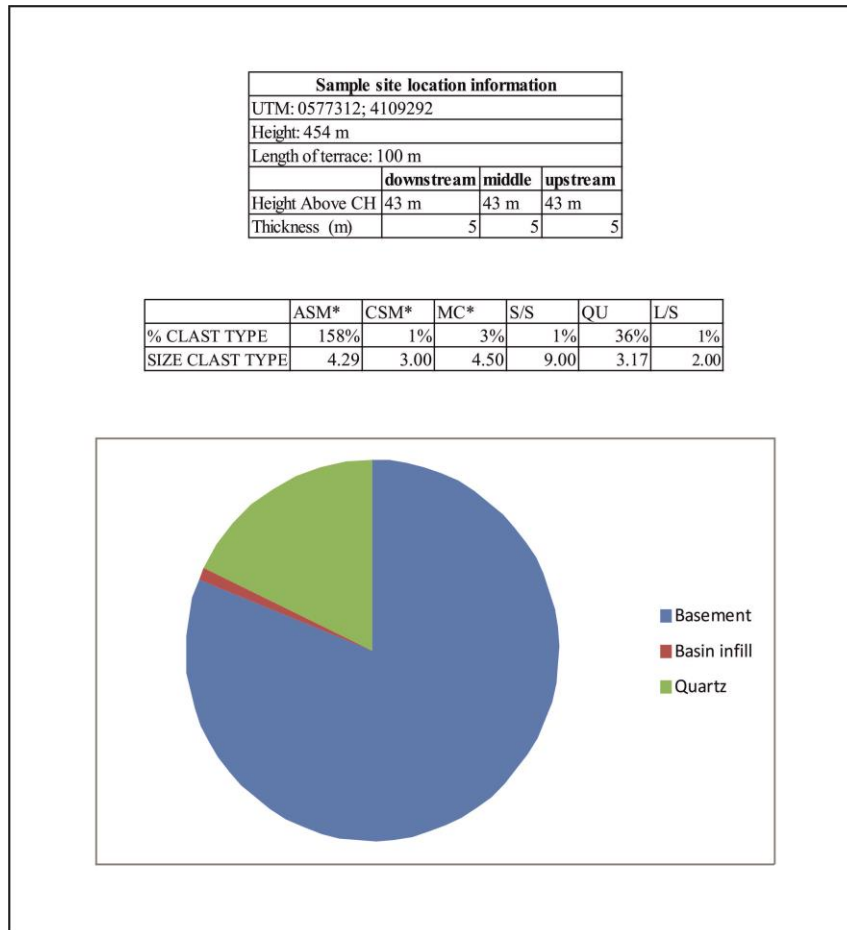


Figure 5.9: Provenance data for the terrace C type locality.

The terrace sediments contain 40 cm thick weakly cross stratified beds which can be traced laterally across the section. The cross-bed foresets strike NW/SE and dip at around 20°. Figure 5.11 is a sedimentary log taken from the exposure shown in photo B (Figure 5.12).

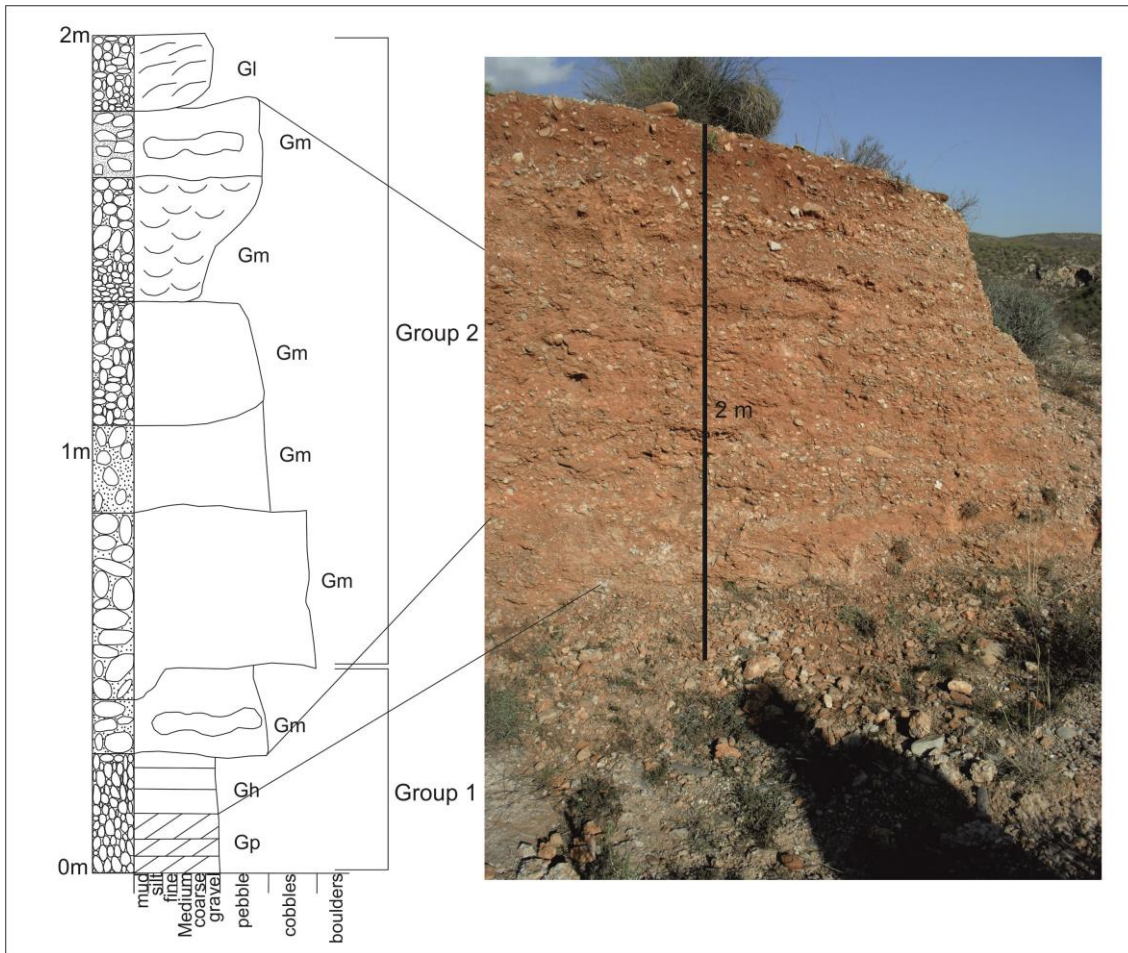


Figure 5.10: Sedimentary log for the type locality G3

The G3 section can be sub-divided into two groups; Group 1 is dominated by cross stratified (Gp) and horizontally bedded sediments (Gh) whilst Group 2 is characterised by massive structureless beds (Gm). The subdivision of the sediments into stratigraphic units is based on sedimentary characteristics and the presence of bounding surfaces.

Group 1 occurs in basal parts of the section and forms an undulating contact (metre scale) with the underlying Góchar Formation. The basal parts of Group 1 are dominated by the lithofacies Gp with cross stratified sediments build in a northwest direction.

Group 1 is capped by 20 cm of horizontally bedded sediments that contains small cobble clasts that mark the bottom of the individual beds. The clast sizes of the Group 1 are noticeably finer ($D_{max}=3$ cm) than those in Unit 2.

Group 2, which is located in the top few metres of the section, is characterised by massive structureless sediments whose clasts are randomly orientated. Occasionally imbrication of clasts occurs in small pockets of finer sediments. The sediments of Group 2 are coarser in nature than those of Group 1 with an average D_{max} of 5 cm. Large cobbles found in the type locality deposit are generally occur in Group 2. The top of Group 2 is capped by 30 cm of fine pebble clasts with occasional larger clasts floating within the finer matrix.

The terrace exposure is capped by a 20 cm thick red soil (Munsell: 2.5 YR 5 red) which contains calcretes of a stage II/III with a 2 cm hardpan calcrete (stage III) covering the top of the terrace gravels (Figures 5.11 & 5.12).

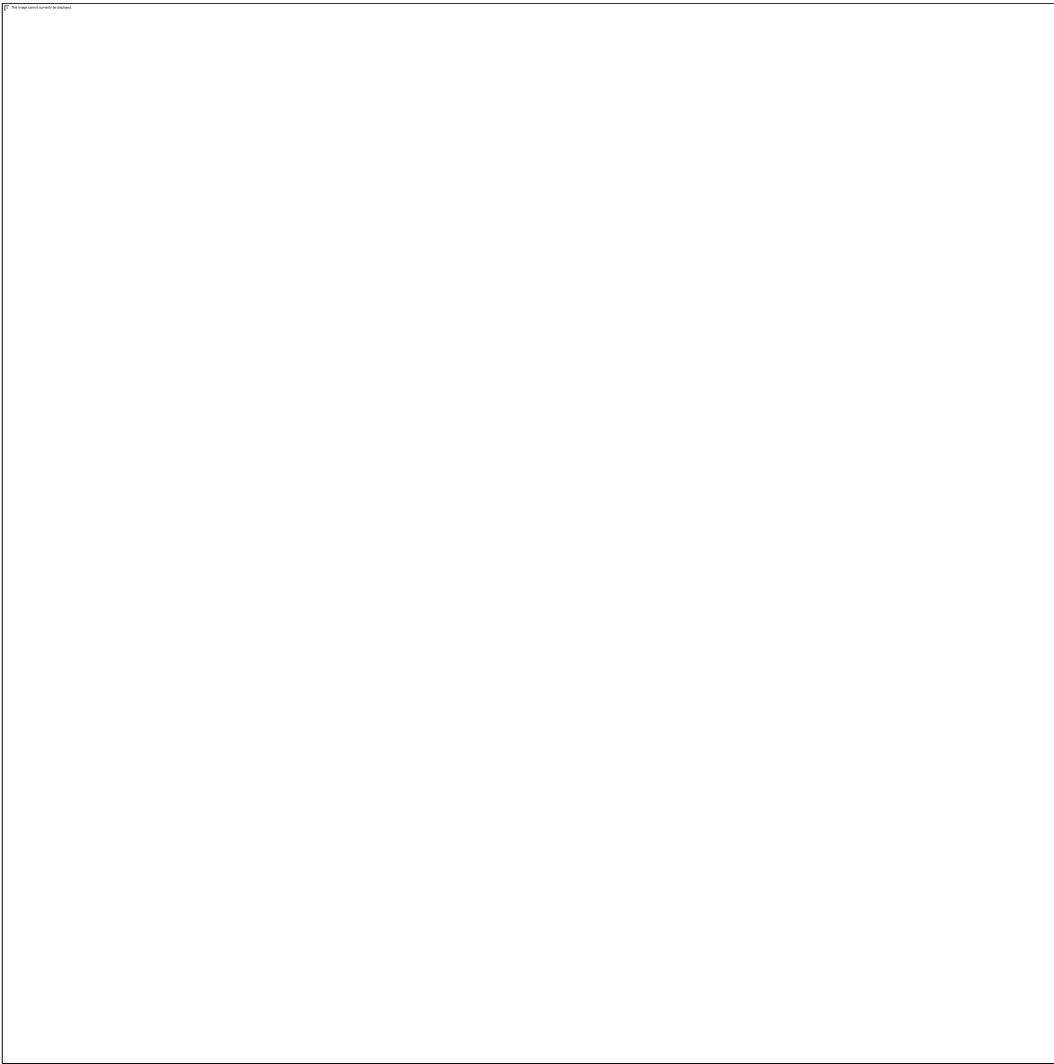


Figure 5.11: Photo and sketch of the type locality for terrace C showing the facies groups present. The section is located in the Rambla de Góchar (Figure 4.10 UTM: 0575574 4111057).

The type locality for terrace C has undergone localised normal faulting that trends NE/SW (section 4.6.5; Figure 4.13). Figure 5.13 illustrates evidence for localised faulting of the section that occurs within Group 1. Deformation of the section is characterised by disruption to the sediments occurs across a 1 m width of sediments where the horizontal layering has been deflected downwards by the faults. Between the two faults the clast organisation has been disrupted so that the gravels appear structureless in nature. Clasts present at the edges of the faulted zone have been displaced so that they are vertical following the path of the fault. The laminar calcrete capping the faulted sediments has not been deformed by the fault. This would suggest

that deformation by the fault occurred before the calcrete formed and was no longer active when the calcrete was forming.

Plio/Quaternary faulting of soft sediments in the Sorbas basin has been described by Mather & Westhead (1993). Regional fault patterns have been described by Stokes (1997; 2008) with a focus on the Vera Basin. Work by Mather & Westhead (1993) and Stokes (1997; 2008) indicates that regional deformation occurs in two directions NNE/SSW and NNW/SSE.

In the Sorbas Basin, deformation of Plio/Quaternary sediments has previously been noted in the Góchar Formation (Mather, 1991; Mather & Westhead, 1993) and in terrace D deposits situated around Urrea (Mather, 1991; Mather *et al.*, 2001; Harvey, 2001). The deformation at Urrea could be related to the Infierno-Marchalico Lineament (after Mather & Westhead, 1993) that crosses this area. The deformation recorded at the terrace C type locality follows the regional direction of NE/SW. The deformation pattern is believed to have formed as a response to the E/W extension occurring in the region (Mather & Westhead, 1993; Stokes, 2008).

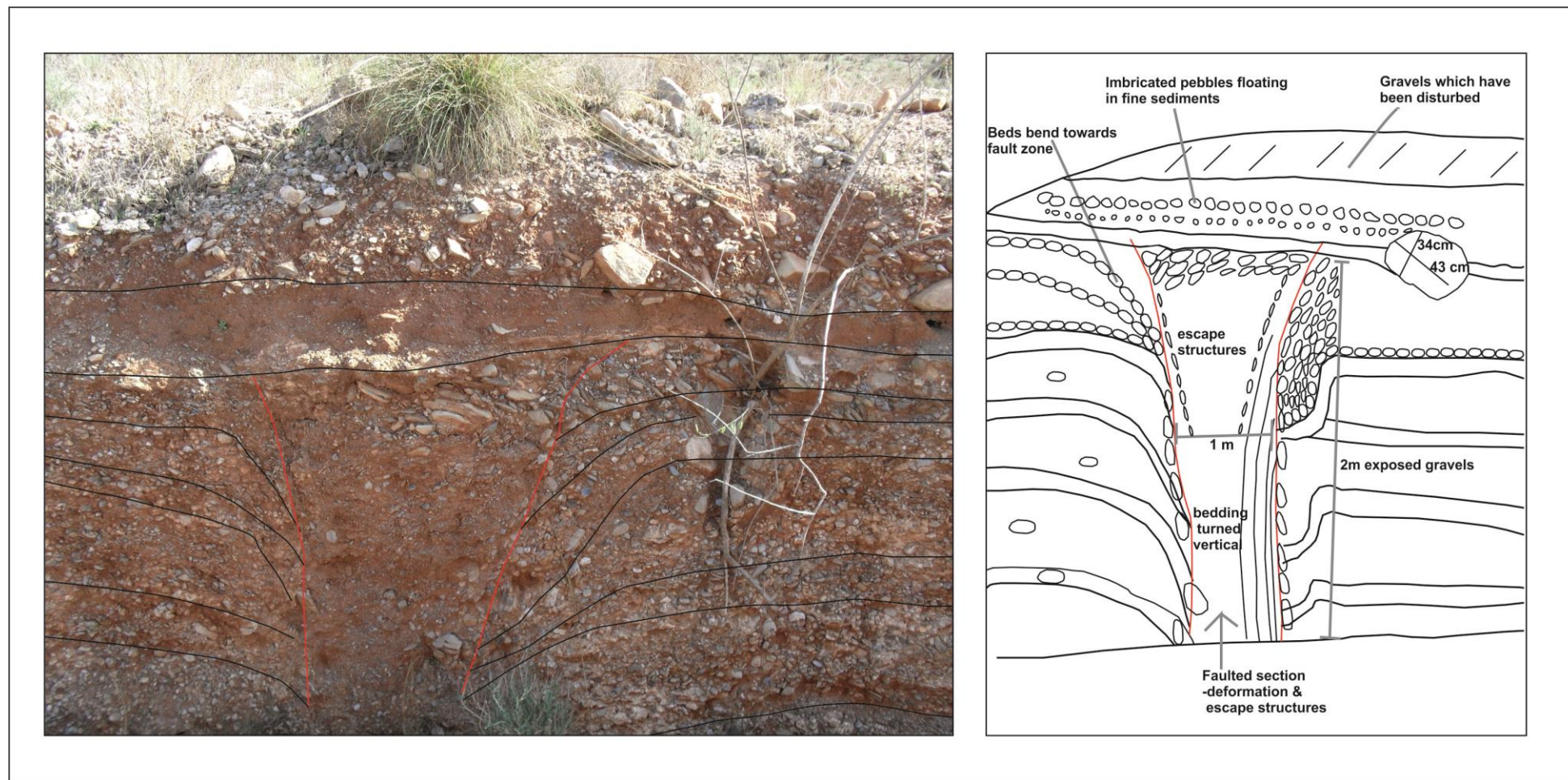


Figure 5.12: Photo and sketch of the faulted sediments present in the type locality for terrace C. The sketch shows the main features of the faults including the disruption of sedimentary structures present.

5.4.2 Interpretation

Imbrication of the terrace C sediments and the roundness of the clasts are evidence that the gravels were transported by fluvial processes. The sediments and sedimentary facies present in the terrace C type locality indicate that the fluvial system was a braided system at the timing of deposition with clasts being transported by sediment rich flows.

Terrace C deposits show a general coarsening upwards trend. This trend can be seen most clearly in a terrace exposure located near Sorbas town (UTM: 0578475: 4105825) where terrace gravels grade from sands to cobble conglomerates (Figure 5.14). The change in grain size could be an indication that there was an increase in stream power during this period enabling larger clasts to be transported.

The cross stratified sediments (Gp facies) of Group 1 at the G3 section are a common feature of all terrace C deposits. The presence of cross stratified gravels indicates that lateral accretion is taking place possibly in bar forms. The low angle nature of the cross stratification present, together with the Gm facies of Group 2, indicates that they were deposited as part of a longitudinal bar in a braided river system (Hein & Walker, 1977; Lewin & Gibbard, 2010).

Group 2 contains medium to coarse pebble/cobble grain sizes indicating that the sediments were transported by high energy flood events with the massive structureless conglomerates (Gm) being transported in thin diffuse sheets that only move during periods of peak flow. The Gm facies were probably deposited at times of bankfull discharge (Hein & Walker, 1977). Occasional imbrication of the clasts indicates that although the flows were clearly sediment rich there was some water present.

Soil development then took place once the terrace deposit had been abandoned by the river with a hardpan calcrete forming to cap the gravels.



Figure 5.13: Sketch log of the Forge deposit showing how the Terrace C deposits become coarser towards the top of the deposits.

5.5 Analysis of the palaeohydrological data

Palaeohydrological analysis can be used to reconstruct the largest floods can be recorded during valley floor aggradation (Chapter 2). The data presented here comes from across the catchment of the Proto Aguas/Féos and is mainly focused on terrace B, C and D deposits which represent the best preserved terrace deposits in the Río Aguas catchment. A summary of the palaeoflood estimates using the Clarke maximum boulder technique is presented in Table 5.1. The quantification methods used to obtain the palaeoflood discharge values are described in Chapter 3 (section 3.6.5). The discharges and the mean depth flows have been calculated for each of the terrace levels.

Palaeochannel widths and maximum boulder sizes were measured in the field (Section 3.6.5). The channel slopes were calculated using the dip of the terrace base assuming no tilting from deformation has taken place. Figure 5.15 shows the reaches of the river referred to in the following text. The proximal reach of the Proto Aguas/Féos includes the headwaters of the Río Aguas. The middle reach is defined as the area from Sorbas town, where the headwaters converge in the main Río Aguas channel, to the capture point. The distal reach includes the Féos valley and the area just downstream of the transverse reach. This section explores the palaeohydrology results in more depth and considers whether these results reveal any spatial and temporal patterns of palaeoflood discharges. The factors driving any changes are also considered.

5.5.1 Palaeoflood results

- Pre terrace A erosion surface

The Pre terrace A erosion surface is only present in the proximal reaches of the Proto Aguas/Féos catchment (Section 5.1, Figure 5.15) with minimal outcrop therefore only one palaeoflood result is presented for the erosion surface. A channel width of 272 m has been used to calculate the palaeohydrological values with a channel slope of 3°. The largest flood recorded by the pre terrace A erosion surface has a low discharge of 123 m³/s with a flow depth of 0.37 m.

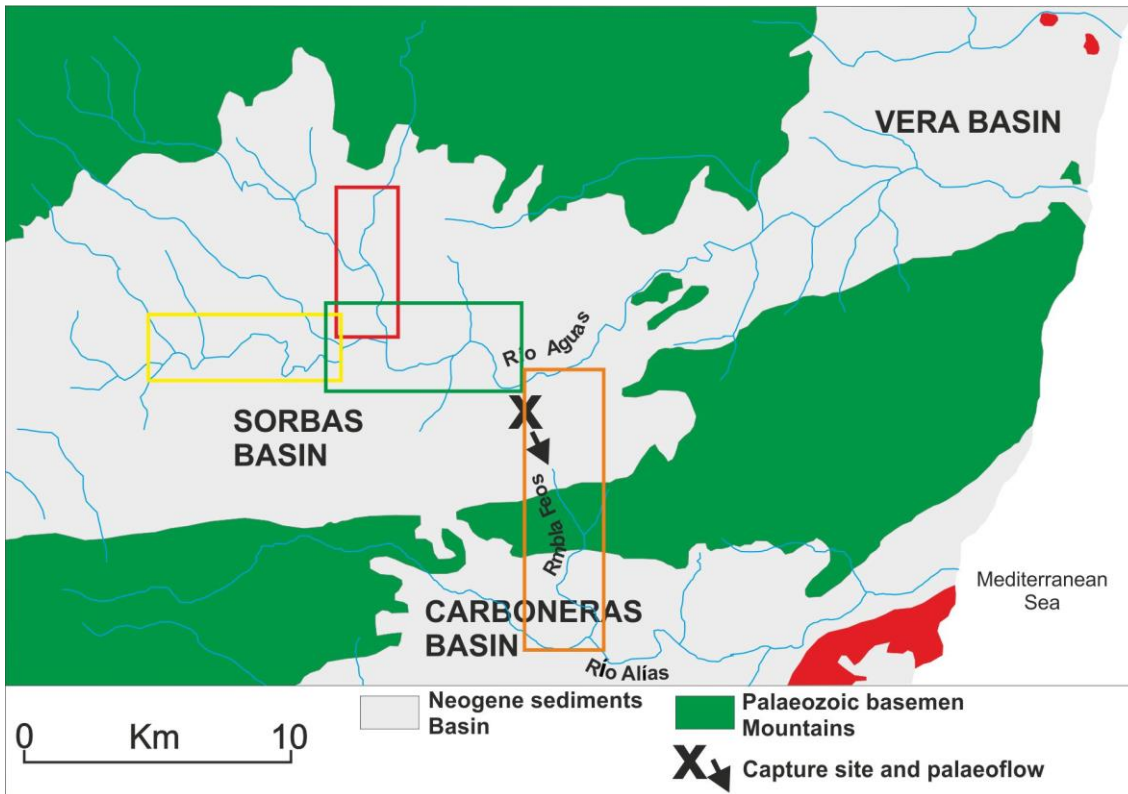


Figure 5.14: Map showing reaches of the Río Aguas as referred to in the text; Proximal (yellow & red boxes), Middle (Green box) and Proximal (orange box).

- Terrace A deposits

Palaeoflood data has been collected from all reaches of the Proto Aguas/Feos for terrace A deposits. Terrace A deposits are rare and fragmentary compared to younger deposits therefore less data is available for palaeoflood analysis. The palaeoflood values for the proximal reach have been calculated from an abandoned meander which recorded an average channel width of 272 m. Palaeoflood values range between 181 m³/s to 340 m³/s with flow depths ranging from 0.47 to 0.91 m. The lowest palaeoflood sizes were recorded in the proximal reaches. The maximum clast size indicates that the largest floods occurring during valley floor aggradation have a discharge of 181 m³/s. The mean flow depth is indicated as being 0.47 m.

Fluvial architecture for terrace deposits in the middle reach indicates that the channel width was 184 m. Terrace A deposits in the middle reach record maximum discharges

of 340 m³/s with a flow depth of 0.86 m. Distal terrace A deposits preserve a channel width of 150 m and the largest flood recorded has a discharge of 305 m³/s with a flow depth of 0.91 m.

- Terrace B deposits

Data was collected from five terrace B locations in the proximal reach of the Proto Aguas/Féos. Channels in the proximal reaches range from 150 m to 300 m in width. The minimum palaeofloods recorded in this area are found in the Rambla de Cinta Blanca (discharges of 417 m³/s; mean flow depths of 0.75m) whilst the largest flood event of 592 m³/s (mean flow depth 1.36 m) is recorded by deposits in the Rambla de Góchar. In the Rambla de Mora flood discharges of 435 m³/s and 438 m³/s were recorded.

Data from the middle reach comes from the Rambla de Sorbas near the town of Sorbas. Channel widths recorded range from 145 to 200 m. Palaeoflood discharges of 460 m³/s and 493 m³/s have been calculated for terrace B deposits in this area with mean flow depths ranging from 1.03 m to 1.19 m.

The largest flood discharges are recorded in the distal reaches of the Proto Aguas/Féos. The channel widths in the distal reach range from 273 m to 283 m. The largest boulder recorded had an A axis of 117 m. The discharge values recorded range from 892 m³/s (mean flow depth 1.22 m) to 1039 m³/s (mean flow depth 1.30 m).

- Terrace C deposits

Data has been collected from a total of nine sites across the fluvial system to gain an insight into the size of floods occurring during the aggradation of the valley floor.

Palaeochannel widths for terrace C deposits measured between 140 m to 400 m.

Maximum clast sizes in terrace C deposits suggest that floods with discharges ranging from 149 m³/s to 692 m³/s were taking place with flow depths peaking at 1.31 m. The flow depths range between 0.50 m to 1.31 m

The minimum palaeodischarge recorded (149 m³/s) was calculated from data collected in the lower Féos valley. A flow depth of 0.61 m was calculated for the minimum palaeodischarge. The maximum palaeodischarge (692 m³/s) of the dataset was recorded by deposits situated in the proximal reach of the Proto Aguas/Féos (the Rambla de Mora).

Fluvial architecture for terrace C deposits in the proximal reach show palaeochannel widths ranging from 140 m to 227 m. The largest clasts found in terrace C deposits in the proximal reach indicate that flood discharge reached 692 m³/s. The palaeodischarge values for the proximal reach range between 488 m³/s and 692 m³/s with mean flow depths of between 0.98 m to 1.31 m.

Terrace C deposits in the middle reach of the fluvial system record palaeochannel width of 400 m. The field data suggests that floods with a discharge of 520 m³/s and a mean flow depth of 1.31 occurred in this reach.

In the distal reaches of the Proto Aguas/Féos, three sites have been used to calculate the largest flood that took place. Palaeochannel widths in this area range from 144 m in the transverse reach to 282 m at the exit of the transverse reach. The palaeodischarge range from 149 m³/s (0.61 m) to 339 m³/s (mean flow depth of 0.67 m).

- Terrace D deposits

There are a large abundance of preserved palaeomeanders relating to terrace D deposits which allows for accurate channel width estimates. The majority of the palaeohydrological data collected for terrace D deposits comes from palaeomeanders. The clast assemblages of terrace D deposits records maximum floods of between 76 to 421 m³/s with flow depths ranging from 0.40 m to 1.14 m. Channel widths recorded vary between 140 m to 272 m. The maximum palaeodischarge recorded by terrace D deposits was found in the middle reach of the Proto Aguas/Féos near Urrea where the average palaeochannel width is 214 m. The clast assemblages of terrace D deposits in the distal reach (Lower Feos valley) record the smallest floods (76 m³/s).

Palaeochannel widths of 200 m have been preserved in the proximal reach. The largest clast present in the deposits in the proximal reach indicates that flood events had discharges ranging from 327 m³/s (mean flow depth of 0.80 m) to 363 m³/s (flow depth of 0.86 m).

In the middle reach, the palaeochannel widths recorded in the field ranged from 144m to 250 m. Palaeodischarges of 314 m³/s and 316 m³/s have been calculated from the maximum clasts present in the terrace D deposits in the middle reach of the Proto Aguas/Féos.

The distal reach contains the lowest estimates for flood size. The channel width estimates for terrace D deposits range from 146 m to 272 m in this reach. Palaeoflood events in the distal reach had discharges ranging from 76 m³/s to 203 m³/s .

Terrace	Location	UTM	Material	Channel width	Maximum boulder dimensions (D-max)			Discharge	Mean flow depth	Manning's
				(m)	A (cm)	B (cm)	C (cm)	(m ³ /s)	(m)	'n'
Pre TA	Rambla de Góchar	0575756, 4109450	SST	272	27	11	4	123	0.37	0.0971
A	Rambla de Mora	0577719, 4110493	AMS	272	60	10	5	181	0.47	0.0971
A	Rambla de Sorbas	0578742, 4107109	AMS	184	70	50	10	340	0.86	0.0971
A	Lower Feos Valley	0580590, 4097059	AMS	150	75	45	13	305	0.91	0.0971
B	Rambla de Mora	0577758, 4111564	AMS	242	52	40	16	438	0.85	0.0971
B	Rambla de Mora	0576999, 4110482	AMS	250	60	36	14	435	0.83	0.0971
B	Rambla de Góchar	0577312, 4109292	AMS	150	90	80	30	592	1.36	0.0971
B	Rambla de Cinta Blanca	0575599, 4108071	AMS	300	33	27	26	467	0.78	0.0971
B	Rambla de Cinta Blanca	0575195, 4108104	AMS	285	40	25	20	417	0.75	0.0971
B	Sorbas Town	0578120, 4106700	AMS	145	82	52	30	460	1.19	0.0971
B	Sorbas Town	0577999, 4106854	AMS	200	85	39	21	493	1.03	0.0971
B	Lower Feos Valley	0585217, 4098517	SST	285	117	61	25	1039	1.30	0.0971
B	Lower Feos Valley	0580600, 4098059	SST	273	103	58	23	892	1.22	0.0971
C	Rambla de Mora	0577317, 4110011	AMS	200	68	40	25	488	1.02	0.0971
C	Rambla de Mora	0577813, 4111283	AMS	227	80	50	20	592	1.06	0.0971

Terrace	Location	UTM	Material	Channel width	Maximum boulder deminsons (D-max)			Discharge	Mean flow depth	Manning's
				(m)	A (cm)	B (cm)	C (cm)	(m ³ /s)	(m)	'n'
C	Rambla de Mora	0577808, 4111552	AMS	223	63	49	19	551	0.98	0.0971
C	Rambla de Góchar	0575574, 4111057	AMS	140	90	55	33	492	1.27	0.0971
C	Rambla de Mora	0577802, 4111780	AMS	186	77	54	45	692	1.31	0.0971
C	Sorbas Town	0578475 4105825	LST	400	50	30	10	520	0.70	0.0971
C	Lower Feos Valley	0585249, 4098340	AMS	282	48	26	10	339	0.67	0.0971
C	Lower Feos Valley	0585958, 4099465	AMS	281	40	20	5	210	0.50	0.0971
C	Lower Feos Valley	0585402, 4099592	AMS	144	46	21	9	149	0.61	0.0971
D	Rambla de Mora	0577651, 4111899	AMS	200	65	20	20	327	0.80	0.0971
D	Rambla de Mora	0577950, 4111600	LST	200	70	30	16	364	0.86	0.0971
D	Río Aguas	057962, 4105248	AMS	250	70	20	10	316	0.69	0.0971
D	Río Aguas	057962, 4105248	AMS	250	70	20	10	316	0.69	0.0971
D	Río Aguas	058050, 4106572	LST	144	100	50	21	421	1.14	0.0971
D	Lower Feos Valley	0585363, 4097787	MC	272	43	23	4	203	0.50	0.0971
D	Lower Feos Valley	0585253, 4098999	BMS	146	32	13	4	76	0.40	0.0971

Table 5.1: Palaeohydrology data for the Proto Aguas/Féos catchment

Terrace level	Proximal		Mid		Distal	
	Discharge	mean flow depth	Discharge	mean flow depth	Discharge	mean flow depth
	(m ³ /s)	(m)	(m ³ /s)	(m)	(m ³ /s)	(m)
Pre Terrace A	123	0.37				
A	181	0.47	340	0.86	305	0.86
B	470	0.91	477	1.11	965.5	1.26
C	563	1.13	520	0.70	233	0.59
D	345	0.83	351	0.84	139	0.45

Table 5.2: Average palaeohydrology data for the proximal, middle and distal reaches of the Río Aguas. The Pre Terrace A erosion surface is only present in the Proximal reach.

5.5.2 Discussion of palaeohydrology data

The palaeohydrology data in this study show both downstream trends and trends between terrace levels. A summary of the estimated average palaeodischarge is presented in Table 5.2 and it shows that palaeodischarge has increased through time until terrace C deposits. The values for the terrace D deposits show a slight reduction in the estimated average discharges for palaeofloods. An increase in estimated flood discharge is recorded in a downstream direction for all of the terrace levels until the distal reach of the Proto Aguas/Féos. This is probably reflecting the increase in stream order as the tributaries converge into the main channel. This pattern is not seen in the distal reach, however, as the results in the Lower Féos are complicated by the capture of the headwaters of the Proto Aguas/Féos by the Lower Aguas.

The terrace C deposits in the proximal and middle reaches of the river system have larger palaeoflood discharges (maximum discharge: 617 m³/s) recorded then the equivalent terrace B deposits (maximum discharge: 545 m³/s) and terrace A deposits (maximum discharge: 340 m³/s). This indicates that larger floods may have been occurring during the deposition of level C deposits.

In the distal reaches of the river system the data trend is reversed with the terrace B deposits recording a significantly larger maximum discharge value of 1039 m³/s than the terrace C deposits (maximum discharge: 339 m³/s). The location of the terrace B deposit recording the maximum discharge is however, located at the exit to a transverse route and would therefore be expected to record a larger discharge value. The lower values in the terrace C deposits could be reflecting the flushing through of larger boulders with smaller boulders being deposited in the waning of the flood event.

Discharge values in the Féos valley vary between 76 m³/s and 1039 m³/s with mean flow depths varying between 1.30 m to 0.40 m. The highest discharge values are associated with terrace B deposits and the lowest with terrace D deposits. There is a four time difference between the terrace B palaeoflood discharge value and the terrace D discharge value with a significant decrease in discharge of about 850 m³/s from terrace B to terrace D deposits.

The distal reach of the Ríó Aguas in this studied is defined as the area downstream of Los Molinos including the Féos valley (Figure 5.15). This area was affected by the river capture event leading to a reduction in the catchment area of the Rambla de los Féos (Harvey & Wells, 1987; Stokes et al., 2002; Maher, 2005; Maher et al., 2007; Maher & Harvey., 2007; Whitfield & Harvey, 2012).

Maher's (2005) PhD thesis covers the Ríó Alias catchment and studied the effects of river capture on a beheaded system. The research showed that the post capture terrace deposits in the Rambla de los Féos record a significant drop in stream power in their sedimentology. The terrace D sediments in this area are significantly finer grained than the older terraces with sand and gravel sized particles dominating the deposits (Maher, 2005).

The palaeodischarge results for terrace D deposits from this study confirm the drop of stream power recorded by the terrace sediments and indicate that the size of flood discharge is half of that seen in the proximal and middle reaches of the Proto Aguas/Féos system.

Overall the palaeohydrology data for the Proto Aguas/Féos fluvial system produces viable discharge values. Discharges calculated for the palaeofloods vary from 149 m³/s to 1039 m³/s. The values obtained by this study for palaeofloods are reasonable compared with another study done on Pleistocene river terraces by Stokes et al., (2012a) who studied the Río Almanzora (located in the Vera Basin). The study on the Río Almanzora river terraces produced palaeoflood estimates ranging from 40 m³/s to 2859 m³/s. These palaeoflood results were considered reasonable when compared with the modern flood records for the Río Almanzora (Stokes et al., 2012a). The upper estimate from this study fits within the range of the Stokes et al., (2012a) study suggesting that the results presented here are viable.

The terrace deposits in the proximal and middle reaches of the Río Aguas catchment appear to show an increase in palaeoflood size between terrace B and terrace C deposits. The discharge values for the terrace C deposits are approximately 100 m³/s larger than for the terrace B deposits. Assuming that the palaeohydrology results are reasonable then the palaeohydrology data could be recording changes in the fluvial system either as a result of fluctuating climatic conditions or regional tectonic activity that is driving the drainage network reorganisation. This is further discussed in chapter 8 along with new chorological database for the Proto Aguas/Feos.

5.6 Chapter summary

This chapter has presented field data collected from the terrace deposits of the Proto Aguas/Féos. Detailed sedimentological analysis of the data collected has been presented for each of the terrace levels as well as the top basin fill surface. Calculations of palaeofloods based on field observations have been presented showing that the fluvial system was sensitive both to climate fluctuations and fluvial events (river capture). The information in this chapter is combined with the cosmogenic dates reported in chapter 7 to calculate incision rates for the Proto Aguas/Féos in chapter 8. The data is also used to create a terrace formation model in chapter 9.

Chapter 6: The Río Jauto

6.1 Introduction

This chapter presents field data from the Río Jauto fluvial archive. The Jauto fluvial system, both in its current form and also its past course, using the fluvial deposits that are present in the catchment, are described. The terrace levels have been mapped, their sedimentary characteristics recorded and analysed. Incision amounts presented for each terrace level are given as height of the terrace base above the modern river bed based upon field surveying and mapping. The sedimentary processes and environment associated with each major terrace level are described. Sedimentary logs are presented to illustrate the key facies types present. Photos and sketches are used to illustrate and provide a description of sedimentary style and processes.

The chapter aims to address a number of aims presented in chapter 1:

- Can a formal stratigraphy be constructed for the Río Jauto fluvial archive?
- Can a relative stratigraphy be created for the Río Jauto using stratigraphic information and sedimentology data?
- Can a model be created to represent the evolution of the Río Jauto fluvial system using depositional and environmental data collected in the field? Did the Río Jauto always follow the modern course?
- Can the application of palaeohydrology equations on field data be used to identify the magnitude of flood events in the Sorbas Basin?

6.2 The Río Jauto

The Río Jauto is a major tributary of the Río Aguas (Figure 6.1). It flows along the foothills of the Sierra de los Filabres, from the settlement of Cariatiz, through the

Chapter 6: The Río Jauto

northern edge of the Sorbas basin to the village of Alfaix where it joins the Río Aguas (Chapter 5). The modern catchment area of the river covers an area of 22 km² and the Jauto is 25 km in length. The modern Río Jauto is an ephemeral meandering valley system with braided sections and bedrock gorges. The river valley is characterised by several gorge and wide open valley reaches possibly related to the local geology and its structural configuration (Appendix 2). There are four major terrace levels present in the Jauto catchment which appears to correspond to similar numbers of terrace levels located elsewhere in fluvial systems in the area (Harvey & Wells, 1987 [Río Aguas]; Stokes, 1997 [Antas and Almanzora]; Nash & Smith, 2003 (Rambla de Tabernas); Maher, 2005 [Feos and Alias]; Meikle, 2009 [Almanzora]). The fluvial terrace deposits consist of gravel/cobble conglomerates that are up to 10 m in thickness. Figure 6.2 shows a long profile of the Río Jauto along with the height of the terrace bases above the current river channel. The following text describes the sedimentology characteristics of the terrace levels present. Spatial changes in the terrace deposits are described with the Río Jauto course split into proximal, middle and distal reaches (Figure 6.1). The proximal reach is defined as the course of the river downstream from the source area (near the village of La Cruz) to the north end of the Loma Orodoña ridge (UTM: 0583948 4111373). This reach contains a gorge, though limestone (Cantera Member, Turre Formation), and a wide dissected valley incised into marls (Turre Formation). The reach is 11 km in length and is strike orientated. The middle reach of the Río Jauto fluvial system is defined as the area downstream of the Loma Orodoña ridge to the knick point before the Alfaix gorge (Figure 6.1). The river course in this reach is strike orientated though the Turre Formation at the top of the reach. This section of the river course is characterised by a wide open valley. Towards the middle and end of the reach the channel becomes entrenched into basement rocks. The reach is 9 km in length. The distal reach of the river is 5 km in length and is defined as the course of the river

Chapter 6: The Río Jauto

downstream from the start of the Alfaix gorge. The river channel in this reach is superimposed onto the local basement geology. At the junction with the Aguas, the valley becomes wider where there is a switch into the softer lithologies of the Turre Formation.

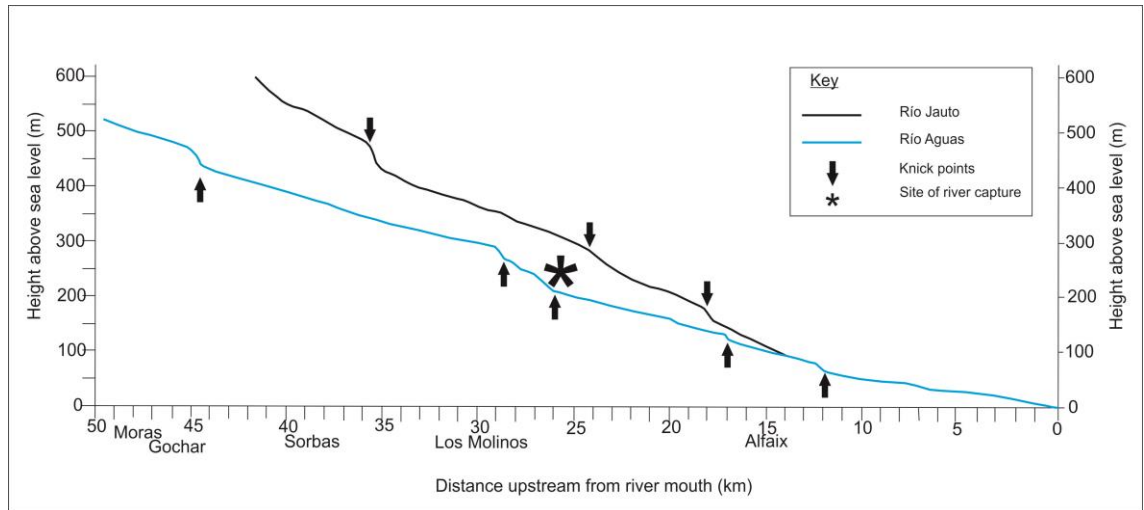


Figure 6.1: Río Jauto long profile showing major knick points and key settlements

Chapter 6: The Río Jauto

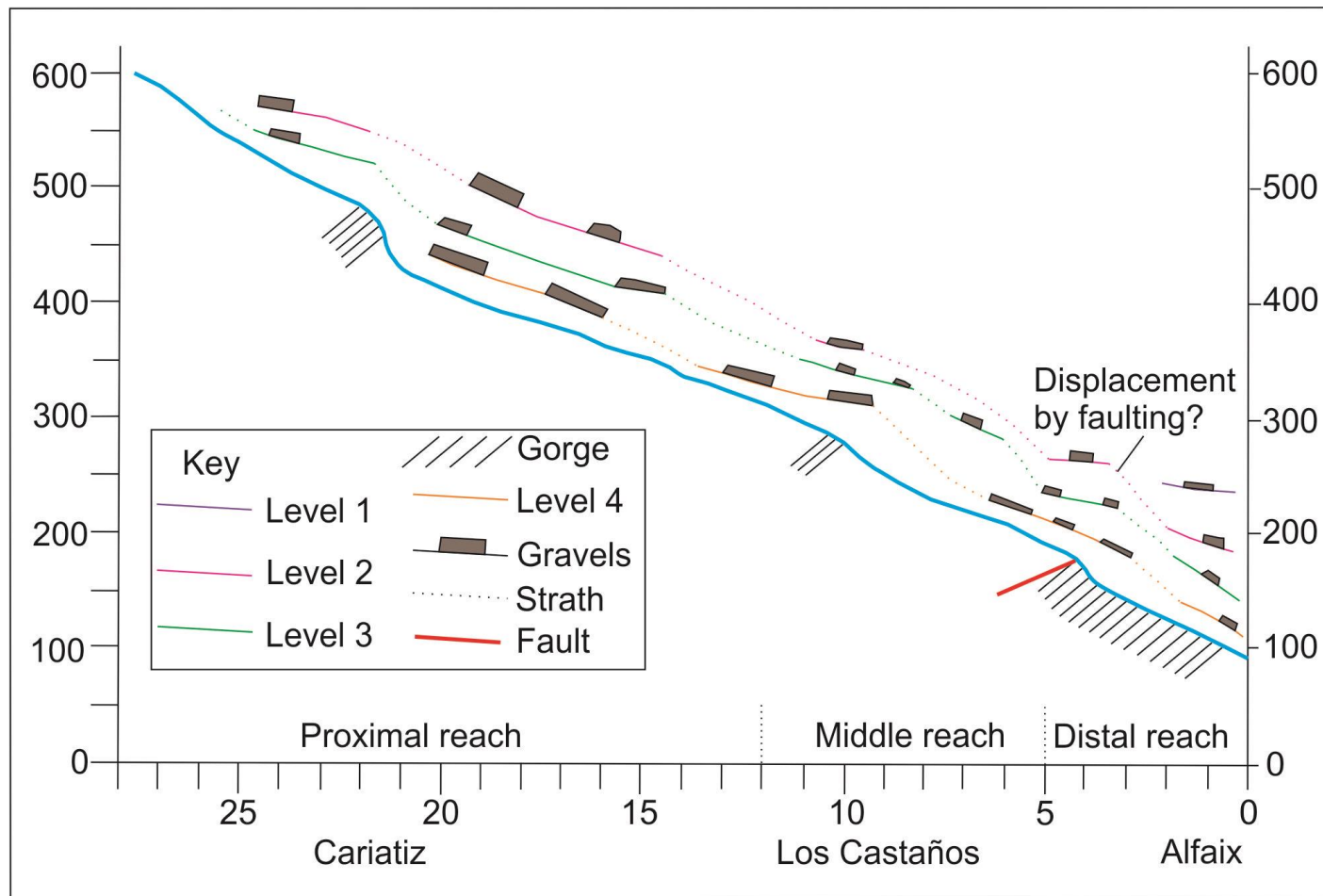


Figure 6.2: Profile of the Río Jauto with associated terrace levels, reaches and key villages.

Chapter 6: The Río Jauto

6.3 Level 1 Terraces

The level 1 terraces are fragmentary and rarely preserved, with the most commonly preserved occurrences being erosional bedrock benches sometimes covered with thin (<1 m) veneers of fluvial gravels. Occurring at 420-196 m.a.s.l. the deposits are positioned from between 4.3 to 14.9 m above the modern channel before the Alfaix gorge (Figure 6.2). In the proximal reaches of the Jauto the river channel is incised into a relict Plio-Quaternary alluvial fan (part of the basin fill Góchar Formation) and has formed a gorge through reef limestones of the Cantera Member of the Turre Formation (Mather, 1991; Martín and Braga., 2001). This has limited the formation of terrace levels in this area as the channel is too confined and vertical incision has dominated within the hard bedrock. Level 1 terraces are best preserved downstream in an area immediately upstream of the Alfaix gorge (Figure 6.2). Here level 1 deposits appear to relate to a period before gorge incision occupying a high level some 180 m above the current channel. In this area, the level 1 deposits are preserved in 20 m wide palaeo-valleys related to the former Jauto channel (Figure 6.3 & 6.4). Any terrace gravels preserved at this level are strongly cemented making analysis challenging due to masking of structures (Figure 6.3). Soil formation on level 1 deposits is best preserved in the distal reach of the Río Jauto.

6.3.1 Type Locality

The level 1 type locality (UTM: 0590705; 4112419) is situated to the north of the town of Alfaix in the distal reach. The gravels are exposed in a valley side which has been incised into a preserved palaeovalley. The gravels occur 180 m above the current channel (240 m.a.s.l) which forms a gorge through the local geology.

Chapter 6: The Río Jauto

The type locality consists of one 6 m long exposure orientated in an east-west direction that is dominated by the lithofacies Gm. The terrace gravels are 0.9 m thick and consist of clast supported, coarse clastic pebble to cobble conglomerates ($D_{50}=6$ cm), which are randomly organised (Figure 6.5). The clasts are sub angular to sub rounded in nature and very poorly sorted. The maximum clast size present is 20 cm. The terrace gravels are highly cemented. There is no rubification of the sediments.

Analysis of the clast assemblage indicates a local source area for the system with tourmaline gneiss (42%) and limestone (36%) forming the main component lithologies of the terrace gravels (Figure 6.6). There is no marble present indicating that the level 1 deposits were not receiving clasts from the Rambla de Chive.

The level one deposits indicate that the Jauto system formed as a headwards eroding system that developed highly incised channels into the basement of the Sierra de los Filabres.

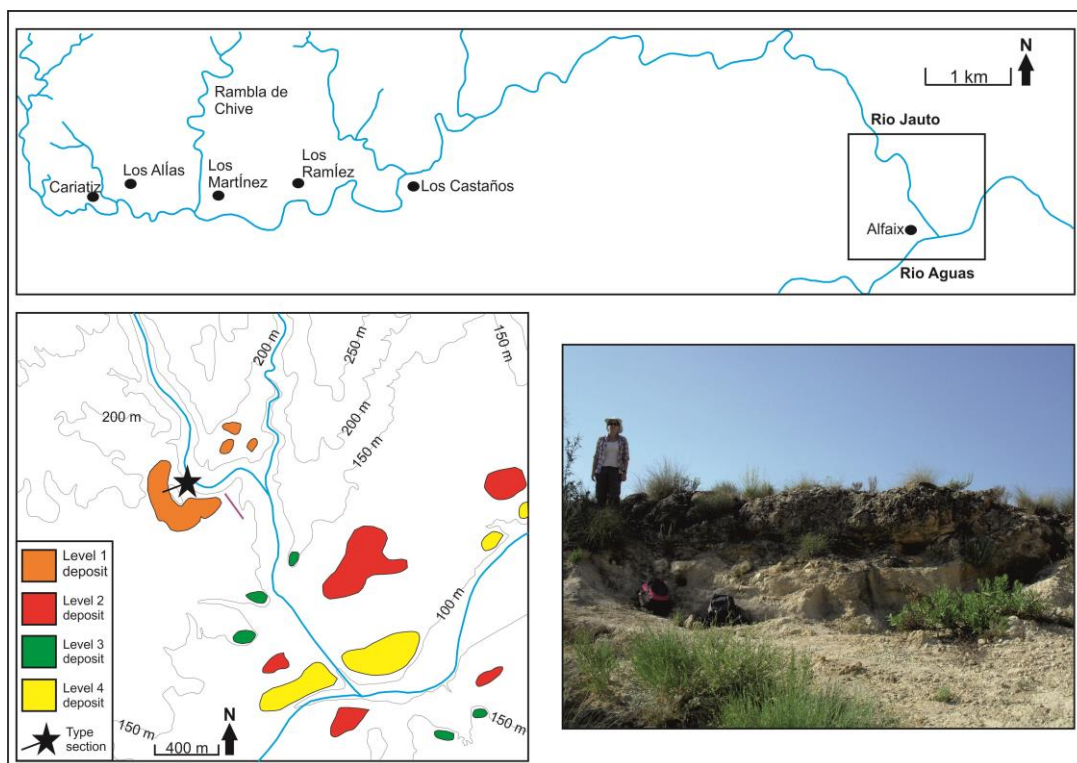


Figure 6.3: Type locality for Level 1 deposits located near Alfaix (UTM: 0590705; 4112419). Palaeovalley location shown by purple line.

Chapter 6: The Río Jauto



Figure 6.4: Photos showing palaeovalleys related to Level 1 deposits. Location of palaeovalley can be found in Figure 6.3.

Chapter 6: The Río Jauto

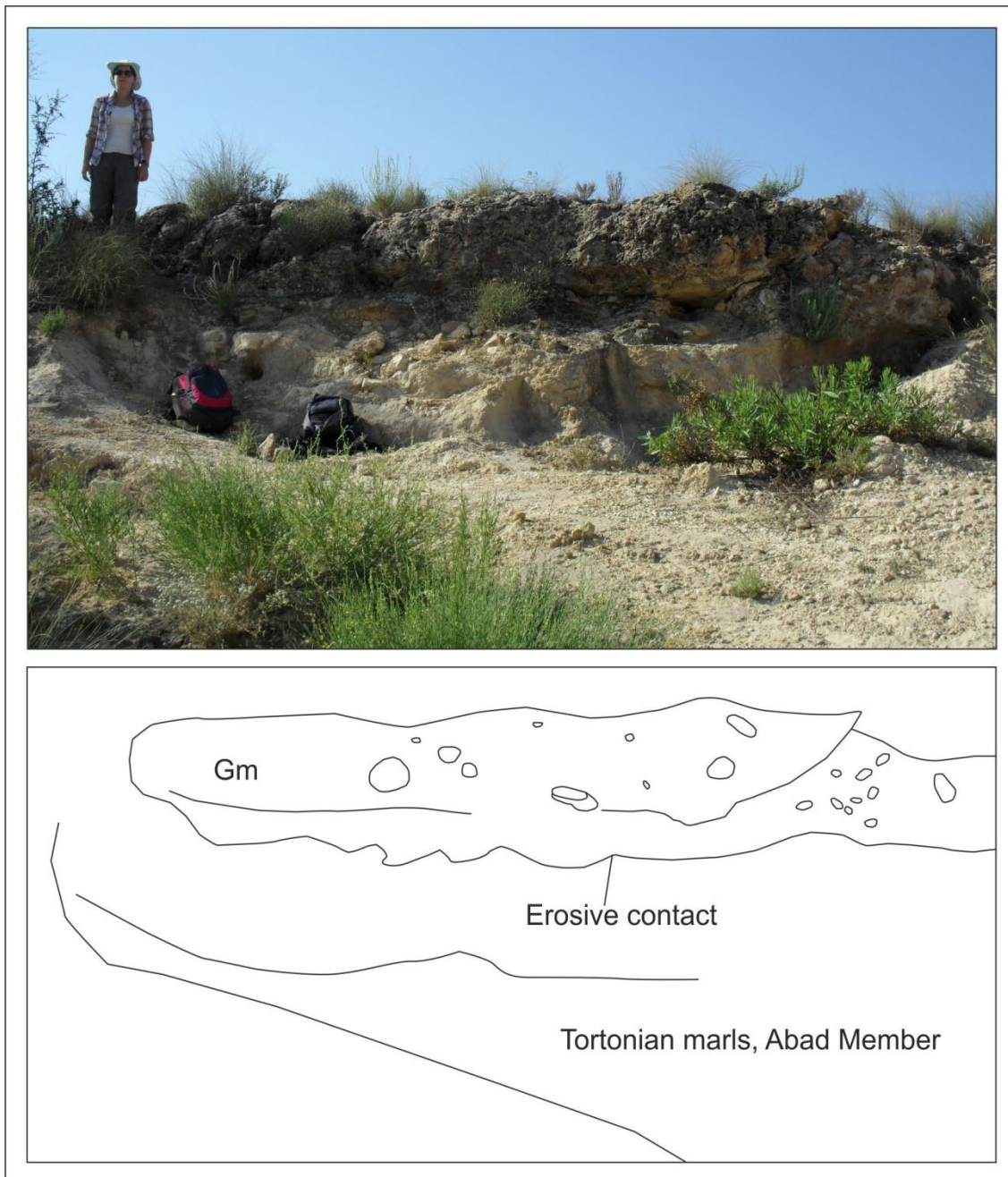


Figure 6.5: Photo sketch of the Level 1 type locality (UTM: 0590705; 4112419).

Chapter 6: The Río Jauto

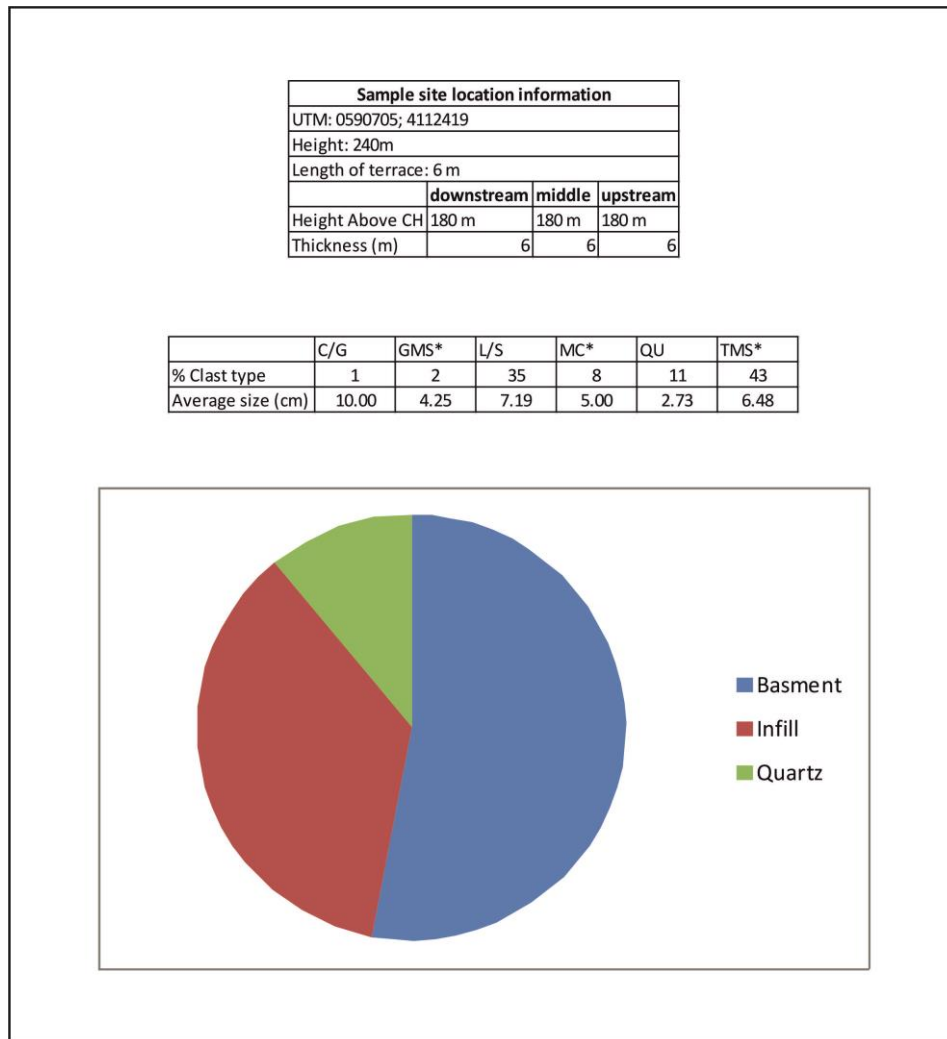


Figure 6.6: Clast assemblage data for Level 1 type locality

Chapter 6: The Río Jauto

6.4 Level 2 Terraces

The level 2 terraces are present as isolated hills and single terrace landforms deposited on outcrops of more resistant basement geology. The level 2 deposits occur in all the reaches of the fluvial system. The terraces consist of up to 8 m of fluvial gravels the bases of which are preserved 35 -25 m above the modern river channel. The terraces range in height from 409-353 m.a.s.l. The gravels tend to be highly cemented making observation of structures within the gravels difficult. Soil formation is also very poor at level 2 with little evidence for rubification.

6.4.1 Type Locality

The type locality is a single terrace landform located in the town of Los Castaños (UTM: 0584912 4111726; Figure 6.7) on the southern valley side in the middle reach.

The terrace gravels are located on a rocky outcrop 23 m above the modern channel (353 m.a.s.l). The gravels are exposed in a natural exposure in the corner of a meander bend formed by the modern river. The type locality consists of one 30 m long exposure orientated in a N/S direction.

The terrace gravels, which are 2 m thick, consist of coarse clastic pebble to cobble conglomerates ($D_{50} = 12.1$ cm) which are randomly organised. The clasts are sub angular to sub rounded in nature and are very poorly sorted. The gravels display a slight fining upwards with boulder sized clasts ($D_{max} = 37$ cm) present at the base of the deposit. The contact between the terrace gravels and the underlying geology is sharply erosive.

Chapter 6: The Río Jauto

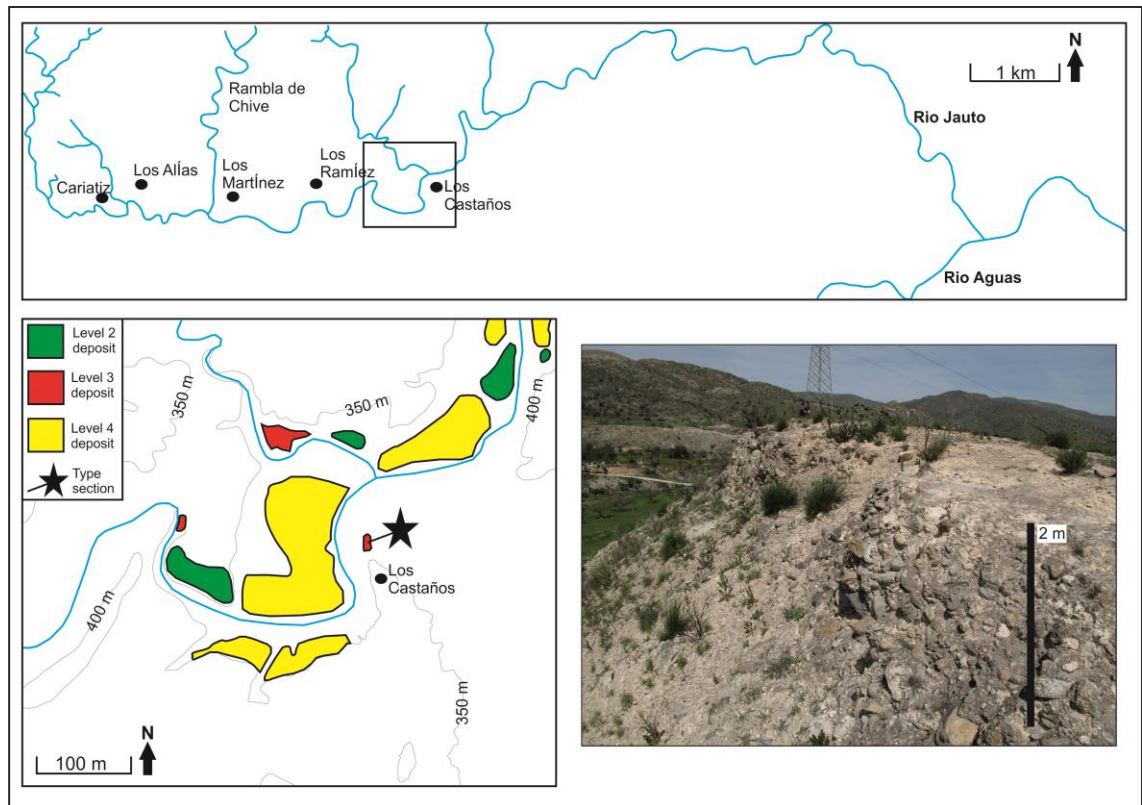


Figure 6.7: Location map, geomorphic map and photo of the Level 2 type section, Los Castaños, Río Jauto (UTM: 0584912 4111726).

The gravels of the type locality are dominated by clasts sourced from the metamorphic basement (Sierra de los Filabres). Local basement lithologies, limestone and marble are also present in the clast assemblage (Figure 6.9).

The gravels present at the type locality are clast supported pebble conglomerates (Gm) which occasionally display weak horizontal bedding (Gh) towards the top of the section. Weak low angle ($< 7^\circ$) cross bedding (G1) is also present formed of poorly sorted pebble/ cobble conglomerates. The lithofacies Gh grades laterally into the lithofacies G1 (Figure 6.8). A coarse sandy matrix occurs in the pebble lenses that are in the section. The pebble lenses display weak imbrication to the NE. The gravels are highly cemented with carbonate. A 10 cm hardpan calcrete covers the surface of the terrace deposit (Figure 6.8).

Chapter 6: The Río Jauto

The Gh/Gm lithofacies are present as sheet forms and probably signify deposition as diffuse sheets during high stage flows. The thin sand drapes and pebble lenses probably represents the waning flood conditions where fine grains enter the clast framework during low flow velocities (Miall, 1996).

The sediments in the Level 2 type section are likely to represent weak longitudinal bar formation. The Gh and Gm facies represent the main bar formation whilst the low angle cross bedding of the G1 facies reflects the downstream migration of the longitudinal bar (Bridge, 1993, Miall, 1996).

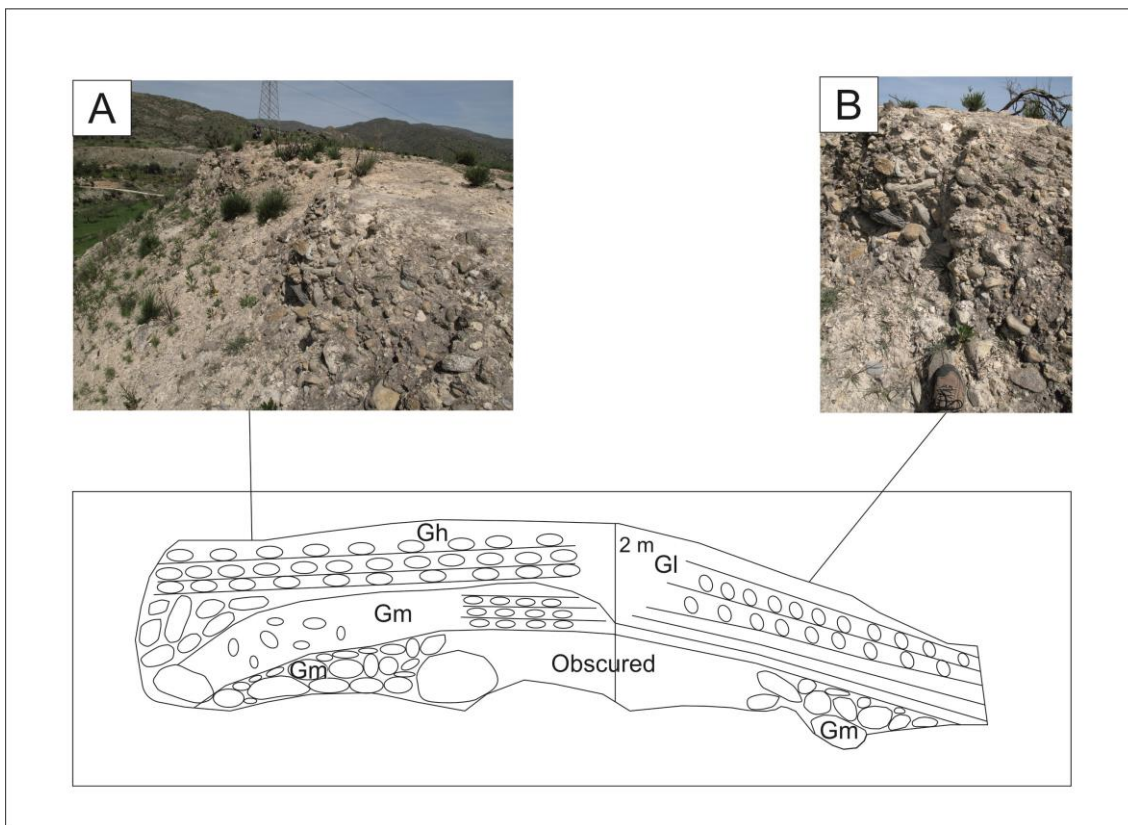


Figure 6.8: Photo-sketch of the Level 2 type locality, Río Jauto (UTM: 0584912 4111726).

Chapter 6: The Río Jauto

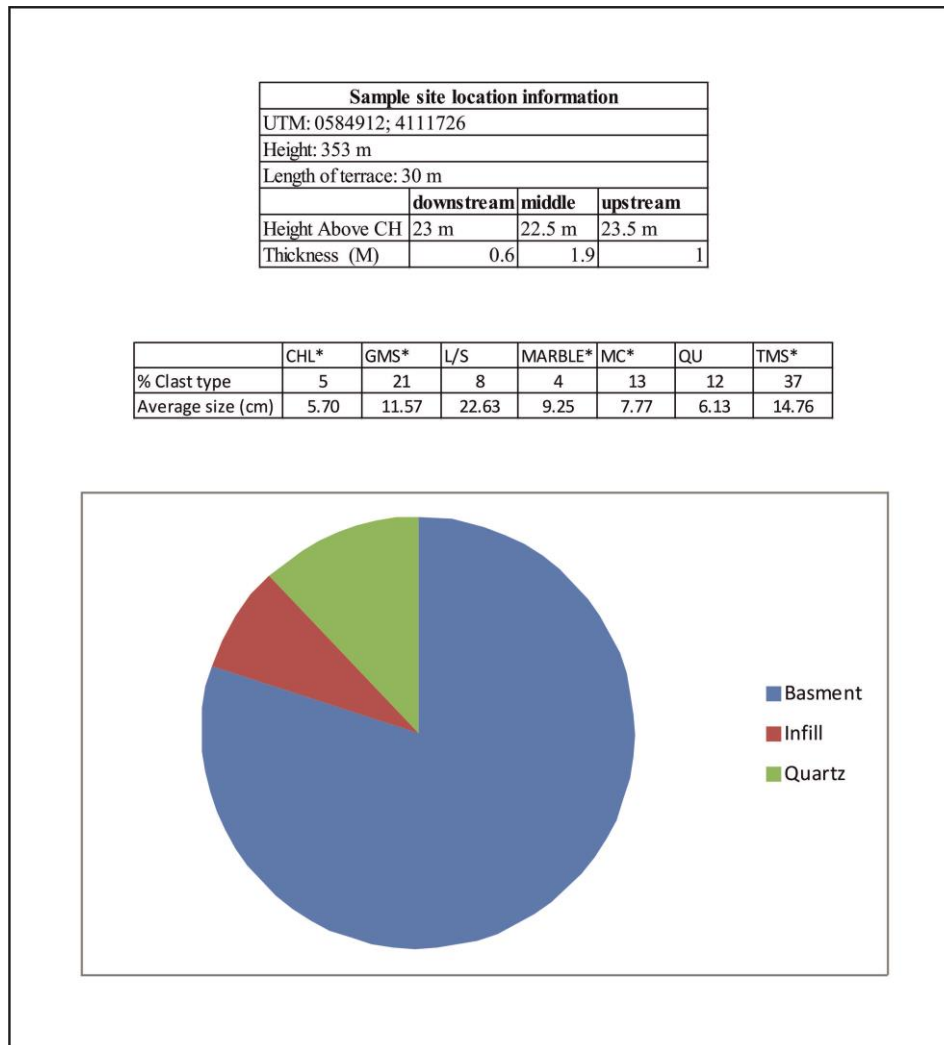


Figure 6.9: Clast assemblage data for the Level 2 type section (UTM: 0584912 4111726). Basement lithologies marked by *. Lithologies codes: chlorine mica schist (CHL), garnet mica schist (GMS), limestone (LST), metacarbonate (MC), quartz (QU) and tourmaline Gneiss (TMS).

6.5 Level 3 Terraces

Level 3 terraces are common along the length of the Río Jauto with the fluvial deposits only being absent in the river gorge reaches. The bases of the terraces are present at heights of 393-220 m above sea level, 15-7 m above the modern river channel. The terrace gravels vary in thickness between 3.6 m to 4 m with some soil development in the middle reach in the region of Los Castaños (Figure 6.6). Type III/IV calcretes are present at the terrace outcrops.

Chapter 6: The Río Jauto

6.5.1 Type Locality

The level 3 type locality (UTM: 0585399; 4112136) is a single terrace landform that forms part of a cluster of level 3 and 4 river terraces that are located to the north east of Los Castaños (Figure 6.10) in the middle reach of the system. The terraces have been deposited where the main Jauto channel dog legs north and is joined by a tributary. The terrace sits on the northern valley side of the modern Río Jauto and is located 15 m above the modern river channel.

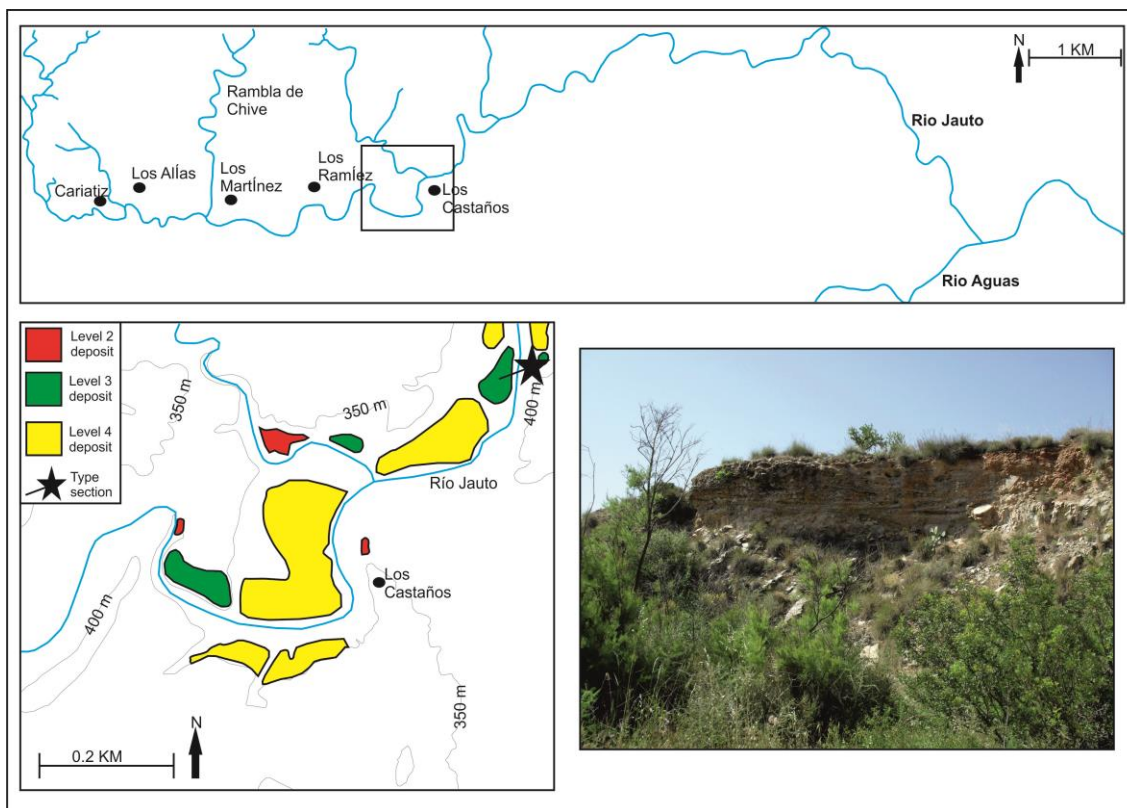


Figure 6.10: The level 3 type locality (UTM: 0585399; 4112136).

The type locality consists of 4 m of terrace gravels. The base of the deposit sits 10 m below the level 2 deposits. The gravels are exposed in a natural exposure in a meander bend. The section is exposed in a 30 m NW/SE orientated exposure. At the base of the exposure is an erosive contact with the underlying tourmaline gneiss basement (Nevado-Filabride nappe). The contact undulates on a metre scale. The gravels consist of clast-supported, poorly to well sorted, pebble boulder conglomerates ($D_{50}=10$ cm).

Chapter 6: The Río Jauto

The largest clasts in the deposit ($D_{\max}=146$ cm) occur at the base of the deposit although boulders can be found throughout the exposure. The clasts in the deposit are sub angular to sub rounded and are often imbricated with the main palaeo-direction being NNE.

Clasts sourced from the metamorphic basement dominate the assemblage although there is also a significant number of clasts sourced from the locally outcropping basin fill Turre Fm (Figure 6.11).

The sediments at the type locality display both low angle ($10-15^\circ$) cross beds (G1) and also horizontal bedding (Gh) (Figure 6.8). Numerous erosion surfaces can be seen in the deposits. Concave erosion surfaces are in-filled by finer pebble and sand sediments which are cross bedded on a 20 cm scale. Lens shaped structures formed from gravels, pebbles and coarse sand are present in the terrace exposure (Figure 6.12).

The low angled cross bedding with metre scale foresets are developed in cobble/pebble grade sediments. The horizontally bedded pebble/cobble conglomerates occur at the south eastern end of the exposure.

The type locality is capped by a 30 cm dark red soil which has a Munsell value of 5 YR 5/6 (red). There is also a hardpan calcrete capping the deposit and clast coatings can also be observed.

Chapter 6: The Río Jauto

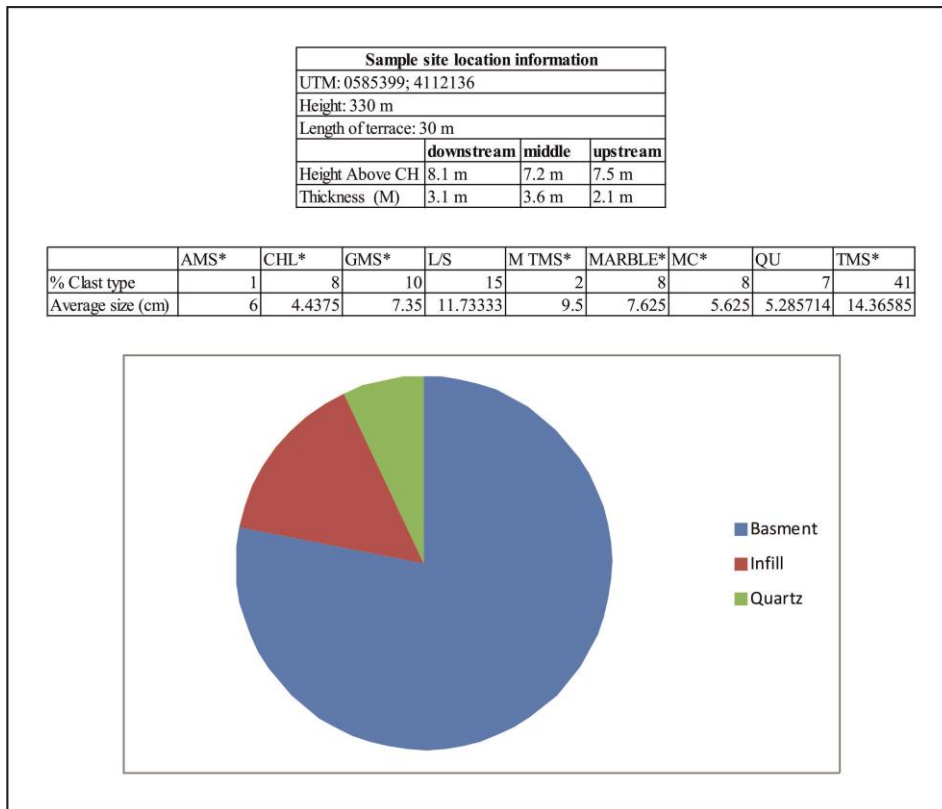


Figure 6.11: Clast assemblage data for Level 3 type section. Basement lithologies marked by *.

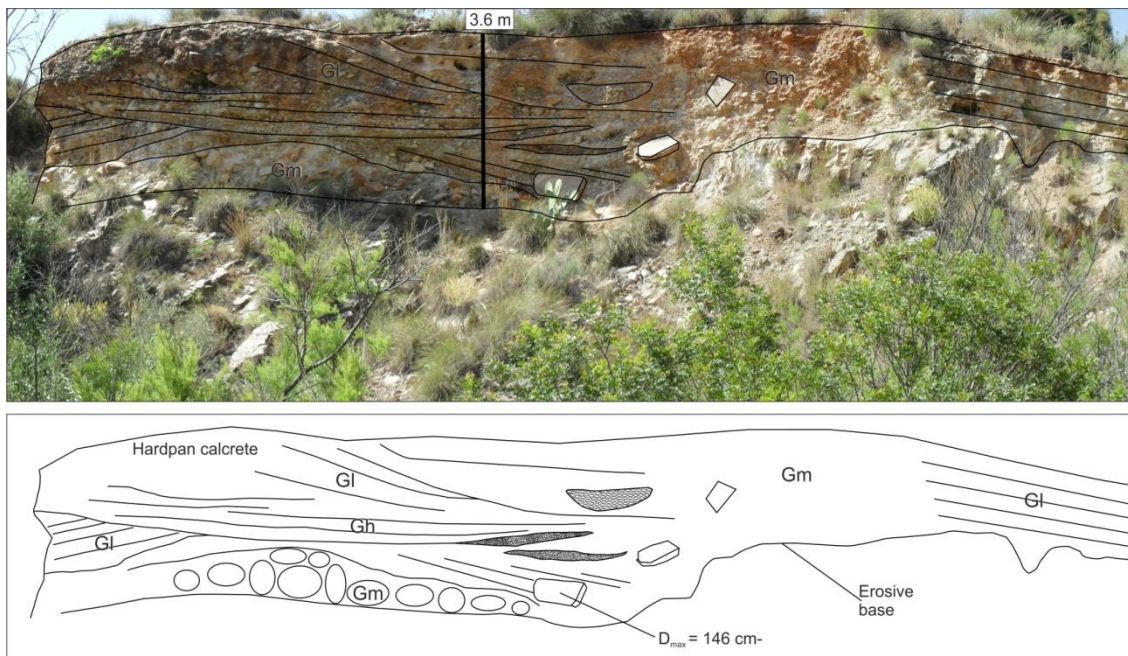


Figure 6.12: Photo-sketch of the type section for level 3 terrace deposits located downstream of Los Castaños (UTM: 0585399; 4112136).

Chapter 6: The Río Jauto

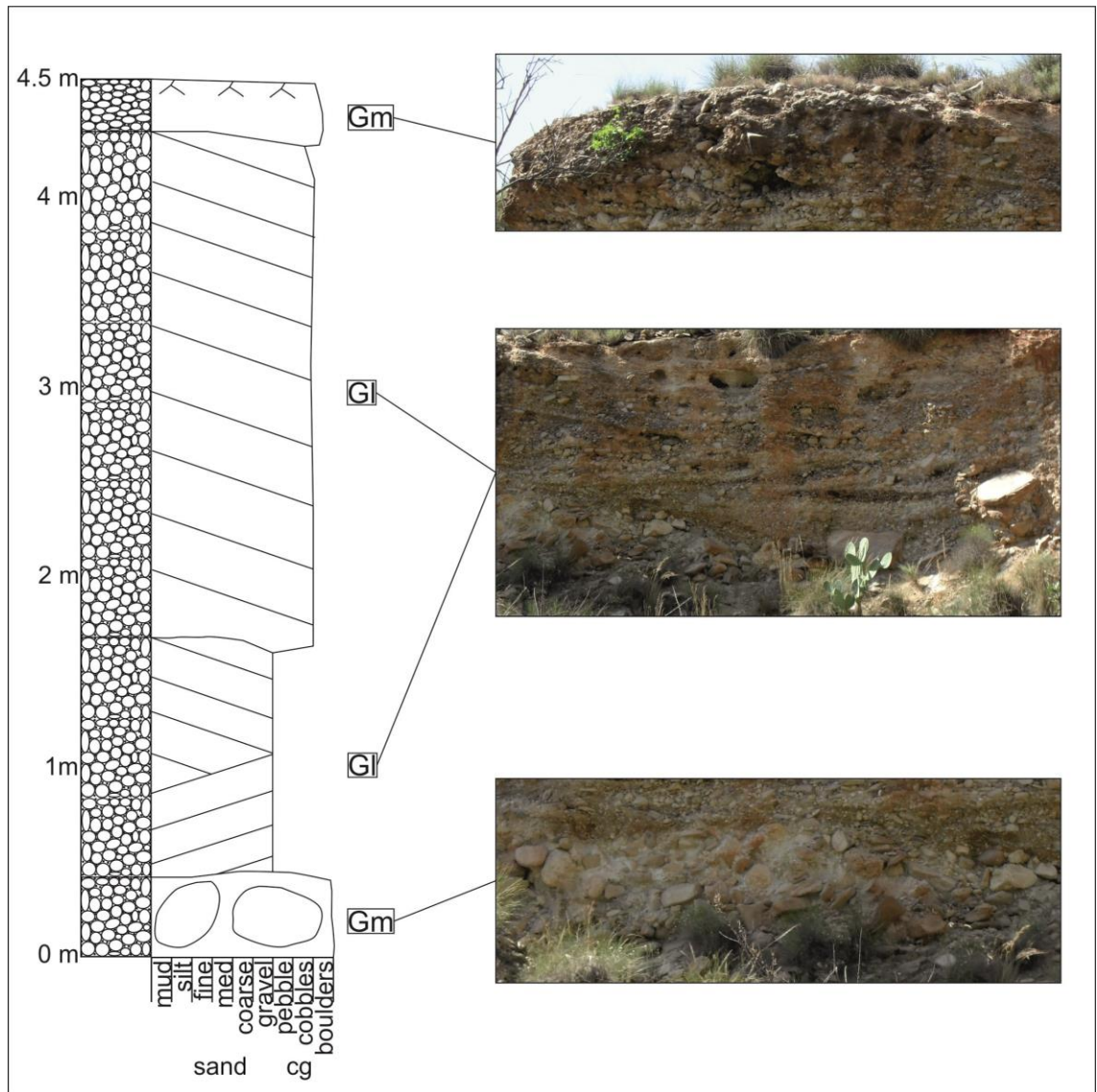


Figure 6.13: Sedimentary log of the Level 3 type section (UTM: 0585399; 4112136).

The sediments present in the level 3 type locality represent a lateral bar that has been migrating downstream. Lateral bars migrate obliquely to the main channel and generally represented by horizontal bedding along with low angle foresets. The bar form has been dissected by numerous reactivation surfaces where channels have shifted cutting through the bar form (Bridge, 1993).

The base of the section is marked by an erosive contact and is possibly scouring caused by an erosive flood event that led to the deposition of the coarse basal sediments. The coarse basal sediments (Gm) facies appear to form a bar core with fine low angle cross

Chapter 6: The Río Jauto

bedded gravel/ sand building from the coarse conglomerate. These are cut by an erosive surface over which horizontally bedded and low angle cross bedded sediments sit (Figure 6.13).

The horizontal bedding (Gh) is present in 20 cm thick sheet forms which were probably deposited as diffuse sheets of sediments. The low angle cross beds form downstream of the horizontal bedding and are generated by sediment avalanching down the front face of the bar form (Miall, 1996). The cross bedding foresets represent downstream migration of the bar form.

Soil formation takes place once the terrace gravels have been abandoned by the river channel. The formation of calcrete coatings on the clasts also form once the terrace deposit is stable.

Overall the level 3 deposits represent a braided river environment in which bar form development is occurring.

6.6 Level 4 Terraces

Level 4 terraces are the most common and well preserved landform present in all the reaches of the Río Jauto. The bases of the level 4 deposits occur at a height of 420-196 m.a.s.l and are 5.2-4.3 m above the modern channel. Thickness of the deposits ranges between 1 m to 8 m. The terrace surfaces rarely display any calcrete or rubification and are normally buried between 1 to 6 m of fine sediments sourced from the local hill slopes.

Chapter 6: The Río Jauto

6.6.1 Type Locality

The level 4 type locality (UTM:0581409 4111344) is part of a series of level 3 and 4 terraces that occur around the village of Los Alias (proximal reach) located near the northern boundary of the Sorbas basin (Figure 6.14). The river valley in this area is wide having just exited a confined gorge through reef limestone of the Cantera Member. The deposit sits at a height of 393 m.a.s.l on the southern valley side of the Rambla Castaños.

The type locality consists of a 144 m long exposure of terrace gravels orientated E-W which occurs 5.3 m above the modern river channel. The gravels form an erosive undulating contact with the underlying sands and marls of the Turre Formation. Above the erosive contact there are 5.2 m of clast supported well sorted gravel/cobble conglomerates ($D_{50}=8$ cm; $D_{max}=45$ cm) deposited in sheet and lens forms. The sub-angular to sub-rounded clasts are imbricated with a main palaeocurrent direction to the NE. The clasts are mainly sourced from the metamorphic basement of the northern basin margin (Sierra de los Filabres).

Chapter 6: The Río Jauto

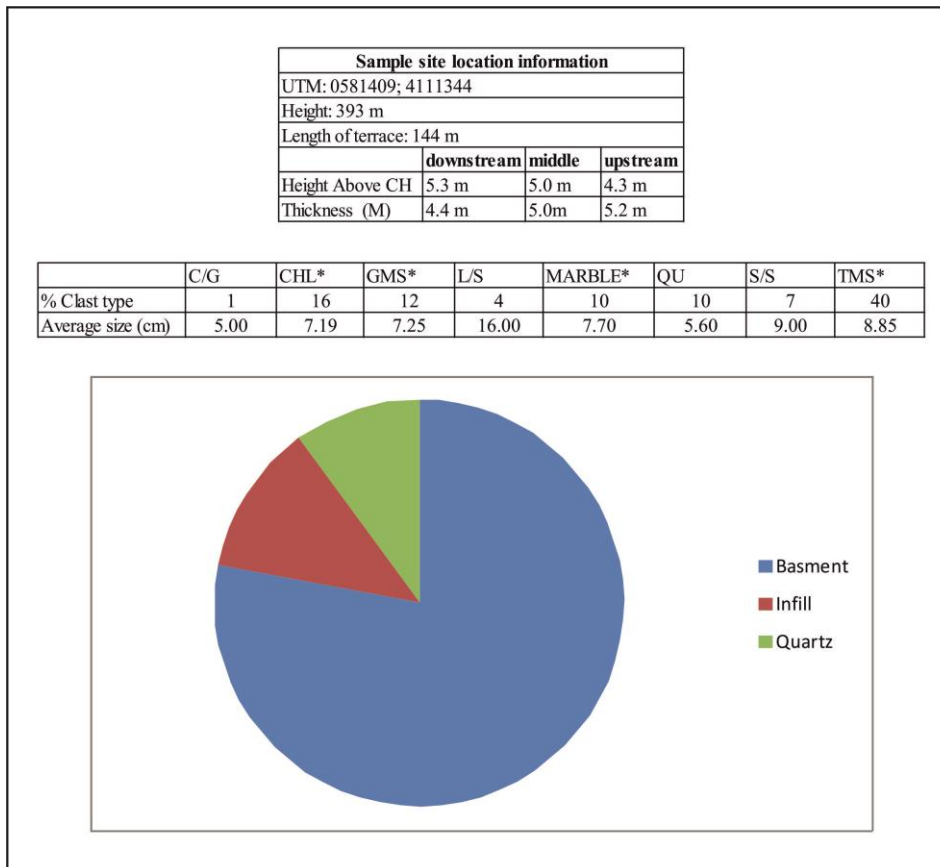


Figure 6.14: Clast assemblage data for the Level 4 type section (UTM: 0581409 4111344). Basement lithologies marked by *.

Figure 6.15 shows the sedimentary structures present in the type locality section. The low angled (20°) cross bedding (G1) that occurs across the whole of the section is formed from well sorted, clast supported, gravels which build towards the east. The cross beds build out towards the west from a massive, structureless, coarse cobble/boulder conglomerate that is located on the eastern edge of the terrace deposit. Also present at the type locality are lenses of structureless cobble conglomerates (Gm). These massive conglomerates are present at the base and also on the western side of the section (Figures 6.16 & 6.17). An erosion surface caps the structureless conglomerates. Above the erosion surface cross bedded gravels (G1) are present. A second large concave erosion surface occurs on top of the low angle cross beds which is in-filled by coarse, cross bedded and laminated sands, massive gravel/cobble conglomerates and low angle cross bedded conglomerates. The whole section is capped by up to 2 m of

Chapter 6: The Río Jauto

fine orange coloured marls which occasionally contains pebble clasts. There is no soil rubification or calcrete development present in the terrace surface.

Chapter 6: The Río Jauto

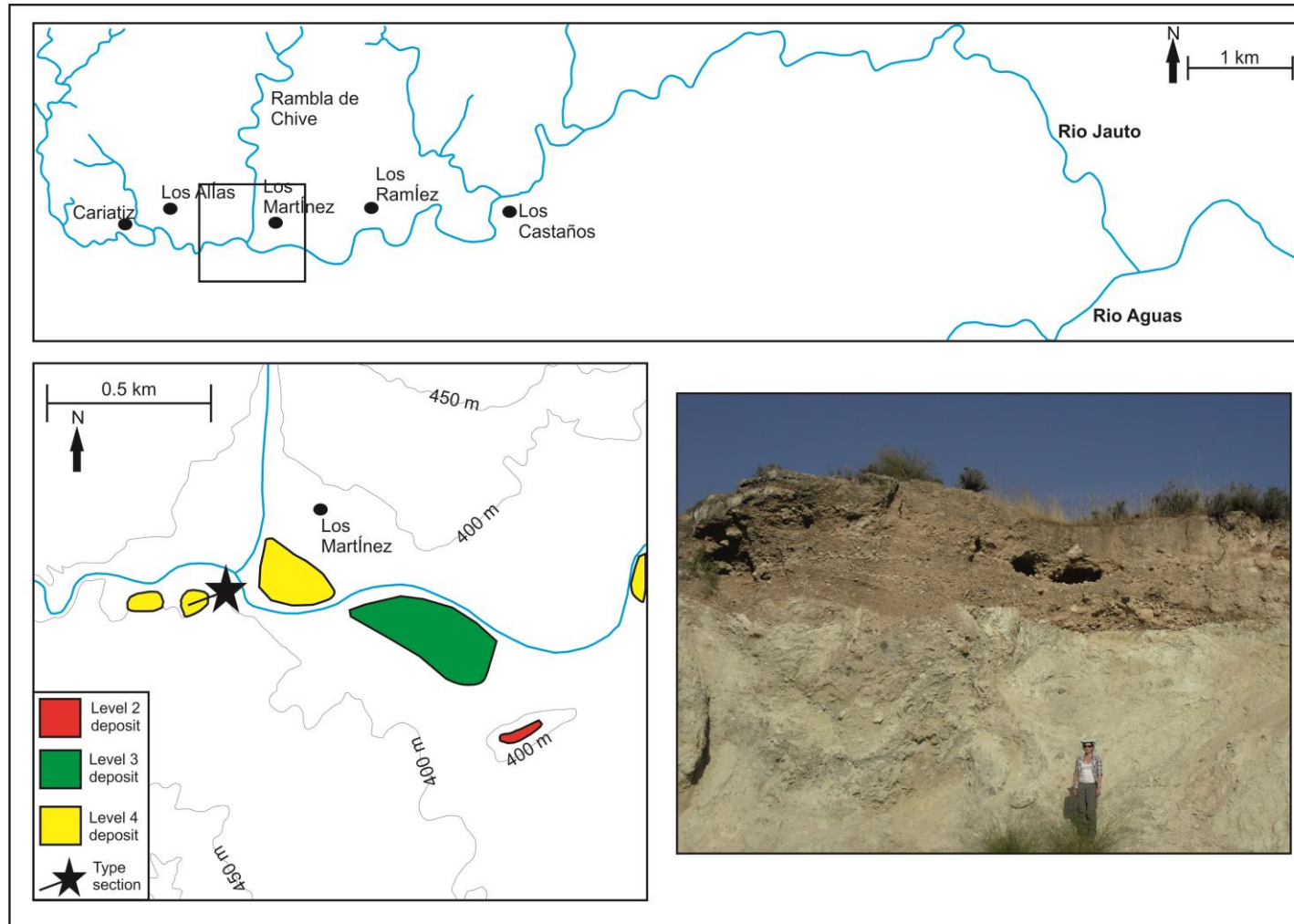


Figure 6.15: Location map for the Level 4 type section (UTM: 0581409 4111344).

Chapter 6: The Río Jauto

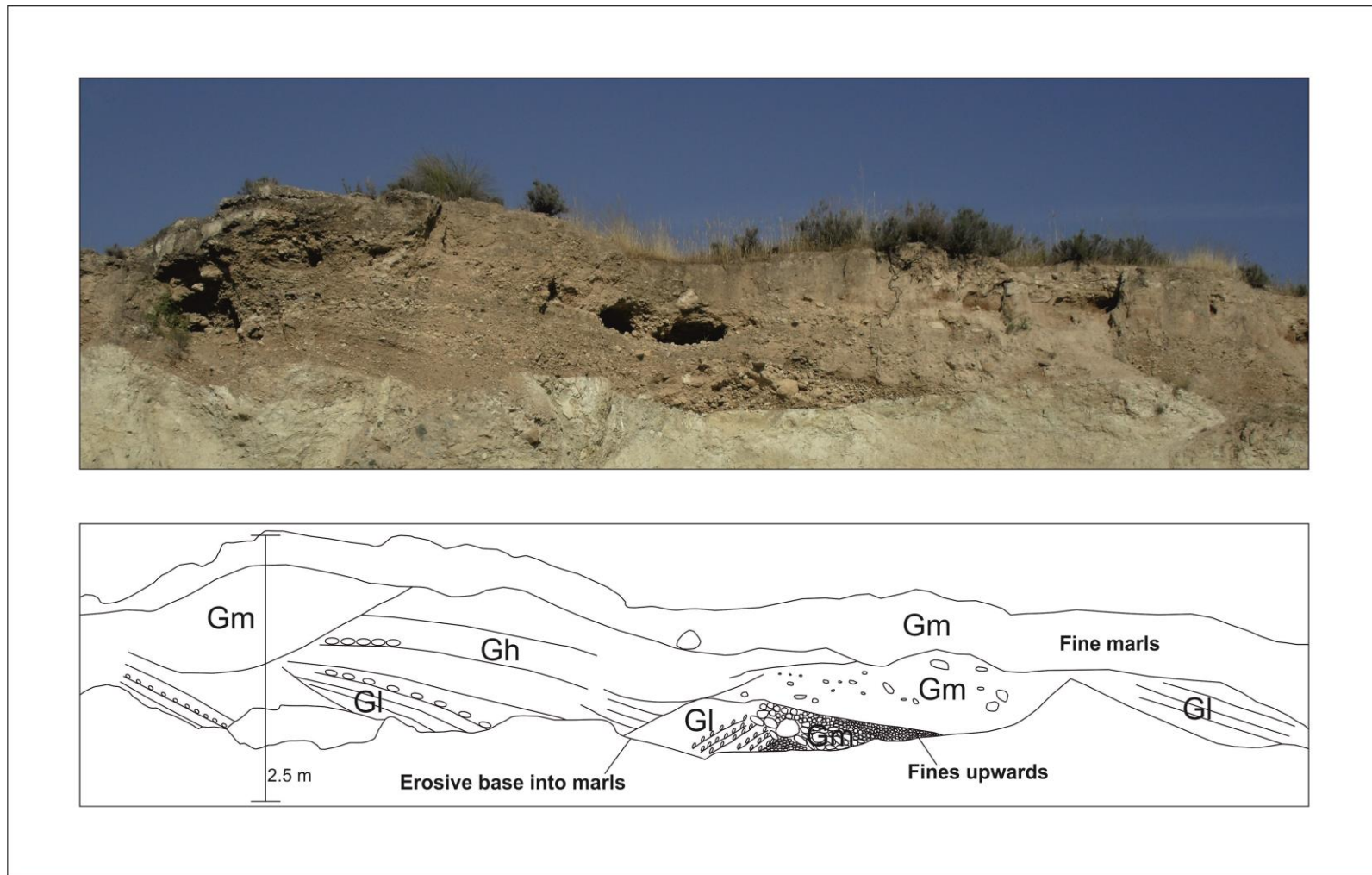


Figure 6.16: Photo-sketch of the type locality for level 4 terrace deposits in the Río Jauto (UTM: 0581409 4111344).

Chapter 6: The Río Jauto

The level 4 terrace gravels represent a bank attached lateral accretion bar which is building outwards from a channel margin. Reactivation surfaces could represent the shifting of the bars in the channel or multiple channels in the main channel.

The base of the deposits is an erosive contact suggesting that it was formed by a strong flow or flood event leading to scour at the base of the channel.

The Gm facies form both at the margins of the channel and also create a core from which the low angle cross beds can laterally aggrade into the channel centre (Miall, 1996). The G1 facies have also prograded over the top of the Gm facies as the channel has shifted. Erosion of the G1 facies has occurred probably as a result of bar form dissection by small shifting channels contained within the main river channel (Bridge, 1993).

The numerous erosion surfaces in the terrace deposit have acted as reactivation surfaces with sediments infill the concave down erosion surfaces and low angle cross bedding prograding over the top possibly representing weak longitudinal bar formation.

The sediments preserved by level 4 terrace deposits were deposited by a braided river that had both lateral accretion bars and longitudinal bar present within the system.

Chapter 6: The Río Jauto

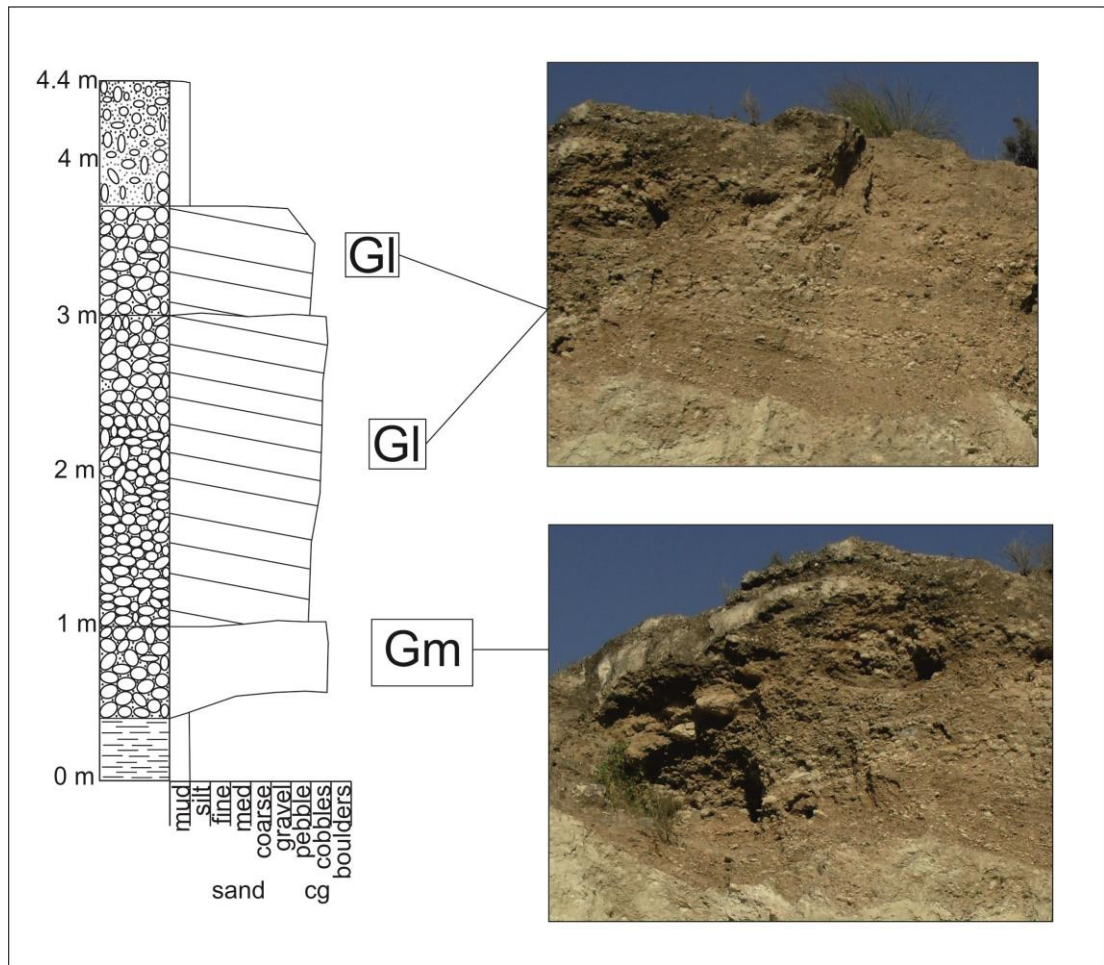


Figure 6.17: Sedimentary log for the Level 4 type section (UTM: 0581409 4111344) showing the major sedimentary facies.

6.7 Palaeohydrology analysis

Palaeohydrological analysis has been used to reconstruct the size of the palaeofloods that deposited the sediments in terrace deposits (Chapter 2). The data presented here comes from across the catchment of the Río Jauto with the bulk of the data coming from the level 3 and 4 deposits. The calculation of the channel width used in the palaeohydrology calculations depends on the preservation of the terraces. Level 1 and 2 terrace deposits are poorly preserved therefore there was only a limited number of outcrop where appropriate field data could be collected.

The discharge results obtained by applying the maximum boulder technique to the Río Jauto deposits are provided in Table 6.1 and Table 6.2 (Full data table can be viewed in

Chapter 6: The Río Jauto

Appendix 4). Figure 6.2 shows the reaches of the river referred to in the following text.

The calculation used to obtain these results is described in Chapter 3 and section 5.6.

6.7.1 Palaeoflood results

6.7.1.1 Level 1

The preservation of palaeo-valleys in the distal reach (figure 6.18) allows estimation of channel width for palaeohydrological analysis on the gravel deposits of level 1 terraces.

The valley forms present indicate a channel width of ~137m (Figure 6.18). The

maximum clast size occurring in the level 1 deposits has an A axis of 22 cm. The

palaeohydrological calculations indicate that the discharge of the floods was around 70

m³/s. It is likely due to the poor preservation and lack of exposure of the deposits that

the maximum boulder moved by the palaeofloods has not been documented in this

work.

6.7.1.2 Level 2

Palaeoflood data has been collected from two sites in the middle and one site in distal

reaches of the Río Jauto for level 2 deposits. Level 2 deposits are rare and fragmentary

compared to younger deposits therefore less data is available for palaeoflood analysis.

Field data collected for level 2 terraces from the modern valley widths indicate that

channel widths varied between 228 m to 400 m. The maximum clasts recorded ranged

from 37 cm to 54 cm (a axis). The calculated flood discharge values range from 343

(mean flow depth 0.75 m) to 631 m³/s (mean flow depth 0.79 m).

Chapter 6: The Río Jauto

The maximum discharge recorded in the middle reach of the Río Jauto was $631 \text{ m}^3/\text{s}$ whilst in the distal reach the maximum palaeoflood discharge recorded was $363 \text{ m}^3/\text{s}$.



Figure 6.18: Aerial image of the level 1 palaeovalleys showing the measured valley width (image sourced from Google earth & DigitalGlobe-Permission has been granted to reproduce this image by Google Earth). See Figure 6.3 for location.

6.7.1.3 Level 3

Data has been collected from 13 sites across the fluvial system to gain an insight into the size of floods occurring during the aggradation of the valley floor. Many of the channel measurements for the level 3 deposits come from abandoned meanders. Five sites are located in the proximal reaches of the Río Jauto, six in the middle reach and two are located in the more confined distal reaches of the fluvial system. The channel widths measured in the field for level 3 deposits ranged between 200 m to 400 m with

Chapter 6: The Río Jauto

recorded maximum clast sizes of 23 cm to 143 cm (a axis). The field measurements indicate that palaeodischarges ranged from 152 m³/s to 1683 m³/s.

In the proximal reach of the Río Jauto palaeochannel widths range between 200 m to 400 m. Maximum clasts recorded range between 48 cm and 108 cm. The largest clasts found in the proximal reach indicate that the largest floods occurring had a discharge of 754 m³/s. The palaeodischarges for the proximal reach range between 302 m³/s to 754 m³/s with mean flow depths of 0.60 m to 1.26 m.

Level 3 deposits in the middle reach of the fluvial system record palaeochannel widths of 200m to 300 m calculated from a preserved palaeomeander. The maximum clast sizes range between 40 cm to 146 cm. The calculated palaeodischarges range from 194 m³/s to 1683 m³/s. Mean flow depths range from 0.54 m to 1.63 m. The maximum palaeodischarge recorded by level 3 deposits was recorded by deposits in the middle reach of the Río Jauto.

A palaeomeander has been used to calculate the former maximum flood discharges occurring in the distal reach. The channel width measured from the preserved meander is 200 m. The maximum clasts ranged from 23 cm to 62 cm. The palaeodischarges ranged from 152 m³/s to 385 m³/s with mean flow depths of 0.51 m to 0.88 m. The minimum palaeodischarge calculated from the maximum clast size in level 3 deposits was found in this area.

6.7.1.4 Level 4

A total of 15 level 4 deposits across the fluvial system were used to calculate maximum flood events in the Jauto. Palaeomeanders, present in all the reaches of the fluvial system, were used to calculate the channel widths. The channel widths ranged from 200

Chapter 6: The Río Jauto

m to 371 m. Maximum clast size in the terrace deposits ranged from 23 cm to 184 cm. Maximum palaeodischarge values varied from 81 m³/s to 1753 m³/s with mean flow depths of 0.35 m to 1.72 m.

Three sites in the proximal reach of the Río Jauto have been used to calculate the maximum flood discharges. The channel widths ranged from 200 m to 350 m with maximum clast sizes of 23 cm to 70 cm recorded. The palaeodischarges ranged from 81 m³/s to 984 m³/s with mean flow depths of 0.35 m to 1.10 m recorded by the deposits.

A total of 11 sites in the middle reach were suitable for palaeohydrology measurements. The recorded palaeochannel width of 200 m to 371 m was preserved by a palaeomeander. The maximum clast sizes found in the deposits ranged from 40 cm to 184 cm. Calculated discharges ranged from 263 m³/s to 1753 m³/s. Mean flow depths of 0.70 to 1.72 were calculated. The maximum palaeoflood discharge for the Río Jauto was calculated from field measurements collected in the middle reach.

A palaeomeander was used to calculate the discharge for maximum flood events in the distal reach. The channel width preserved by the palaeomeander was 200 m. The maximum clast size found in the deposit was 62 cm. The discharge calculated from the field data was 471 m³/s with a mean flow depth of 1.00 m. The smallest maximum flood discharge was recorded by level 4 deposits was found in this section.

6.7.2 Discussion of palaeohydrology data

A summary of the mean palaeoflood estimates using the Clarke maximum boulder technique is presented in Table 6.2. The mean discharges and the mean depth flows have been calculated for each of the terrace levels. Maximum and minimum values are also reported. The data presented in table 6.2 is separated into proximal, middle and

Chapter 6: The Río Jauto

distal reaches respectively in order to determine any downstream trends that may be present in the data set.

Terrace level	Proximal		Middle		Distal	
	Discharge m ³ /s	Mean flow Depth (m)	Discharge m ³ /s	Mean flow depth (m)	Discharge m ³ /s	Mean flow depth (m)
1	n/a	n/a	n/a	n/a	40	0.38
2	n/a	n/a	487	0.77	363	0.75
3	502	0.90	781	1.20	316	0.78
4	319	0.77	778	1.04	471	1.00

Table 6.1: Data table showing the mean palaeohydrological data for the Río Jauto.

Palaeoflood mean discharge values in the Río Jauto varies between 40 and 781 m³/s.

The largest mean discharge is recorded by the level 3 deposits (781 m³/s) and the minimum by level 1 deposits (40 m³/s). The data indicates that the discharges increase in a downstream direction between the proximal and middle reaches of the river system as the stream order increases. However, in the distal reaches of the Jauto the palaeoflood discharges decrease for all the terrace levels. The distal reach of the Río Jauto is marked by the 180 m deep lower gorge. The narrow nature of the valley both at the gorge and just upstream of the gorge area limits the space for the deposition of river terraces. The reduced palaeoflood discharges could therefore be due to the limited accommodation space for the deposition of fluvial terraces leading to boulders being transported downstream into the Río Aguas where there is a wide open valley for terrace deposition.

Table 6.3 contains the maximum and minimum values recorded by the terrace deposits.

The maximum palaeoflood discharge (1753 m³/s) is recorded by level 4 deposits. The minimum values (10 m³/s) are recorded by the level 1 deposits.

Terrace	Minimum	Maximum
1	10 m ³ /s	70 m ³ /s
2	343 m ³ /s	631 m ³ /s
3	152 m ³ /s	1683 m ³ /s
4	81 m ³ /s	1753 m ³ /s

Table 6.2: Palaeoflood data collected from the Río Jauto catchment.

Chapter 6: The Río Jauto

The data indicates that palaeoflood discharges increased substantially between terrace levels 2 and 3 with the maximum palaeoflood discharges recorded being more than two times larger for level 3 and 4 than in level 2 terraces. The differences in palaeoflood discharges could be related to either climatic fluctuations, as described in chapter 5 (section 5.6), or to the base level drop created by differential uplift.

6.8 Development of the Río Jauto drainage system

The modern day course of the Río Jauto follows the foothills of the Sierra de los Filabres on the northern margin of the Sorbas basin to join the Río Aguas near the village of Alfaix. The river system collects several north south flowing systems as it flows along the Sierra de los Filabres and it is suggested that the Jauto developed as a headward eroding system. By studying the clast assemblage of the terrace deposits it may be possible to identify when or if the rivers captured the north south flowing streams.

This section also aims to address whether the Río Jauto has shifted its course to flow round the north side of the ridge instead of the south side. In the middle reach, near the village of Los Castaños, the landscape is highly dissected. To the south of the Lomas Orodña ridge, there is an area of flat land in filled by slope material (Figure 6.19). Any resulting terrace gravels could have been buried by slope material such as those seen on the capping the level 4 terrace deposits. Another area where the former course of the Jauto is uncertain is around the town of Los Castaños where the river currently passes to the northeast of the town. There is a valley to the east of Los Castaños where the river could have formally flowed following the A370 to join the Río Aguas near the village of Almcaizar (Figure 6.20).

Chapter 6: The Río Jauto



Figure 6.19: Photo showing where the modern river channel is currently positioned and a valley where the Río Jauto could have previously been. Facing south.

6.8.1 Development of river course

Level 1 deposits in the distal reach of the Río Jauto indicate that the river system developed as small headward eroding streams that followed structures in the basement geology. Clast assemblage data indicates that limited incision had taken place into the basin sedimentary infill with lithologies sourced from the local area dominating the deposits. There is no marble within the clast assemblage (Figure 6.21). Marble only outcrops to the north of the village of Cariatiz in the catchment of the Rambla de Chive. The absence of this lithology therefore indicates that the river system was not yet part of the Jauto system.

Chapter 6: The Río Jauto



Figure 6.20: Los Castaños river valley showing course of modern river channel and possible former route of river channel. Facing northeast looking towards the town of Los Castaños.

Mable clasts begin to be present in small percentages in level 2 deposits (Figure 6.20). The percentage of marble present in the clast assemblage increases through the terrace levels with level 4 deposits containing the most marble clasts. This suggests that the Rambla de Chive was part of the Río Jauto fluvial system at the time of aggradation of level 2 deposits. The percentage of clasts sourced from the sedimentary infill increases through time reflecting the entrenchment of the fluvial system into the basin sediments.

Chapter 6: The Río Jauto

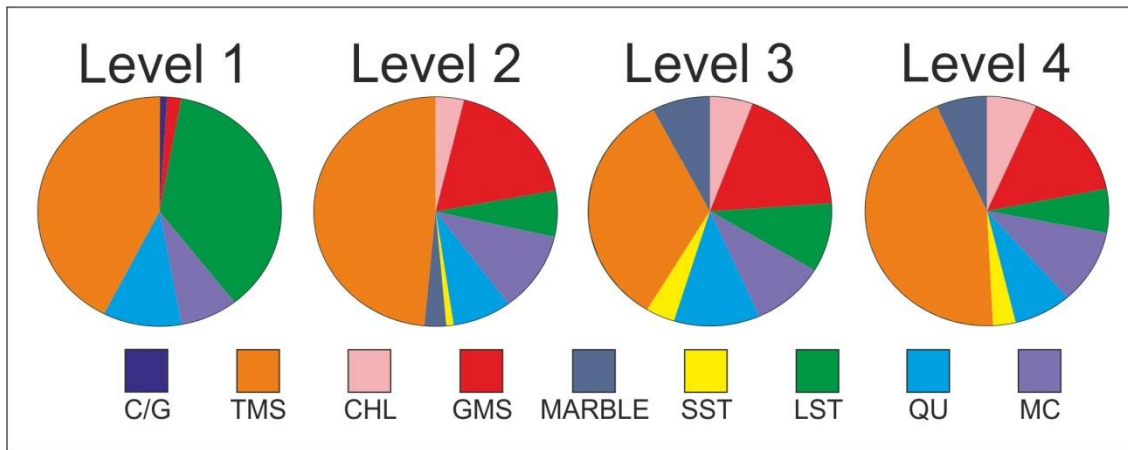


Figure 6.20: Clast assemblage data for the Río Jauto showing the increasing % of marble and sedimentary infill through time (C/G= conglomerate, TMS= tourmaline gneiss, GMS= garnet mica schist, SST= sandstone, LST= limestone, QU= quartz, MC= meta carbonate).

6.8.2 Los Castaños valley

The area downstream of Los Castaños is dominated by a highly dissected valley surrounding a ridge of basement rock (Level 1 erosion surface). The flat nature of the valley floor to the south of the Loma Orodoña ridge (Figure 6.19) indicates that the Río Jauto could have previously flowed to the south of the ridge of tourmaline gneiss.

The Río Jauto currently flows round to the northeast of Los Castaños town; however, there is a valley to the east of the town where the river could have previously flowed.

The area to the south of the Loma Orodoña ridge and to the west of Los Castaños was investigated to see whether there were any terrace gravels that would indicate whether the Río Jauto had flowed through the area.

The flat valley floor to the south of the Loma Orodoña ridge has numerous gullies running through the surface. Gullies further to the north below Los Castaños town contain level 4 gravels however, the gullies to the south of the ridge do not contain any river gravels indicating that the river has not flowed in that area. A well to the south of

Chapter 6: The Río Jauto

the valley did not contain any gravels where as one at the southern tip of the ridge did.

This is evidence that the river has always flowed around the north side of the ridge.

The area around Los Castaños town was also studied and any terrace gravels present in the streams to the west of the town were investigated. Studies of the clast assemblage in deposits to the east of the town had no clasts originating from the Caños Formation which outcrops only to the south of the Río Jauto catchment (Appendix 3). There was also no chlorine mica schist present in the gravels which originates from the Góchar formation (chapter 2). The level 2 type section (section 6.4) at Los Castaños town displays palaeocurrents to the northeast. This suggests that the river channel developed to the northeast of the town through the basement metamorphic and did not flow to the east of Los Castaños.

6.9 Establishing a chronological framework

This section aims to establish a relative chronological framework for the Jauto fluvial archive. There is currently no chronology for the Jauto fluvial archive with no absolute or relative dates for the fluvial terrace deposits. Relative dating methods which could be employed are relative stratigraphy (including height relationship above the modern river and incision between terrace levels), soil chronology (rubification and pedogenic calcretes), biostratigraphy and comparison of sedimentary characteristics (including lithostratigraphy) with the Río Aguas fluvial system. In this case biostratigraphy is not used as no fossils have been found in the terrace deposits. This is common in semi arid areas where there is little preservation of organic material.

The use of soils as a relative dating methodology has been widely applied in the Sorbas basin on the Río Aguas terraces (Harvey & Miller, 1995; Maher, 2005). A number of

Chapter 6: The Río Jauto

assumptions are used when utilising soil as a chronological marker. Firstly, it is assumed that soils on terrace levels form simultaneously on all terrace surfaces of the same age. However, the abandonment of terrace formation may be diachronous and therefore any age must be treated with caution. The rate of soil formation also differs in different climatic conditions (Yaalon, 1997) and this makes the estimation of the age of soils more complex (Harvey & Miller, 1995).

An issue with relative dating is that it only provides an order of events rather than the actual date of an event. In order to use them as a chronological reference for terrace incision, absolute dating is needed to place the terrace surfaces in chronological order. In this study cosmogenic dating has been employed in the Río Aguas catchment to date fluvial terraces. However, in the Río Jauto catchment the terrace deposits were not possible for dating using the profiling method of cosmogenic dating due to the lack of man-made sections, a lack of opportunity to excavate a site and the degraded nature of outcrops of terrace gravels. An attempt to date a level 1 erosion surface did not yield a date due to oversaturation by atmospheric Neon (section 7.5).

The lack of an absolute chronology for the Jauto system means that currently only a tentative framework can be established using relative dating methods. Relative dating has been undertaken using sedimentological data and soil data from the terraces along with relative stratigraphy. Relative dating information can then be linked to the Río Aguas system where the fluvial archive has an absolute chronological framework based on U-series dating (Candy *et al.*, 2004; 2005) and cosmogenic dating (this study).

In a fluvial landscape the oldest fluvial landforms are those that are highest above the current river channel (assuming that no tectonic displacement has taken place) so in the case of the Río Jauto catchment terrace level 1 is the highest and therefore the oldest.

Chapter 6: The Río Jauto

Terrace level 4 is the closest to the modern stream bed and is the youngest terrace level present.

Unlike in the Aguas system where there is a clear soil chronology (Section 3.7.1), with the majority of the terrace surfaces displaying some soil formation (Bt, Bk and K horizons), in the Jauto system there is limited preservation of soil formation with often only K horizons present. This could be due to the intensive farming that has occurred on the surface of the terraces. The Río Jauto deposits show increasing calcretes with relative age. The level 2 deposits are capped by type IV calcretes, the level 3 deposits type III/IV deposits and level 4 type II calcretes.

In the distal reaches of the Jauto catchment where level 1 deposits are isolated in the landscape by the formation of the lower gorge, preservation of Bt and Bk horizons occurs. The soils give an average Munsell colour chart reading of 2.5 YR. Terrace A and B deposits in the Río Aguas system provide readings of 2.5 YR indicating that the level 1 deposits are at least equivalent to the terrace B deposits and are more likely to be the same age as terrace A.

In the middle reach of the Jauto, level 3 terraces display soil formation with red colouration of Bt horizons clearly seen on the surfaces of the terraces. Munsell colour chart readings for the level 3 terraces produces an average of 5.0 6/5 (red) YR. This is the same as the terrace C deposits in the Aguas system, from which an average Munsell reading of 5.0 YR is recorded, suggesting that the level 3 terraces are equivalent to the terrace C of the Aguas system.

Chapter 6: The Río Jauto

Relative age		Late to Mid Pleistocene			Late Pleistocene
Terrace Level (Río Aguas)		A	B	C	D
Characteristic soil properties	Approx depth (cm)		150-200		>150
	CaCO ₃ stage	IV	III-IV	II-III	I-II
B Horizon					
Hue		2.5YR	2.5YR	5YR	7.5YR
Redness index (mean)		14	12.7	9.1	4.2

Terrace Level (Río Jauto)		1	2	3	4
Characteristic soil properties	Approx depth (cm)				
	CaCO ₃ stage	IV	III-IV	II-III	I
B Horizon					
Hue		2.5YR		5YR	
Redness index (mean)		12.4		7.8	

Table 6.3: Soil data for the Río Aguas and Río Jauto. Río Aguas data sourced from Mather *et al.* (2001).

The lowest level deposits in the Jauto, level 4 deposits, are capped by a minimum of 1 metre of fine sediments. In the Río Aguas, the lower terraces (terrace D) are also capped by fine material. This suggests that the lower terraces in the Jauto are of the same age as the Terrace D deposits in the Aguas system. The relative chronology of the Río Jauto is discussed further in Chapter 8 (section 8.1.2).

6.10 Summary

This chapter has covered the Quaternary stratigraphy of the Jauto catchment using sedimentary data collected in the field. It has been established that there are four major terrace levels in the Río Jauto fluvial archive and the fluvial environment in which the deposits were deposited have been described. Finally, a tentative relative chronology has been proposed for the Río Jauto fluvial achieved based a relative stratigraphy, plus sedimentological and soil data. A comparison has been made between the Río Jauto and

Chapter 6: The Río Jauto

Río Aguas fluvial archive. The timing of terrace deposition is discussed further in chapters 6 and 7.

Chapter 7: Cosmogenic exposure dating results

7.1 Introduction

The following chapter presents the results from the cosmogenic exposure dating methodologies, described in Chapter 4, that have been applied to landforms in the Sorbas basin. The sampling strategies and methodology are described in chapter 4 (section 4.4). Overall seven fluvial terraces, one landslide and one erosion surface were dated using cosmogenic exposure dating. The terraces were dated using the concentration profile method of cosmogenic dating (section 4.6). In some cases paired cosmogenic isotopes (^{10}Be & ^{26}Al) were used to date the terraces. Table 7.1 provides an overview of the cosmogenic isotopes utilised during this study. Minimum, maximum and best-fit ages are reported for all river terrace sites. Burial ages are reported where possible. Sample site descriptions are provided in chapter 4 for the erosion surface and landslide. The sample sites are described in chapters 4 and 5. The main aim of this chapter is to present the cosmogenic exposure ages and to compare the cosmogenic data with the existing U-Series database of pedogenic calcretes used to date fluvial terraces in the Río Aguas catchment. This chapter demonstrates that the concentration profile method is a viable method to use to date fluvial terraces.

7.2 Calculating exposure ages

The following section describes the process of modelling the concentration profile data to produce an age for the terrace deposits. Mathematical modelling of the cosmogenic isotope data was done in the Matlab programme with additional code sourced from Balco et al. (2008) CRONOUS calculator. Matlab is a numerical computing and programming language that can be used for mathematical modelling. The CRONOUS calculator is an internet-based means of calculating cosmogenic exposure dates and

erosion rates. The calculator can also be used to calculate attenuation lengths and production rates.

7.2.1 Calculation of production and attenuation lengths

The raw ^{10}Be concentration profile produced by the AMS (Table 4a) for a sample is first used, along with information from the field about sample location (such as longitude, latitude & shielding [section 4.4] - see appendix 5), to produce an expected production rate and attenuation lengths. Production rate is the amount of cosmogenic nuclides produced during the interactions of cosmic rays with target elements. The attenuation length of a cosmic ray is the amount of rock that a cosmic ray has to pass through before it drops below the binding energy of an atom (section 4.2). Production rates and attenuation lengths were calculated using the Matlab code from the CRONUS calculator produced by Balco et al. (2008). The code was modified to fit muon interaction cross sections described by Braucher et al. (2013), Balco et al. (2013) and references found therein. Instead of the original values determined experimentally by Heisinger, the following values in the CRONUS Matlab code were used: $K_{\text{neg10}} = 1.2916\text{e-}04$, $K_{\text{neg26}} = 0.0016$, $\sigma_{190_10} = 3.7822\text{e-}29$ and $\sigma_{190_26} = 6.9599\text{e-}28$.

Sample name	[Be-10] atoms g-1	Error atoms g-1
G30M	4.725E+05	1.483E+04
G30.5M	2.529E+05	8.902E+03
G31.0M	1.545E+05	5.434E+03
G31.5M	9.671E+04	3.359E+03
G32M	6.685E+04	2.462E+03
GTB 0M	9.621E+05	3.115E+04
GTB 0.5M	6.855E+05	2.382E+04
GTB 1.0M	4.257E+05	1.468E+04
GTB 1.5M	3.482E+05	1.142E+04
GTB 2.0M	3.096E+05	1.078E+04

Table 7.1: Table showing the output data from the AMS analysis for two of the terraces that were sampled. The first column shows the concentration of ^{10}Be in the sample, the second column is the analytic error.

7.2.2 Modelling of data

Modelling can be achieved using a simple exposure model or a complex exposure model. A simple model assumes constant exposure to cosmogenic rays and therefore constant production rates. A complex model does not assume a simple exposure history and enables modelling of hiatuses in the form of periods of erosion. The decision on whether to use a simple or complex exposure model is based on the AMS concentration profile. Figure 7.1a shows a profile that would be modelled using a simple exposure model and Figure 7.1b is a profile that would be modelled using a complex exposure model. A cosmogenic concentration curve should be exponential with depth (Figure 7.1a) if no shielding or mixing of the terrace sediments has taken place since deposition of the terrace (Chapter 4, section 4.3.1). If the terrace gravels have been disturbed or shielded post deposition, then the concentration of nuclides will not decrease steadily with depth as clasts with different amounts of ^{10}Be and ^{26}Al will have moved around. Figure 7.2 illustrates the different profile shapes that may occur if shielding or mixing has taken place.

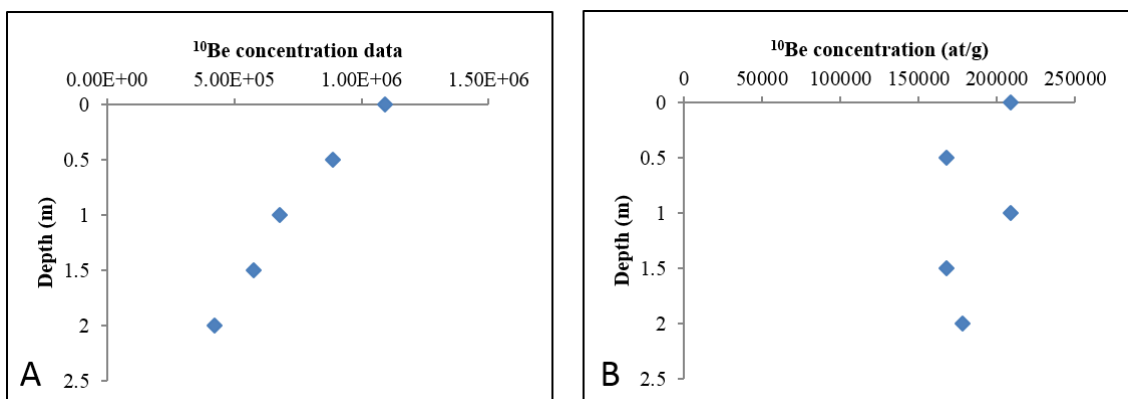


Figure 7.1: A) A curve that can be modelled using a simple exposure model B) A curve which would be modelled by a complex exposure model.

A) Simple exposure models

To each of the data sets Lal's (1991) nuclide accumulation models were fitted using Matlab. Accumulation models are mathematical models that have been calculated to

Chapter 7: Cosmogenic exposure dating results

predict how much cosmogenic nuclide would be present after a defined time period (Lal, 1991). The Chi squared minimization method (minimises the differences observed between the ^{10}Be and ^{26}Al experimental and modelled data) (Rhodes *et al.*, 2011) was used to fit Lal's (1991) equations considering concentration and depth uncertainties.

Fminsearch Matlab function was used within *optimset* ('*TolFun*', 0.005, '*maxFunEvals*', 500) options. Inheritance (accumulations of cosmogenic nuclides built up by previous exposure to cosmogenic rays-section 4.3.1) and density were determined from discrete data (input densities (g/cm^3) = 1.6, 1.7, 1.8, 1.9, 2.0, 2.1, 2.2; input inheritance = 100 values between 0 and the minimum concentration of the profile).

Density values are important because they can affect the production rate of nuclides (section 7.3). A range of densities are used to reflect the differences in density between parts of the section where calcrete is present compared to parts where no calcretes are present. Age and erosion values were determined by chi squared minimization from 200 age discrete values logarithmically distributed between 10^3 and 10^7 years to achieve a 5% precision in age results (always better than 1 sigma model results). 10^7 years models are considered saturated (infinity age). Burial ages have been calculated for profiles which have been sampled for both ^{10}Be and ^{26}Al . Burial ages are calculated using the ratio of $^{10}\text{Be}:^{26}\text{Al}$ in the oldest sample and can be used to give an indication of the maximum age of the deposit. Determination of apparent averaged basin erosion rates and maximum burial ages were based on Granger & Muzikar (2001). An average basin altitude of 500 m was considered to calculate an average production rate for the burial calculations.

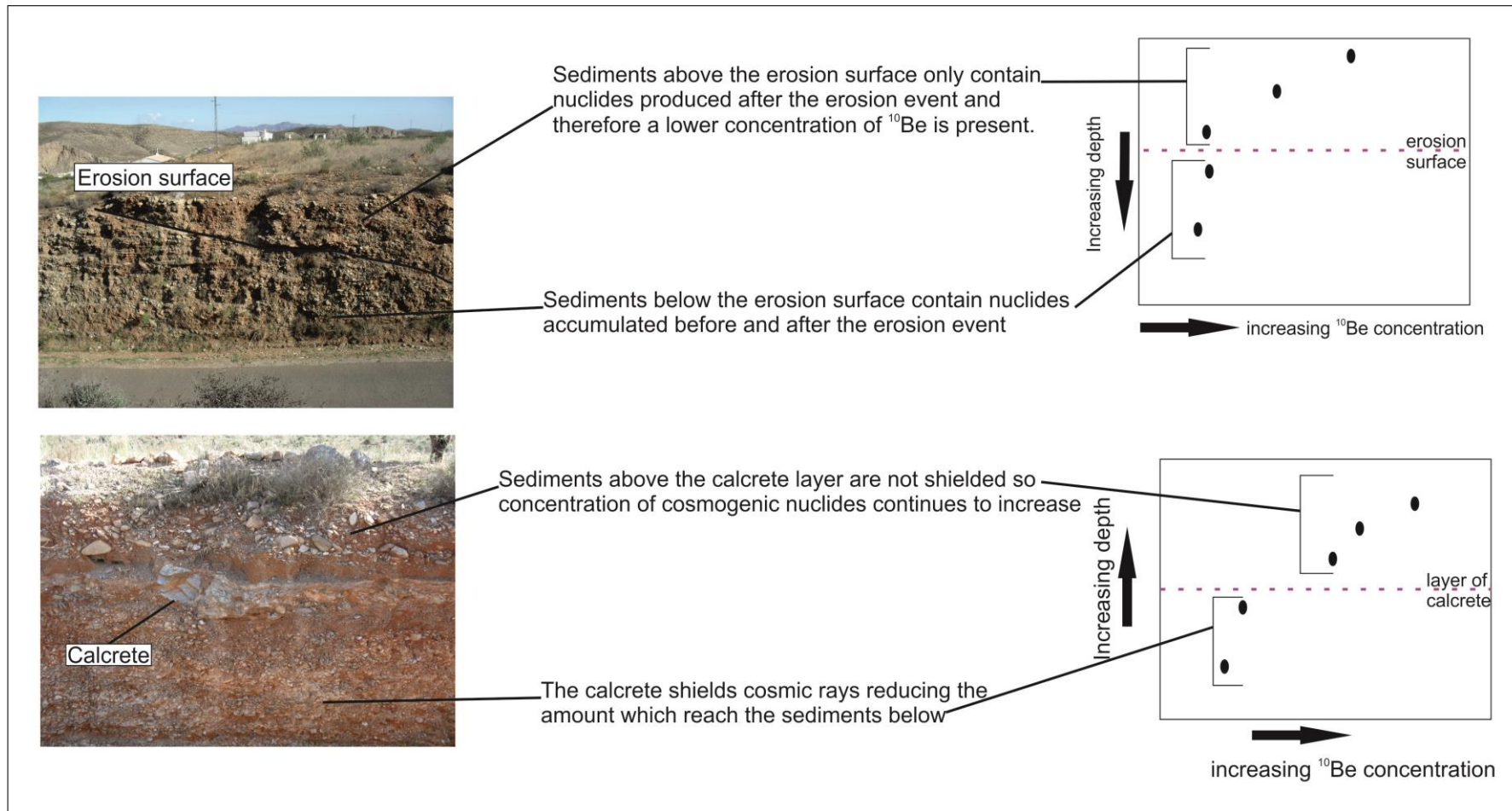


Figure 7.2: Expected shape of concentration profiles if erosions/ mixing or shielding of the terrace sediments has occur during or after deposition.

B) Complex exposure models

Profiles that indicate a complex exposure history were modelled using two unit exposure models. The models consider a first unit of sedimentation t_1 years ago and a second unit of sedimentation t_2 years ago with a period of hiatus of t_1 years at the depth of the anomaly within the concentration profile. The erosion rate of the surface was considered constant. Two profiles were considered suitable for the modelling process: MTC and TBP. These models were run considering the same parameters as the single exposure models with two exceptions; t_1 and t_2 values (total age) was tested for 100 discrete values logarithmically distributed between 10^3 and 10^7 years. Secondly 11 linearly distributed values were assigned to t_1 and t_2 for each tested age.

7.2.3 Chi-squared minimization method

A chi squared equation minimises the differences observed between the ^{10}Be and ^{26}Al concentration profiles and the concentration profiles predicted by models (Siame *et al.*, 2004).

Equation 1

$$C(x, \epsilon, t) = C_{inh} \cdot e^{-\lambda t} + \frac{P_0 \cdot p_n}{\lambda + \epsilon/\Lambda_n} \cdot e^{-x/\Lambda_n} (1 - e^{-t(\lambda + \epsilon/\Lambda_n)}) + \frac{P_0 \cdot p_s}{\lambda + \epsilon/\Lambda_s} \cdot e^{-x/\Lambda_s} (1 - e^{-t(\lambda + \epsilon/\Lambda_s)}) + \frac{P_0 \cdot p_f}{\lambda + \epsilon/\Lambda_f} \cdot e^{-x/\Lambda_f} (1 - e^{-t(\lambda + \epsilon/\Lambda_f)}).$$

C is the predicted ^{10}Be concentration as a function of time and is calculated by taking into account inherited cosmogenic nuclides (C_{inh}), the decay constant (λ) and total surface production rate (P_0). The decay constant is the rate at which cosmogenic nuclides decay and the total surface production rate is the rate at which cosmogenic

nuclides are formed at the Earth's surface. P_n (neutrons), p_s (slow muons) and p_f (fast muons) are the relative contributions of different particles in percentages. The effective attenuation lengths of these particles (λ_n , λ_s and λ_f) are also used in the calculation. The calculated C value is then used in the second equation.

Equation 2

$$\chi^2 = \sum_{i=1}^n \left[\frac{C_i - C}{\sigma_i} \right]^2$$

The second equation calculates the exposure age of the terraces. C_i is the measured ^{10}Be concentration at a given depth in the sampled terrace; σ_i is the analytical uncertainty at that depth, n is the total number of samples collected for the profile and C is the predicted ^{10}Be concentration value that was calculated in the first equation.

The χ^2 fit modelling for both single isotopes and paired isotopes takes into account nuclide concentration, depth and the density uncertainties. It can be used to produce values for both inheritance and erosion rates as well as estimating an age for the terrace surface. Only one value that minimises the χ^2 values is expected to fit the model however, there are uncertainties which are not considered by the model. To overcome the errors created by the uncertainties an χ^2 best fit value ($\chi^2 \text{ min}$) is created and then the $\chi^2 \text{ min}$ values is accessed with a quality factor to see if it is the best fit for the distribution of the data. The quality factor ranges from 0 to 1, with the best fitting data having a higher value, and is calculated using the following calculation:

$$Q_f = 1 - P(V/Z; \chi^2 \text{ min}/2)$$

With V being the degree of freedom of the model calculated by the number of samples minus the number of modelled parameters. The value of inheritance, erosion and age that fit the data within 1σ or 2σ confidence levels is obtained from the χ^2 distribution.

7.3 Concentration profile results

The next section presents the results produced by the concentration profile methodology. Minimum, maximum and best fit ages are provided for all sections.

Burial ages are present where calculated. Erosion and inheritance values are also reported. The dates are presented in stratigraphic order and the data for each profile is assessed for its quality.

7.3.1 GS sample site (Pre Terrace A erosion surface)

7.3.1.1 AMS data

Paired isotopes, ^{10}Be and ^{26}Al , have been measured in the landform to enable the age of the Góchar surface/erosion surface to be accurately constrained. This enables the calculation of an erosion rate, an age and a maximum burial age for the surface of the terrace deposit.

The concentration data produced by AMS analysis presented in Figure 7.3 & 7.4 show a good match in the shape of the curve between the ^{10}Be and the ^{26}Al data sets with no outliers present. This indicates that there has been no mixing of the profile and no hiatus in sediment deposition during cosmogenic nuclide formation in the sampled section.

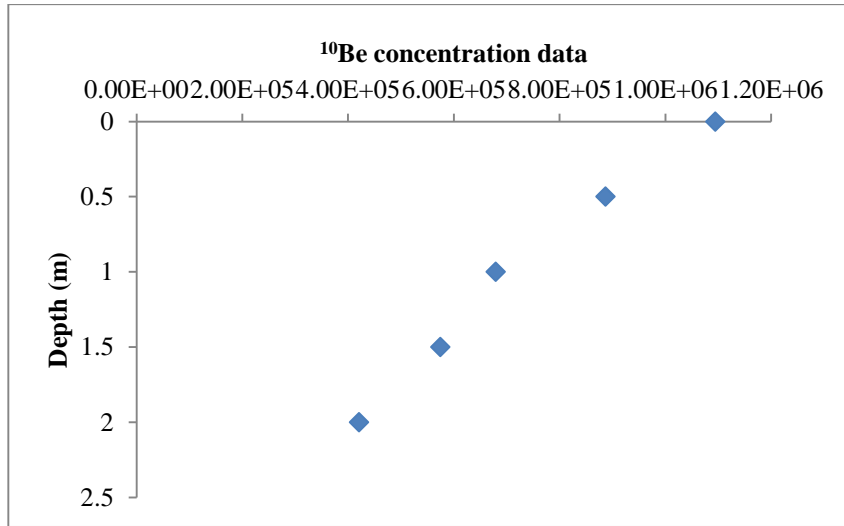


Figure 7.3: Graph of concentration profile for ¹⁰Be data from the G.S site showing the curve of the data with no outliers

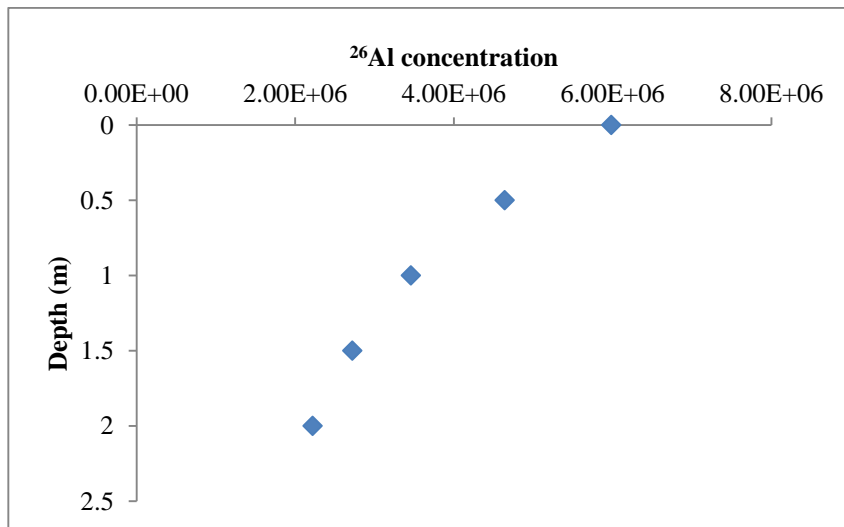


Figure 7.4: Graph of the ²⁶Al concentration data from the G.S site. The curve follows the same pathway as the ¹⁰Be data.

7.2.1.2 Concentration profile & Burial Age

The GS sample site ¹⁰Be exposure model results are shown in Fig 7.5. ²⁶Al exposures models yield similar results in terms of age and erosion rate. The resulting erosion rates of 0.8 mm/ka is not high for a sediment surface.

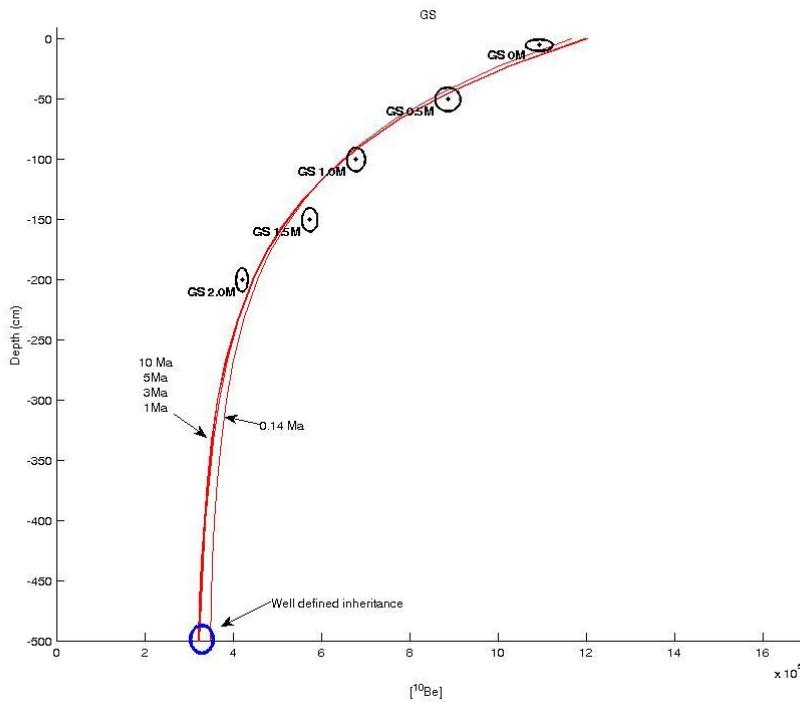


Figure 7.5: Modelled ages for the G.S ^{10}Be data showing the wide variability in ages which fit the experimental curve.

Modelled densities (1.6-1.8) also look sensible for these deposits. The results of the age modelling are imprecise because the profile seems to be saturated with cosmogenic isotopes (i.e. it is compatible with a large set of erosion rate-age pairs).

Erosion rate - age pairs fitting the GS ^{10}Be profile data within 1 sigma confidence level are represented in Fig. 7.6. Again, the ^{26}Al profile yields a very similar graph. Fig. 7.7 shows the probability of each age based on the same models. This means that the "best fit" of the exposure models that are saturated (i. e.: are compatible with any age from minimum to infinite) means nothing because the probability of the best fit is almost the same as the probability of any other age. Thus, in this case the best fit of 3 Ma is just an artefact.

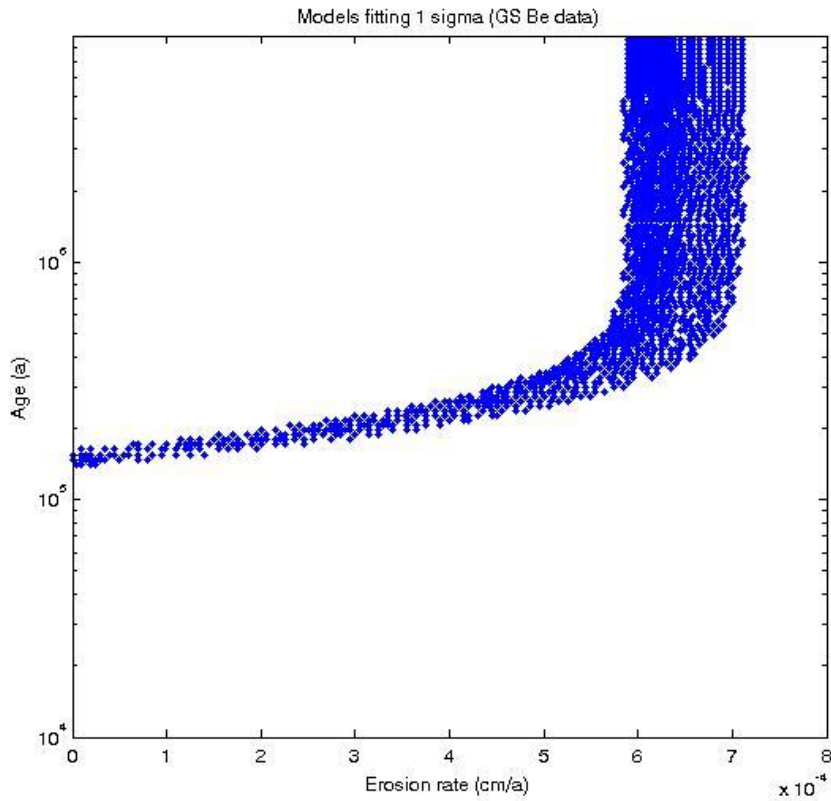


Figure 7.6: The modelled erosion rate for the G.S sample site.

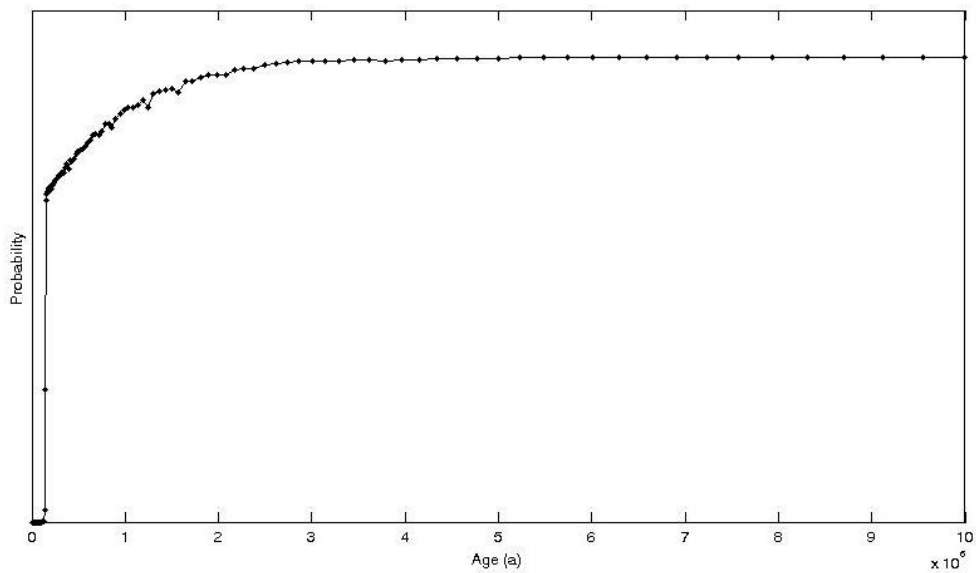


Figure 7.7: This probability data graph shows that there are a wide number of ages that could fit the G.S cosmogenic isotope curves.

However, the one parameter of the exposure models that is very well defined in the GS

^{10}Be and ^{26}Al profiles is the amount of inherited ^{10}Be and ^{26}Al .

Chapter 7: Cosmogenic exposure dating results

^{26}Al and ^{10}Be are produced at the surface with a ratio of $^{26}\text{Al}/^{10}\text{Be}$ of c. 6.7, but this ratio is depleted with time because of the different ^{10}Be and ^{26}Al decay rates producing the characteristic curve seen in the graphs. Inheritances can be used to calculate the "burial age" of the sediments since its first exposure (section 4.0; Granger and Muzicar, 2001). It cannot be assumed that these sediments were deposited by the last depositional event due to their depth in the section, therefore the burial age should be considered as a maximum age of the landform deposition. Using ^{10}Be and ^{26}Al model results a burial age can be calculated by plotting the inherited concentrations in a "banana plot" (see Fig. 7.8). These results indicate that the erosion surface sediments were deposited after 1.5 Ma.

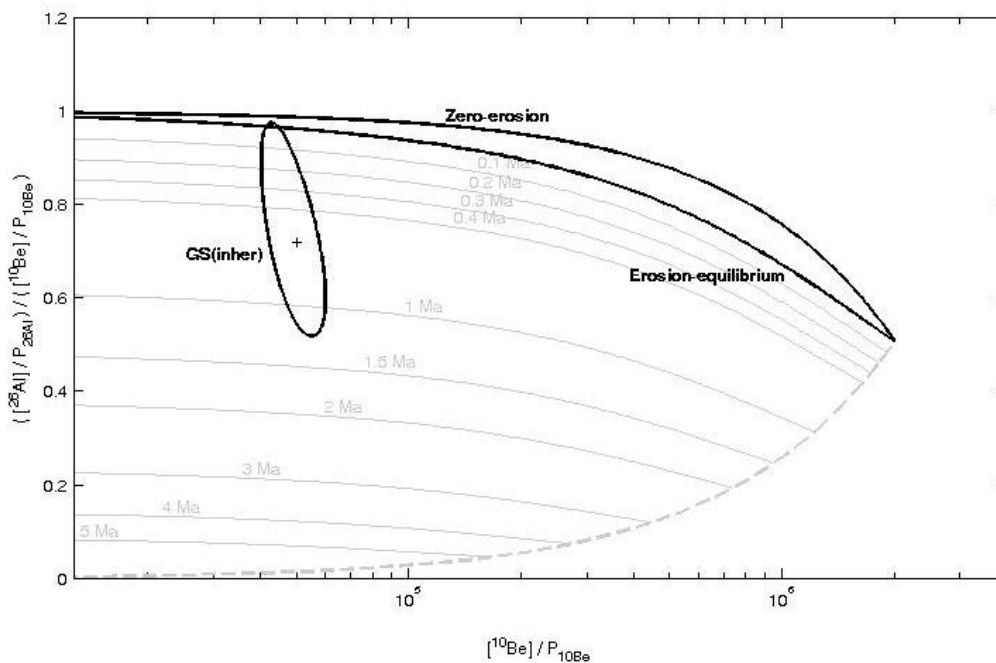


Figure 7.8: A banana plot showing the burial age for the G.S data.

By considering the age probabilities of the exposure model and the age probabilities of the burial dating based on the inheritance, it can be argued that the deposition age of the GS sediments should be between 0.2 and c. 1.3 Ma within 1 sigma confidence level (Fig. 7.9). The "best-fit" age seem to be around 1 Ma. This seems to be compatible with an "upper Matuyama" paleomagnetic age for the "Rañas".

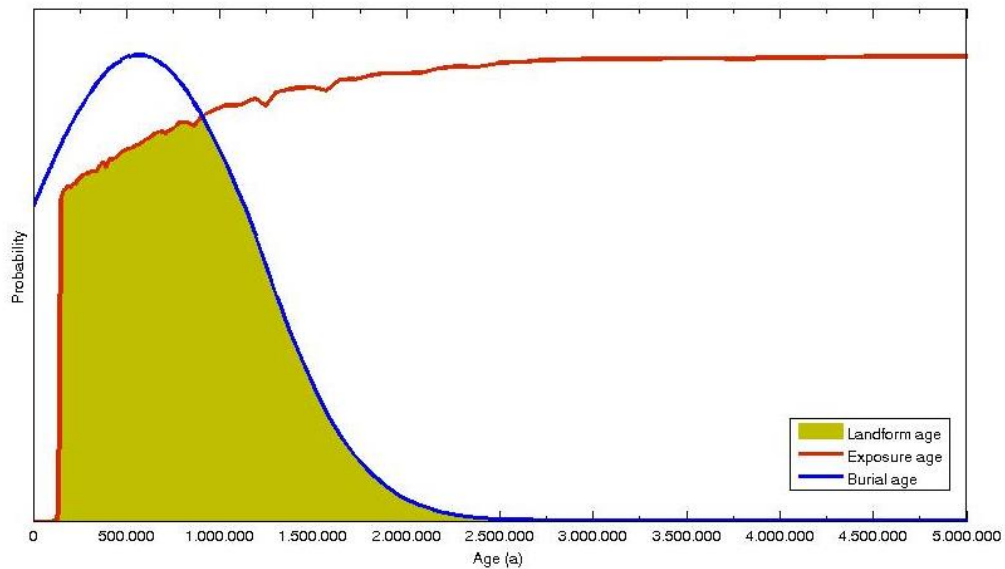


Figure 7.9: Graph showing the expected age of the Pre Terrace A erosion surface when comparing the burial age with exposure age.

7.3.2 GTB sample site (Terrace B)

7.3.2.1 AMS data

A single isotope, ^{10}Be , was measured for the GTB sample site. Paired isotopes were not applied in this case as the age of the terrace was believed to be below 500ka. The data presented in the graph below (Figure 7.10) show a good exponential curve with depth. There are no outliers present. This indicates that there has been no mixing or disruption of the sampled profile by faulting or erosion.

7.3.2.2 Concentration profile Age

The ^{10}Be concentration present in the GTB sample site profile produces a best age of 140 ka and a minimum age of 130ka (Figure 7.11). The low chi squared value (1.5) is representative the well constrained nature of this sample. The models indicate an erosion rate of 6m/ma at the sample site. Inheritance values are high at this site with a calculated value of 0.25×10^6 atoms.

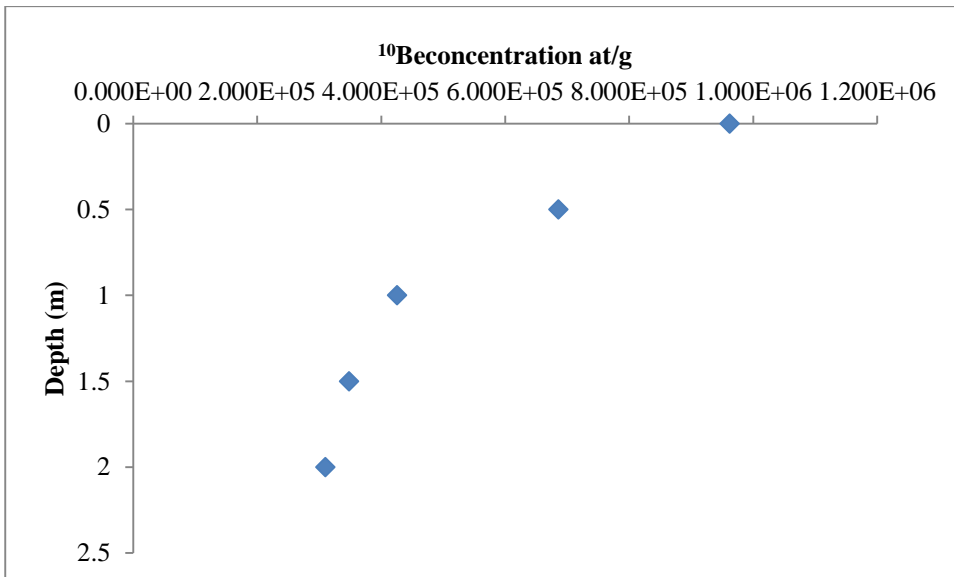


Figure 7.10: AMS data for the GTB sample site. Concentration of ^{10}Be is show with depth.

7.3.2.3 Burial age

A burial age for the GTB sample site could not be calculated as this involves the use of paired isotopes.

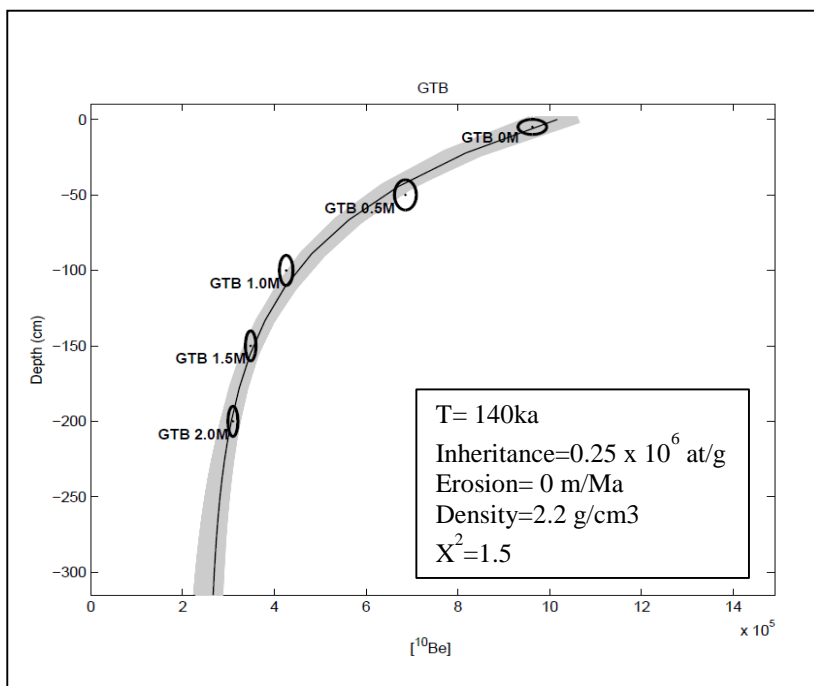


Figure 7.11: Chi squared minimisation model curve for ^{10}Be data from the GTB sample site.

7.3.3 CB sample site (Terrace B)

7.3.3.1 AMS data

Paired isotopes, ^{10}Be and ^{26}Al , have been measured in the landform to enable the age of the CB sample site to be accurately constrained (Figure 7.12 & 7.13). Although the AMS profile data for the ^{10}Be and ^{26}Al cosmogenic nuclides have matching curve shapes they do both contain an anomalous value. This will affect the ability to match the modelled curves to the data curves reducing the accuracy of the method. The value indicates a lower than expected concentration of nuclides at a depth of 1 m in the profile. The presence of an anomalous data value at the same location in both profiles rules out an experimental error and indicates that there was an increased amount of cosmogenic nuclides present in the sediment.

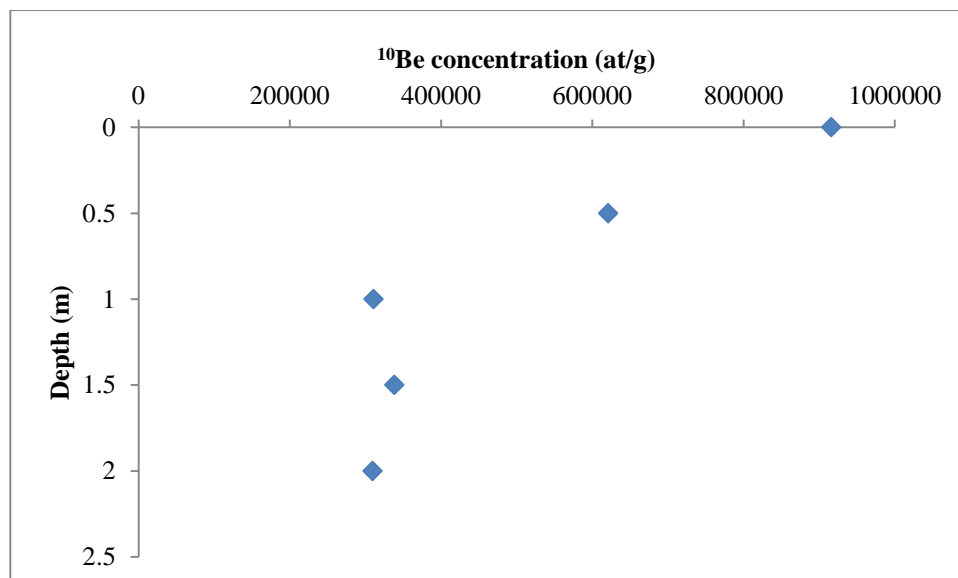


Figure 7.12: Graph showing the ^{10}Be profile for the C.B sample site

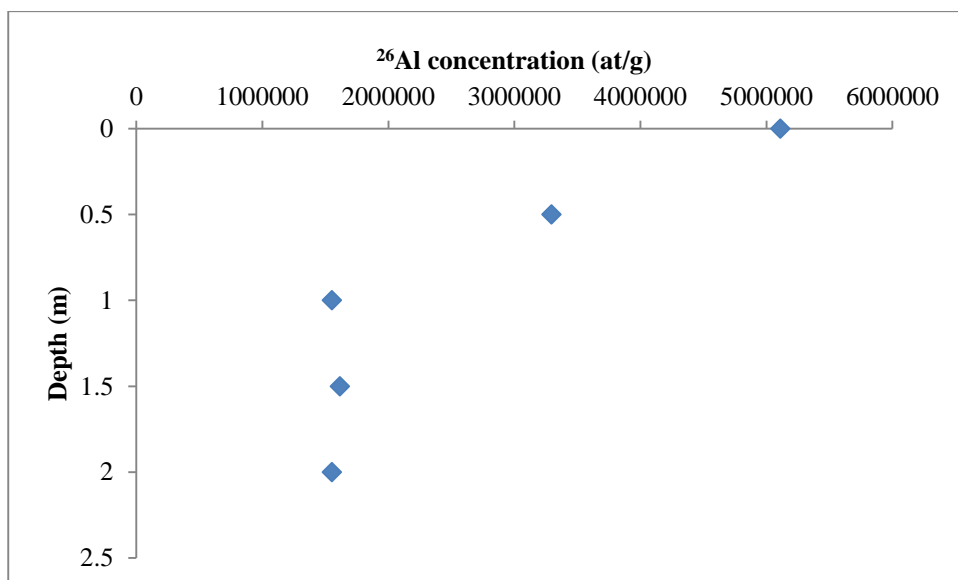


Figure 7.13: Graph showing the ²⁶Al profile for the C.B sample site

7.3.3.2 Concentration profile Age

The data for the CB sample site were modelled in a single exposure model. Modelling of the data (Figure 7.14 & 7.15) shows that the best fit curve with a statistically most likely age of 130 ka and low erosion rates of 1m/ma. Inheritance levels are high with 0.24×10^6 atoms for ¹⁰Be and 1.30×10^6 atoms for ²⁶Al. The chi square value for type ¹⁰Be fit is 20.6 which is a good statistical match.

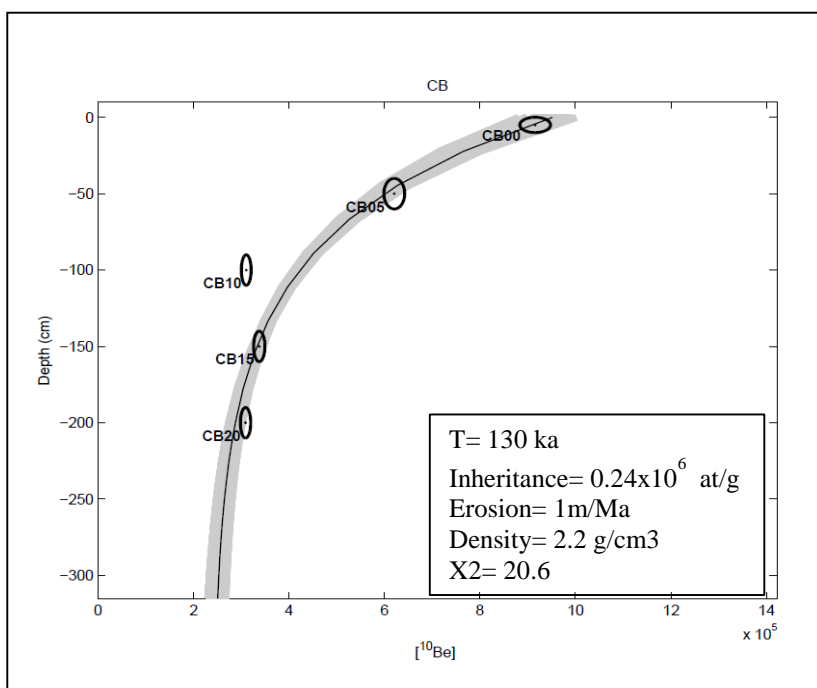


Figure 7.14: Single exposure model results for the CB sample site based on ¹⁰Be concentrations

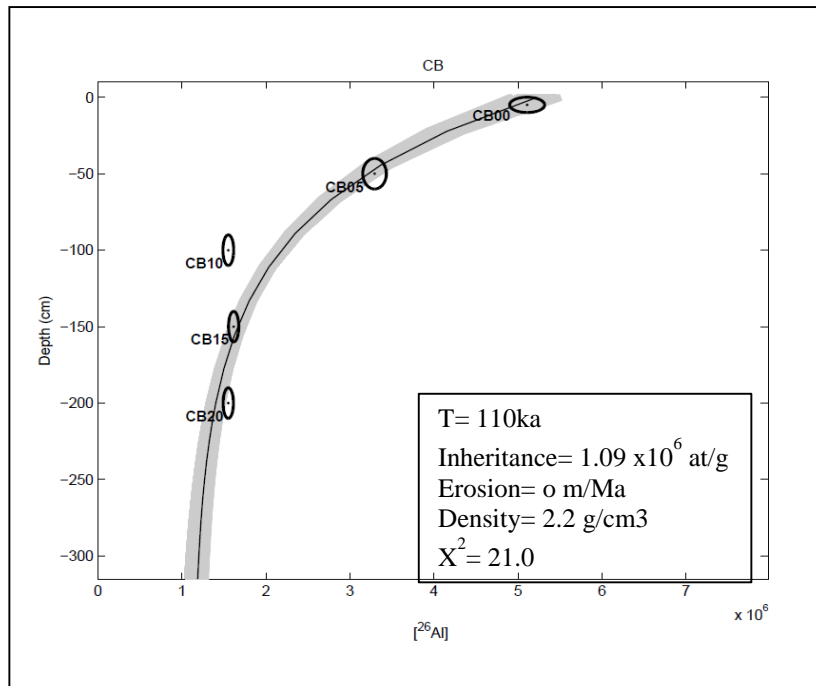


Figure 7.15 Single exposure model results for the CB sample site based on ^{26}Al concentrations

7.3.3.3 Burial age

Burial age dating using the concentration of cosmogenic nuclides present in the deepest sample suggests a maximum age of 573 ka for the deposit.

7.3.4 TBP sample site (Terrace B)

7.3.4.1 AMS data

For the TBP sample site, both ^{10}Be and ^{26}Al were both measured to ascertain the age of the deposit (Figure 7.16 & 7.17).

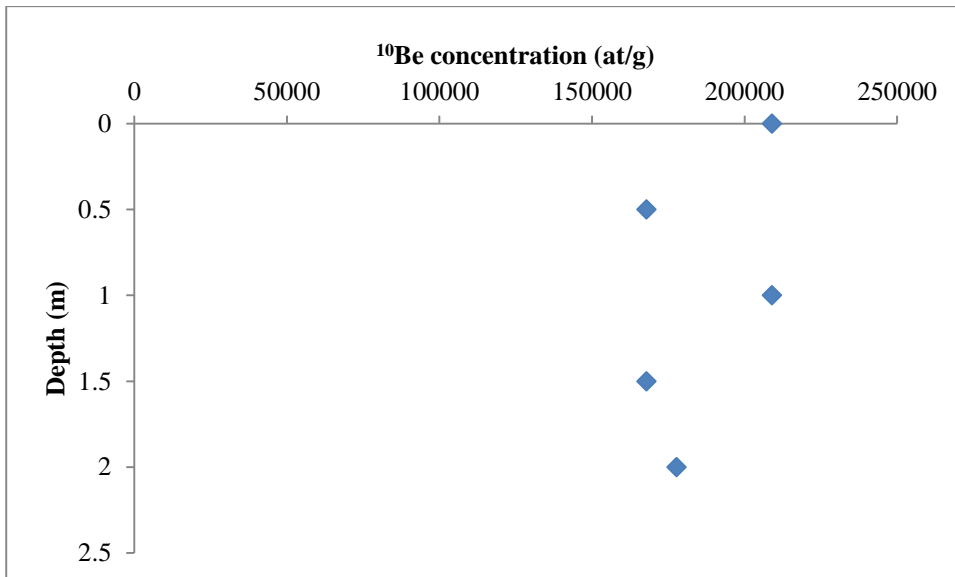


Figure 7.16: Concentration profile for ^{10}Be from the TBP sample site

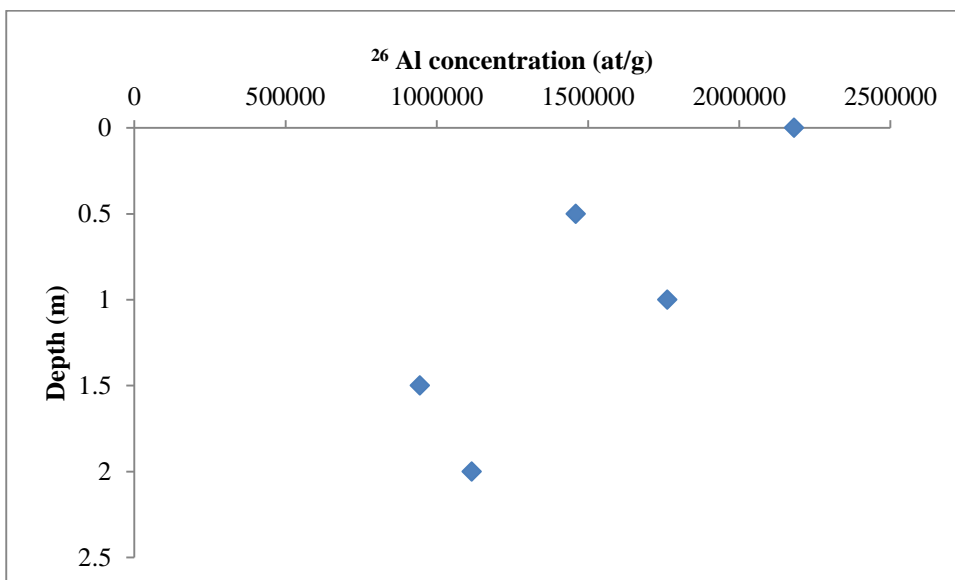


Figure 7.17: Concentration profile for ^{26}Al (TBP sample site)

The TBP profile for both the ^{10}Be and ^{26}Al show anomalies in the profile, with two points (1m & 2m) having a higher than expected concentration (Figure 7.1a) indicating that some mixing has taken place by deformation. The process of sedimentation could also have been interrupted by erosion events. This would lead to the sediments above the erosion surface having a lower amount of nuclides than in the sediments deposited before erosion event took place (Figure 7.2). The sediments deposited below the erosion surface would have been exposed to cosmic rays for longer. Another reason for anomalous values within a profile could be the presence of a calcrete capping sediments

and shielding them from cosmic rays. Shielding would produce values with a lower than expected concentration of cosmic rays. The anomalous points in the profile have a higher than expected concentration therefore shielding has not occurred. The calcrete could, however, have formed along the erosion surface masking it.

7.3.4.2 Concentration profile Age

The data for the TBP sample site were modelled in two model types, firstly in simple exposure model and secondly in a complex exposure model. The single exposure model assumes one single exposure event whereas the complex exposure model assumes multiple exposures.

A) Single exposure model

The results for the single exposure model are presented in Figure 7.18 & 7.19. The single exposure model has produced dates that are too young (40 ka for ^{10}Be best fit) or too old with a maximum age of 1.72 Ma calculated (^{10}Be). The maximum age is too old to be stratigraphically correct and the best fit age is too young. The model curves are a poor match for the data and this is reflected in the chi square values for the model (29.5 for ^{10}Be and 41.6 for ^{26}Al) which are high.

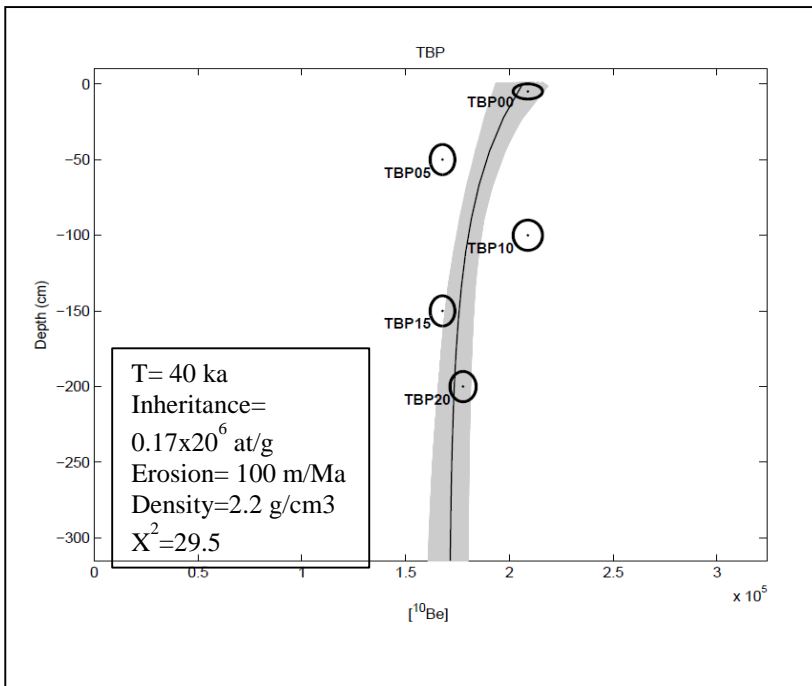


Figure 7.18 Single exposure model results for the TBP sample site based on ^{26}Al concentrations

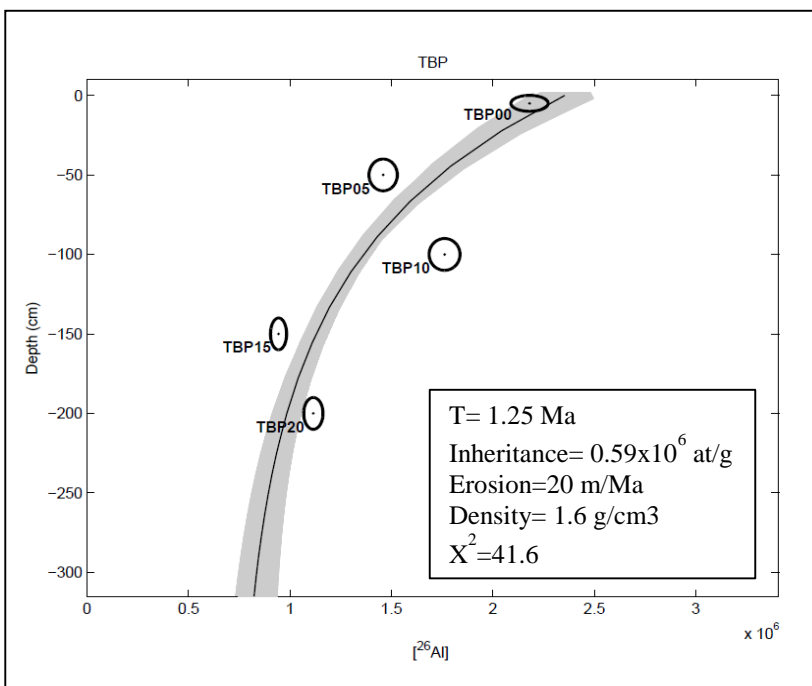


Figure 7.19 Single exposure model results for the TBP sample site based on ^{26}Al concentrations

B) Complex exposure model

In order to produce a better model which is more representative of the data, a complex exposure model was devised with a period of erosion used to reflect the points with higher nuclide concentrations than expected. Both beryllium and aluminium data were

Chapter 7: Cosmogenic exposure dating results

run through the complex exposure model (Figure 7.20 & 7.21). The age produced by the model is 2.72 Ma (^{10}Be) and 170 ka (^{26}Al). The ^{10}Be age is too high for the sample site and indicates that there is probably a high amount of inheritance present in the terrace sediments.

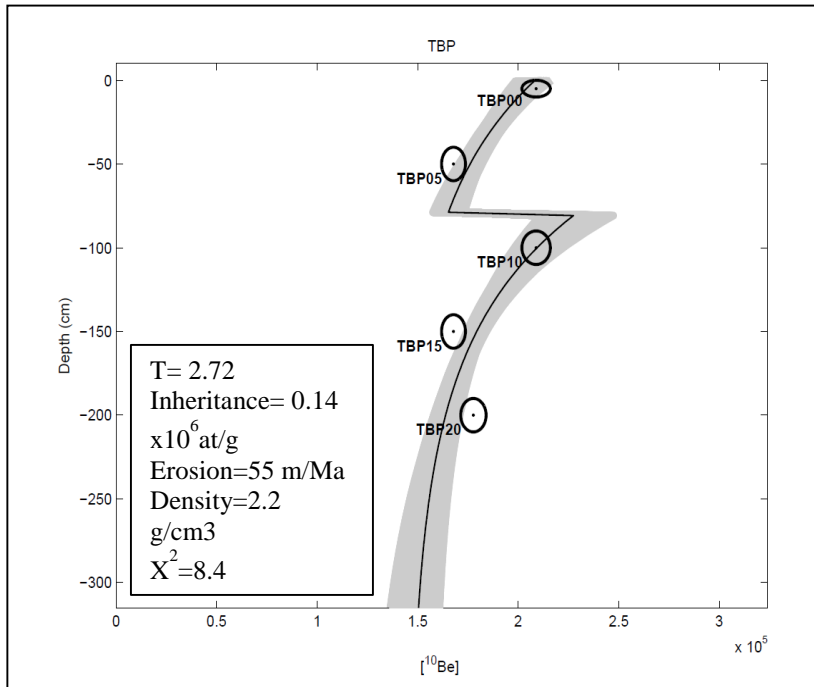


Figure 7.20 Complex exposure model for the ^{10}Be cosmogenic nuclide concentration profile for the TBP sample site.

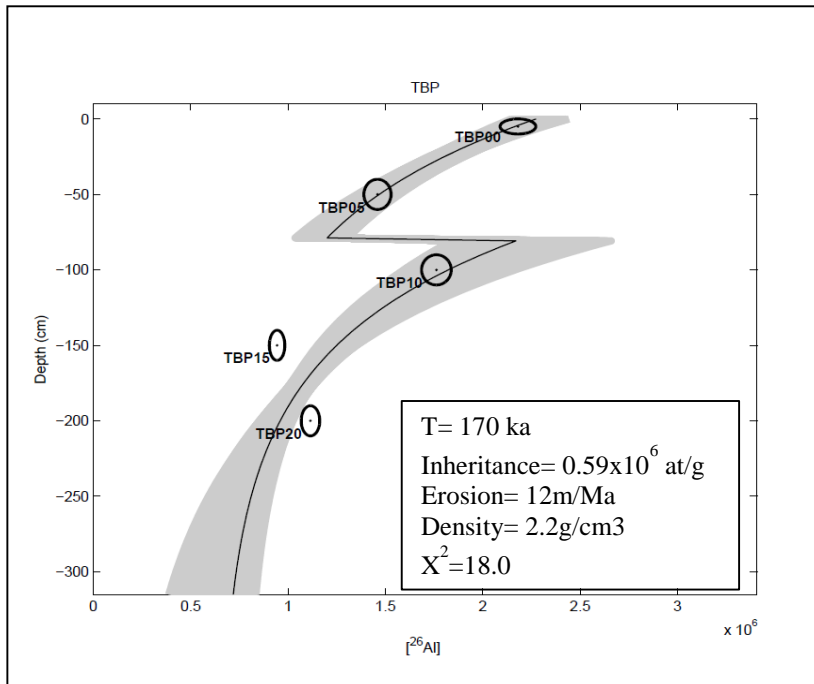


Figure 7.21 Complex exposure model for the ^{26}Al cosmogenic nuclide concentration profile for the TBP sample site.

7.3.4.3 Burial age

The deepest samples for the TBP profile have been used to provide a maximum burial age for the surface sediments of the terrace. The best fit maximum age for the surface is 161 ka. This is a good maximum age for the deposit and also stratigraphically correct.

7.3.5 G3 sample site (Terrace C)

7.3.5.1 AMS data

A single isotope, ^{10}Be , was measured for the G3 sample site. The concentration profile (Figure 7.22) displays a smooth profile when converted to graphical form indicating no hiatus in sediment deposition. No mixing of the profile by faulting has taken place. This confirms that faults present in the G3 section were successfully avoided (Chapter 4).

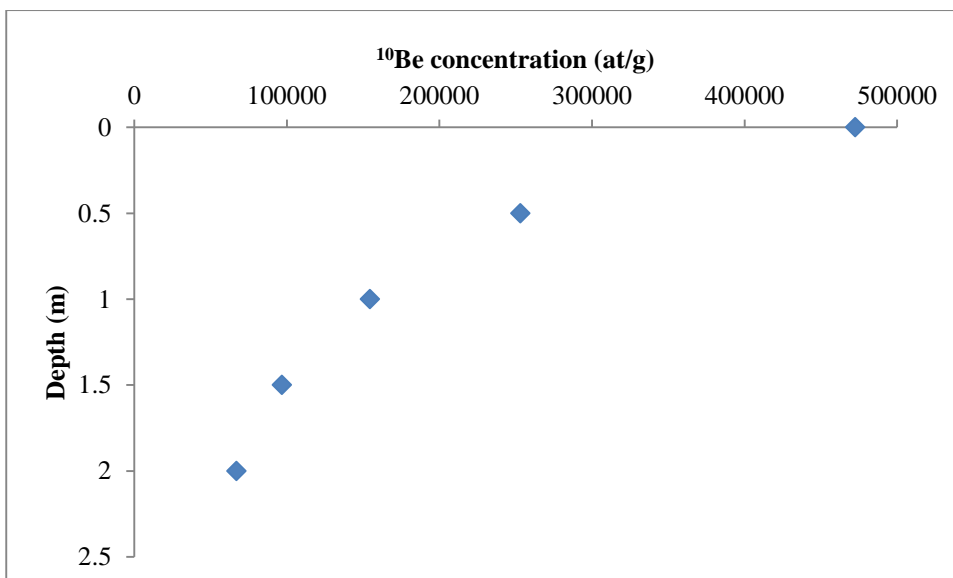


Figure 7.22 AMS data for the G3 sample site. Concentration of ^{10}Be is show with depth.

7.3.5.2 Concentration profile Age

The best fit age for the chi squared model for G3 is 120 ka with a minimum age of 70 ka (Figure 7.23). This model suggests an erosion rate of 6 m/ma with inheritance of 0.03×10^6 atoms. The chi square value for this model is very low at 0.3 indicating that there is a very good statistical fit.

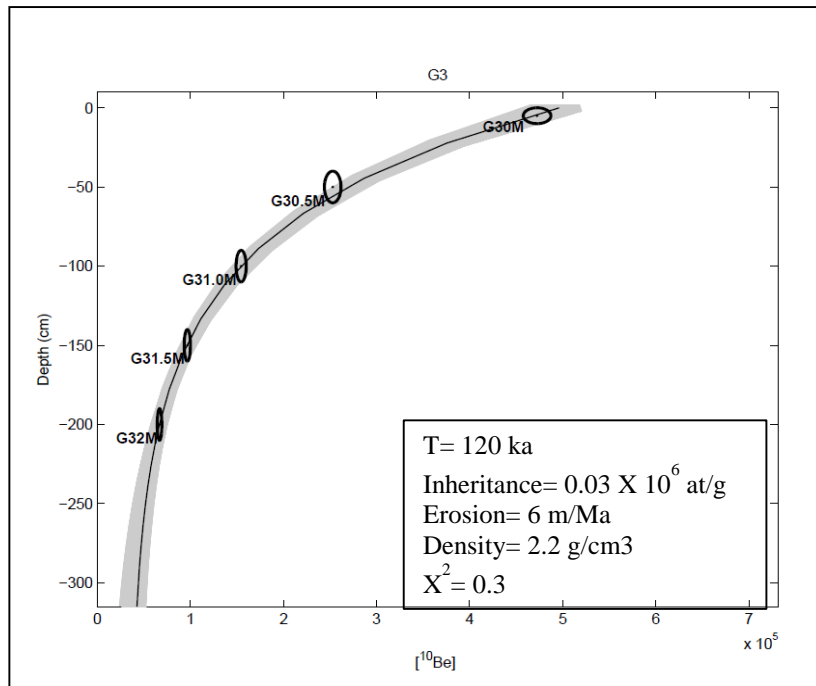


Figure 7.23 Single exposure model results for the G3 sample site based on ¹⁰Be concentrations

7.3.5.3 Burial age

A burial age for the G3 sample site could not be calculated as this involves the use of paired isotopes.

7.3.6 TCF sample site (Terrace C)

7.3.6.1 AMS data

Both ¹⁰Be and ²⁶Al have been used to produce an age and erosion rate for the TCF sample site. The two profiles match very well with an anomaly present in both samples at a depth of 0.5 m (Figure 7.24 & 7.25). The anomalous value has a lower cosmogenic nuclide concentration than would be expected suggesting some mixing with the sediment layer below. There could also have been shielding of the sediment at this level in the deposit decreasing the amount of cosmic rays reaching this point. It would be expected that the samples below the anomalous value would also have a reduced concentration of nuclides as they also would be shielding from the cosmic rays. This is

not reflected in the profile indicating that mixing of the profile rather than shielding is a more likely cause for the anomalous value.

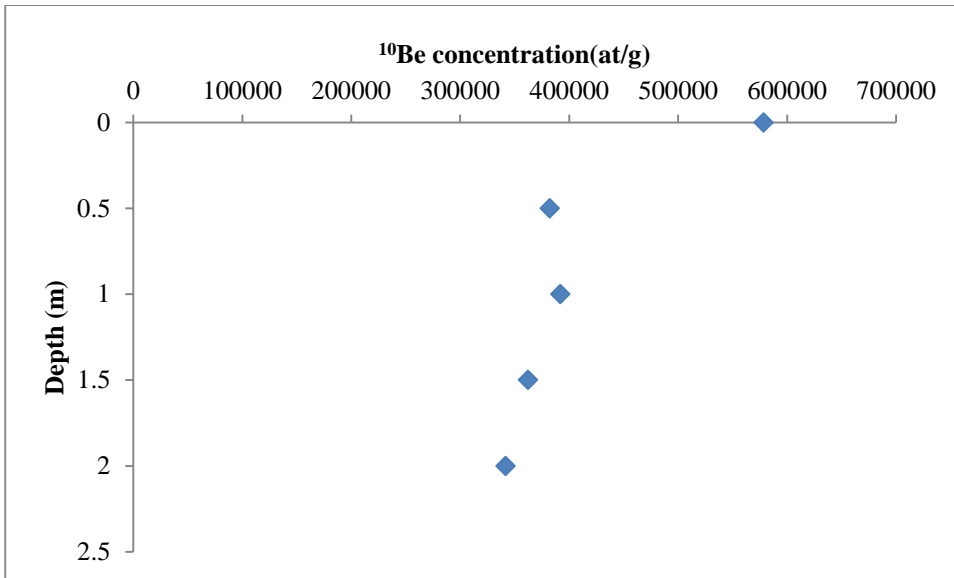


Figure 7.24 AMS data for the TCF sample site. Concentration of ^{10}Be is show with depth.

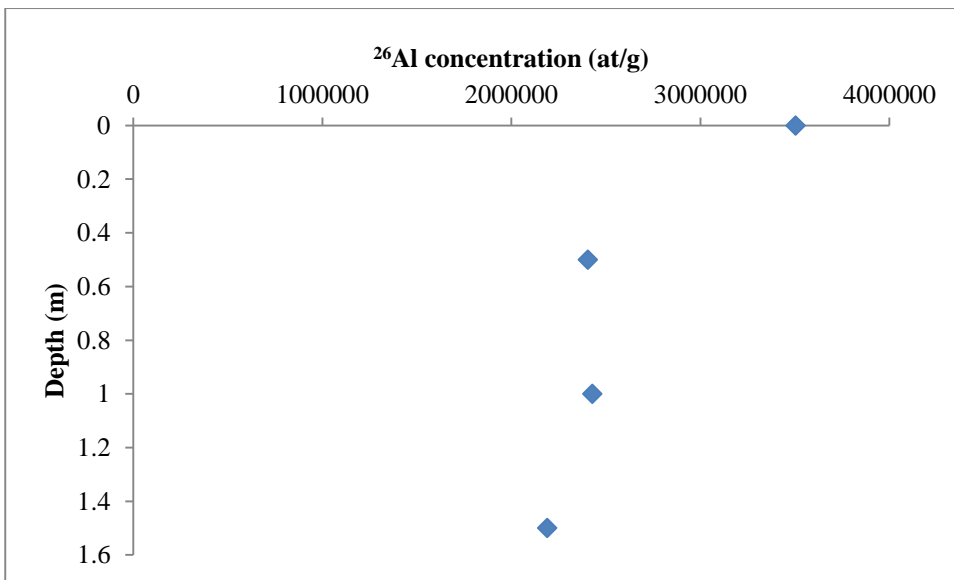


Figure 7.25 AMS data for the TCF sample site. Concentration of ^{26}Al is show with depth.

7.3.6.2 Concentration profile Age

The ages produced by modelling the data in the chi squared equation are presented in Figure 7.26 and 7.27. The results indicate that the surface sediments were deposited 79 ka (^{10}Be best fit). The ^{26}Al inheritance input to the deposit is quite large at 1.93×10^6 atoms. The chi square values indicate that the modelled curves are a good fit. The erosion rate calculated for the TCF site is between 5-7 m/Ma.

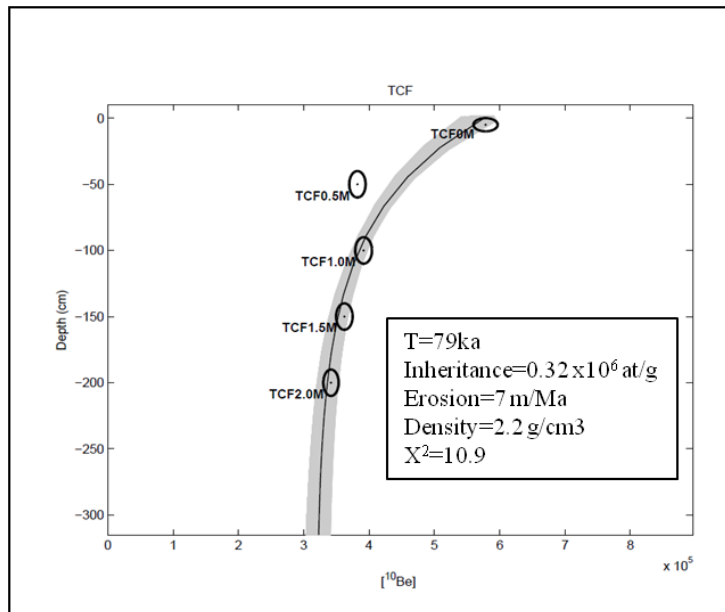


Figure 7.26: Single exposure model results for the TCF sample site based on ^{10}Be concentrations

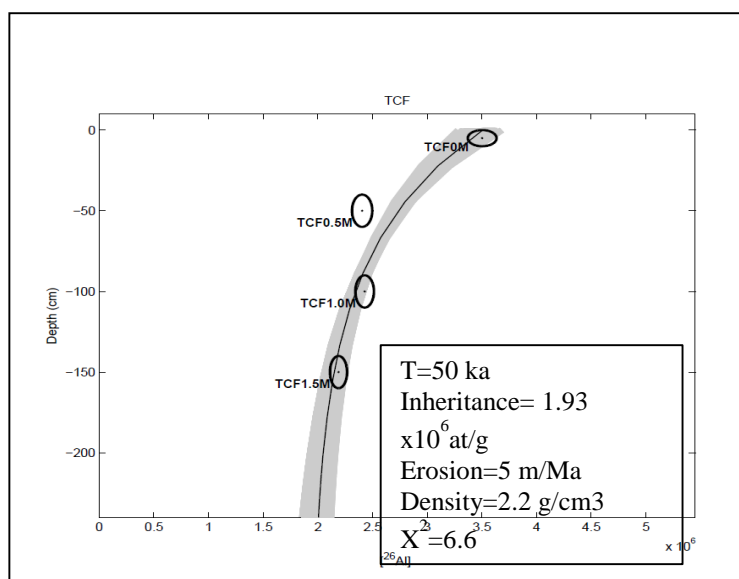


Figure 7.27: Single exposure model results for the TCF sample site based on ^{26}Al concentrations

7.3.6.3 Burial age

The burial age data indicates that the maximum age of the terrace C surface deposits is 231 ka. This is quite old and indicates that inheritance is a significant problem for some of the terrace deposits.

7.3.7 MTC sample site (Terrace C)

7.3.7.1 AMS data

The cosmogenic nuclide concentrations measured in the AMS for the MTC site show a good match indicating limited laboratory uncertainties. Both profiles show two curves (Figure 7.28 & 7.29). The first curve consists of the top two samples of the profile (0 & 0.5 m) and the second curve covers the bottom 1 m of the profile. This indicates that an erosional event or a hiatus in deposition followed by a second period of deposition leading to a lower concentration of nuclides than expected in the top two samples of the profile.

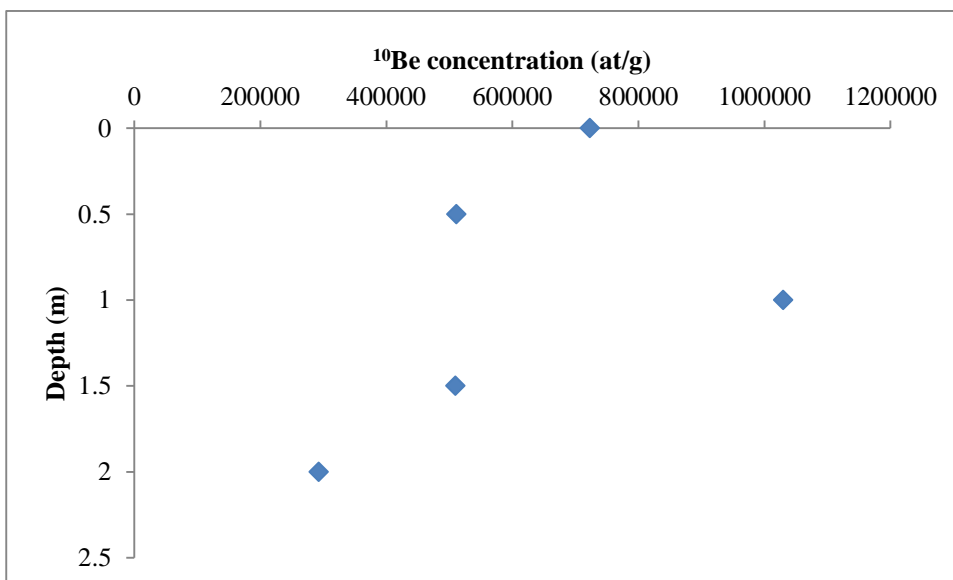


Figure 7.28: ^{10}Be concentration profile from the MTC sample site.

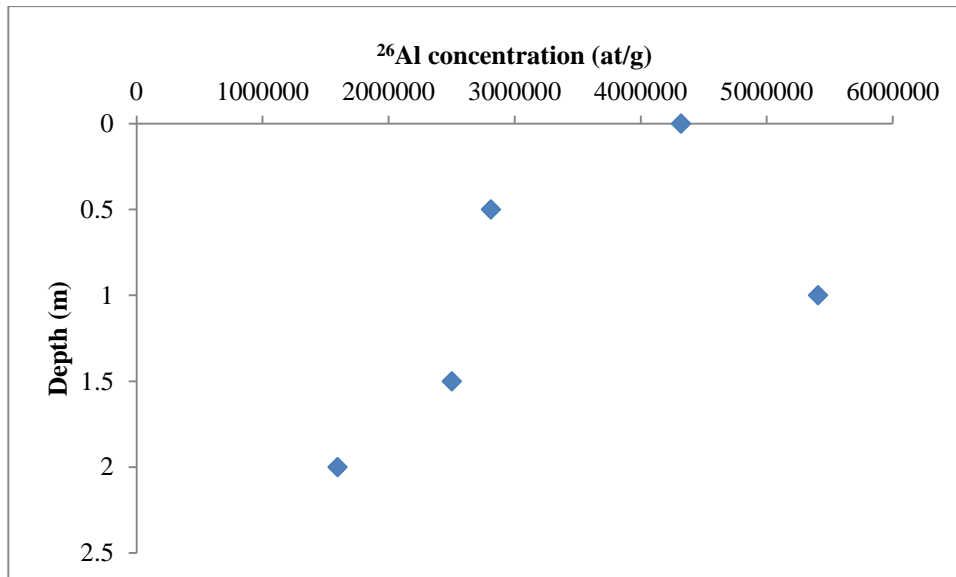


Figure 7.29: ²⁶Al concentration profile for the MTC sample site.

Although a layer of calcrete is present in the deposit at a depth of 80 cm (Chapter 4), this is unlikely to be solely responsible for the spilt in the curve. If the calcretes alone was responsible for two curves being present, it would be expected that the lower curve would have a nuclide concentration much lower than that of the top curve. A lower concentration would be expected because the calcrete would be shielding the sediments below from the cosmic rays, reducing the formation of cosmogenic nuclides (Figure 7.2). As indicated earlier (Section 7.2.4), calcretes can form along erosion surfaces therefore the most likely explanation is that there has been a period of erosion removing the top layer of sediment, then a second period of deposition. The laminar calcretes has then form along the erosion surface. This would account for the lower concentration of cosmogenic nuclides in the top metre of gravel above the calcrete.

7.3.7.2 Concentration profile Age

The data for the MTC sample site were modelled in two model types, firstly in simple exposure model and secondly in a complex exposure model. The complex model is used to attempt to represent the erosion then deposition of the top layers of sediment.

Chapter 7: Cosmogenic exposure dating results

A) Single exposure model

The single exposure models for the MTC profile (Figure 7.30 & 7.31) indicate a surface age of 470 ka with a minimum age of 370 ka. The ^{26}Al dates indicate 10 Ma for the maximum age and 90 ka for the minimum age. These ages are too old for the surface which is believed to be within the age range of 70-90 ka. The minimum age for the ^{26}Al is at the top of this range. The range of ages in the model reflects the poor fit of model curves with the experimental data.

B) Complex exposure model

The complex exposure models, presented below, indicate a surface age of between 460 to 510 ka with a minimum age of ~225 ka (Figure 7.32 & 7.33). These ages are again far too high for the expected age of the deposit which is inset below the terrace B deposits of TBP and should be around the same age of the G3 deposit (120 ka).

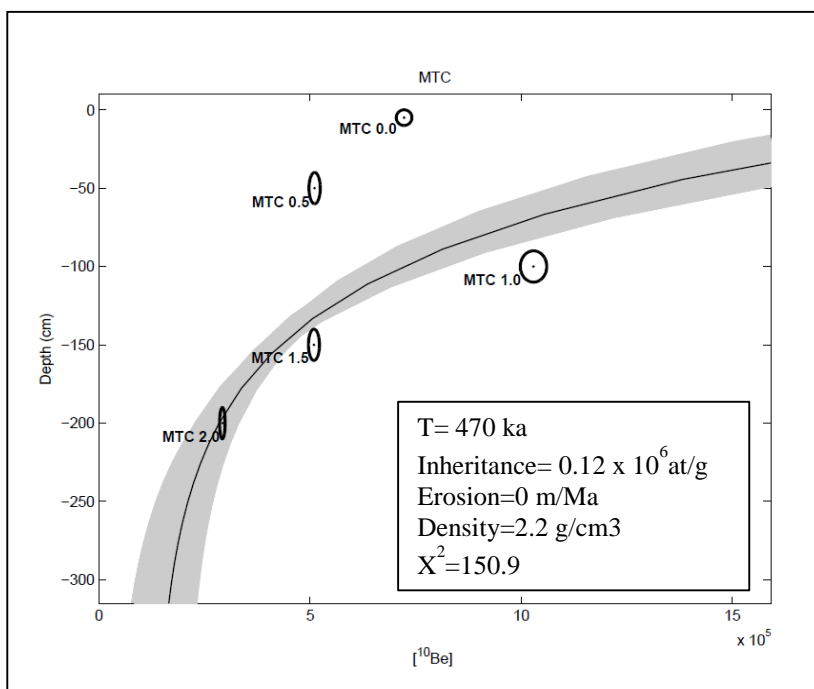


Figure 7.30: Single exposure model for the ^{10}Be concentration curve present at the MTC sample site.

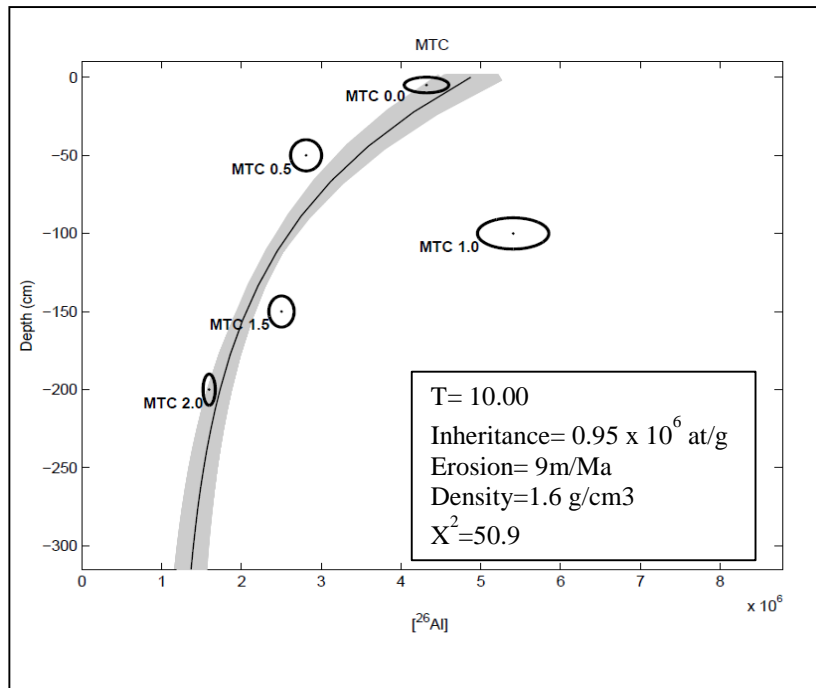


Figure 7.31: Single exposure model for the ^{26}Al concentration curve present at the MTC sample site.

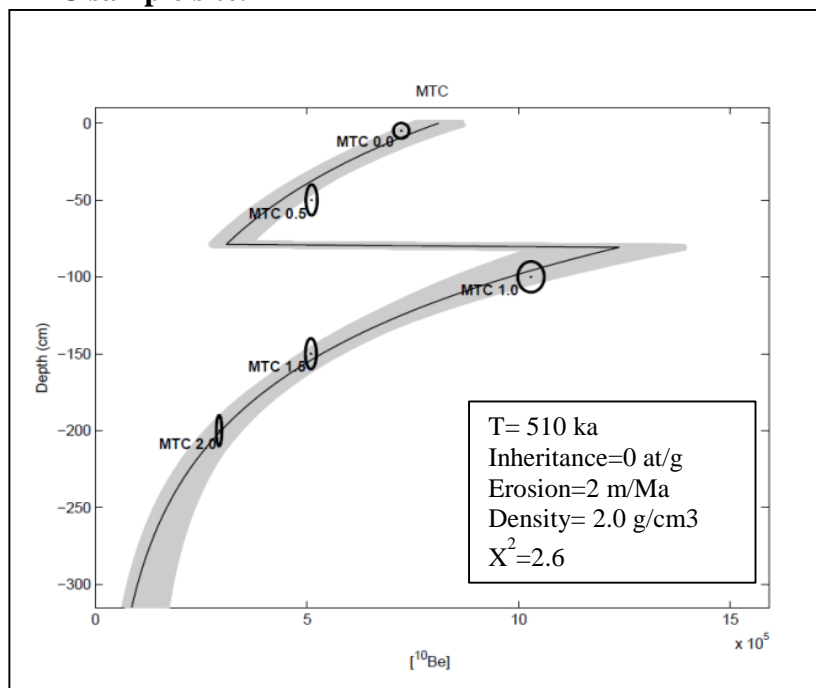


Figure 7.32: Complex exposure model for the ^{10}Be cosmogenic nuclide concentration profile for the MTC sample site.

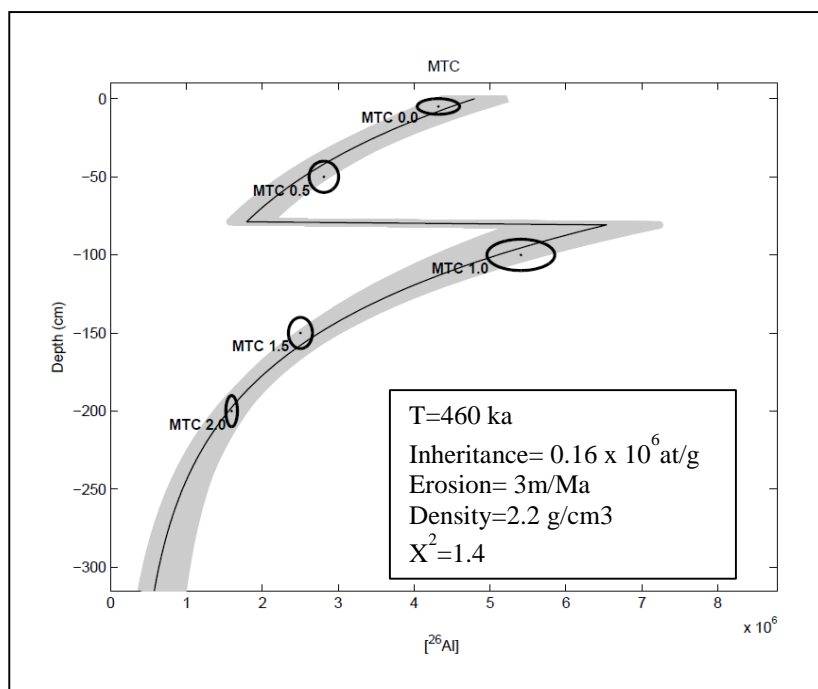


Figure 7.33: Complex exposure model for the ^{26}Al cosmogenic nuclide concentration profile for the MTC sample site.

7.3.7.3 Burial age

The burial age calculated using the paired isotope values give a best fit age of 412ka.

This is again too old for the deposit and suggests that inheritance is a big problem in this deposit.

7.4 Causes of anomalies in cosmogenic nuclide profiles

Several of the sample sites show unexpected anomalies in the measured concentration curves of ^{10}Be and ^{26}Al . The presence of anomalies within a cosmogenic nuclide concentration profile indicates that there has been some mixing of the concentration curve. This could have been caused by erosion of the section, faulting or deformation of the sediments, shielding of the sediments (by landforms or via calcrete formation) and mixing of the vertical profile either during sampling of the profile or when the terrace section was first created.

Chapter 7: Cosmogenic exposure dating results

The sedimentary characteristics of the terraces levels are further explored in Chapter 2; however, there was no evidence of faulting or deformation found in the area of the sample sites which were sampled. The sample sections were specifically chosen because there was no evidence of removal of sediment of the top of the terrace surface. The presence of the calcrete and soil layer which develop at the terrace surface when aerial exposure occurs was taken to indicate that there had been no significant removal of sediment from the surface of the terrace. Based on the results of this study other properties of sample sites need to be taking into consideration when modelling concentration curves.

A) Erosion surfaces

It is very important to know the geomorphic context of the samples. Especially important for the concentration profile method is to know where erosion surfaces are present in the sample section as these could represent a significant hiatus in deposition and could be reflected in the profile. The presence of erosion surfaces are a characteristic of fluvial deposits, especially in bar deposits.

The issue with erosion surfaces seems to be where there has been a major erosion event. However, these are not necessarily easy to pick out unless deep scouring has happened as a result of the erosion. The best practise maybe to avoid any erosion surface all together as it may have had an effect on the profile although this may prove impossible in fluvial terraces.

B) Calcrete

The presence of hardpan calcretes in the sections has presented a number of problems during this research in relation to sampling methodology. Highly cemented terrace

Chapter 7: Cosmogenic exposure dating results

gravels make sampling more complicated as it is harder to remove the quartz clasts from the section. This makes it difficult to collect a large number of clasts from the sample site.

Calcretes also present an issue with density values of sediments as demonstrated by Rhodes et al (2012). Calcretes are often localised in the sediments, being present towards the surfaces of the sample section. Cemented sediments have a higher density value than sediments which are not cemented. This means that the lower sediments of a section often have lower densities than the higher sediments. Calcrete thickness also varies over time increasing density amounts as it forms. In this study the density issues caused by calcrete presence were dealt with by introducing a viable range of densities into the model reflecting the changing calcrete amounts over time.

C) Stability of the sampled section

The majority of the sections sampled were very stable; the only exception was the TCF sample site which was very unstable. This presented a challenge as mixing of the profile could occur. If clasts are moved either up or down the profile then the concentration curve would be disrupted. Due to the unstable nature of the deposits extra care was taken when collecting the sample to ensure no mixing of the profile occurred. Sample bags were kept closed whilst quartz clasts were selected to ensure no clasts entered the bag and only clasts which were firmly embedded into the terrace sediments were collected. This limited the possibility of mixing occurring.

Whilst the sampling methodology was adapted to deal with the instability of the Forge sample site (Chapter 4), it appears that some mixing of the profile took place leading to an outlier in the concentration profile. The clasts could have been displaced when the

Chapter 7: Cosmogenic exposure dating results

sampling of the terrace was undertaken; however, the sampling strategy was designed to prevent this with samples collected from a clearly marked level. Also the clasts that were collected were very firmly imbedded into the terrace profile so they are unlikely to have been displaced from higher up the profile.

The mixing of the concentration profile could have taken place pre sampling when the section was created by a digger. This data from this sample site, although providing a good geomorphically significant date, indicates that using sampling from unstable sections is not advised to avoid mixing of the profile.

D) Faulting

Sections which are faulted are potentially problematic as profiles could be mixed by the deformation of the gravels. This could potentially make it very difficult to produce an accurate model for the terrace. The G3 sample site had faults present in the terrace; however, these were carefully avoided when choosing the exact place to sample. The G3 model is statically very good and therefore shows that by careful selection of the sample site, a terrace that has undergone some form of deformation can be successfully dated.

7.5 Chlorine 36 dating results

Sample ID	CaO	K ₂ O	Cl	³⁶ Cl	³⁶ Cl age	³⁶ Cl age
	(wt-%)	(wt-%)	(µg/g)	(10 ⁵ at/g)	(a)	(a)
					Phillips	Stone96
L1	54.70±1.2 2	<0.01	14.78±0.6 0	0.694±0.02 6	2873±14 7	3785±19 4
L2	52.54±1.1 8	0.058±0.00 2	15.19±0.7 2	0.707±0.07 8	3027±18 7	3997±24 0

Table 7.2: Data table of cosmogenic dating results for Chlorine dating of the Maleguica landslide. Ages (in bold) were calculated using the CHLOE3 programme (courtesy of F.Phillips).

Table 7.2 displays the results of the chlorine 36 dating of the limestone blocks from the Maleguica landslide. The concentration of chlorine present in the landslide samples indicated that the age of the section of the Maleguica landslide sampled was ~4 ka. The difference of 900 years between the Phillips and Stone calculation methods are a result of differences between the two methods documented elsewhere (Vincent et al., 2010). In samples with high K values, the Phillips methodology gives higher ages whereas in samples with low K values the Stone methodology will produce the higher age. The results indicate that failure of the part of the landslide sampled occurred around 3 -4 ka.

This indicates that the failure did not occur at or around the time of the capture event but has occurred due to destabilisation of the valley sides that has taken place after the capture event. However, as the landslide is likely to have formed by a series of smaller failures rather than one large failure, it is possible that the cosmogenic date has dated the last big failure of the Maleguica landslide. In order to test whether the landslide fails in a series of mass movements, multiple samples would need to be taken at several locations on the landslide.

7.6 Neon dating results

The atmospheric neon content of the samples from the erosion surface proved too high to be able to utilise neon to calculate an age for the surface. This problem has been encountered previously in Spain (Pers. Comms Fin Stewart, 2011) making it impossible to date landforms accurately. Being unable to date the erosion surface in the Río Jauto catchment using absolute methods in this study means that the chronological framework has to be constrained by relative methods (Chapter 6).

7.7 Discussion of results

Six terrace deposits and one erosion surface have been dated using the concentration profile of cosmogenic exposure dating in the Río Aguas catchment. Viable dates have been produced for 6 of the 7 landforms dated spanning from the pre terrace A erosion surface to terrace C deposits. A summary of the cosmogenic dates calculated for the Río Aguas terrace staircase by this study are presented in Table 7.3.

Terrace level	Sample site	Concentration profile age		Burial age		
		min (ka)	best fit (ka)	Min (ka)	best fit (ka)	Max (ka)
Pre terrace A	GS	70	1200	200	1000	1300
Terrace B	GTB	130	140	n/a	n/a	n/a
Terrace B	CB	110	130	503	573	693
Terrace B	TBP	40	40	90	161	291
Terrace C	G3	70	120	n/a	n/a	n/a
Terrace C	TCF	30	79	121	231	302
Terrace C	MTC	370	470	342	412	503

Table 7.3: Cosmogenic exposure dating results for the terrace deposits of the Río Aguas. Concentration profile and burial dates are reported.

Figure 7.34 shows the stratigraphic order of the river terraces, inset into the Góchar Formation, as observed in the field. The majority of the ages of the sample sites, presented in Table 7.3, fit in with the stratigraphic framework. The exceptions are sample sites MTC and TBP. Field mapping indicates that the MTC sample site is a terrace C deposit and is therefore expected to be around the same age as the G3 sample site (~120 ka). The concentration profile method produced an age of 470 ka for the MTC site with burial dating indicating that the maximum age of the deposit is 503 ka. These ages are far older than expected.

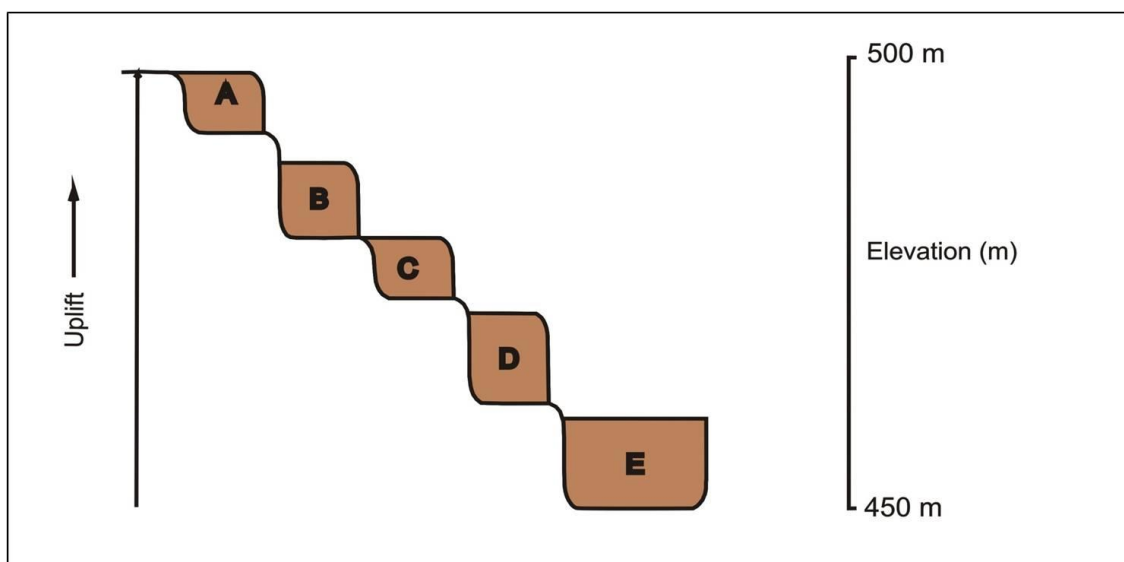


Figure 7.34: Stratigraphic order of river terraces present in the Rio Aguas catchment.

The burial ages consistently overestimate the ages of the deposits. The exception is the GS site where the age of the erosion surface has been underestimated. The burial date for the pre terrace A erosion surface indicates that it is younger than the terrace B sample site CB. This is highly unlikely as the CB sample site is morphostratigraphically lower in the landscape than the GS sample site. The burial dates for terrace B deposits suggests maximum ages of between 693 to 291 ka whilst for terrace C deposits the maximum ages range between 503 to 302 ka. The old ages produced from burial age calculations suggests that inheritance is a significant problem for these deposits.

The terrace deposits of the Río Aguas have previously been dated absolutely using U-Series dating on the pedogenic calcretes capping the terrace deposits (Kelly *et al.*, 2000; Schulte, 2002; Candy *et al.*, 2004; 2005; Schulte *et al.*, 2008). The cosmogenic dates produced by this study should be broadly similar to the existing U-Series chronology because both methods date the abandonment of the terrace surfaces and thus constrains incision. The U-Series chronology for the Río Aguas is presented in Table 7.4 to allow comparison to the cosmogenic chronology.

The U-Series chronology for the Río Aguas terrace deposits indicates that terrace A was abandoned by 304 ± 26 ka, terrace B between 207- 112 ka and terrace C by 104-67 ka. The majority of the cosmogenic dates for both terrace B and C deposits fall within the ranges of the U-Series dating. The dates for two of the terrace B deposits, GTB and C.B, (140-130 ka) fall at the lower end of the time period expected from the U-Series database (207-112 ka). This indicates that for the older terrace deposits that the U-Series methodology was possibly overestimating the age of the calcretes capping the deposit. The TBP deposit has a best fit age of 40 ka. This is very young for a terrace B deposit, and unlikely to be a true reflection of the age of the deposit. The model age more likely reflects the poor fit of experimental data to the modelled data.

Location	Terrace level	UTM	Best fit age	Max burial age	U-Series date (ka)
Proximal	Pre Terrace A	0575763, 41049446	1.0 Ma	543 ka	No date
Proximal	B	0577312, 4109292	140 ka	n/a	207-112
Mid	B	0575599, 4108071	130 ka	693ka	207-112
Distal	B	0583753, 4095355	40 ka	291 ka	207-112
Proximal	C	0575374, 41110571	120 ka	n/a	104-67
Mid	C	0578450, 4105837	79 ka	302 ka	104-67
Capture point	C	0581425, 4106200	470 ka	503 ka	104-67

Table 7.4: Database of terrace formation in the Río Aguas fluvial system. U-Series dates after Candy *et al.*, (2005).

The terrace C age of 79 ka for sample site TCF falls within the expected range for the deposit from the U-Series dating (104-67 ka). The G3 sample site indicates that incision into the terrace surface started 120 ka slightly outside the U-Series range. The age from the distal reach of the Proto Aguas/Feos is outside of the expected range for both terrace C and B. Indeed it is more in the expected range for a terrace A deposits. This leaves

Chapter 7: Cosmogenic exposure dating results

two possibilities for the date; first that there has been too much inheritance in the gravels of the MT.C deposit which has led to the age of the deposit to be overestimated or secondly that the terrace deposit is older than it has been assigned on a relative scale. The latter option is unlikely as mapping was undertaken before sampling showing this deposit to be a terrace C deposit.

There is no U-Series date for the Pre terrace A erosion surface. The cosmogenic exposure date produced for the Pre-terrace A erosion surface indicates that incision of the basin sediments had begun by 1.5 Ma. The data then indicates that incision continued at a slow rate until the deposition and abandonment of the terrace deposits occurs. Terrace A deposits were probably abandoned 230-240 ka with the terrace B deposits abandoned around 130 ka and the terrace C around 79 ka. This indicates that incision rapidly sped up around 240 ka possibly as a result of regional tectonic uplift.

Incision into the surfaces of terraces B and C appears to be linked to the transitional periods between glacial and interglacial periods. The abandonment of terrace B took place during the transition from the stage 6 glacial to the stage 5 interglacial. Terrace C surface sediments were abandoned during the stage 5 interglacial. These dates indicate that the climate cycles have some influence over the deposition and abandonment of terraces in the Río Aguas system. However, there are many major climatic transitional stages (16/15, 12/11 or 10/9 for example [Gibbard & Lewin, 2009]) that have not been recorded by the Río Aguas staircase indicating that climate may not be the controlling external influence over incision in the Sorbas basin.

7.8 Summary

Cosmogenic methods used on landslide deposits and fluvial terraces have provided viable results that will be used to further explore the incision history of the Río Aguas.

Chapter 7: Cosmogenic exposure dating results

The results from using the profile methodology on terrace deposits indicates that the methodology works well for gaining accurate ages for the abandonment of terraces. The use of burial dating can also give an indication of the timing of deposition of the sediments.

The results presented in this chapter show that cosmogenic exposure dating is a versatile method that can be applied to a range of geomorphic environments in order to create detailed geochronological databases. Discussion of the dates in the context of the timing of terrace formation, climatic and tectonic cycles and existing terrace formation models is undertaken in Chapter 8.

Chapter 8: Controls on incision in the Sorbas Basin

Chapter 8.1 Introduction

This chapter is used to discuss the dates obtained by cosmogenic dating in relation to climatic cycles and tectonics. A terrace formation model is presented for terraces B and C using the cosmogenic dates produced by this study. This chapter uses data presented in this thesis to address three main questions:

- 1) When did incision start in the Sorbas Basin? Is it synchronous with other basins in the Iberian Peninsula and does the dating of a long term fluvial record provide information about long term regional fluvial incision patterns?
- 2) Does cosmogenic exposure dating of river terrace landforms provide any insights into the relationships of the timings between terrace formation (fluvial aggradation), abandonment and river downcutting (fluvial incision) and glacial/interglacial climate cycles?
- 3) Can the application of palaeohydrology equations on field data be used to identify the magnitude of flood events during terrace building periods in the Sorbas Basin? Do the terrace deposits of the Río Jauto and Aguas show any spatial and or temporal variability? If patterns are identified then is there a climatic link?

8.2 When did incision start in the Sorbas Basin?

Cosmogenic dating has been used to date the surface deposits of fluvial landforms and therefore gives the age of surface abandonment. The cosmogenic dates reported in Chapter 7 allow new analysis of the Plio/Pleistocene incisional history of the Sorbas

Chapter 8: Controls on incision in the Sorbas Basin

basin to be undertaken. The new data can be integrated with existing dates from other Pliocene deposits from surrounding basins as well as paleontological and palaeomagnetic data from the Pliocene deposits in the Sorbas basin. The data can then be used to test whether incision is synchronous across the Neogene basins.

The final stage of Sorbas basin infilling is represented by the Góchar Formation. The top of the Góchar Formation forms a low relief undulating surface in the west of the Sorbas Basin which consists of the true depositional surface with erosion surfaces set into it (section 5.1). Inset into the basin fill are five major terrace levels (A-E).

Cosmogenic exposure dating of the Góchar Formation erosion surface gives an age of exposure of 1.0 Ma, indicating that the incision of the Río Aguas began after this time (Figure 8.1).

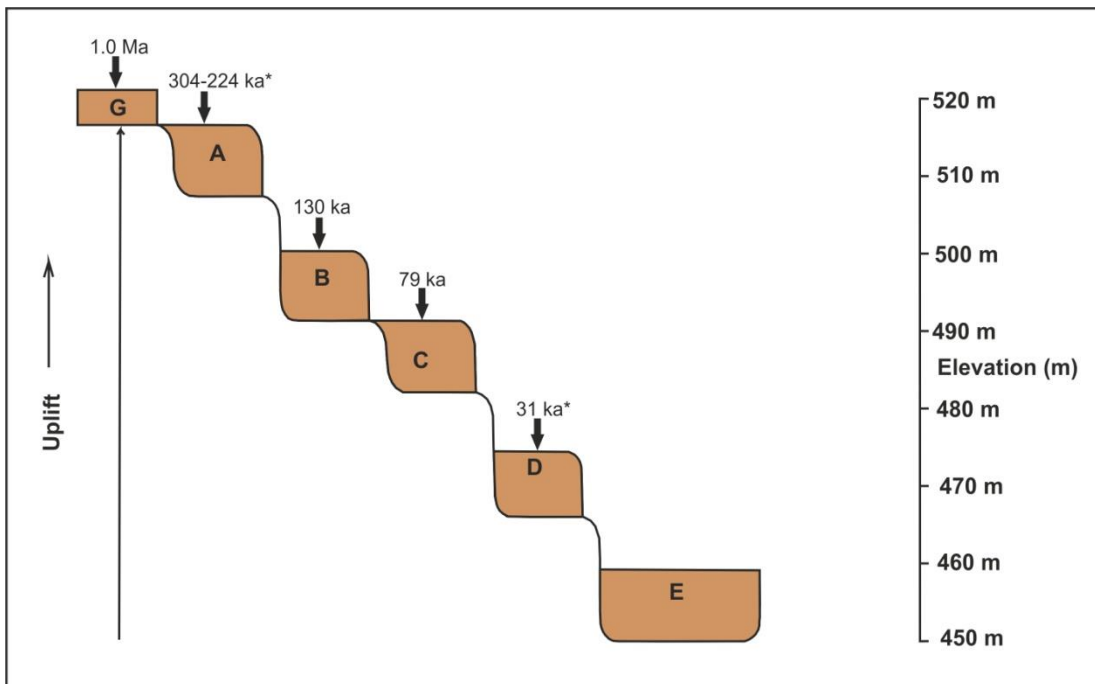


Figure 8.1: New chronological framework for the Pleistocene terrace deposits of the Río Aguas, Sorbas Basin. *Dates from Candy et al (2005).

A date for the erosion surface allows for new constraints of the age of the Góchar Formation which is currently undated. The age of the base of the Góchar Formation is currently locally constrained by paleontological and magnetostratigraphy data (Martin-

Chapter 8: Controls on incision in the Sorbas Basin

Suarez *et al.*, 2000) from the underlying Zorreras Member of the Cariatiz Formation (Chapter 2). The top of the Cariatiz Formation (Figure 8.2) is marked by the Zorreras Member which is capped by a yellow basin wide marine unit which contains bivalves and brachiopods (Mather, 1991). The Zorreras Member is of reverse polarity, belonging to the magnetostratigraphic polarity unit C3r which places the age of the member close to the Miocene/Pliocene boundary (Martin-Suarez *et al.*, 2000). The marine band contains bivalves and brachiopods that indicate an early Pliocene age (Ott d'Estevou, 1980; Martin-Suarez *et al.*, 2000). Cosmogenic dating of the erosion surface has indicated that the surface was abandoned during the Early Pleistocene (1.0 Ma, Calabrian age). This suggests that the Góchar Formation was deposited during the early to middle Pliocene through to the Early Pleistocene (~4.0 Ma to 1.0 Ma) after which incision into the top basin fill began.

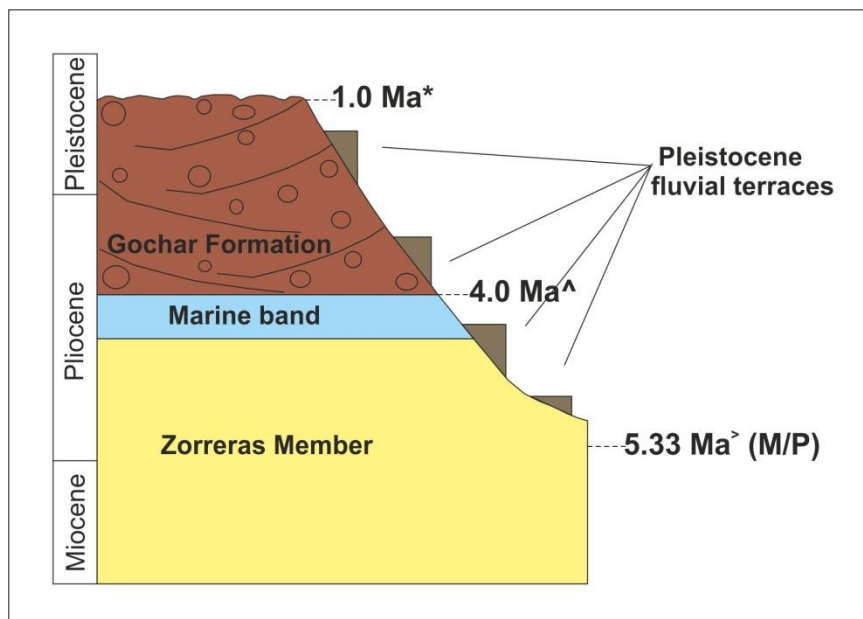


Figure 8.2: Sedimentary log showing the dates available for the Pliocene/Pleistocene stratigraphy of the Sorbas basin (* Cosmogenic exposure date, this study; ^ Paleontological data, Ott d'Estevou, 1980; Martin-Suarez *et al.*, 2000; > Magnetostratigraphic data; Martin-Suarez *et al.*, 2000)

In the neighbouring Vera basin, the sedimentary basin fill is capped by the Salmerón Formation which consists of alluvial fan sediments (Stokes & Mather, 2000). The age of the Salmerón Formation is constrained by Electron Spin Resonance dating (ESR) which

Chapter 8: Controls on incision in the Sorbas Basin

has been used on shallow marine and travertine carbonate that mark the lower (2.3 Ma) and upper (1.6 Ma) boundaries respectively (Wenzens, 1992). The error on the ESR date is quite large (~ 255 ka). There is no date for the first terrace, the Gordo Allomember (after Meikle, 2009) although the age of the base of the terrace was estimated to be 1.3 Ma using uplift rates (Meikle, 2009). Without an absolute date of either the deposits or the surface of the deposit it is impossible to say whether this estimate is correct. Therefore there remain uncertainties about when the incision started in the Vera Basin.

Although the surrounding basins (Carboneras, Pulpi and Almería) contain Plio-Pleistocene equivalents to the Góchar and Salmerón Formations, no absolute dates exist for them. Most of the formations, based on stratigraphic bracketing, are believed to be Pliocene in age, with fluvial systems forming in the Pleistocene.

It is proposed that in the Sorbas basin incision into the top basin fill would have begun before incision in the surrounding basins due to differential uplift of the Betic Cordilleras. The lack of absolute dates for the Plio/Pleistocene deposits of the older Neogene basins in the local area makes it difficult to confirm this theory.

In other basins around the Iberian Peninsula, some paleontological and palaeomagnetic data has been collected for top basin fill surfaces although there is no absolute dates. In the Guadiana Basin, the top basin fill is represented by the La Raña deposits. The La Raña deposits are localised lithofacies consisting of a cobble piedmont sheet with pseudogley soils (Aguirre, 1997). Detailed palaeontological studies have indicated that the basin infilling ended between 1.9 Ma to 1.5 Ma (Mazo, 1999). Palaeomagnetic data provides an age of 1.75 Ma (Matuyama/Olduvai) for end of basin infilling in the Guadalquivir system suggesting a similar age for the end of basin infilling as in the Guadiana Basin (Baena and Díaz del Olma, 1997).

Chapter 8: Controls on incision in the Sorbas Basin

Larger inland systems (e.g. Tajo, Guadalquivir) have longer terrace records and appear to record a long period of incision then smaller coastal systems such as the Río's Aguas or Almanzora. For example, in the Tajo Basin, the upper most sedimentary deposits have been assigned a Pienzian/Gelasian age by palaeomagnetic dating (Matuyama/Gauss boundary; ~2.58 Ma) (Torres et al., 1994; Santisteban & Schulte, 2007). Whilst this is a tentative age due to the lack of absolute dating, it does demonstrate the range of dates attributed to top basin fill surfaces (~2.58 Ma-1.0 Ma). This suggests that the onset of fluvial incision in Spain could be diachronous (Santisteban & Schulte, 2007).

8.3 Climate and tectonic controls on terrace formation

Rivers in the Sorbas (Aguas & Jauto), Vera (Almanzora) and Almería (Alias) basins all show four levels of major terrace formation relating to the Middle/Late Pleistocene. This suggests that there is a regional control on terrace formation in this area. The Río Aguas and Almanzora both show significant time gaps between the apparent onset of fluvial incision and the subsequent preservation of terrace landforms (~300 ka). This suggests that there has been a trigger for terrace formation, abandonment and preservation during the Pleistocene (climatic cycles or tectonic uplift?).

There are two types of dates available for the terrace deposits of SE Spain; those that date incision (e.g. cosmogenic exposure dating and U-series dating) and ones that date aggradation (e.g. OSL and radiocarbon dating) (Figure 8.3). These two types of dates enable the inference of timing of aggradation and incision with relation to climatic cycles.

Chapter 8: Controls on incision in the Sorbas Basin

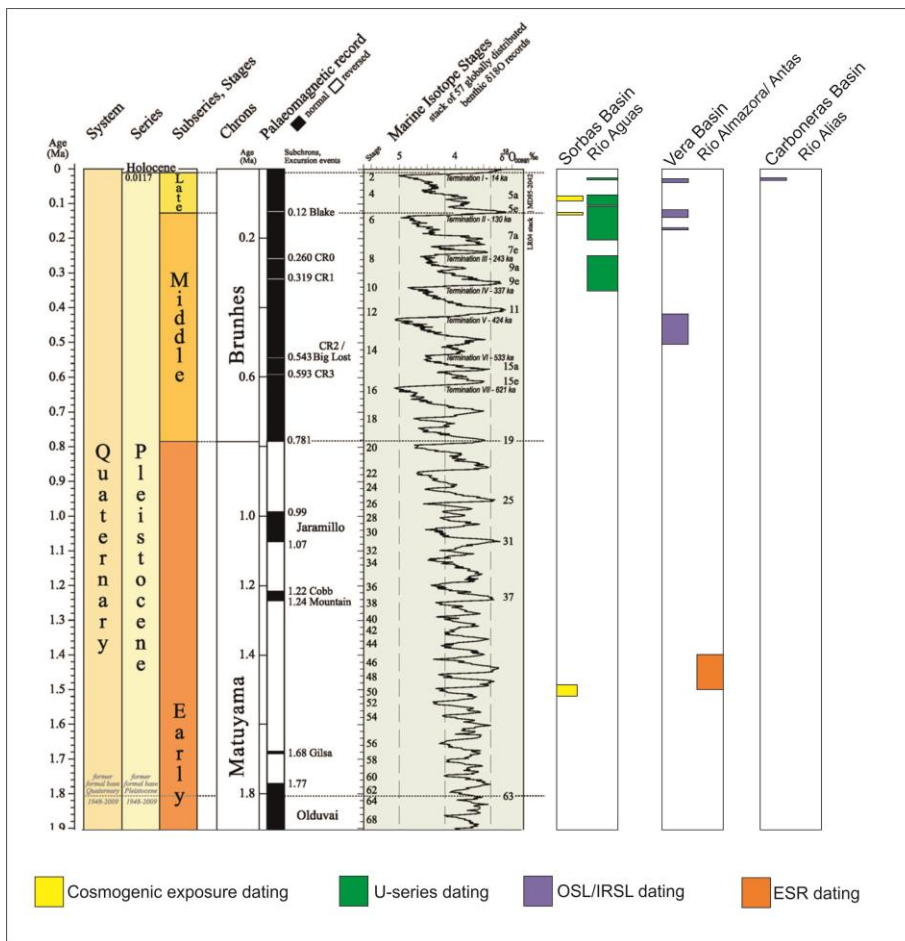


Figure 8.3: Stratigraphical position of the Quaternary terrace sequences of the Río's Aguas, Almanzora/Antas, and Alias based on absolute dating results. U-series data sourced from Candy *et al.* (2004; 2005); OSL/IRSL data from Meikle (2009); ESR date from Wenzens (1992). Stratigraphy sourced from strat.org.

The classical models of terrace formation proposed that fluvial incision occurred in the interglacials whilst fluvial aggradation took place during glacial periods (Gibbard & Lewin, 2002; Vandenberghe, 2003 and refs therein). Fluvial incision during interglacials would occur because periods of high run off would coincide with maximum vegetation cover on the slopes with low rates of sediment supplied to the fluvial system. Aggradation was believed to take place during glacial periods where maximum rates of sediment supply would occur due to limited vegetation cover on the slopes and high rates of mass movement. More recent studies of fluvial archives indicate that fluvial aggradation and incision may have taken place during glacial to interglacial transitional periods (Bridgland & Westaway, 2008 and refs therein; Vandenberghe, 2008) with little or no activity during interglacial periods. Climatic

Chapter 8: Controls on incision in the Sorbas Basin

instability in the transitions is linked to increased incision in the fluvial system. With the development of dating techniques, which enabled chronological frameworks to be developed for Pleistocene terrace deposits, it has been confirmed that fluvial activity can be linked to the transitional periods between glacial and interglacial cycles (Bridgland & Westaway., 2008; Vandenberghe, 2008).

Bridgland and Westaway (2008) present a model of terrace formation in response to climatic forcing giving several scenarios of timing of terrace deposition relating to climatic cycles. Figure 8.4 is a diagram showing a synthesis of the Bridgland and Westaway model. This model builds on a previously published model (Bridgland, 2000) that proposed downcutting at warming transitions. The revised model adds two new scenarios, rivers that incise at both warming and cooling transitions and rivers just incising at cooling transitions. The model demonstrates that incision can occur at both warming and cooling transitions due to climatic deterioration in these periods. Fluvial systems in different climatic regions respond in different ways to climate cycles with some systems, such as the River Somme in northern France, only incising during cold transitions (Bridgland & Westaway, 2008).

New dates produced by this study show that the surface of the terrace deposits were abandoned and incised into during transitional periods between climatic cycles (Figure 8.3). The surface of terrace B was incised into during stage 5a (~130 ka) of MIS 6/5. This is a transitional period between the stage 6 glacial to the stage 5 interglacial and is known as a warming transition. A burial date for a terrace B deposit gave an age of 160 ka (section 7.2.4.3). This suggests that terrace B was aggradated during the stage 6 glacial. Dates for the timing of incision into terrace C indicate incision either during the interglacial period (~120 ka) or late in the stage 5/4 transition (~79 ka). The highest quality date for the terrace C deposits is the G3 exposure date of 120 ka. This suggests

Chapter 8: Controls on incision in the Sorbas Basin

that terrace C was abandoned during the interglacial periods. Burial dates for terrace C were inconclusive (231 ka & 412 ka) due to a large inheritance component (section 7.2.6).

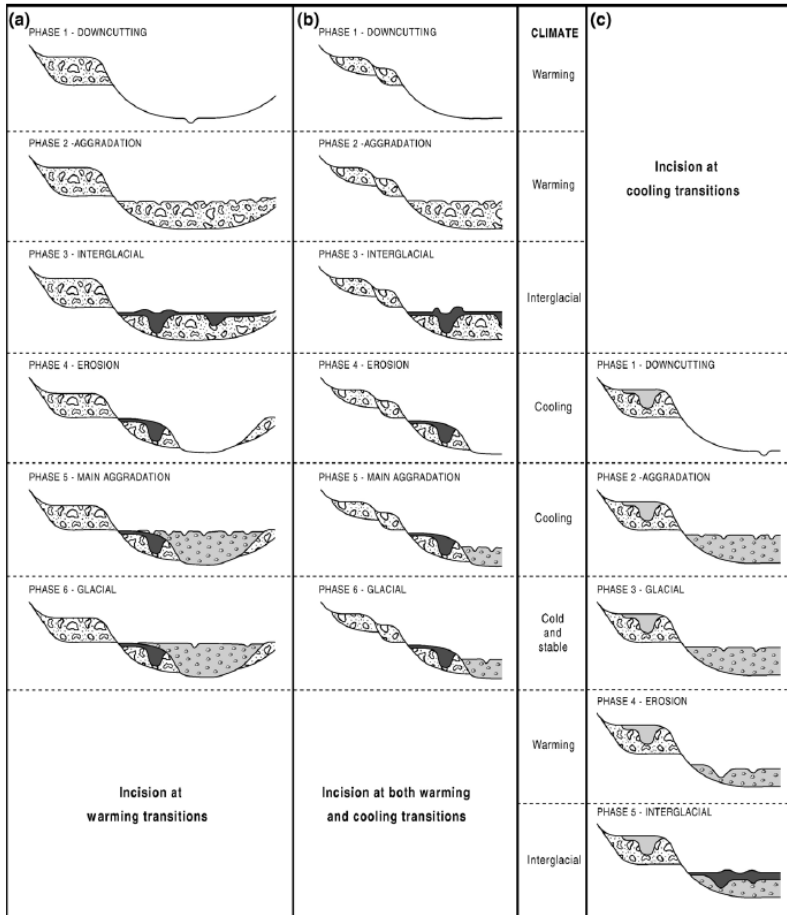


Figure 8.4: Bridgland & Westaway (2008) model of terrace formation in response to climatic forcing. The diagram shows three possible responses by rivers to climatic cycles.

The only data available for terrace A comes from U-series dating (224-304 ka) which also dates surface abandonment and therefore incision. Based upon the link of incision to transitional periods or interglacials, the terrace A deposits could have been isolated in either MIS 9/8 (300 ka) or 8/7 (243 ka) transitions. Given the tendency of the U-series dating methodology to overestimate the age of the surface of older Pleistocene deposits (section 7.6) it is likely that the terrace A deposits (U-series dated to 224-304 ka) relate to the younger MIS 8/7 transitional period or stage 7 interglacial.

Chapter 8: Controls on incision in the Sorbas Basin

Incision at both warming and cooling transitions suggests the Río Aguas fluvial system was very sensitive to climatic changes in the Pleistocene. The amount of incision occurring at transitions varies according to the type of incision with deeper incision occurring at warmer transitions than at cooling transitions (Bridgland & Westaway, 2008). This however, is not the case in the Río Aguas with more incision having occurred post terrace C (at a cooling transition) than between level B and C terraces (a warming transition). This could indicate an increase of uplift rates due to increased tectonic activity. However, a river capture event occurred after terrace C was deposited, which has amplified incision in the Río Aguas and therefore complicated the sequence of incision.

The new age control on the Río Aguas terrace deposits suggests that the fluvial archive spans a shorter and more recent timescale than existing studies (albeit with little/no age control) indicated (Harvey & Wells, 1987; Candy *et al.*, 2003; 2004; Schulte *et al.*, 2008). The chronology also shows that there is a significant gap (~1.2 Ma) between the initiation of incision into the top basin fill and the formation and incision into the surface of the terrace A deposit. There is then a much shorter period of time in which four terrace levels are deposited. This suggests that there has been a change in conditions which has enabled the river to incise and aggrade.

The pattern of a slow start to incision/ terrace development followed by an increase in the rate of incision with a number of terraces being formed in a short period of time is related to the tectonic setting of the area (Westaway, 2012). In large river systems in tectonically active areas, such as the Rhine, a slow rate of incision is recorded by the fluvial archive until the Middle Pleistocene when incision rates rapidly increased (Van Balen *et al.*, 2000). In smaller systems, such as the Río Aguas, that are formed in an area that are tectonically active due to young thin mobile crust, an abrupt increase in

Chapter 8: Controls on incision in the Sorbas Basin

uplift pattern is also recorded. This is possibly a response to the Mid Pleistocene revolution (Westaway, 2012).

The formation of terrace deposits from the middle Pleistocene could be related to the switching from 40 ka climatic cycles to 100 ka Milankovitch cycles. Referred to by some researchers as the Mid Pleistocene Revolution (Bridgland & Westaway, 2008; Gibbard & Lewin, 2009), in this period Milankovitch forcing climate cyclicality changed from obliquity driven 40 ka cycles to 100 ka eccentricity driven cycles. The switch to 100 ka cycles may have allowed the rivers to form terrace deposits through increasing the rate of sediment input to the river systems (Bridgland & Westaway, 2008). The Mid Pleistocene Revolution took place between 1.2 Ma and 500 ka (Gibbard & Lewin, 2009). In the Sorbas basin, the Mid Pleistocene revolution appears to have triggered erosion and incision into the Góchar Surface around 1.0 Ma.

There have been several major glacial cycles since the Mid Pleistocene Revolution (for example MIS 16/15, 12/11 or 10/9) but it appears that only the MIS 7/6 (or 8/7), 6/5 and 5/4 transitional periods have been recorded by the Río Aguas. This could mean that there is another external control, for example tectonic uplift, controlling the timing of terrace aggradation and fluvial incision.

The rate that incision is taken place may also impact on the preservation of terraces. It may be the case that older terraces (i.e pre terrace A deposits) were formed but because incision was so slow laterally erosion has occurred destroying the terrace deposits.

Fluvial systems with higher numbers of terraces preserved may have higher incision rates which isolated the terrace deposit before lateral erosion could destroy them.

Chapter 8: Controls on incision in the Sorbas Basin

8.4 Tectonic uplift

Active tectonics can generate regional topographic gradients which can lead to incision in river systems oblique to the tilting and deflection of river systems running parallel to the tilting (Keller & Pinter, 1996). In the Neogene basins of the Iberian Peninsula, ongoing tectonic uplift promoted by the regional tectonic setting (Chapter 2) has been proposed as a mechanism for regional-scale drainage re-arrangement, integration and expansion which has occurred during the Quaternary (Mather & Harvey, 1995; Stokes & Mather, 2003, Maher, 2008). Differential uplift of the Betic Cordilleras (Table 8.1) has led to the Sorbas Basin being uplifted higher than the neighbouring Vera basin leading to aggressive incision by the Lower Aguas and capture of the Proto Aguas/Feos during the Late Pleistocene (~80 ka). The capture event is believed to relate to a pulse of tectonic activity in the Middle Pleistocene which enhanced uplift rates (Mather & Westhead, 1993; Mather & Harvey, 1995; Stokes & Mather, 2003).

Calculation of time averaged uplift rates in the Sorbas basin using Pliocene marine deposits has suggested uplift rates of between 0.06 m ka^{-1} to 0.16 m ka^{-1} (Mather, 1991; Mather & Harvey, 1995; Braga *et al.*, 2003). Marine sediments can be used to calculate uplift rates because their ages are often well constrained by fossil and stable isotope data and the past sea levels are well constrained thus providing a clear geomorphic datum. This means that the main components for calculating uplift rates (present day altitude of the base of the deposit, its absolute age and sea level at the time of deposition) can be determined. One issue with these studies is that they produce a time average rate that is constant over the time period for which it is calculated and which therefore does not account for epeirogenic nature of the uplift. Rates calculated for a long time period tend to give low averages as the short term variability in uplift rates gets flattened out. These studies calculate uplift rates using Pliocene marine deposits therefore the rates probably

Chapter 8: Controls on incision in the Sorbas Basin

are not applicable for the Pleistocene fluvial systems. With a better age control for the fluvial terraces provided by cosmogenic exposure dating and a more reliable shortened timescale uplift rates for the Sorbas basin can be re-evaluated.

The use of river terraces to calculate uplift rates is contentious because of the number of external variables (e.g. climate, sea-level and tectonics) that control terrace formation.

An uplift model was developed by Maddy (1997) using river terrace deposits in the upper Thames valley, southern England. The model, which used estimated ages of terraces and terrace heights, discounted variables other than tectonics or climate as a factor in fluvial incision. The river basin chosen for testing the model was located slightly inland to minimise the affects of sea-level change and had an estimated age control framework for the river terraces using palaeomagnetic and paleontological data. The results of the model showed good agreement with previously existing uplift rate estimates for southern England indicating that river terraces could be useful for calculating uplift rates in specific circumstances.

8.4.1 Published uplift rates

Uplift rates for the Sorbas basin area, presented in Table 8.1, have been produced by three studies using the Pliocene marine deposits (Mather, 1991; Mather & Harvey, 1995; Braga *et al.*, 2003). Uplift rates of between 0.08-0.16 m ka⁻¹ have been proposed by Mather (1991) and Mather & Harvey (1995). These uplift rates were calculated from the early to mid Pliocene marine bands of the Zorreras Member. Rates of uplift appear higher for the south of the basin (Sierra Alhamilla/Cabrera: 0.16 m ka⁻¹) than in the north of the basin where uplift rates of ~0.06 m ka⁻¹ occur.

Chapter 8: Controls on incision in the Sorbas Basin

Basin	Study	Time average uplift rate
Sorbas Basin	Mather, 1991 Pliocenemarine deposits above present	0.16 m ka ⁻¹
Sorbas Basin	Mather & Harvey, 1995 Pliocenemarine deposits above present	0.08 m Ka ⁻¹ - 0.16 m ka ⁻¹
Sorbas basin	Braga <i>et al.</i> , 2003 Pliocenemarine deposits above present	0.07 m ka ⁻¹ - 0.10 m ka ⁻¹
Vera Basin	Stokes, 1997 Pliocene shoreline above present	0.015 m ka ⁻¹
Vera Basin	Stokes & Mather, 2003 Pliocene shoreline above present	0.02 m ka ⁻¹
Vera Basin	Meikle, 2009 MIS 5e Raised beach deposit	0.07 m ka ⁻¹
Eastern Vera Basin	Booth-Rea <i>et al.</i> , 2004 Pliocene shoreline above present	0.05 m ka ⁻¹
Huercal-Overa Basin	Stokes & Mather, 2003 Pliocene shoreline above present	0.05 m ka ⁻¹
Almeria Basin	Zazo <i>et al.</i> , 2003 MIS 5e Raised beaches above present	0.04 m ka ⁻¹
Cope Basin	Zazo <i>et al.</i> , 2003 MIS 5e Raised beaches above present	0.023 m ka ⁻¹

Table 8.1: Time averaged uplift rates for the Neogene Basin of SE Spain. The range of values demonstrates the differential nature of uplift in the Betic Cordilleras.

Chapter 8: Controls on incision in the Sorbas Basin

Basin	Study	Time averaged uplift rate
Sorbas Basin	Mather, 1991 Pliocene deposits	0.16 m ka ⁻¹
Sorbas Basin	Mather & Harvey, 1995 Pliocene deposits	0.08-0.16 m ka ⁻¹
Sorbas Basin	Braga et al., 2003 Pliocene deposits	0.07-0.10 m ka ⁻¹

Table 8.2: Published uplift rates for the Sorbas basin.

Braga et al (2003) calculated uplift rates of between 0.07 to 0.10 m ka⁻¹ for the Pliocene deposits of the Sorbas basin. These rates are slightly lower than previous rates suggested for the basin.

8.4.2 Terrace spacing & uplift rates

The spacing between terrace deposits provides an indication of whether tectonic uplift has occurred during the formation of the terrace staircase. Starkel (2003) produced a series of diagrams showing the spacing between terraces in areas that are being tectonically uplifted versus areas that are tectonically stable. In areas that are being uplifted the spacing between the terraces is wide creating a terrace staircase. In areas that are not being uplifted there is little or no space between the terraces. In the Sorbas basin there is clear spacing between all terrace levels in the terrace staircases however the picture is complicated by river capture, variability in uplift rates and rock strength.

In areas where tectonic uplift has occurred during fluvial incision, the spacing between terrace levels also increases in a downstream direction. This pattern is seen both in the Río Aguas and the Río Jauto catchment (Figures 2.8 and 6.2).

Chapter 8: Controls on incision in the Sorbas Basin

The uplift rates can be used to calculate the spacing that would be expected for the Río Aguas and Jauto terrace staircase by using the cosmogenic exposure dating results.

Table 8.3 presents the actual spacing between the terraces in both the Río Aguas and Jauto fluvial systems. The spacing that would be expected between terraces for the various uplift rates has been calculated and is presented in Figures 8.5 & 8.6 (calculation tables can be found in Appendix 6). The expected distance between the terrace levels have been calculated using the time gap between the terrace deposits and multiplying by selected uplift rates (0.07 m ka^{-1} , 0.08 m ka^{-1} and 0.16 m ka^{-1}). The uplift rates selected have been chosen because they represent the minimum and maximum rates of uplift proposed for the Sorbas basin.

Río Aguas Terrace Level	Age	Time gap	Spacing
A	264ka	1.2 Ma*	20 m*
B	130ka	134ka	28m
C	79ka	51ka	20m
D	31ka	48ka	34m

Río Jauto Terrace Level	Age	Time gap	Spacing
1	264ka	1.2 Ma*	0
2	130ka	134ka	29
3	79ka	51ka	20
4	31ka	48ka	8
Modern river	0	31ka	4

Table 8.3: Spacing, time gaps and age of the terrace deposits in the Sorbas Basin. * From/ below the Góchar surface

Chapter 8: Controls on incision in the Sorbas Basin

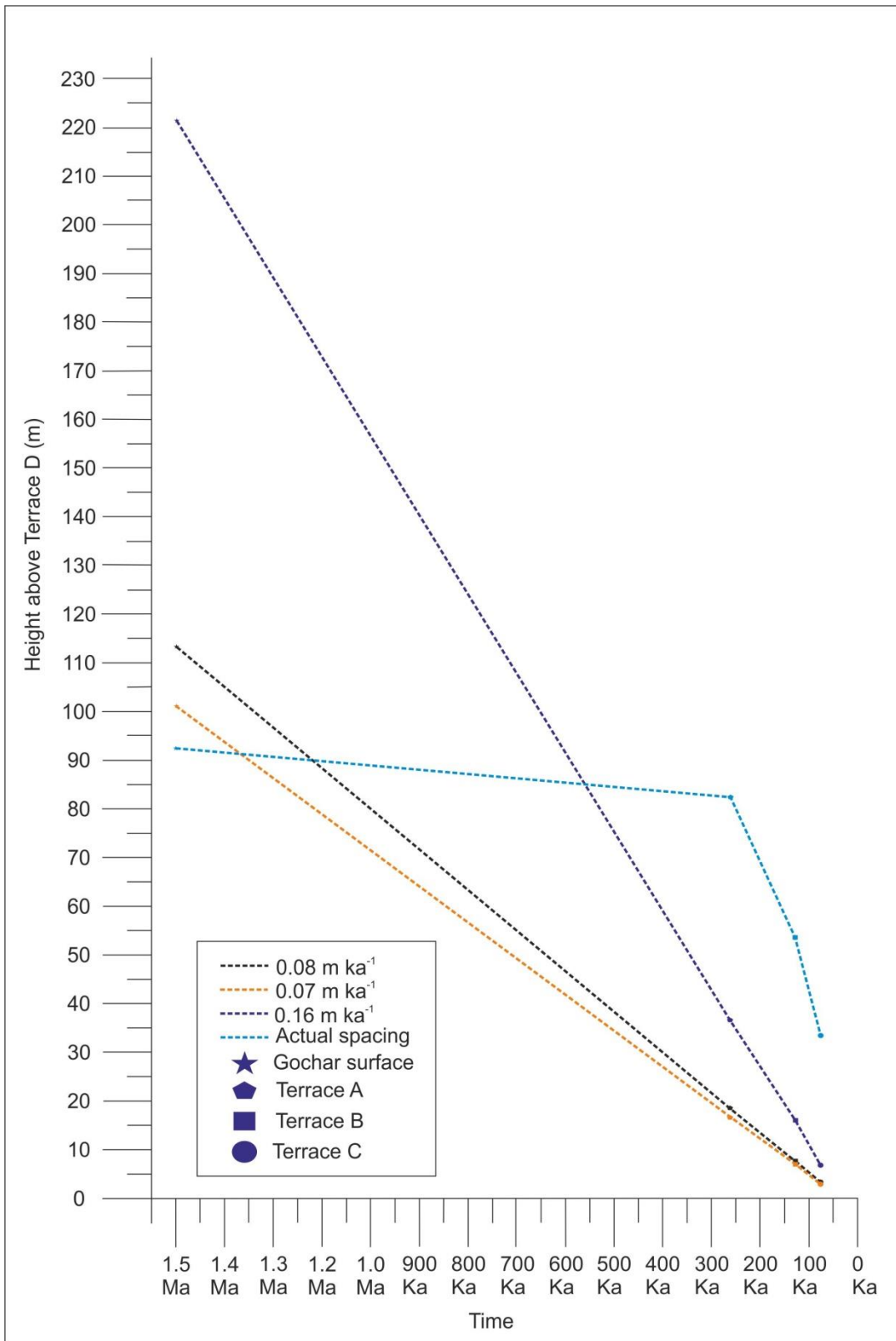


Figure 8.5: Predicted and actual spacing between river terraces in the Río Aguas fluvial system using the uplift rates in published literature.

Chapter 8: Controls on incision in the Sorbas Basin

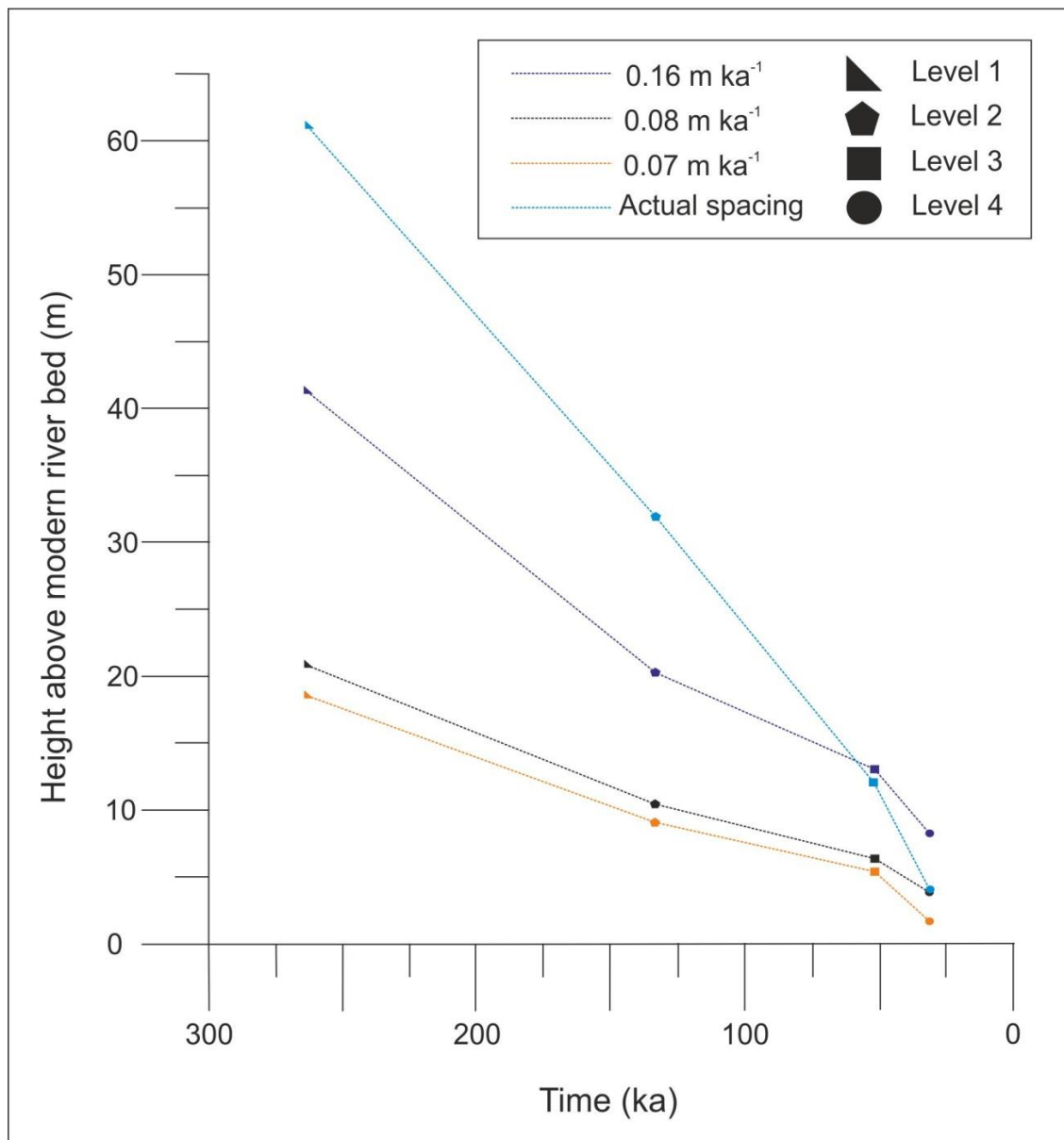


Figure 8.6: Predicted and actual spacing between terraces in the Río Jauto fluvial system using the uplift rates in published literature.

The predicted spacing between terrace levels in the Sorbas basin is compared to the actual distance between terrace levels in figures 8.5 and 8.6. For an uplift rate of 0.16 m ka⁻¹, it is predicted that the highest terrace level should be 192 m below the top basin fill surface (Terrace A or level 1), the second terrace (B or level 2) should be 21 m below the first terrace, the third terrace level (C or Level 3) should be 8.16 m below that. There should be 7.68 m between the third (C or Level 3) and fourth terrace level (D or Level 4).

Chapter 8: Controls on incision in the Sorbas Basin

All three of the uplift rates overestimate the amount of incision that has occurred between the Góchar surface and terrace A (20 m), whilst under estimating the actual incision that has taken place between terraces A, B, C and D (Table 8.3). The biggest underestimation occurs for the distance between terrace C and D. The predicted gap between the two terraces is 7.68 m for 0.16 m ka^{-1} , 4.08 m for 0.08 m ka^{-1} and 3.57 for the uplift rate of 0.07 m ka^{-1} . The actual gap between the two terrace levels is around 34 m. These two levels are however affected by accelerated incision related to the capture event and therefore the spacing probably reflects this rather than an increased uplift amount. The extent of increased incision related to the capture event reaches 20 km upstream, to the town of Sorbas; therefore terrace deposits occurring beyond the extent of the wave of incision may reflect a better picture of uplift rates. The base of terrace D occurs 8 m below the surface of terrace C. This is closer to the distance predicted by an uplift rate of 0.16 m ka^{-1} .

The predicted spacing between terraces also overestimates the distance between to the level 1 deposits in the Río Jauto system. The spacing between levels 2, 3 and 4 are underestimated (Table 8.3). The largest underestimation of the distance between terrace deposits is produced for Level 3 deposits with a difference of 12 m between the actual and predicted space using the uplift rate of 0.16 m ka^{-1} .

8.4.3 Discussion

The previous uplift rates appear to underestimate the uplift rates recorded by the fluvial deposits in this Sorbas basin. This could be due to the time averaged nature of the previous rates calculated which assume that uplift rates were continuous over the time period accounted for. It is more likely that uplift is dynamic in nature with periods of

Chapter 8: Controls on incision in the Sorbas Basin

higher uplift rate. A shorter time period allows for a 100 ka tectonic cycles to be explored.

The spacing between the terraces in the Aguas system increases as the terraces get younger. In the Jauto system the terrace spacing increases until level 3 terraces where upon it decreases. Both systems appear to record high uplift rates in the middle Pleistocene and lower uplift rates in the early Pleistocene. The absolute chronology for the Aguas system indicates that there was a long time period between the incision into the Góchar surface and the incision into the surface of terrace A. This indicates that there was a low uplift rate during this period and this is reflected by the actual spacing between the terraces compared to the predicted gaps show in Figure 8.5.

From the increased incision between terrace levels A, B and C, it is suggested that the uplift rate has increased during this period. The increase in distance between the terrace deposits as they get younger suggests that the system may have been responding to increasing uplift rates during terrace aggradation and incision.

There is evidence of local tectonic activity recorded by terraces and sediments in the Sorbas basin. In the southwest of the basin, a NNE-SSW lineament (Infierno Marchalico Lineament) cuts through the basin offsetting the main channel of the Río Aguas (Mather & Westhead, 1993). In the north of the basin, localised faulting occurs in a terrace C deposit (section 5.4.1).

The sinuosity of a river channel and the number of abandoned meander loops provides evidence of localised active tectonics (Harvey, 2007). In the Ramble de Góchar (UTM: 0577312 4109292) sinuosity of the channel increases from terrace A through B, C and D (Harvey, 2007). The number of preserved meanders also increases from terrace A through to terrace D.

Chapter 8: Controls on incision in the Sorbas Basin

In the Río Jauto, there is also an increase in abandoned meanders observed through level 3 and 4. The abandoned meanders are also mostly observed to be on the south side of the river. It was noted by Harvey (2007) that this could be a result of structural flexuring of the river system. The increase in sinuosity and abandoned meanders observed in both the Río Aguas and Jauto could be a reflection of the increasing uplift rates with time.

Uplift rates calculated from the cosmogenic dates and spacing between the fluvial terraces has provided some suggested uplift rates for the Río Aguas and Jauto over the timescale of the terrace staircase (Table 8.4). Uplift rates are provided for each terrace level and for the Río Aguas they indicate that tectonic uplift is increase as the terraces get younger. The rate of uplift appears to double between B and C. The uplift rate between terrace C and D seems very high, however, this area is affected by the river capture event and therefore the uplift rate of 0.70 m ka^{-1} can be discounted due to the enhanced incision in the area.

Terrace level	Age	Time gap	Spacing	Uplift rate
A	264ka	1.2 Ma	20	0.02 m ka^{-1}
B	130ka	134ka	28	0.21 m ka^{-1}
C	79ka	51 ka	20	0.40 m ka^{-1}
D	31 ka	48ka	34	0.70 m ka^{-1}

Terrace Level	Age	Time gap	Spacing	Upliftrate
1	264ka	1.2 Ma	0	$<0.01 \text{ m ka}^{-1}$
2	130ka	134ka	29	0.22 m ka^{-1}
3	79ka	51 ka	20	0.40 m ka^{-1}
4	31 ka	48ka	8	0.18 m ka^{-1}
Modern river	0	31 ka	4	0.14 m ka^{-1}

Table 8.4: Calculated uplift rates for the Río's Aguas (top) and Jauto (bottom).

Chapter 8: Controls on incision in the Sorbas Basin

To discount the effects of the river capture related incision on the calculated uplift rates, they were recalculated for terrace deposits located in an area of the river not affected by the wave of incision. This area was selected by choosing a section of river above the last capture related knick point. Uplift rates were calculated for all the terraces to test the difference in uplift rates for the centre and the edges of the basin (Table 8.5). The suggested rates for the Góchar area indicate that uplift was occurring at a lower rate but was still increasing during the Pleistocene.

Using a terrace deposit that is in part of the Río Aguas catchment not affected by the wave of incision created by the capture event, the rate of uplift for terrace D is calculated as being 0.25 m ka^{-1} . This is closer to the maximum rate suggested by Mather (1991) and far less than the 0.70 m ka^{-1} indicated for the centre of the basin.

Previous research by Mather & Harvey (1995) indicated that uplift rates were lower on the northern margin of the basin than on the southern edge. Recent research focusing on the tectonic geomorphology of the Sierra Alhamilla supports the occurrence of tectonic activity during the Pleistocene (Giaconia et al., 2012). Several geomorphic indices measured indicate that the North Alhamilla Reverse Fault (NARF) was active during through the Pleistocene, Holocene and through to the modern day (Giaconia et al., 2012; 2013). The results for the Góchar area come from near the north margin whereas the results from Sorbas town are from the centre of the basin. The results indicate that the centre is uplifting faster than the northern edge. The higher rates of uplift in the south and centre of the Sorbas Basin could have caused the speed of propagation of the wave of incision to increase through the Río Aguas system. The uplift rates for the Jauto also indicate lower rates for the northern margin, where the Jauto flows along the foothills of the Sierra de los Filabres then in the Río Aguas. This could reflect a

Chapter 8: Controls on incision in the Sorbas Basin

difference in uplift rates for the north margin or could be a reflection on the different nature of the geology through which the two systems flow.

A

Terrace level	Age	Time gap	Spacing	Uplift rate
A	264ka	1.2 Ma	20	0.02 m ka ⁻¹
B	130ka	134ka	28	0.21 m ka ⁻¹
C	79ka	51 ka	20	0.40 m ka ⁻¹
D	31 ka	48ka	34	0.70 m ka ⁻¹

B

Terrace level	Age	Time gap	Spacing	Uplift rate
A	264ka	1.2 Ma	20	0.02 m ka ⁻¹
B	130ka	134ka	8	0.06 m ka ⁻¹
C	79ka	51 ka	8	0.16 m ka ⁻¹
D	31 ka	48ka	12	0.25 m ka ⁻¹

Table 8.5: Uplift rates calculated from the spacing between the terrace deposits and the time gaps derived from the cosmogenic exposure dating database (Top table Sorbas town, bottom table near Góchar).

8.5 Lithological controls on terrace formation in the Río Jauto

The geology through which a river system flows can directly influence the type of river valley that forms and the fluvial processes that occur (Bull, 2009). The Río Aguas has exploited a weak band of marls, allowing it to erode headwards and expand the drainage network of the system. The Río Aguas also follows the strike of the bedding which is controlled by the weakly synclinal folding of the basin created due to the uplift of the mountain ranges. In the Río Jauto system lithology therefore exerts a strong control on terrace formation and valley type. There are several gorges present in the Río Jauto catchment which are cut into the metamorphic basement lithologies of the Sierra de los Filabres. There are no fluvial terraces present in the gorges which form narrow slot like features. Whilst there are level 1 deposits around the Alfaix gorge, the deposits in this

Chapter 8: Controls on incision in the Sorbas Basin

area occur above the gorge, but are not present in the gorge itself (Figure 8.7a). Steeper channel gradients are also recorded in the gorges (Figure 6.1). In areas where there is softer geology (e.g. marls), there are numerous terrace deposits present and the younger fluvial deposits are often preserved in palaeomeanders (Figure 8.7b). Field observations show that where the rock resistance is high vertical incision has dominated whilst where the lithology is softer lateral erosion is the primary action of the fluvial system. This suggests that where the river cuts through the basement rocks the river become locked into a slot like feature and is unable to laterally erode and does not have the space for aggradation to take place. In areas where the local lithology is soft the river is able to laterally erode creating space for aggradation to take place.

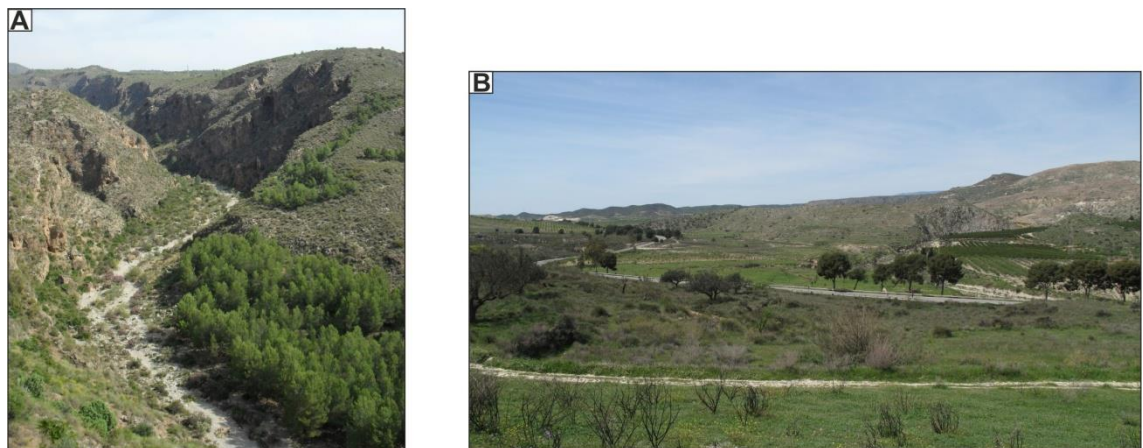


Figure 8.7: Lithological controls on terrace formation in the Río Jauto: A) Alfaix Gorge B) Highly dissected valley, Los Castaños.

Hard lithologies can also act as a buffer zone in systems and slow down erosion rates (Harvey, 2007). The differential uplift of the Betic Cordillera led to drainage rearrangement and river capture taking place in many systems. In the Sorbas basin headward erosion by the Lower Aguas led to the capture of the Proto Aguas/Feos. The Río Jauto would also have been affected by the base-level drop occurring in the Lower Aguas as uplift took place. Knick points along the long profile of the Jauto show that the base level drop in the Río Aguas caused affected the Río Jauto, however deep

Chapter 8: Controls on incision in the Sorbas Basin

incision in the Río Jauto has only propagated 10 km upstream. The presence of the metamorphic basement could have acted as a buffer to any base-level drop that occurred as a result of the lower Aguas down the propagation of headward erosion and limiting the extent of incision in the Jauto catchment. This slowing down of the headward erosion in the Río Jauto probably prevented it from capturing the headwaters of the Proto Aguas/Féos and from becoming the master drainage system in the Sorbas basin. The headward erosion was able to propagate fast up the Lower Aguas and capture the Proto Aguas /Féos due to the strike orientated system following a weak band of marls (Abad Member, Turre Formation).

8.6 Palaeoflood estimates for the Pleistocene deposits of the Sorbas Basin

Palaeohydrological analysis has been undertaken on the Pleistocene terrace deposits of the Proto Aguas/Feos and the Río Jauto (Chapter 5 & 6). A summary of the major findings from the analysis is presented here along with a discussion of any data trends determined. This research helps to form a picture of the long-term regional hydrological conditions under which the river terraces formed. Regional hydrological conditions are linked to long term climate variably discussed earlier (section 8.3).

Table 8.6 presents the maximum discharges for the reaches of the Río Jauto and Aguas. Maximum flood discharge for terrace A increases in a downstream direction until the distal reach where it decreases slightly. For terrace B and C a decrease in discharge is seen between the proximal and distal reach. This decrease could be due to the maximum clast not being exposed by the limited exposures of terrace gravels. The maximum clast carried by the flood might also not been deposited but flushed through the system and out to sea. Terrace D deposits show an increase from the proximal to middle reach and then a decrease in the proximal reach. The proximal reach has been beheaded by the Río

Chapter 8: Controls on incision in the Sorbas Basin

Aguas capture event and the palaeohydrology calculations are therefore reflecting the loss of drainage area.

Terrace level	Proximal (m³/s)	Middle (m³/s)	Distal (m³/s)
Level 1	-	-	70
Level 2	-	631	363
Level 3	1683	1683	421
Level 4	1753	1753	471

Terrace level	Proximal (m³/s)	Middle (m³/s)	Distal (m³/s)
A	181	340	305
B	592	493	1039
C	692	520	339
D	364	421	203

Table 8.6: Maximum flood discharge for the Río's Jauto (top table) and Aguas (Bottom table) calculated using the maximum boulder size method of Clark (1996).

Terrace deposits in the Río Jauto show a downstream increase in flood discharge until the distal reach. In the distal reach the maximum flood discharges recorded by the terraces are significantly reduced. The distal reach of the Río Jauto is dominated by a gorge which limits the lateral space for terrace aggradation. The outcrops in the distal reach are generally thinner than exposed elsewhere in the catchment. This is especially true when compared with the middle reach where several of the lower terraces are cut by gully systems which expose terrace gravels. The smaller outcrops reduce the chance that the largest boulder carried by a flood was exposed in the sections of terrace gravels.

Palaeoflood estimates for the terrace deposits in the Sorbas basin indicate that palaeoflood discharge has increased thought time (Table 8.7). In the Proto Aguas/Feos

Chapter 8: Controls on incision in the Sorbas Basin

systems terrace C deposits record maximum palaeoflood discharge values $100 \text{ m}^3/\text{s}$ higher than those which recorded by the terrace B deposits. In the Jauto the difference between the level 2 and 3 terrace is more significant with a 3 times increase in maximum palaeoflood discharge recorded in level 3 and 4 deposits (Table 8.7). Significantly higher values of maximum flood discharges are recorded in the Río Jauto deposits then in the Aguas terrace deposits (Table 8.6 & 8.7). This could be reflecting the position of the Río Jauto drainage system to the Sierra de los Filabres. The system flows through the foothills of the Sierra de los Filabres collecting north-south flowing stream. The higher flood discharge could be reflecting the higher precipitation on the higher ground. The increase in flood discharge could also be reflecting the increase in catchment area from the gained headwaters.

Río Aguas Terrace Level	Maximum (m^3/s)	Río Jauto Terrace Level	Maximum (m^3/s)
A	340	Level 1	70
B	592	Level 2	631
C	692	Level 3	1683
D	364	Level 4	1753

Table 8.7: The maximum palaeoflood discharges recorded by terrace deposits in the Sorbas basin.

The palaeoflood data could be showing reflecting climatic cycles as well as tectonic activity. SE Spain is the site of a diffuse plate boundary where the African plate is colliding with the Iberian plate. This has led to the formation and tectonic uplift of the Betic Cordilleras which are still uplifting today. The Lower Aguas experienced steepening channel gradients due to the regional tectonic uplift leading to headwards erosion and river capture. The river capture event was recorded by the terrace deposits

Chapter 8: Controls on incision in the Sorbas Basin

of the Rambla de Féos and the Río Alias with the post capture deposits having significantly different sedimentary characteristics (smaller clast sizes, localised source for clast assemblage) to the pre capture terraces (Maher, 2005). The palaeoflood data from the Proto Aguas/Féos system also reflects that the beheading of the Féos by the Lower Aguas had a significant effect on the flood events taking place in the Féos system with a marked decrease in calculated maximum palaeodischarge seen between pre (terrace levels A, B & C) and post capture terrace deposits (terrace D) (Table 8.6) with a fall from a maximum discharge of 692 m³/s to 364 m³/s.

The apparent increase in maximum flood discharge found in terrace C deposits, and the equivalent level 3 deposits in the Río Jauto, could be reflecting climatic events taking place during the deposition period. Regional patterns of palaeo-precipitation have been investigated by Hodge *et al* (2008) using $\delta^{13}\text{C}$ variations in a speleothem.

Concentrations of $\delta^{13}\text{C}$ are affected by two major factors; firstly the abundance of C3 to C4 plants and, secondly, soil microbial activity and vegetation respiration (Hodge *et al.*, 2008). In SE Spain the first factor is not present as C4 plants did not grow in the Mediterranean region during the Late Quaternary (Hodge *et al.*, 2008).

Soil microbial activity and vegetation respiration are controlled by temperature and moisture availability during the growing season. Moisture availability is the largest control on vegetation respiration in SE Spain due to limited variation in the temperature and therefore any variation seen in $\delta^{13}\text{C}$ values are controlled by effective precipitation (Hodge *et al.*, 2008).

The research conducted by Hodge *et al* (2008) provides some regional insights into the palaeo-precipitation patterns from MIS 8-3 (~226 ka- 46 ka). The $\delta^{13}\text{C}$ records from the speleothem documents a steady rise in effective precipitation during MOIS 8 to 7. Precipitation then decreased during MIS 6 and then went on to rise rapidly during

Chapter 8: Controls on incision in the Sorbas Basin

MIS 5 (from ~ 128 ka). Around 11ka rainfall began to steadily decrease, with some fluctuations, into MIS 4-2 (Hodge *et al.*, 2008; Schulte *et al.*, 2008). Cosmogenic dating of the terrace C deposits show that the terraces were abandoned ~120-79 ka which suggests that the terrace gravels were deposited during late stage of the MIS 6 glacial through to the early MIS 6/5 transition when sediment supply to the channel would have been high. This would indicate that it is very likely that the terrace gravels are recording the increased precipitation relating to MIS 5 (Figure 8.8). The increased rainfall recorded in the speleothem record coincides with Termination II and is probably related to a Heinrich event.

The climatic changes that took place in MIS 6/5 have been recorded by the Río Jauto system with a significant increase in the palaeoflood discharges recorded by level 3 deposits (Chapter 6). If, as suggested by this research, the level 3 deposits are equivalent to the terrace C deposits of the Río Aguas then the increase in rainfall related to Termination II could have led to larger flood events occurring in the Jauto system. The increase in maximum palaeoflood discharge rates by 1000 m³/s seems to confirm this theory.

The increased palaeoflood discharge levels are also recorded in Level 4 terraces (Table 8.1). The level 4 terraces are believed to relate to the MIS 4/2 glacial. However, precipitation is believed to have decreased during this period (Stokes *et al.*, 2012b). The level 4 terraces could be recording the fluctuations in rainfall. Alternatively the increase in palaeoflood discharge could be related to the differential uplift of the Betic Cordilleras. Although the Río Jauto was not affected by the river capture event in the Río Aguas, the headward erosion of the Lower Aguas that caused the capture event has propagated up the Jauto river system. Increased incision is recorded in the Jauto channel, with the river valley becoming slot like for up to 10 km upstream from the

Chapter 8: Controls on incision in the Sorbas Basin

junction with the Río Aguas. The increased incision reaches until just upstream of the town of Los Castaños (Figure 6.2) and is probably caused by the base level drop occurring in the Río Aguas channel. The increase incision would have led to network expansion by headward erosion expanding the catchment of the Río Jauto. The expanding catchment would lead to an ability to generate progressively larger floods by collecting more water.

The palaeohydrology data suggests that the Río Jauto and the Proto Aguas/Féos is sensitive to both climatic and tectonic changes taking place in the Sorbas basin. The data from the Féos valley shows that when fluvial systems are affected by river capture, the river terraces store the signals from the event and the relationship between climate and maximum palaeoflood discharge is masked. Where the system is unaffected by the capture event, the deposits record the increased rainfall that occurred during Termination II (Figure 8.8).

Chapter 8: Controls on incision in the Sorbas Basin

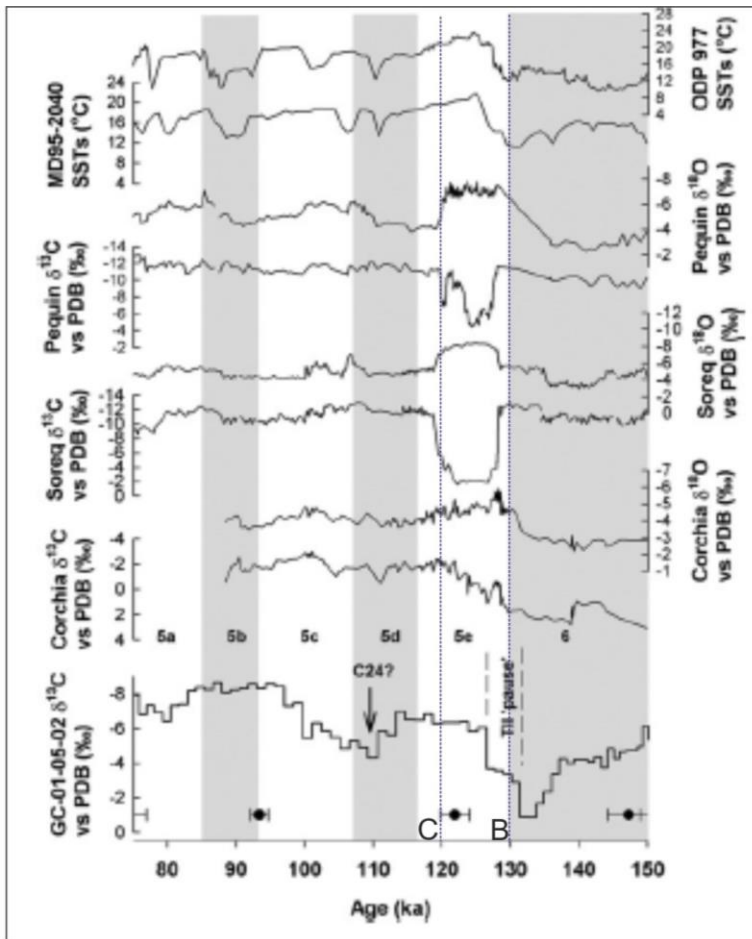


Figure 8.8: Isotope curves from Hodge et al. (2008) with the timing of terrace abandonment of terrace levels C & B superimposed (purple lines).

8.7 Landslides: The keep up vs. catch up model

Chlorine 36 dating has been used to date the Maleguica landslide complex in order to determine when the landslide was initiated and to assess its relationship to the river capture event. Whilst previous studies have shown that the landslides in the Sorbas basin cluster around the river capture site and upstream around Sorbas Town where increased incision has led to canyon development, the timing of the landslides is unknown.

Rapid incision creates instability in river catchments because it leaves little time for the affected hill slopes to adjust to the steepening of gradient by toe removal. This means that the landscape becomes inherently unstable. Although it is clear that the landslides in the Río Aguas catchment must be related in some way to the wave of incision created

Chapter 8: Controls on incision in the Sorbas Basin

by the capture event it is unclear as to the exact timing of failure. It is possible that the landscape reacted instantaneously (in geological terms) to the increased incision and that successive landslide slippages occurred as the incision took place (i.e. it kept up with incision). Alternatively the landslides could have occurred later on once the wave of incision had passed upstream (i.e. catching up with incision) and could be linked to subsequent climate variability, with landsliding occurring during the wetter climatic phases as thought to be the case with the La Cumbre slide by the Mather et al (2003) of a large inactive (fossil) landslide complex.

Cosmogenic exposure dating of the Maleguica landslide has shown that a period of failure took place 3-4 ka. Pollen data collected from the Alfaix travertine (Schulte et al, 2008) for this period shows an increase in arboreal and mesic pollen taxa indicating that the climate was dominated by more humid conditions (Figure 8.9). The increase in humid conditions is confirmed by the development of haploxerolls (organic rich soils) which have been dated at 4.6 ka and 3.6 ka. The failure of the Maleguica landslide during a wetter climatic period suggests that the landslide was triggered by the increase in storm events.

Chapter 8: Controls on incision in the Sorbas Basin

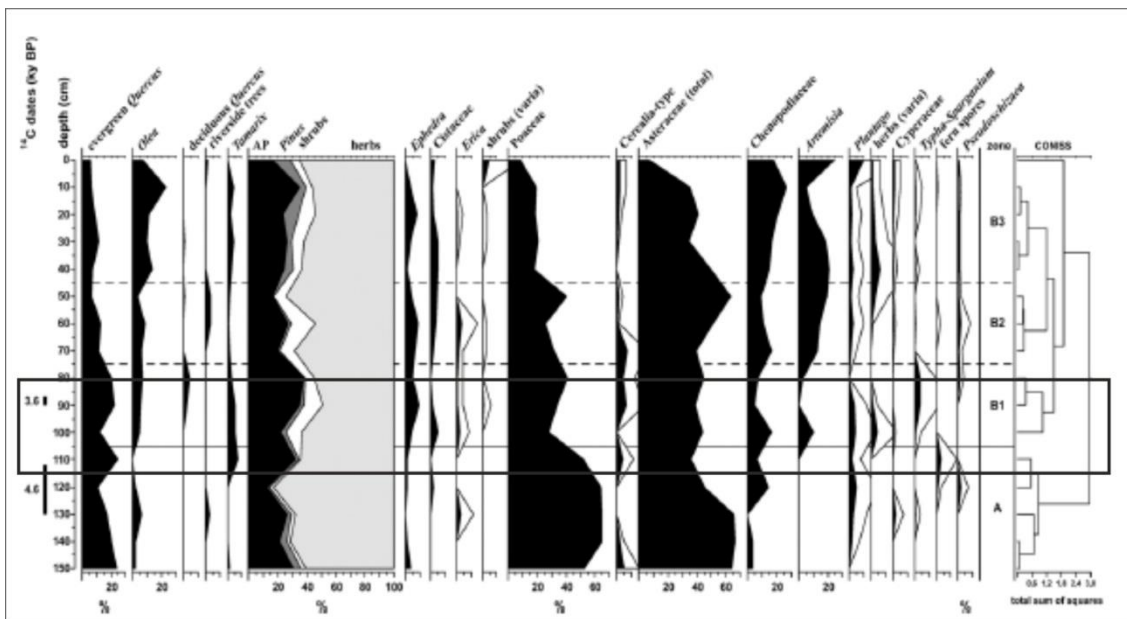


Figure 8.9: Pollen diagram from Schulte et al (2008) showing the increase in Arboreal pollen around 3-4 ka.

The failure of the landslide at 3-4 ka suggests that the landscape is catching up with the river capture related incision rather than keeping up with it. However, the Maleguica landslide is a large scale failure that covers an area of 1 km with a volume of $3.14 \text{ m} \times 10^6 \text{ m}^3$ (Hart, 2004). The landslide is described as a complex landslide (Hart, 2004) with a number of failure mechanisms identified (rock falls, rock topples and non rotational landslides). The multiple failure mechanisms along with the presence of tension cracks and multiple rotational blocks indicate that the landslide has failed multiple times. It is therefore likely that the cosmogenic date does not reflect the first failure of the landslide, but the last major failure of the complex. The complex nature of the landslide could suggest that the landscape is still adjusting to the widespread incision created by the capture event.

In order to fully assess whether the landscape in this area kept up with the wave of incision or is catching up with it, multiple dates for the landslide are needed from several different locations. This may help indicate whether one side of the landslide failed first and if the first failure occurred much earlier than the chlorine 36 date suggests.

Chapter 8: Controls on incision in the Sorbas Basin

8.8 Palaeoenvironmental model of terrace formation

This section presents a suggested model of terrace evolution in the Sorbas basin for terrace B and C using data presented above. The model focuses on terrace deposits B and C because these deposits have the best age control. The model takes into account the cosmogenic, tectonic, climatic and palaeohydrology data relating to the terrace deposits. Table 8.8 details the conditions expected to occur during a climatic cycles whilst Figure 8.10 shows the conditions recorded by the terrace B and C sediments.

A) Glacial period-Stage 6

During the MIS 6 glacial period the climate in the Sorbas basin was dry and cold (Schulte *et al.*, 2008; Hodge *et al.*, 2008). Limited precipitation occurred with floods having a maximum discharge of 592 m³/s. The vegetation cover was restricted to small amounts of herbaceous shrubs and steppe vegetation (Schulte *et al.*, 2008). The cold and dry conditions would have restricted vegetation growth leading to reduced slope stability caused by the limited root mass. The sediment supply to the river would have been high due to freeze thaw and mass movement processes taking place on the bare slopes. The high sediment supply plus the low precipitation rate, indicated by pollen data (Schulte *et al.*, 2008), would have limited the ability of the rivers to incise and therefore aggradation of the terrace B in a braided river channel occurred.

B) Glacial to interglacial transition

The transitional period between glacial and interglacial conditions can be split into two parts based on river activity; the early transition (warm to cold) and the late transition (cold to warm). During the early part of the transition minor aggradation took place in

Chapter 8: Controls on incision in the Sorbas Basin

the river system due to the increasingly stormy weather increasing the sediment supply off the valley slopes. The vegetation was still sparse during this period as there is a time lag in the recovery of vegetation to the slopes (Schulte *et al.*, 2008). During the late transition the climate becomes warmer and the sediment supply from the slopes decreases due to vegetation re-growth (Schulte *et al.*, 2008). With sediment supply reduced incision processes took over in the fluvial systems leading to abandonment of terrace deposits as the river incises below the surface of the terrace B deposit around 130 ka.

C) Interglacial period-stage 5

Interglacial periods on the Iberian Peninsula are generally characterised by warm and dry conditions (Tzedakis, 2009). However, during the stage 5 interglacial a gradual increase in effective precipitation occurred from 128 ka relating to Termination II (Hodge *et al.*, 2008). Larger flood events took place (maximum discharge: 629 m³/s) The increased rainfall could have destabilised valley sides leading to landslides increasing the sediment supply to the river system leading to the aggradation of terrace C. Effective precipitation continued to rise throughout the stage 5 interglacial and along with increasing rates of tectonic uplift (0.40 m ka⁻¹) possibly triggered a switch to incision causing the abandonment of terrace C around 120-70 ka.

Chapter 8: Controls on incision in the Sorbas Basin

Getting younger	Stage	sub-stage	Climatic conditions	vegetation	Sediment supply	fluvial mode
	Glacial	Glacial	Cold and dry	Limited vegetation	High	Aggradation
	Transition	Early transition	warming and wet	Limited vegetation	High	Aggradation
	Transition	Late transition	warming and drier	Increasing vegetation	Low	Incision
	Interglacial	interglacial	hot and dry	Highly vegetated	Low	Incision
	Transition	Early transition	cooling and wet	Highly vegetated	Low	Incision
	Transition	Late transition	cooling and drier	Decreasing vegetation	Increasing	Aggradation

Table 8.8: Table showing the conditions occurring during a climate cycle in the Sorbas basin (Schulte et al., 2008; Tzedakis, 2009; Olszak, 2011)

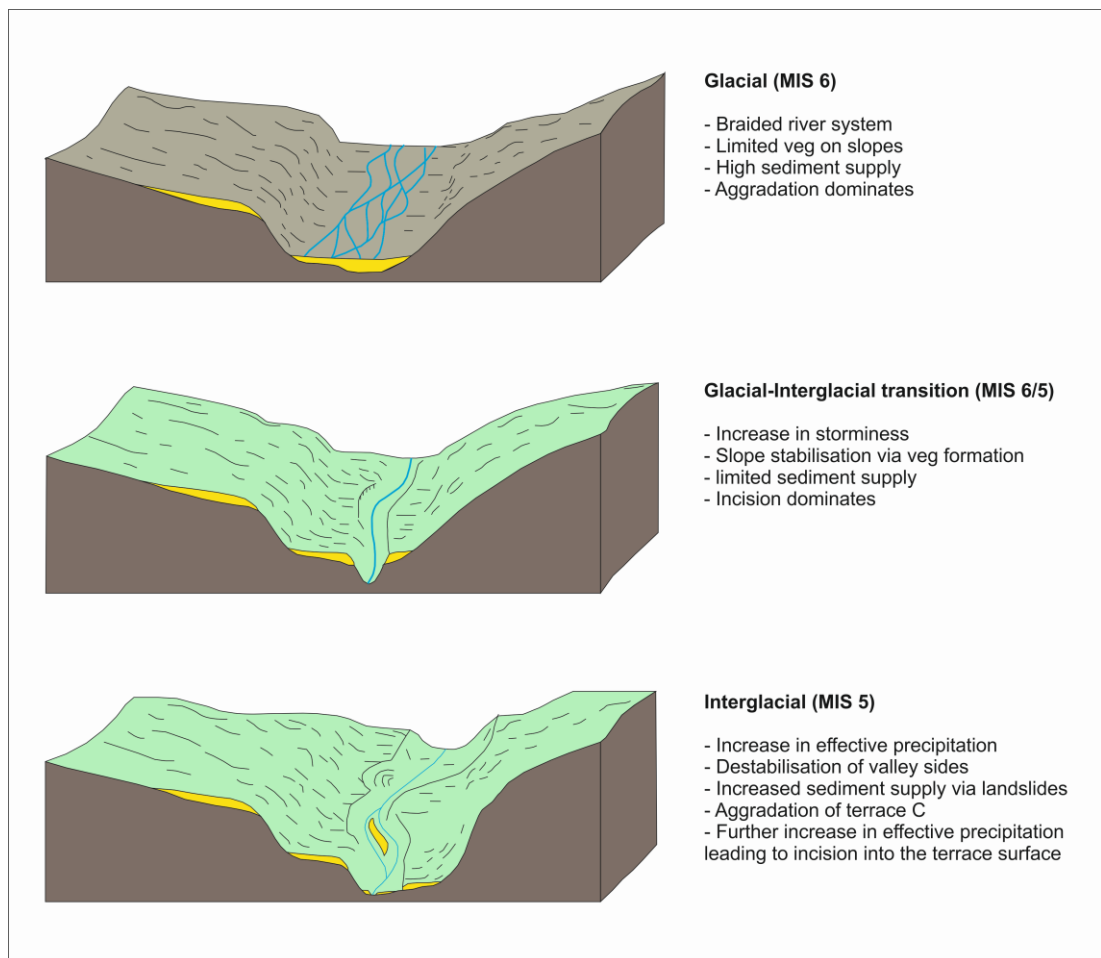


Figure 8.10: Model of terrace formation (adapted from Olszak, 2011).

Chapter 8: Controls on incision in the Sorbas Basin

The terrace formation model present here for terraces B and C is different to models previously presented (i.e. the general model of Bridgland & Westaway (2008) and Meikle's, (2009) model of the Río Almanzora). Previous models suggest that the main phases of aggradation and incision occur at transitions between cycles. The Río Aguas has been shown to respond to the Stage 6 glacial and the stage 5 interglacial. It is significant that the aggradation and abandonment of Terrace C has taken place during an interglacial period as they are generally considered to be periods of stability with little/no incision or aggradation occurring.

8.9 Summary

The terrace staircases in the Sorbas basin are created by interplay between the differential uplift of the area and climatic cycles. Climatic deterioration at the MIS 6/5 transitional period led to thresholds being crossed allowing for terrace abandonment. Aggradation of terrace B happened during the stage 6 glacial. Terrace C abandonment occurred during the stage 5 interglacial. Tectonic uplift has created a sustained base-level drop creating spacing between the periods of aggradation leading to terrace staircase formation. Tectonic uplift of the Sorbas Basin has increased since the Mid Pleistocene causing increased incision and along with a switch to 100 ka climatic cycles has create a terrace record which records 1.5 Ma of incision in the Sorbas Basin. Tectonic uplift rates for the Sorbas basin have been recalculated and appear to be higher than previously recognised. Uplift rates for the northern margin are lower than those calculated for the centre of the basin reflecting previous research. Palaeohydrological data has shown that the fluvial archives record signals from the climate, in form of increased or decreased rainfall amount, and also records any drainage expansion or reduction taking place in a fluvial system. Overall the fluvial systems in the Sorbas

Chapter 8: Controls on incision in the Sorbas Basin

basin record 1.0 Ma incision that has occurred due increasing rates of tectonic uplift with climatic signatures superimposed upon the tectonic signals.

Chapter 9: Conclusions

The principle aim of this project was to apply a developing chronological technique, the cosmogenic profiling method, to fluvial terraces in a system that has undergone base level lowering linked to differential tectonic uplift and drainage network reorganisation via a basin scale capture event. The cosmogenic exposure dating method was applied to calculate exposure ages for the abandonment of fluvial terraces by incision. Burial ages were calculated for deposits, where paired isotopes have been collected, to provide a maximum age for the surface sediments and an indication of the timing of aggradation. The resultant geochronological database has been used to quantify spatial and temporal patterns of fluvial system incision. Both mega scale (10^6 - 7) and macro scale (10^4 - 5) patterns were investigated. The link between landslides and climate was also investigated using chlorine 36.

9.1 Conclusions: Cosmogenic exposure dating

Cosmogenic exposure dating and the profile methodology has been successfully applied to the river terraces in the Río Aguas fluvial system with viable dates recorded for the top basin fill surface and terrace deposits in the Río Aguas system. The chronological database created by this method indicates that the aggradation of terrace B is linked to glacial conditions, whilst the deposition and abandonment of terrace C took place during an interglacial. Incision also took place during transitional periods (Chapter 8).

Cosmogenic exposure dating has been proved to be a useful method for dating fluvial landforms that are outside the age range of the normal techniques applied to fluvial terraces (Chapter 7). It is also can be used in areas where sediments are affected by bleaching (which limits the usefulness of quartz OSL dating) as this does not impact on

Chapter 9: Conclusions

the cosmogenic nuclide content of the sediments. U-series dating has been successfully used in the Sorbas basin (Chapter 1) however U-series dating has been shown to overestimate the age of landforms that are at the limit of its range (Chapter 7). U-series dating for terrace B indicated that the surface of the deposit had been abandoned between 207-112 ka whereas cosmogenic dating provided an age of 130 ka for the terrace B deposit. Another issue with U-series dating is the multi-phase development of calcretes and the potential for inclusions. Although methodologies have been developed to overcome both of these issues they still remain as a boundary to producing reliable dates (chapter 1). Cosmogenic dating is not without its own issues; inheritance remains a big problem leading to overestimating of dates and oversaturation of samples. Whilst the profile methodology goes some way to solving this issue by using a multiple sample approach, it remains a challenge when dealing with sediments that are recycled from older deposits. Burial dating helps overcome inheritance by providing a maximum age for the deposits and providing an indication of the amount of inheritance present. Cosmogenic exposure dating does present researchers with an opportunity to constrain both incision and aggradation when multiple isotopes are used (profile method and burial dating) as well as constraining surface erosion rates. Both cosmogenic dating and U-series dating are useful to date Late Pleistocene river terrace deposits and present researchers with options for creating chronological databases of fluvial deposits. A multi-proxy approach could also be considered in areas where some terraces do not meet the strict criteria for the profile methodology.

Cosmogenic exposure dating has also been applied to a landslide and an erosion surface by collecting rock samples from the landforms. Neon dating was unsuccessful due to the high concentration of atmospheric neon in the samples (chapter 7). This could be avoided in future by collecting a sample at the surface and collecting a shielded sample

Chapter 9: Conclusions

from a quarry if possible. Unfortunately in this case, this was not possible as the ridge has not been quarried.

Cosmogenic exposure dating using chlorine has successfully been applied to the Maleguica landslide, near Sorbas town, producing an age of 3000 ka (Chapter 7) suggesting that the landscape did not react instantaneously in geological terms to the river capture event. The failure is linked a period of wetter climatic conditions that occurred around 3-4 ka. However, due to the mechanism of failure in the landslide complex it is suggested that the cosmogenic date may simply reflect the latest failure. The landslide may have undergone multiple failures along the back scar and therefore applying multiple sample methodology may help produce a timeline of failures (Chapter 8). This may show further whether the landslide failures are linked to specific climatic conditions (e.g. slope loading due to wetter conditions) and if the landslide first occurred nearer to the time of the river capture event. Overall cosmogenic exposure dating has provided useful dates for fluvial related landforms in the Sorbas basin enabling detailed studies of the history of incision to take place.

9.2 Conclusions: Timing of fluvial incision

Cosmogenic exposure dating along with detailed field and palaeohydrological studies (Chapter's 5& 6) has provided insights into fluvial archive development in the Sorbas Basin (Figure 9.1). Cosmogenic dating indicates that incision into the Góchar surface began 1.0Ma (Chapter 7) and therefore constrains the deposition of the Góchar Formation to between ~4.0 Ma to 1.0 Ma (Chapter 8). The incision probably began in response to the Mid Pleistocene Revolution during which period tectonic activity was accelerated. The rate of tectonic uplift during this period was around 0.02 m ka^{-1} (Chapter 8).

Chapter 9: Conclusions

The aggradation of terrace B occurred during the MIS 6 glacial (160 ka) when sediment supply to the river was high. This period was marked by an increase in effective precipitation (recorded by $\delta^{13}\text{C}$ isotopes) until 130 ka which is reflected by the palaeodischarge values calculated for terrace B deposits (Chapter 5). The Level 2 deposits of the Río Jauto were probably deposited during this period (Chapter 6). The Río Aguas started to incise around 130 ka (Chapter 7) during a period when uplift rates of 0.21 m ka^{-1} were occurring suggesting that tectonic activity in the Sorbas basin has intensified (Chapter 8).

The MIS 5e interglacial coincides with the aggradation and abandonment of terrace C (Chapter 8). This period is also marked by increased precipitation leading to larger floods taking place (Chapter 8). These are recorded by the Terrace C ($693\text{ m}^3/\text{s}$) and Level 3 ($1683\text{ m}^3/\text{s}$) deposits (Chapter's 6&5). Uplift rates during this time period increased to 0.40 m ka^{-1} . Incision into the terrace C surface began between 120 to 79 ka during the stage 5 interglacial. The incision into the surface could be a response to the increased rainfall as a response to termination II (Chapter 8).

9.3 River capture

The basin-scale river capture event which occurred when the Lower Aguas captured the headwaters of the Proto Aguas/Feos has been further constrained. The river capture is believed to have taken place after the deposition of terrace C (Chapter 2). Dating of a terrace C deposits located 10 km upstream of the capture site, using ^{10}Be , indicates that the terrace surface was abandoned $\sim 79\text{ ka}$ giving a maximum age limit to the river capture event. This was during a period of high incision rates and increasing tectonic uplift. The highest rates of uplift occurred in the centre and southern areas of the Sorbas Basin, where the capture event occurred (Chapter 8). The propagation of the wave of

Chapter 9: Conclusions

incision created by the capture event was probably amplified by the increasing rates of uplift along with the increased precipitation recorded during this period (chapter 8). Although the Río Jauto has shown some reaction to the base-level lowering created by the headward erosion of the Lower Aguas, the amount of incision and the distance which incision has propagated upstream is small compared to the response in the Río Aguas (Chapter 6). This could be down to the lithological controls on the Río Jauto with the relative strength of the metacarbonate basement suppressing incision. It could also be due to the lower uplift rates recorded on the northern margin of the basin (Chapter 8).

9.4 Timeline creation

One of the original aims of this project was to quantify the river capture event by creating timelines. This has not been achieved due to (1) an attempt at dating the terrace C nearest to the capture site did not produce a viable date & (2) Due to the limitations of this study, cosmogenic dating was only applied to terrace deposits older than the capture event. This means that although the date of the capture event has been closely constrained, the timing of the wave of incision has not. The dates for the terrace C deposits tentatively suggest that incision occurs in a downstream direction; however, this is only based on two dates; several more would be needed to confirm this.

9.5 Key conclusions

The key conclusions of this research are:

- Cosmogenic exposure dating and the profile method offer a viable way to date Early and Middle Pleistocene terrace deposits. Combined exposure and burial

Chapter 9: Conclusions

ages approaches using paired isotopes allow for insights into terrace aggradation and fluvial incision timing.

- The fluvial archive in the Sorbas basin records over 1.0 Ma of incision with the onset into the Góchar Formation surface occurring at 1.0 Ma.
- Uplift rates calculated from terrace spacing appear to be much higher than previously indicated for the Middle/Late Pleistocene. Previous values suggested an uplift rate of between 0.07 m ka⁻¹ to 0.16 m ka⁻¹ (Mather, 1991; Mather & Harvey, 1995; Braga et al., 2003). Uplift rates calculated for the Early Pleistocene suggest an uplift rate of 0.02 m ka⁻¹ whilst in the middle Pleistocene uplift rates increased to 0.21 m ka⁻¹. The rate of uplift increased significantly during the Late Pleistocene to 0.40 m ka⁻¹.
- Terrace aggradation has taken place in glacial and interglacial periods
- Terrace abandonment has occurred both at warming transitions and in interglacial periods
- The major capture event that took place in the Sorbas basin occurred before 79 ka.

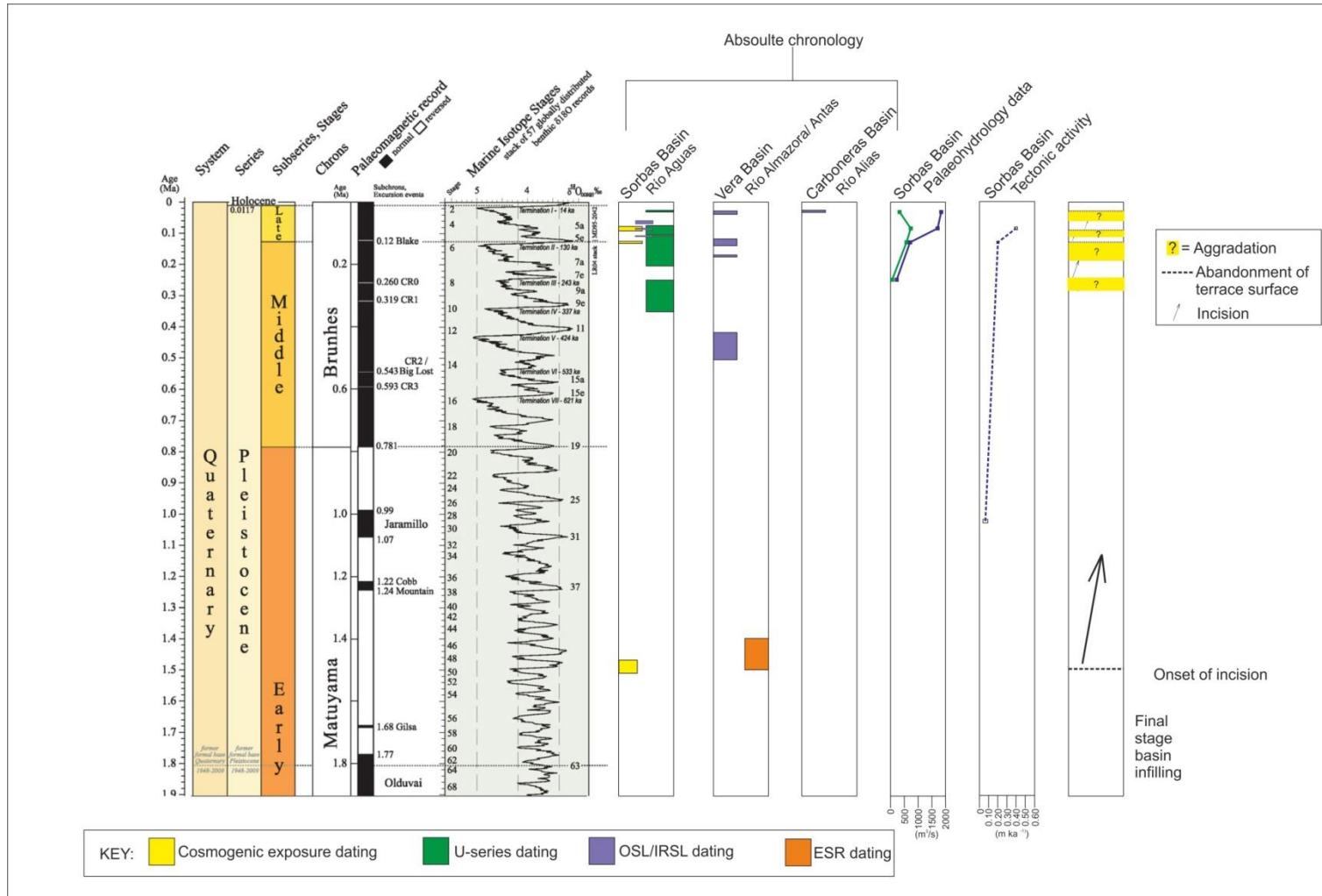


Figure 9.1: Diagram summarising the data collected in this thesis. OSL dates after Schulte, 2008; Maher 2007 & Meikle, 2009; ESR data after Wenzens, 1991; U-series dates after Candy et al., 2004; 2005.

References

- Aguirre, E. 1997. The Pliocene-Pleistocene transition in the Iberian Peninsula. In Couvring, J.A (Editor), *The Pleistocene boundary and the beginning of the Quaternary*. Cambridge university press, Cambridge. 297 pp.
- Alexander, R.W., Spivey, D.B., Faulkner, H and Wilshaw, K., 1999. Badland morphology and geocology: Mocatán system: Processes and patterns. In: Mather, A.E and Stokes, M. (Eds), *BSRG/BGRB SE Spain Field Meeting Guide Book*, University of Plymouth, England, 134-151.
- Alonso-Zarza, A.M. 2003. Palaeoenvironmental significance of palustrine carbonates and calcretes in the geological record. *Earth Science Reviews*, **60**, 261-298.
- Anderson, R.S., Repka, J.L., and Dick., G.S., 1996. Explicit treatment of inheritance in dating depositional surfaces using in situ ^{10}Be and ^{26}Al . *Geology*, **24**, 47-51.
- Anthony, E.Y and Poths, J., 1992. ^3He surface exposure dating and its implications for magma evolution in the Potrillo volcanic field, Rio Grande Rift, New Mexico, USA. *Geochimica et Cosmochimica Acta*, **56**, 4105-4108.
- Bache, F., Popescu, S.M., Rabineau, M., Gorini, C., Suc, J.P., Clauzon, G., Olivet, J.L., Rubino, J.L., Melinte-Dobrinescu, M.C., Estrada, F., Londeix, L., Armijo, R., Meyer, B., Jolivet, L., Jouannic, G., Leroux, E., Aslanian, D., Tadeu Dos Reis, A., Mocochain, L., Dumurdžanov, N., Zagorchev, I., Lesić, V., Tomić, D., Çağatay, M.N., Brun, J.P., Sokoutis, D., Csato, I., Uçarkus, G., Çakır, Z., 2012. A two-step process for the reflooding of the Mediterranean after the Messinian Salinity Crisis. *Basin Research*, **24**, 125-153.

- Baena, R. and Di'az del Olmo, F., 1997. Resultados paleomagneticos de la ran~ a del Hesperico Meridional (Montoro, Co' rdoaba). *Geogaceta*, **21**, 31–34.
- Baggley, K.A., 2000. The late Tortonian-Early Messinian foraminiferal record of the Abad Member (Turre Formation), Sorbas Basin, Almeria, South-east Spain. *Palaeontology*, **43**, 1069-1112.
- Baker, V.R. 1974. Paleohydraulic interpretation of Quaternary alluvium near Golden, Colorado. *Quaternary Research*, **4**, 94-112.
- Baker, V.R. 2008. Paleoflood hydrology: Origin, progress, prospects. *Geomorphology*, **101**, 1-13.
- Balco, G., Stone, J. O.H., Lifton, N. and Dunai, T., 2008. A complete and easily accessible means of calculating surface exposure ages or erosion rates from Be and Al measurements. *Quaternary Geochronology*, **3**, 174-195.
- Balco G., Schaefer J.M., LARISSA group., 2013. Exposure-age record of Holocene ice sheet and ice shelf change in the northeast Antarctic Peninsula. *Quaternary Science Reviews*. **59**, 101-111.
- Ballantyne, C.K., Stone, J.O.H., and Fifield, L.K., 1998. Cosmogenic Cl-36 dating of postglacial landsliding at The Storr, Isle of Skye, Scotland. *The Holocene*, **8**, 347-351.
- Ballantyne, C.K., Stone, J.O.H., and Fifield, L.K., 2009. Glaciation and deglaciation of the SW Lake District, England: implications of cosmogenic ³⁶Cl exposure dating, *Proceedings of the Geologists' association*, **120**, 139-144.
- Ballantyne, C.K., and Stone, J.O., 2013. Timing and periodicity of paraglacial rock-slope failures in the Scottish Highlands. *Geomorphology*, **186**, 150-161.

- Benito, G., Sancho, C., Peña, J.L., Machado, M.J., and Rhodes, E.J., 2010. Large-scale karst subsidence and accelerated fluvial aggradation during MIS6 in NE Spain: climatic and palaeohydrological implications. *Quaternary Science Reviews*, **29**, 2694-2704.
- Biermann, C. 1995. The Betic Cordilleras SE Spain. Anatomy of a dualistic collision-type orogenic belt. *Geologie en Mijnbouw*, **74**, 167-182.
- Birkeland, P.W. 1999. *Soils and geomorphology*. Third edition. Oxford University Press, Oxford, 430 pp.
- Blum, A.J. 2009. Controls on long-term drainage development of the Carboneras Basin, SE Spain. The University of Plymouth, Unpublished PhD Thesis.
- Blum, M. D and Törnqvist, T. E., 2000. Fluvial responses to climate and sea-level change: a review and look forward. *Sedimentology*, **47**, 2-48.
- Blumenthal, M. 1927. Versuch einer tektonischen Gliederung der betischen Cordilleren von Central- und Südwest- Andalusien. *Eclogae geol. Helv.* **20**, 487-532.
- Booth-Rea, G., Azan, J.M., Azor, A and Garcia-Duen, V., 2004. Influence of strike-slip fault segmentation on drainage evolution and topography. A case study: the Palomares Fault Zone (southeastern Betic, Spain). *Journal of Structural Geology*, **26**, 1615-1632.
- Braga, J.C. and Martin, J.M., 1997. Evolución paleogeográfica de la Cuenca de Sorbas y relieves adyacentes (Almería SE España) en el Mioceno superior. In: Calvo, J.P and Morales, J., (eds). *Avances en el Conocimiento del Terciario Ibérico*, Universidad Complutense de Madrid-Museo Nacional Ciencias Naturales, Spain, pp. 61-64.

- Braga, J.C., Martin, J.M. and Quesada, C., 2003. Patterns and average rates of late Neogene- recent uplift of the Betic Cordillera, SE Spain. *Geomorphology*, **50**, 3-26.
- Braucher, R., Bourlès, D., Merchel, S., Vidal Romani, J., Fernandez-Mosquera, D., Marti, K., Léanni, L., Chauvet, F., Arnold, M., Aumaître, G and Keddadouche, K., 2013. Determination of muon attenuation lengths in depth profiles from in situ produced cosmogenic nuclides, *Nuclear Instruments and Methods in Physics Research Section B: Beam Interactions with Materials and Atoms*, **294**, 484-490
- Bridge, J.S. 1993. The interaction between channel geometry, water flow, sediment transport and deposition in braided rivers. In: J.L. Best and C.S. Bristow, (Eds). *Braided Rivers, Special Publication of the Geological Society of London*, **75**, 13–71.
- Bridgland, D.R. (ed) 1986. *Clast lithological analysis*. Quaternary Research Association, Technical Guide, no.3, QRA London.
- Bridgland, D. R. 2000. River terrace systems in north-west Europe: an archive of environmental change, uplift and early human occupation. *Quaternary Science Reviews*, **19**, 1293-1303.
- Bridgland, D.R, Keen, D., and Westaway, R., 2007. Global correlation of Late Cenozoic fluvial deposits: a synthesis of data from IGPC 449, *Quaternary Science Reviews*, **26**, 22-24, Global correlation of Late Cenozoic fluvial deposits: IGPC Project No. 449, November 2007, 2694-2700.
- Bridgland, D.R, and Maddy, D., 2002. Global correlation of long Quaternary fluvial sequences: a review of baseline knowledge and possible methods and criteria for establishing a database. *Geologie en Mijnbouw*, **81**, 265-281.

- Bridgland, D.R and Westaway, R., 2008. Climatically controlled river terrace staircases: A worldwide Quaternary phenomenon. *Geomorphology*, **98**, 285-315.
- Bull, W.E. 1991. Geomorphic responses to climatic change. Oxford University Press, Oxford, 326 pp.
- Bull, W.B. 2009. Geomorphic responses to climate change. Blackburn Press, New Jersey. 326 pp.
- Burbank, D.W and Anderson, R.S., 2001. Tectonic Geomorphology. Blackwell Science Ltd, Oxford. 274 pp.
- Buylaert, J.-P., Jain, M., Murray, A.S., Thomsen, K.J., Thiel, C., Sohbati, R., 2012. A robust feldspar luminescence dating method for Middle and Late Pleistocene sediments. *Boreas*. **41**, 435-451.
- Calaforra, J.M. and Pulido-Bosch, A., 1997. Peculiar landforms in the gypsum karst of Sorbas (Southeast Spain). *Carbonates and Evaporites*, **12**, 110-116.
- Calaforra, J.M. and Pulido-Bosch, A., 2003. Evolution of the gypsum karst of Sorbas (SE Spain). *Geomorphology*, **50**, 173-180.
- Calvos-Cases, A., Harvey, A.M and Paya-Serrano, J., 1991. Process interactions and badland development in SE Spain. In: Sala, M., Rubio, J.L and Garcia-Ruiz, J.M. (Eds), *Soil Erosion Studies in Spain*, Geoforma Ediciones, Logroño, Spain, 75-90.
- Candy, I., Black, S and Sellwood, B.W., 2004. Interpreting the response of a dryland river system to Late Quaternary climate change. *Quaternary Science Reviews*, **23**, 2513-2523.

- Candy, I., Black, S and Sellwod, B.W., 2005. U-series isochron dating of immature and mature calcretes as a basis for constructing Quaternary landforms chronologies for the Sorbas basin, southeast Spain. *Quaternary Research*, **64**, 100-111.
- Chilton, S., Faulkner, H., & Zukowskyj, P., 2008. Moderating accurate topographic EDM survey with expert-derived planimetric geomorphological information: a case study mapping soil pipes, Mocatan, SE Spain. *Journal of Maps*, **4**, 248-257.
- Clarke, A.O. 1996. Estimating probable maximum floods in Upper Santa Ana Basin, Southern California, from stream boulder size. *Environmental and Engineering Geoscience*, **2**, 165-182.
- Cloetingh, S., Van Der Beek, P.A., Van Rees, D., Roep, T.B., Biermann, C and Stephenson, R.A., 1992. Flexural interaction and dynamics of Neogene extensional basin formation in the Alboran-Betic region. In: Maldonado, A. (Ed.), Alboran Basin Special Issue. *Geo-Marine Letters*, **12**, 66-75.
- Cook, K.L., Whipple, K., Heimsath, A.M., Hanks, T.C., 2009. Rapid incision of the Colorado River in Glen Canyon-insights from channel profiles, local incision rates, and modelling of lithologic controls. *Earth Surface Processes and Landforms*, **34**, 994-1010.
- Cockburn, H, and Summerfield, M.A., 2004. Geomorphological applications of cosmogenic isotope analysis. *Progress in Physical Geography*, **28**, 1-42.
- Collins, A.L., Walling, D.E., and Leeks, G.J.L., 1998. Use of composite fingerprints to determine the provenance of the contemporary suspended sediment load transported by rivers. *Earth Surface Processes and Landforms*, **23**, 31-52.
- Cordier, S., Harmand, D., Lauer, T., Voinchet, P., Bahain, J. J., & Frechen, M., 2012. Geochronological reconstruction of the Pleistocene evolution of the Sarre valley

- (France and Germany) using OSL and ESR dating techniques. *Geomorphology*, **165**, 91-106.
- Costa, J.E. 1983. Paleohydraulic reconstruction of flash flood peaks from boulder deposits in the Colorado Front Range. *Geological Society of America Bulletin*, **94**, 986-1004.
- Dabrio, C.J., Esteban, M., and Martín, J.M. 1981., The coral reef of Níjar, Messinian (Uppermost Miocene), Almería province, SE Spain. *Journal of sedimentary petrology*, **51**, 521-539.
- Dawson, M.R., and Gardiner, V., 1987. The general model and a palaeohydrological and sedimentological interpretation of the terraces of the Lower Severn. In: Gregory, K.J., Lewin, J., Thornes, J.B. (Eds.), *Palaeohydrology in Practice. A River Basin Analysis*. John Wiley and Sons Ltd., PP269-305.
- Dronkert, H., 1976. Late Miocene evaporates in the Sorbas Basin and adjoining areas. *Memorie della Societa geologica Italiana*, **16** 341-361.
- Dunne, J., Elmore, D. and Muzikar, P., 1999. Scaling factors for the rates of production of cosmogenic nuclides for geometric shielding and attenuation at depth on sloped surfaces. *Geomorphology* , **27**, 3-11.
- Dunai, T.J. 2010. *Cosmogenics nuclides: Principles, concepts and applications in the Earth surface sciences*. Cambridge University Press, Cambridge. 187 pp.
- Egeler, C.G. 1963. On the tectonics of the eastern Betic Cordilleras. *Geologische Rundschau*, **53**, 260-269.

- Egeler, C.G and Simon, O.J., 1969. Orogenic evolution of the Betic Zone (Betic Cordilleras, Spain), with emphasis on the nappe structures. *Geologie en Mijnbouw*, **48**, 296-305.
- Evenstar, L.A., Hartley, A.J., Stuart, F.M., Mather, A.E., Rice, C.M. and Chong, G., 2009. Multiphase development of the Atacama Planation Surface recorded by cosmogenic He-3 exposure ages: Implications for uplift and Cenozoic climate change in Western South America. *Geology*, **37**, 27-30.
- Fallot, P. 1948. Los Cordilleres Betiques. *Estud.Geol.*, **8**, 83-172.
- Faulkner, H., Spivey, D. and Alexander, R., 2000. The role of some site geochemical processes in the development and stabilisation of three badland sites in Almeria, Southern Spain. *Geomorphology*, **35**, 87-99.
- Faulkner, H., Ruiz, J., Zukowskyj, P and Downward, P., 2003. Erosion risk associated with rapid and extensive agricultural clearances on dispersive materials in southeast Spain, *Environmental Science and Policy*, **6**, 115-127.
- Fenton, C.R., Mark, D.F., Barfod, D.N., Niedermann, S., Goethals, M.M., Stuart, F.M., 2013. $^{40}\text{Ar}/^{39}\text{Ar}$ dating of the SP and Bar Ten lava flows AZ, USA: Laying the foundation for the SPICE cosmogenic nuclide production-rate calibration project. *Quaternary Geochronology*, <http://dx.doi.org/10.1016/j.quageo.2013.01.007>.
- Fenton, C. R., & Niedermann, S., 2012. Surface exposure dating of young basalts (1-200 ka) in the San Francisco volcanic field (Arizona, USA) using cosmogenic ^3He and ^{21}Ne . *Quaternary Geochronology*. <http://dx.doi.org/10.1016/j.quageo.2012.10.003>
- Friedlander, M.W. 1989. *Cosmic Rays*, Harvard University Press, Cambridge. 160 pp.

- Friend, P. F., Slater, M. J., & Williams, R. C., 1979. Vertical and lateral building of river sandstone bodies, Ebro Basin, Spain. *Journal of the Geological Society*, **136**, 39-46.
- Gábris, G., and Nádor, A., 2007. Long term fluvial archives in Hungary: response of the Danube and Tisza rivers to tectonic movements and climate changes during the Quaternary. *Quaternary Science Reviews*, **19**, 667-685.
- García, A. F., Zhu, Z., Ku, T. L., Chadwick, O. A., and Chacón Montero, J., 2004. An incision wave in the geologic record, Alpujarran Corridor, southern Spain (Almería). *Geomorphology*, **60**, 37-72.
- Giaconia, F., Booth-Rea, G., Martínez-Martínez, J. M., Azañón, J. M., Pérez-Peña, J. V., Pérez-Romero, J., & Villegas, I., 2012. Geomorphic evidence of active tectonics in the Sierra Alhamilla (eastern Betics, SE Spain). *Geomorphology*, **145**, 90-106.
- Giaconia, F., Booth-Rea, G., Miguel Martínez-Martínez, J., Miguel Azañón, J., Pérez-Romero, J., & Villegas, I., 2013. Mountain front migration and drainage captures related to fault segment linkage and growth: The Polopos transpressive fault zone (southeastern Betics, SE Spain). *Journal of Structural Geology*. **46**, 76-91.
- Gibbard, P. L and Lewin, J., 2002. Climate and related controls on interglacial fluvial sedimentation in lowland Britain. *Sedimentary Geology*, **151**, 187-210.
- Gibbard, P. L and Lewin, J., 2009. River incision and terrace formation in the late Cenozoic of Europe. *Tectonophysics*, **474**, 41-55.
- Gillen, D., Honda, M., Chivas, A.R., Yatsevich, I., Patterson, D.B., and Carr, P.F., 2010. Cosmogenic ²¹Ne exposure dating of young basaltic lava flows from the

- Newer Volcanic Province, western Victoria, Australia. *Quaternary Geochronology*, **5**, 1-9.
- Giménez, J., Suriñach, E., and Goula, X., 2000. Quantification of vertical movements in the eastern Betics (Spain) by comparing levelling data. *Tectonophysics*, **317**, 237-258
- Glasser, N.F., Hughes, P.D., Fenton, C., Schnabel, C., and Rother, H., 2012. ^{10}Be and ^{26}Al exposure-age dating of bedrock surfaces on the Aran ridge, Wales: evidence for a thick Welsh ice cap at the Last Glacial Maximum. *Journal of Quaternary Science*, **27**, 94-104.
- Granger, D. E., & Muzikar, P. F., 2001. Dating sediment burial with in situ-produced cosmogenic nuclides: theory, techniques, and limitations. *Earth and Planetary Science Letters*, **188**, 269-281.
- Gressly, A. 1838. Observations géologiques sur le Jura soleurais. *Neue Denkschr Allg Schweizerische Gesellsch ges. Naturw*, **2**, 1-112.
- Griffiths, J.S., Hart, A.B., Mather, A.E and Stokes, M., 2005. Assessment of some spatial and temporal issues in landslide initiation within the Río Aguas catchment, south-east Spain. *Landslide*, **2**, 183-192.
- Griffiths, J. S., Mather, A. E. and Hart, A. B., 2002. Landslide susceptibility in the Río Aguas catchment, SE Spain. *Quarterly Journal of Engineering Geology and Hydrogeology*, **35**, 9-17.
- Grün, R. 1989. Electron spin resonance (ESR) dating. *Quaternary International*, **1**, 65-109.

- Gomez-Pugnaire, M. 2001. The basement geology of the Almeria province, In: Mather, A.E., Martín, J.M., Harvey, A.M., and Braga, J.C. (eds), *A Field Guide to the Neogene Sedimentary Basins of the Almería Province, SE Spain*. Blackwell Science Ltd, Oxford, 33-46.
- Gosse, J.C., and Phillips, F.M. 2001. Terrestrial in situ cosmogenic nuclides: theory and application. *Quaternary Science Reviews*, **20**, 1475-1560.
- Haq, B.U., Hardenbol, J. and Vail, P.R., 1988. Mesozoic and Cenozoic chronostratigraphy and cycles of sea-level change. In: Wilgus, C.K., Hasting, B.S., Kendall, C.G.St.C., Posamentier, H.W., Ross, C.A. and Van Wagoner, J.C. (Eds), *Sea-level Changes: an integrated approach*, Special publication, Society of Economic Paleontologists and Mineralogists (SEPM), Tulsa, **42**, 71-108.
- Hart, A.B. 1999. *An introduction to the landslides of the Sorbas Basin*. In: Mather A.E, Stokes, M. (Eds), BSRG/BGRG SE Spain Field Meeting: Field Guide. University of Plymouth, pp 124-133.
- Hart, A.B. 2004. Landslide investigations in the Río Aguas catchment, Southeast Spain. Unpublished PhD Thesis, University of Plymouth.
- Hart, A.B and Griffiths, J.S., 1999. Mass movement features in the vicinity of the town of Sorbas, South-east Spain. In: Griffiths, J.S., Stokes, M.R and Thomas, R.G. (Eds), *Landslides: Proceedings of the Ninth International Conference and Field Trip on Landslides*, Bristol, UK, 5-16th September 1999, A.A. Balkema, Rotterdam, 57-63.
- Hart, A. B., Griffiths, J. S., & Mather, A. E., 2009. Some limitations in the interpretation of vertical stereo photographic images for a landslide

investigation. *Quarterly Journal of Engineering Geology and Hydrogeology*, **42**, 21-30.

Harvey, A.M. 2001. Uplift, dissection and landform evolution: the Quaternary. In: Mather, A.E., Martín, J.M., Harvey, A.M., and Braga, J.C. (eds), *A Field Guide to the Neogene Sedimentary Basins of the Almería Province, SE Spain*. Blackwell Science Ltd, Oxford, 33-46.

Harvey, A. M. 2007. High sinuosity bedrock channels: response to rapid incision: Examples in se Spain. *Revista de Cuaternario y Geomorfología*, **21**, 21-47.

Harvey, A and Wells, S., 1987. Response of Quaternary fluvial systems to differential epeirogenic uplift: Aguas and Feos river systems, southeast Spain. *Geology*, **15**, 689-693.

Harvey, A.M., Miller, S.Y and Wells, S.G., 1995. Quaternary soil and river terrace sequences in the Aguas/Feos river systems: Sorbas Basin, Southeast Spain. In: Lewin, J., Macklin, M.G and Woodward, J.C. (Eds), *Mediterranean Quaternary River Environments*, A.A. Balkema, Rotterdam, 65-76.

Hodge, E. J., Richards, D. A., Smart, P. L., Andreo, B., Hoffmann, D. L., Matthey, D. P., & González-Ramón, A., 2008. Effective precipitation in southern Spain (~ 266 to 46 ka) based on a speleothem stable carbon isotope record. *Quaternary Research*, **69**, 447-457.

Hodgson, D.M. 2002. *Tectono-stratigraphic evolution of a Neogene oblique extensional orogenic basin, southeast Spain.*, Unpublished PhD thesis, University College London, London

- Hancock, G.S., Anderson, R.S., Chadwick, O.A. and Finkel, R.C., 1999. Dating fluvial terraces with ^{10}Be and ^{26}Al profiles: application to the Wind River, Wyoming. *Geomorphology*, **27**, 41-60.
- Hein, F. J., & Walker, R. G., 1977. Bar evolution and development of stratification in the gravelly, braided, Kicking Horse River, British Columbia. *Canadian Journal of Earth Sciences*, **14**, 562-570.
- Hellborg, R. and Skog, G., 2008. Accelerator Mass Spectrometry. *Mass Spectrometry Reviews*, **27**, 398-427.
- Huibregtse, P., Van Alebeek, H., Zaal, M and Biermann, C., 1998. Palaeostress analysis of the northern Níjar Basin and southern Vera basins: constraints for the Neogene displacement history of major strike-slip faults in the Betic Cordilleras, SE Spain. *Tectonophysics*, **300**, 79-101.
- Hurst, V.J. 1977. Visual estimates of iron in saprolite. *Bulletin Geological Society of America*, **88**, 174-176.
- Hsü, K.J., Cita, N.B and Ryan, W.B.F., 1972. The origin of the Mediterranean evaporates. *Initial Reports of the Deep Sea Drilling Project (DSDP)*, **XIII**, pt.2, 695-708.
- Jones, A.P. 1999. Background to sedimentary facies, In: The description and analysis of Quaternary stratigraphic field sections. Technical guide 7. Quaternary Research Association, London, 5-62.
- Keller, J.V.A., Hall, S.H., Dart, C.J and McClay, K.R., 1995. The geometry and evolution of a transpressional strike-slip system-the Carboneras Fault, SE Spain. *Journal of the Geological Society*, **152**, 339-351.

- Keller, E.V and Pinter, N., 2000. Active tectonics: earthquakes, uplift & landscape. 2nd edition. Prentice Hall, Upper Saddle River, 338 pp.
- Kelly, M., Black, S., & Rowan, J. S., 2000. A calcrete-based U/Th chronology for landform evolution in the Sorbas Basin, Southeast Spain. *Quaternary Science Reviews*, **19**, 995-1010.
- Knight, J., Wishart, A.M., and Rose, J., 2011. Geomorphological field mapping. In: Smith, M., Paron, P., and Griffiths, J., (eds). Geomorphological mapping- Methods and applications. *Developments in Earth Surface Processes*, **15**, 1-612.
- Kohl, C. P. and Nishiizumi, K., 1992. Chemical isolation of quartz for measurement of in situ produced cosmogenic nuclides. *Geochimica et Cosmochimica Acta*. **56**, 3583-3587.
- Kozaci, O., Dolan, J., Finkel, R., and Hartleb, R., 2007. Late Holocene slip rate for the North Anatolian fault, Turkey, from cosmogenic ³⁶Cl geochronology: Implications for the constancy of fault loading and strain release rates. *Geology*, **35**, 867-870.
- Krijgsman, W., Fortuin, A.R., Hilgen, F.J and Sierro, F.J., 2001. Astrochronology for the Messinian Sorbas Basin (SE Spain) and orbital (precessional) forcing for evaporate cyclicity. *Sedimentary Geology*, **140**, 43-60.
- Lal, D. 1991. Cosmic ray labelling of erosion surfaces: in situ nuclide production rates and erosion models. *Earth and Planetary Science Letters*, **104**, 424 – 439.
- Larouzière, F.D.De., Bolze, J., Bordet, P., Hernandez, J., Monenat, C and Ott D'Estevou, P., 1988. The Betic segment of the lithospheric Tran-Alboran shear zone during the late Miocene. *Tectonophysics*, **152**, 41-52.

- Leopold, L.B and Bull, W.B., 1979. Base level, aggradation, and grade. *Proceedings of the American Philosophical Society*, **123**, 168-202.
- Leopold, L.B., and Miller, J.P., 1954. A postglacial chronology for some alluvial valleys in Wyoming. Geological Survey Water Supply Paper 1261. United States Government printing office, Washington, 90 pp.
- Leopold, L.B., Wolman, M and Miller, J.P., 1964. Fluvial processes in Geomorphology. Freeman, San Francisco. 522 pp.
- Lewin, J and Gibbard, P. L., 2010. Quaternary river terraces in England: Forms, sediments and processes. *Geomorphology*, **120**, 293-311.
- Lifton, N., Smart, D. and Shea, M., 2008. Scaling time integrated in situ cosmogenic nuclides production rates using a continuous geomagnetic model. *Earth and Planetary Science letters*, **268**, 190-201.
- Lisiecki, L. E and Raymo, M.E., 2005. A Pliocene- Pleistocene stack of 57 globally distributed benthic δ 18O records. *Paleoceanography*, **20**.
- Maddy, D. 1997. Uplift-driven valley incision and river terrace formation in southern England. *Journal of Quaternary Science*, **12**, 539-545.
- Machette, M.N. 1985. Calcic soils within the southwestern United States. In: Weide, D.L (ed), Soils and Quaternary geology in the southwestern United States, special paper, *Geological Society of America*, **203**.
- Maher, E. 2006. *The Quaternary evolution of the Río Alias southeast Spain, with emphasis on sediment provenance*. PhD thesis, University of Liverpool.

- Maher, E. and Harvey, A.M., 2008. Fluvial system response to tectonically induced base-level change during the late-Quaternary: The Rio Alias southeast Spain. *Geomorphology*, **100**, 180-192.
- Maher, E., Harvey, A.M and France, D., 2007. The impact of a major Quaternary river capture on the alluvial sediments of a beheaded river system, the Río Alias SE Spain. *Geomorphology*, **84**, 334-356.
- Maill, A.D. 1996. The Geology of Fluvial Deposits: Sedimentary Facies, Basin analysis and Petroleum Geology. Springer-Verlag Berlin, 582 pp.
- Martín, J.M., Braga, J.C. and Sánchez-Almazo, I.M., 1999. The Messinian record of the outcropping marginal Alborán Basin deposits: significance and implications. *Proceedings of the ODP, Scientific Results*, **161**, PP. 543-551. Ocean Drilling Program, Collage Station, TX.
- Martín, J.M. and Braga, J.C., 2001. Shallow Marine Sedimentation. In: Mather, A.E., Martín, J.M., Harvey, A.M., and Braga, J.C. (eds), *A Field Guide to the Neogene Sedimentary Basins of the Almería Province, SE Spain*. Blackwell Science Ltd, Oxford, 33-46.
- Martín, J.M., Braga, J.C. and Betzler, C., 2003. Late Neogene-recent uplift of the Cabo de Gata volcanic province, Almería, SE Spain. *Geomorphology*, **50**, 27-42.
- Martín-Suárez, E., Freudenthal, M., Krijgsman, W. and Rutger Fortuin, A., 2000. On the age of the continental deposits of the Zorreras Member (Sorbas Basin, SE Spain). *Geobios*, **33**, 505-512.
- Mather, A.E. 1991. *Late Cenozoic drainage evolution of the Sorbas Basin, southeast Spain*. Unpublished PhD Thesis, University of Liverpool, 276 pp.

- Mather, A.E. 1993a. Basin inversion: Some consequences for drainage evolution and alluvial architecture. *Sedimentology*, **40**, 1069-1089.
- Mather, A.E. 1993b. Evolution of a Pliocene fan delta: links between the Sorbas and Carboneras Basins, SE Spain. In: Forstick, L and Steel, R (Eds), *Tectonic controls and signatures in sedimentary successions*. International Association of Sedimentologists, Special Publication, **20**, 277-290.
- Mather, A.E. 2000. Adjustments of a drainage network to capture induced base-level change: an example from the Sorbas Basin, SE Spain. *Geomorphology*, **34**, 271-289.
- Mather, A.E. 2009. Tectonic setting and landscape development. In: Woodward, J.C. (Ed.), *The physical geography of the Mediterranean*. Oxford University Press, Oxford, pp.532.
- Mather, A. E., Griffiths, J. S. and Stokes, M., 2003. Anatomy of a "fossil" landslide from the Pleistocene of SE Spain. *Geomorphology*, **50**, 135-149.
- Mather, A.E, and Hartley, A., 2005. Flow events on a hyper-arid alluvial fan: Quebrada Tambores, Salar de Atacama, northern Chile. In Harvey, A.M., Mather, A.E., Stokes, M. (Eds.), *Alluvial Fans: Geomorphology, Sedimentology, Dynamics*. Geological Society, London, Special Publications, 251, pp.9-24.
- Mather, A.E, and Harvey, A., 1995. Controls on drainage evolution in the Sorbas basin, southeast Spain. In: Lewin, J., Macklin, M and Woodward, J., (Eds) *Mediterranean quaternary river environments*. Balkema, Rotterdam, 65-76.
- Mather, A.E., Martín, J.M., Harvey, A.M., and Braga, J.C. (eds). 2001. *A Field Guide to the Neogene Sedimentary Basins of the Almería Province, SE Spain*. Blackwell Science Ltd, Oxford, 33-46.

- Mather, A.E and Stokes, M., 2001. Marine to Continental Transition. In: Mather, A.E., Martín, J.M., Harvey, A.M., and Braga, J.C. (eds), *A Field Guide to the Neogene Sedimentary Basins of the Almería Province, SE Spain*. Blackwell Science Ltd, Oxford, 33-46.
- Mather, A.E., Stokes, M., and Griffiths, J.S., 2002. Quaternary landscape evolution: a framework for understanding contemporary erosion, southeast Spain. *Land Degradation & Development*, **13**, 89-109.
- Mather, A. E., & Westhead, K., 1993. Plio/Quaternary strain of the Sorbas Basin, SE Spain: evidence from soft sediment deformation structures. *Quaternary Proceedings*, **3**, 57-65.
- Mazo, A.V. 1999. Vertebrados fósiles del Campo de Calatrava (Ciudad Real). In: Aguirre, E., Ra'bano, I. (Eds.), *La huella del pasado. Fósiles de Castilla-La Mancha. Patrimonio Histórico-Arqueología Castilla-La Mancha*, Toledo, pp. 281–291.
- Meikle, C.D. 2009. The Pleistocene drainage evolution of the Río Almanzora, Vera basin, SE Spain. Unpublished PhD thesis, University of Newcastle, UK. 210 pp.
- Meikle, C., Stokes, M., and Maddy, D., 2010. Field mapping and GIS visualisation of Quaternary river terrace landforms: an example from the Río Almanzora, SE Spain. *Journal of maps*, **6**, 531-542.
- Montenat, C., Ott D'Estevou, P and Masse, P., 1987. Tectonic sedimentary characters of the Betic Neogene basins evolving in a crustal transcurrent shear zone (SE Spain). *Bulletin Centres Recherches Exploration-Production Elf Aquitaine Pau*, **11**, 1-22.

- Montenat, C. and Ott D'Estevou, P., 1999. The diversity of Late Neogene sedimentary basins generated by wrench faulting in the eastern Betic Cordillera, southeast Spai. *Journal of Petroleum Geology*, **22**, 61-80.
- Nash, D.J., and Smith, R.F., 2003. Properties and development of channel calcretes in a mountain catchment, Tabernas Basin, southeast Spain, *Geomorphology*. **50**, 227–250.
- Nissen, E., Walker, R. T., Bayasgalan, A., Carter, A., Fattahi, M., Molor, E., Schnabel, C., West, A. J. and Xu, S., 2009. The late Quaternary slip-rate of the Har-Us-Nuur fault (Mongolian Altai) from cosmogenic ¹⁰Be and luminescence dating. *Earth and Planetary Science Letters*, **286**, 467-478.
- Olszak, J. 2011. Evolution of fluvial terraces in response to climatic change and tectonic uplift during the Pliestocene: Evidence from Kamienica and Ochotnica River valleys (Polish Outer Carpathians). *Geomorphology*, **129**, 71-78.
- Ott D'Estevou, P. 1980. *Evolution dynamique du bassin Néogène de Sorbas (Cordillères Bétiques Orientales, Espagne)*. PhD Thesis, Université Paris VII, Denis-Diderot, 264 pp.
- Pagnier, H. 1976. Depth of deposition of Messinian selentic gypsum in the Basin of Sorbas (SE Spain). *Memorie della Societa geologica italiana*, **16**, 363-367.
- Pedrera, A., Pérez-Peña, J.V., Galindo-Zaldívar, J., Azañón, J.M and Azor, A., 2009. Testing the sensitivity of geomorphic indices in areas of low-rate active folding (eastern Betic Cordillera, Spain). *Geomorphology*, **105**, 218-231.
- Pérez-Peña, J. V., Azor, A., Azañón, J. M., and Keller, E. A., 2010. Active tectonics in the Sierra Nevada (Betic Cordillera, SE Spain): Insights from geomorphic indexes and drainage pattern analysis. *Geomorphology*, **119**, 74-87.

- Pla-Pueyo, S., Gierlowski-Kordesch, E.H., Viseras, C and Soria, J.M., 2009. Major controls on sedimentation during the evolution of a continental basin: Pliocene-Pleistocene of the Guadix Basin (Betic Cordillera, southern Spain). *Sedimentary Geology*, **219**, 97-114.
- Reading, H.G. 2004. *Sedimentary Environments: Processes, Facies and Stratigraphy*, Third Edition, Blackwell Science, Oxford, 704 pp.
- Repka, J.L., Anderson, R.S., and Finkel, R.C., 1997. Cosmogenic dating of fluvial terraces, Fremont River, Utah. *Earth and Planetary Science Letters*, **152**, 59-73.
- Rodés, A., Pallàs, R., Braucher, R., Moreno, X., Masana, E., Bourles, D. L., 2011. Effect of density uncertainties in cosmogenic ¹⁰Be depth-profiles: Dating a cemented pleistocene alluvial fan (carboneras fault, se iberia). *Quaternary Geochronology*, **6**, 186 – 194.
- Rinterknecht, V., Braucher, R., Böse, M., Bourlès, D., and Mercier, J.L., 2012. Late Quaternary ice sheet extents in northeastern Germany inferred from surface exposure dating, *Quaternary Science Reviews*, **44**, 89-95.
- Ruegg, G.J.H. 1964. *Geologische Onderzoekingen in Het Bekken Van Sorbas, S Spanje*. Unpublished M.S.c Thesis, Municipal University of Amsterdam, 67 pp.
- Ruiz-Constán, A., Stich, D., Galindo-Zaldívar, J and Morales, J., 2009. Is the northwestern Betic Crdillera mountain front active in the context of the convergent Eurasia-Africa plate boundary? *Terra Nova*, **21**, 352-359.
- Rutter, E.H., Faulkner, D.R and Burgess, R., 2012. Structure and geological history of the Carboneras Fault Zone, SE Spain: Part of a stretching transform fault system. *Journal of structural geology*, **45**, 68-86.

- Santisteban, J. I., & Schulte, L., 2007. Fluvial networks of the Iberian Peninsula: a chronological framework. *Quaternary Science Reviews*, **26**, 2738-2757.
- Sanz de Galdeano, C. 1987. Strike-slip faults in the Southern border of the Vera basin (Almería, Betic Cordilleras). *Estudios Geológicos*, **43**, 435-443.
- Sanz de Galdeano, C. 1990. Geologic evolution of the Betic Cordilleras in the western Mediterranean, Miocene to the present. *Tectonophysics*, **172**, 107-119.
- Sanz de Galdeano, C and Vera, J.A., 1992. Stratigraphic record and palaeogeographical context of the Neogene basins in the Betic Cordillera, Spain. *Basin Research*, **4**, 21-36.
- Sanz de Galdeano, C., Shanov, S., Galindo-Zaldívar, J., Radulov, A., and Nikolov, G., 2010. A new tectonic discontinuity in the Betic Cordillera deduced from active tectonics and seismicity in the Tabernas Basin. *Journal of Geodynamics*, **50**, 57-66.
- Schulte, L. 2002. Climatic and human influence on river systems and glacier fluctuations in southeast Spain since the Last Glacial Maximum. *Quaternary International*, **93**, 85-100.
- Schulte, L., Julia, R., Burjachs, F and Hilgers, A., 2008. Middle Pliocene to Holocene geochronology of the River Aguas terrace sequence (Iberian Peninsula): Fluvial response to Mediterranean environmental change. *Geomorphology*, **98**:13-33.
- Schumm, S., Dumont, J., and Holbrook, J., 2002. Active tectonics and alluvial rivers. Cambridge University Press. Cambridge. 277 pp

Shulmeister, J., Fink, D., Hyatt, O.M., Thackray, G.D., and Rother, H., 2010.

Cosmogenic ^{10}Be and ^{26}Al exposure ages of moraines in the Rakaia Valley, New Zealand and the nature of the last termination in New Zealand glacial systems. *Earth and Planetary Science Letters*, **297**, 558-566.

Siame, L., Bellier, O., Braucher, R., Sébrier, M., Cushing, M., Bourlès, D., Hamelin, B., Baroux, E., de Voogd, B., Raisbeck, G., Yiou, F., 2004. Local erosion rates versus active tectonics: cosmic ray exposure modelling in Provence (south-east France). *Earth Planetary Science Letters*, **220**, 345–364.

Smith, A.G., and Woodcock, N.H., 1982. Tectonic synthesis of the Alpine-Mediterranean region: A review. In: Berckhemer, H and Hsü, K. (Ed.), Alpine-Mediterranean geodynamics, *American Geophysical Union Geodynamics Series*, **7**, 15-38.

Spivey, D. 1997. *Scale, process and badland development in the Almeria Province*. Unpublished PhD thesis, University of Liverpool.

Stapel, G., Moeys, R. and Biermann, c., 1996. Neogene evolution of the Sorbas Basin (SE Spain) determined by paleostress analysis. *Tectonophysics*, **255**, 291-305.

Starkel, L. 2003. Climatically controlled terraces in uplifting mountain areas. *Quaternary Science Reviews*, **22**, 2189-2198.

Stokes, M. 1997. *Plio-Pleistocene drainage evolution of the Vera Basin, SE Spain*. Unpublished PhD Thesis, University of Plymouth, 390 pp.

Stokes, M. 2008. Plio-Pleistocene drainage development in an inverted sedimentary Basin: Vera Basin, Betic Cordillera, SE Spain. *Geomorphology*, **100**, 193-211.

- Stokes, M., Cunha, P and Martins, A., 2012 (a). Techniques for analysing Late Cenozoic river terrace sequences. *Geomorphology*, **165-166**: 1-6.
- Stokes, M., Mather, A.E and Harvey, A.M., 2002. Quantification of river-capture-induced base level changes and landscape development, Sorbas Basin, SE Spain. *Geological Society, London, Special Publications*. **191**, 23-35.
- Stokes, M., Griffiths, J and Mather, A., 2012(b). Palaeoflood estimates of Pleistocene coarse grained river terrace landforms (Río Almanzora, SE Spain). *Geomorphology*, **149-150**:11-26
- Stokes, M., & Mather, A. E., 2000. Response of Plio-Pleistocene alluvial systems to tectonically induced base-level changes, Vera Basin, SE Spain. *Journal of the Geological Society*, **157**, 303-316.
- Stokes, M. and Mather, A.E., 2003. Tectonic origin and evolution of a transverse drainage: the Río Almanzora, Betic Cordillera, Southeast Spain. *Geomorphology*, **50**, 59-81.
- Stone, J. O., Allan, G. L., Fifield, L. K. and Cresswell, R. G., 1996. Cosmogenic chlorine-36 from calcium spallation. *Geochimica et Cosmochimica Acta*, **60**, 679–692.
- Torres, T., Cobo, R., Garcia Cortes, A., Hoyos, M., Garcia Alonso, P., 1994b. Cronoestratigrafia de los depositos fluviokarsticos del Cerro dela Oliva (Patones, Madrid). *Geogaceta*, **15**, 90–93.
- Trochim, W. 2006. The Research Methods Knowledge Base, 2nd Edition. Internet www page at URL : > <http://www.socialresearchmethods.net/kb/dedind.php> (Last accessed 4th June 2013).

- Troelstra, S.R., Van de Poel, H.M., Huisman, C.H.A., Geerlings, L.P.A and Dronkert, H., 1980. Palaeoecological changes in the latest Miocene of the Sorbas Basin, SE Spain. *Géologie Méditerranéenne*, **7**, 115-126.
- Tucker, M.E. 1996. Sedimentary rocks in the field. Second edition. J. Wiley and Sons, Chichester, 153 pp.
- Tucker, M.E. 2003. Sedimentary rocks in the field. Third Edition. John Wiley and Sons, Chichester, 234 pp.
- Tubía, J.M., Cuevas, J., Navarro-Vila, F., Álvarez, F and Aldaya, F., 1992. Tectonic evolution of the Alpujarride complex (Betic Cordilleras, southern Spain). *Journal of Structural Geology*, **14**, 193-203.
- Twidale, C.R. 2004. River patterns and their meaning. *Earth Science Reviews*, **67**, 159-218.
- Tyráček, J., and Havlíček, P., 2009. The fluvial record in the Czech Republic: A review in the context of IGCP 518. *Global and Planetary change*, **68**, 311-325.
- Tzedakis, C. 2009. Cenozoic climate and vegetation change. In: Woodward, J. (Ed.), The physical geography of the Mediterranean. Oxford University Press, Oxford, 89-137 pp.
- Van Balen, R. T., Houtgast, R. F., Van der Wateren, F. M., Vandenberghe, J., & Bogaart, P. W., 2000. Sediment budget and tectonic evolution of the Meuse catchment in the Ardennes and the Roer Valley Rift System. *Global and Planetary Change*, **27**, 1, 113-129.
- Van Bemmelen, R.W. 1927. Bijdrage geologie der Betisvhe Ketens in de provincie Granada. PhD thesis, University of Delft, the Netherlands.

- Vandenbergh, J. 2003. Climate forcing of fluvial system development: an evolution of ideas. *Quaternary Science Reviews*, **22**, 2053-2060.
- Vandenbergh, J. 2008. The fluvial cycle at cold-warm-cold transitions in lowland regions: a refinement of theory. *Geomorphology*, **98**, 275-284.
- Vincent, P. J., Wilson, P., Lord, T. C., Schnabel, C. and Wilcken, K. M., 2010. Cosmogenic isotope (^{36}Cl) surface exposure dating of the Norber erratics, Yorkshire Dales: Further constraints on the timing of the LGM deglaciation in Britain. *Proceedings of the Geologists' Association*, **121**, 24-31.
- Vis, G.J., Kasse, C and Vandenbergh, J., 2008. Late Pleistocene and Holocene palaeogeography of the Lower Tagus Valley (Portugal): effects of relative sea level, valley morphology and sediment supply. *Quaternary Science Reviews*, **27**, 1682-1709.
- Vissers, R.L., Platt, J.P. and Van Der Vaal, D., 1995. Late orogenic extension of the Betic Cordilleras and the Alboran Domain: a lithospheric view. *Tectonics*, **14**, 786-803.
- Völk, H.R. 1967a. Relation between Neogene sedimentation and late orogenic movements in the Eastern Betic Cordilleras (SE Spain). *Geologie en Mijnbouw*, **46**, 471-474.
- Völk, H.R. 1967b. *Zur Geologie und Stratigraphie des Neogenbeckens von Vera, Südost-Spanien*. Unpublished PhD Thesis, Municipal University of Amsterdam, 160 pp.
- Völk, H.R. and Rondell, H.E., 1964. Zur Gliederung des Jungtertiars im Becken von Vera, Südostspanien. *Geologie en Mijnbouw*, **43**, 310-315.

- Walker, M. 2005. Quaternary Dating Methods. John Wiley and Sons, Chichester, 304 pp.
- Walther, J. 1894. Einleitung in die Geologie als Historische Wissenschaft, Bd. 3. Lithogenesis der Gegenwart, 535-1055. Fischer Verlag, Jena.
- Watchman, A.L and Twidale, C.R. 2002. Relative and absolute dating of land surfaces. *Earth Science Reviews*, **8**, 1-49.
- Weijermars, R. 1991. Geology and tectonics of the Betic Zone, SE Spain. *Earth Science Reviews*, **31**, 153-236.
- Weijermars, R., Roep, T.H.B., Van Den Eekhout, B., Postma, G and Kleverlaan, K., 1985. Uplift history of a Betic fold nappe inferred from the Neogene-Quaternary sedimentation and tectonics (in the Sierra Alhamilla and Almeria, Sorbas and Tabernas Basins of the Betic Cordillera, SE Spain). *Geologie en Mijnbouw*, **64**, 379-411.
- Wenzens, G. 1991. Die mittelquartaäre Reliefentwicklung am Unterlauf des Río Almanzora (Südostspanien). *Freiburger Geographische*, **33**, 185– 197.
- Wenzens, G. 1992. The influence of tectonics and climate on the Villafranchian morphogenesis in semiarid Southeastern Spain. *Zeitschrift für Geomorphologie*, **84**, 173-184.
- Westaway, R. 2012. A numerical modelling technique that can account for alternations of uplift and subsidence revealed by Late Cenozoic fluvial sequences. *Geomorphology*, **165**, 124-143.

- Westaway, R., Bridgland, D., Sinha, R and Demir, T., 2009. Fluvial sequences as evidence for landscape and climatic evolution in the Late Cenozoic: a synthesis of data from IGCP 518. *Global and Planetary Change*, **68**, 237-253.
- Whitfield, E and Harvey, A.M., 2012. Interactions between the controls on fluvial system development: tectonics, climate, base level and river capture- Rio Alias, Southeast Spain. *Earth Surface Processes And Landforms*, **37**, 1387-1397.
- Wilcken, K. M., Freeman, S. P. H. T., Dougans, A., Xu, S., Loger, R. and Schnabel, C. 2009. Improved ^{36}Cl AMS at 5 MV. *Nuclear Instruments and Methods B*, **268**, 748-751.
- Wright, V.P and Tucker, M.E., 1991. Calcretes: an introduction. In: Wright, V.P and Tucker, M.E (Eds), Calcretes. Reprint Series volume 2 of the international Association of Sedimentologists, Blackwell, Oxford, pp1-22.
- Yaalon, D. 1997. Soils in the Mediterranean region: What makes them different? *Catena*, **28**, 157-169.
- Zazo, C., Goy, L.J., Dabrio, C.J., Bardaji, T., Hillaire-Marcel, C., Ghaleb, B., Gonzalez-Delgado, J and Soler, V., 2003. Pleistocene raised marine terraces of the Spanish Mediterranean and Atlantic coasts: records of coastal uplift, sea-level highstands and climate changes. *Marine Geology*, **194**, 103-133.
- Zeck, H.P. 2004. Rapid exhumation in the Alpine Belt of the Betic-Rif (W Mediterranean): Tectonic Extrusion. In: Buforn, E., Martín-ávilla, J and Udías, A. (Eds.) *Geodynamics of Azores-Tunisia*. Birkhäuser, Basel, pp 477-487.
- Zitellini, N., Gràcia, E., Matias, L., Terrinha, P., Abreu, M.A., DeAlteriis, G., Henriët, J.P., Dañobeitia, J.J., Masson, D.G., Mulder, T., Ramella, R., Somoza, L and

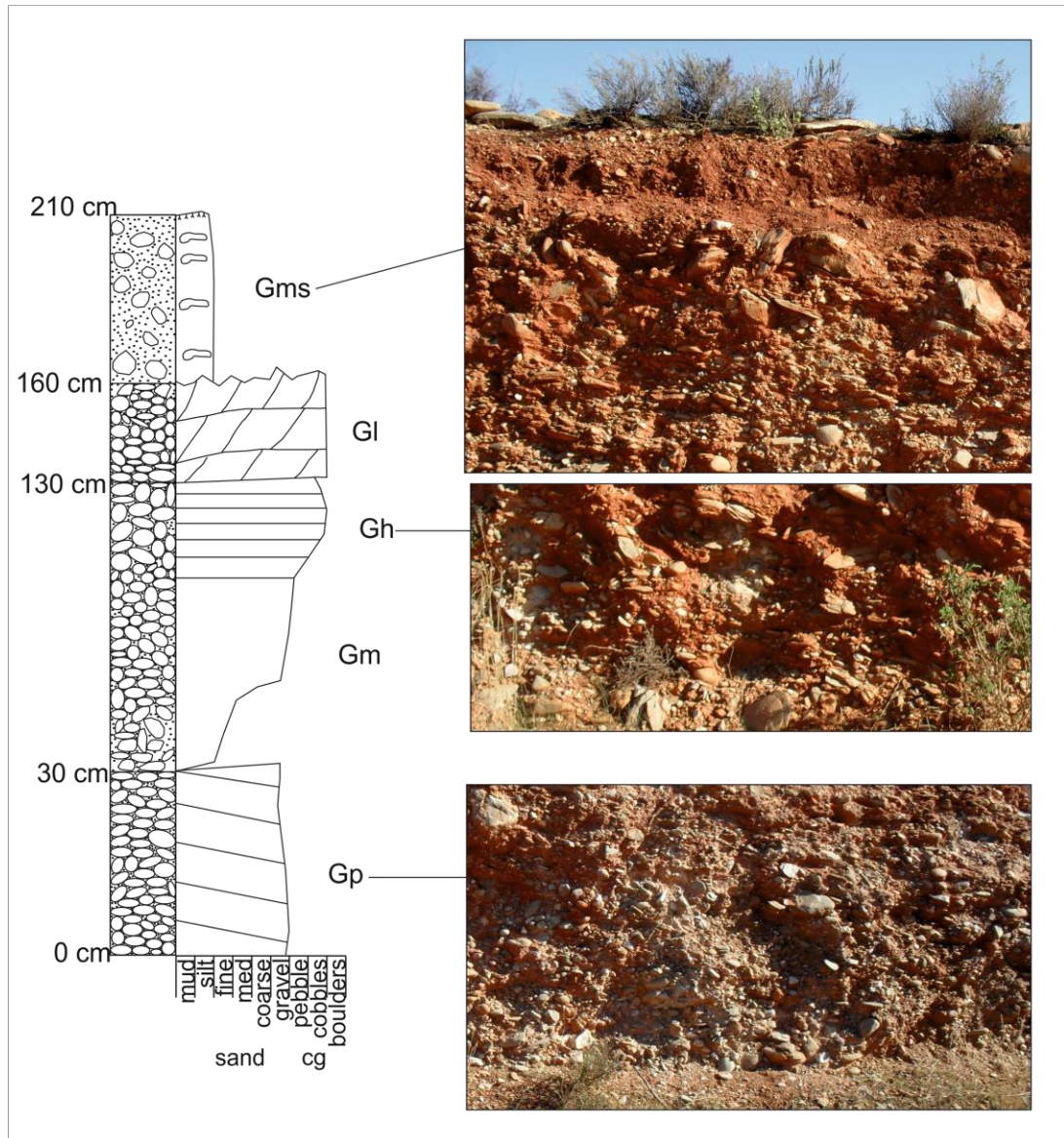
Dies, S., 2009. The quest for the African-Eurasia plate boundary west of the Strait of Gibraltar. *Earth and Planetary Science Letters*, **280**, 13-50.

Appendix 1

Sedimentary data for cosmogenic sample sites

(Chapter 4)

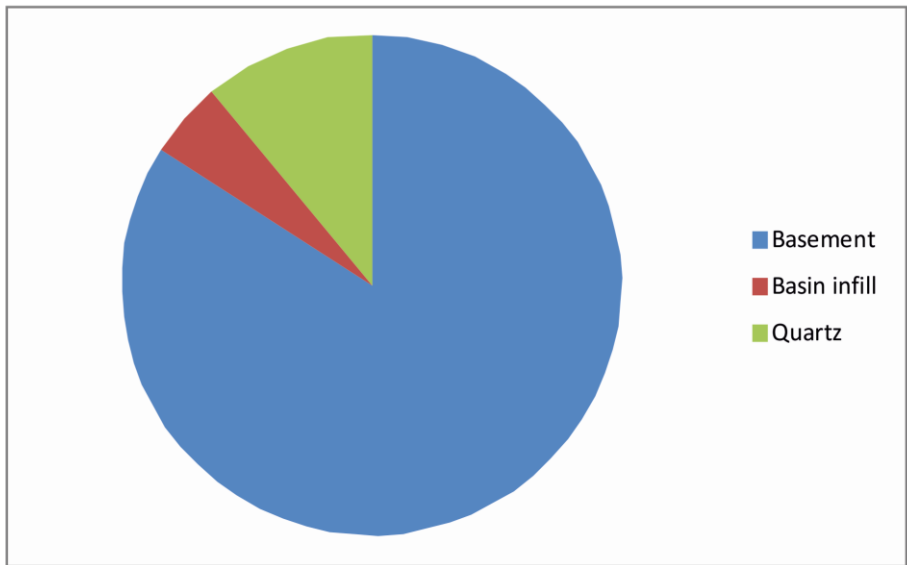
A1.1: Sedimentary log for the C.B sample site



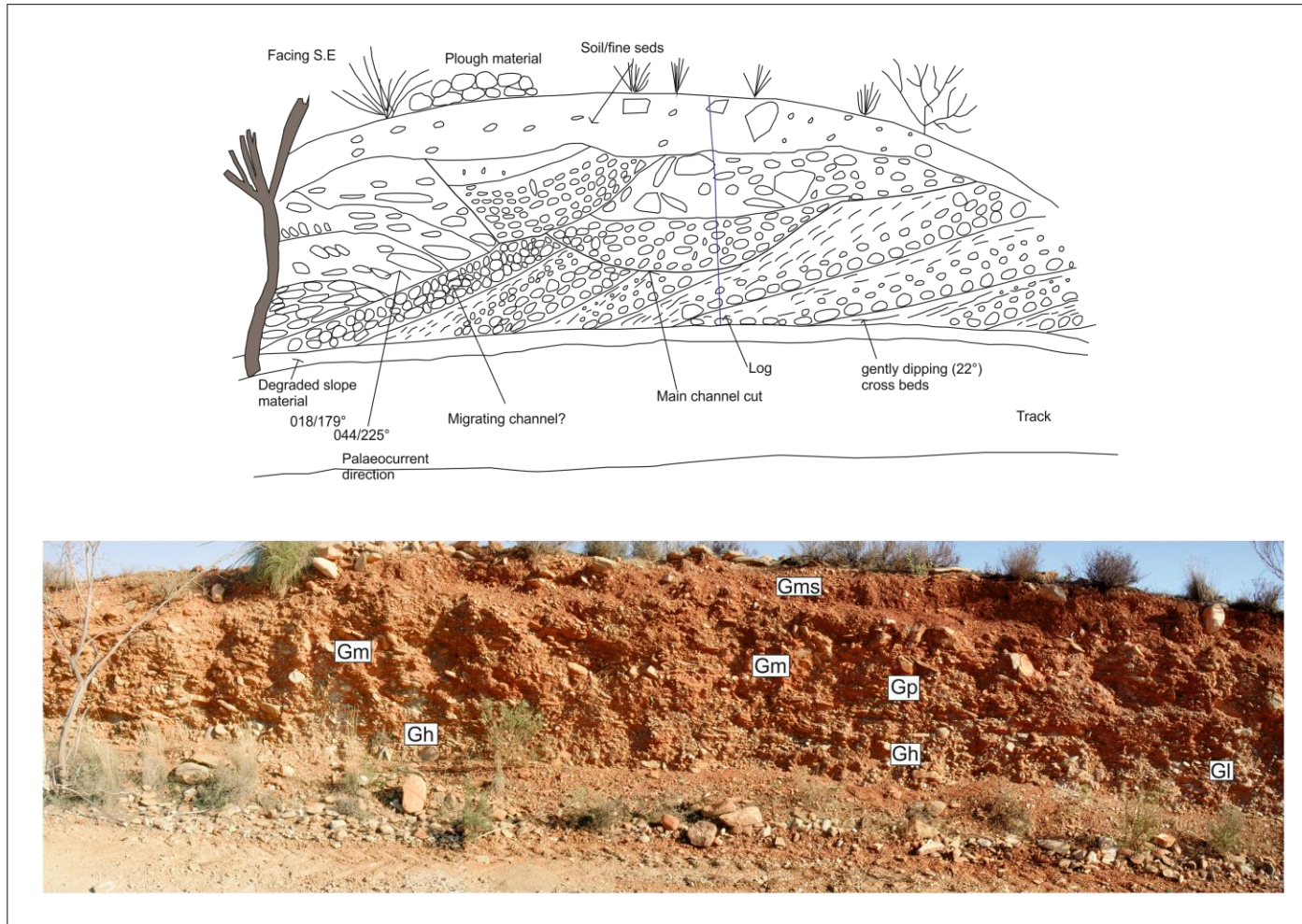
A1.2: Clast assemblage data for C.B

Sample site location information			
UTM: 0575600; 4108254			
Height: 480 m			
Length of terrace: 200 m			
	downstream	middle	upstream
Height Above CH	40 m	40 m	40 m
Thickness (M)	3.40	4.00	3.60

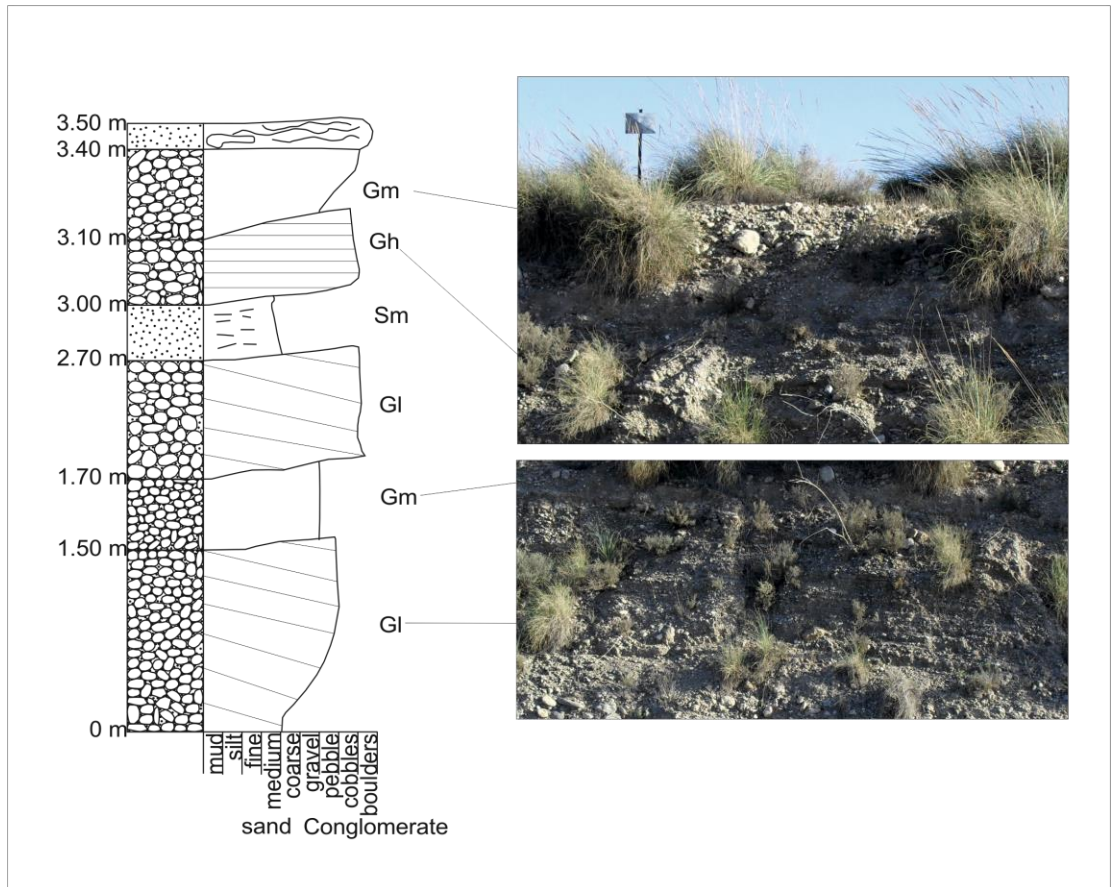
	ASM*	CSM*	MC*	S/S	QU
% CLAST TYPE	67%	9%	8%	5%	11%
SIZE CLAST TYPE	8.36	9.22	6.88	8.40	5.36



A1.3: Sedimentary photo sketch for the C.B sample site



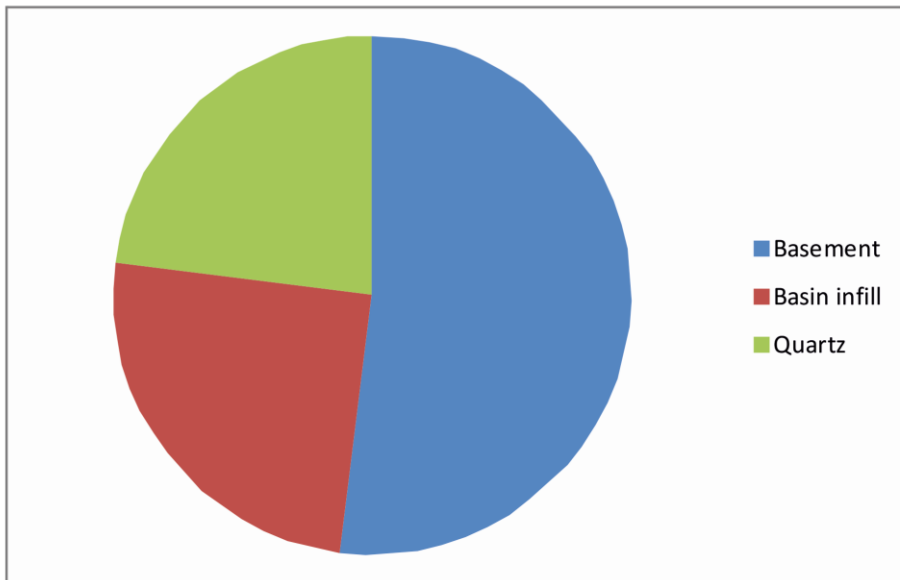
A1.4: Sedimentary log for the T.B.P sample site



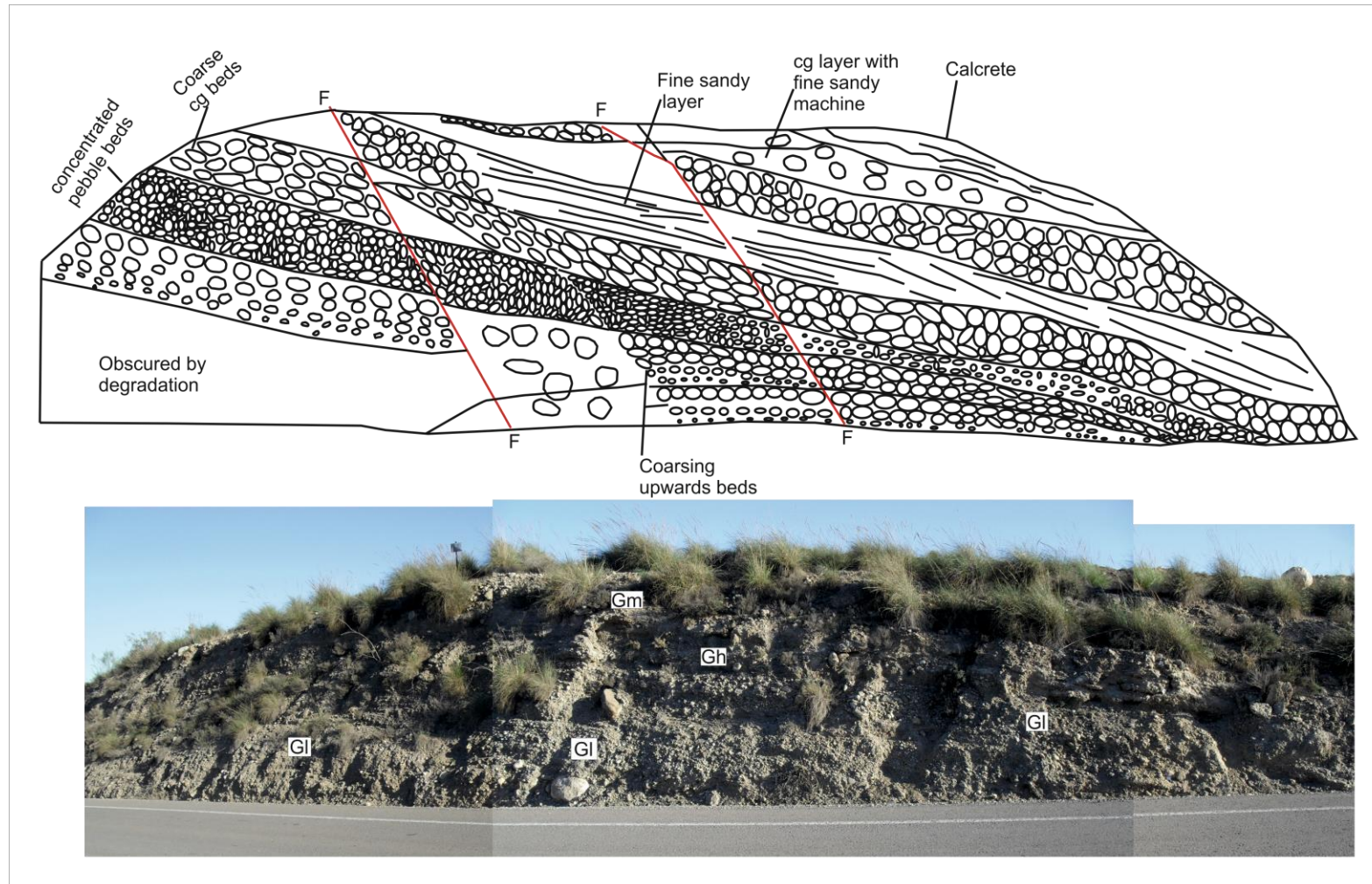
A1.5: Clast assemblage data for the T.B.P sample site

Sample site location information			
UTM: 0583950: 4095100			
Height: 230 m			
Length of terrace: 400 m			
	downstream	middle	upstream
Height Above CH	30 m	30 m	30 m
Thickness (M)	4.00	4.00	4.00

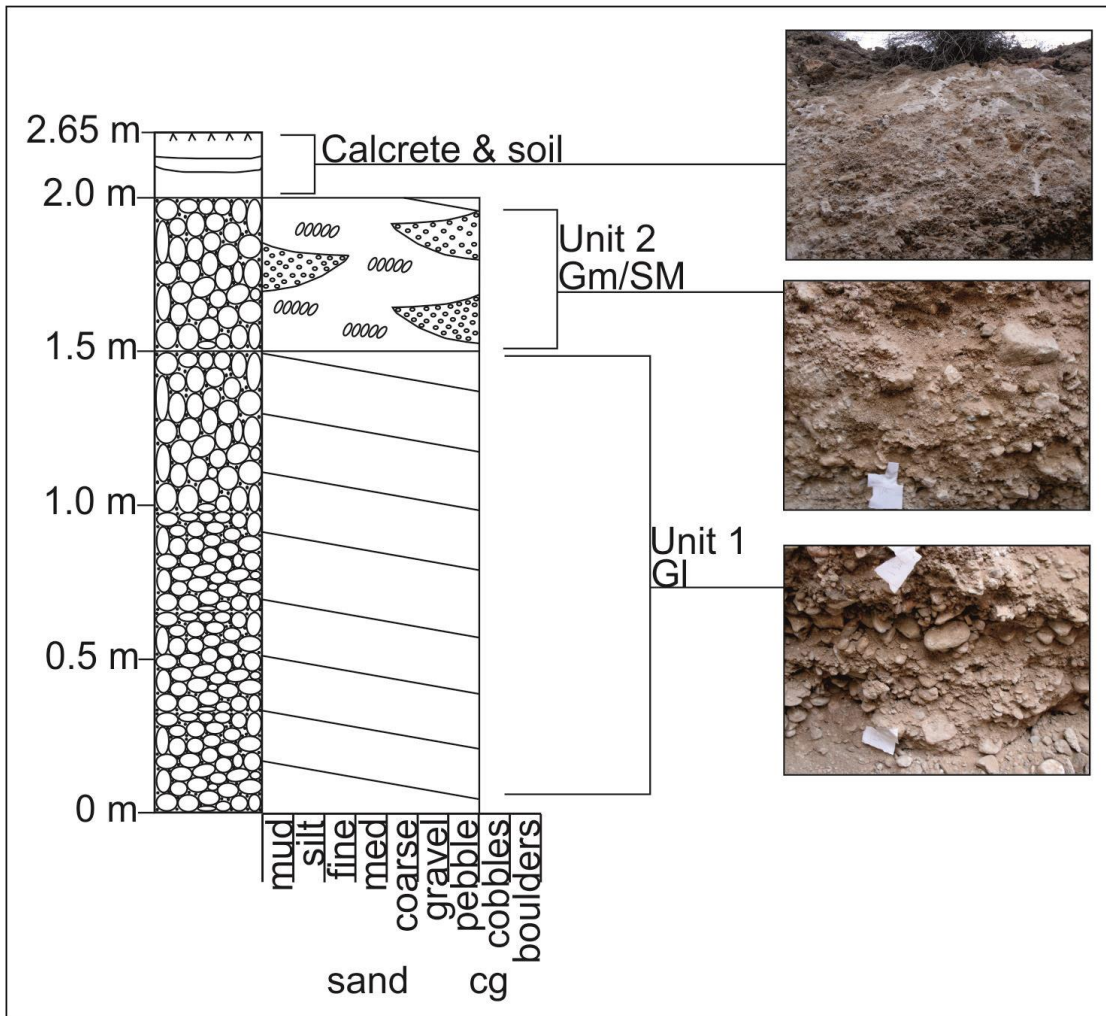
	ASM*	CSM*	GMS*	LST	MC*	S/S	QU
% CLAST TYPE	30%	1%	2%	15%	19%	10%	23%
SIZE CLAST TYPE	7.60	5.00	7.5	7.23	6.53	8.10	5.87



A1.6: Photo sketch of the T.B.P sample site showing the main sedimentological features



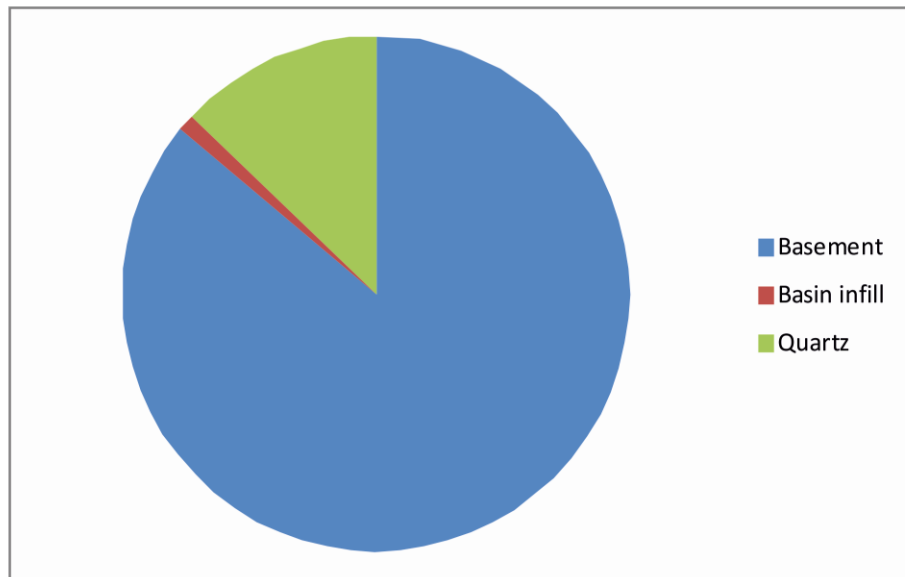
A1.7: Sedimentary log from the M.T.C site



A1.8: Clast assemblage data for the M.T.C. sample trench

Sample site location information			
UTM: 0581425; 4106200			
Height: 380 m			
Length of terrace: 200 m			
	downstream	middle	upstream
Height Above CH	60 m	60 m	60 m
Thickness (M)	4.00	4.00	4.00

	ASM*	CSM*	MC*	S/S	QU
% CLAST TYPE	82%	1%	3%	1%	13%
SIZE CLAST TYPE	4.97	3.00	4.50	9.00	4.23



Appendix 2

GIS map of the Góchar Formation surface

(Chapter 4)

Appendix 3

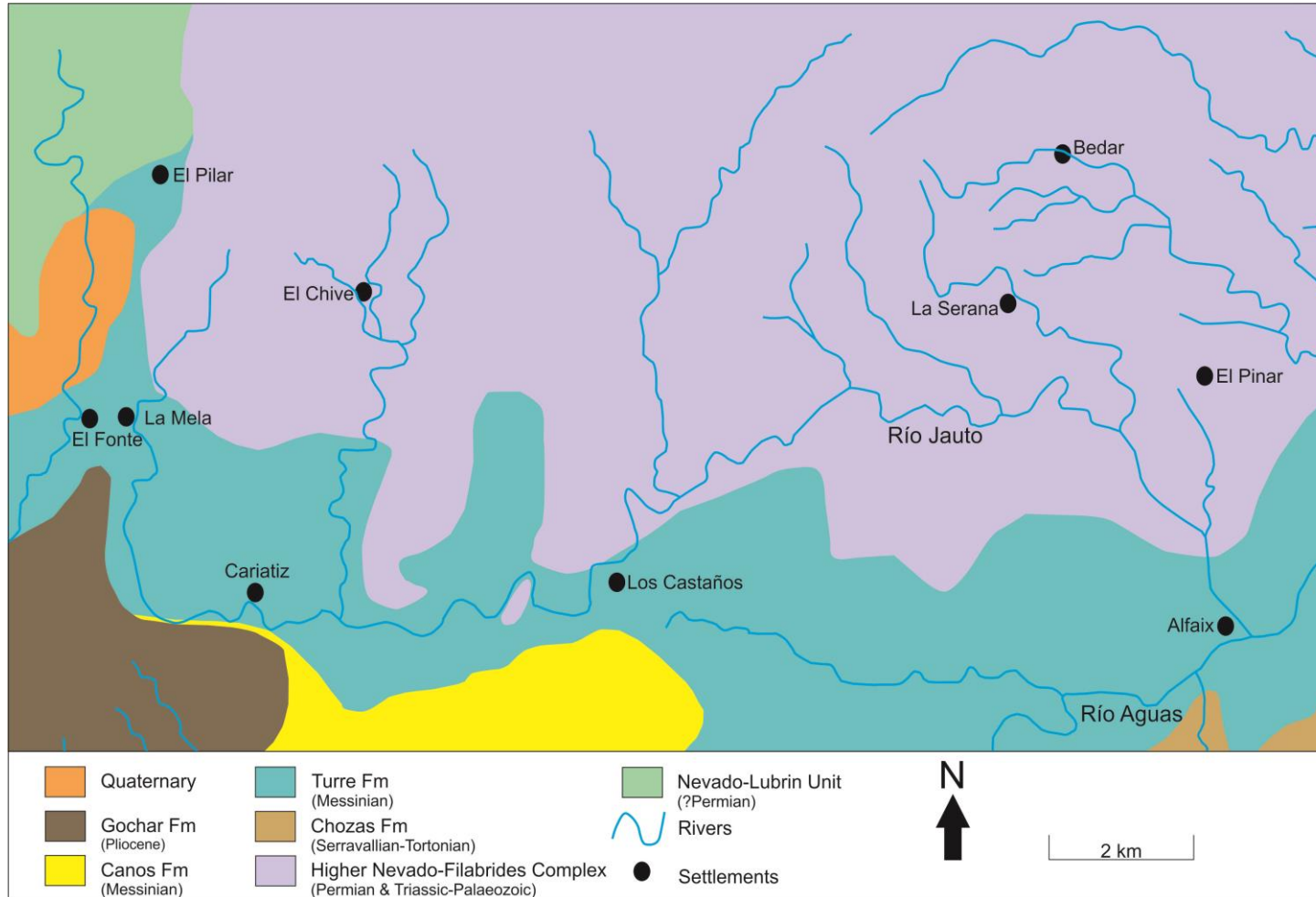
Geological maps of the Sorbas Basin

(Chapter 5 & 6)

Appendix 3.1: Geological map of the Sorbas Basin showing the main Formations



Appendix 3.2: The geological formations of the Río Jauto catchment (after Weijermars, 1991; Mather, 1991; Stokes, 1991).



Appendix 4

Palaeohydrology data for the Río Jauto

A 4.1 Palaeohydrological data for the Río Jauto fluvial system

Terrace	Location	UTM	Material	Channel width	Maximum boulder deminsons (D-max)			Discharge	Mean flow depth	Manning's
				(m)	A (cm)	B (cm)	C (cm)	(m ³ /s)	(m)	'n'
1	Mine Gorge	0590705; 4112419	LST	137.8	20	13	6	70	0.40	0.0971
1	Mine Gorge	0590714; 4112530	LST	24.8	22	9	5	10	0.35	0.0971
2	Los Castanos	0584912; 4111726	LST	400	37	34	19	631	0.79	0.0971
2	Mine valley	0590505; 4113682	Meta S/S	250	47	22	19	363	0.75	0.0971
2	Cerro De Solano	0588114; 4113850	TMS	228	54	33	12	343	0.76	0.0971
3	Cortijo del Hoyo	0584878; 4112063	LST	230	85	42	32	696	1.16	0.0971
3	los Ramirez	0584205; 4111665	TMS	400	60	47	13	754	0.87	0.0971
3	Cerro De Solano	0585399; 4112136	TMS	300	146	82	37	1597	1.63	0.0971
3	los Ramirez	0583093; 4111020	TMS	300	48	17	10	302	0.60	0.0971
3	Los Castanos G	0584405; 4111499	TMS	300	146	80	43	1683	1.68	0.0971
3	Mine valley	0589844; 4113660	TMS	200	62	31	20	385	0.88	0.0971
3	Mine valley	0590332; 4114078	MC	200	23	15	12	152	0.51	0.0971
3	D Cerro de Solano	0587749; 4113235	TMS	229	40	15	8	194	0.54	0.0971
3	D Cerro de Solano	0588626; 4113365	TMS	228	72	39	20	513	0.97	0.0971
3	Cerro De Solano	0588184; 4113830	TMS	200	77	31	20	421	0.93	0.0971
3	Upper Caratiz	0580488; 4111500	LST	200	108	46	32	695	1.26	0.0971
3	Upper Caratiz	0580422; 4111471	LST	200	50	34	16	333	0.81	0.0971
3	Upper Caratiz	0580534; 4111399	LST	200	60	30	27	424	0.94	0.0971

Terrace	Location	UTM	Material	Channel width	Maximum boulder deminsons (D-max)			Discharge	Mean flow depth	Manning's
				(m)	A (cm)	B (cm)	C (cm)	(m ³ /s)	(m)	'n'
4	Los Martinez	0582020; 4111567	TMS	350	70	38	36	984	1.10	0.0971
4	Los Castanos G	0584371; 4111502	TMS	300	184	64	47	1753	1.72	0.0971
4	Los Castanos t	0584531; 411280	LST	371	68	56	20	948	1.05	0.0971
4	Los Castanos t	0584586; 411276	LST	371	62	60	44	1305	1.27	0.0971
4	Los Castanos t	0584680; 4111285	TMS	371	40	22	12	416	0.64	0.0971
4	Los Castanos t	0584634; 4111322	LST	371	104	54	30	1320	1.28	0.0971
4	Los Castanos t	0584786; 4111377	TMS	371	72	50	13	774	0.93	0.0971
4	Los Castanos t	0585216; 4112009	TMS	200	96	40	38	670	1.23	0.0971
4	Los Castanos t	0585320; 4112010	TMS	200	55	25	13	280	0.73	0.0971
4	Los Castanos t	0585128; 4112011	TMS	200	81	53	16	490	1.02	0.0971
4	Los Castanos t	0585045; 4111995	TMS	200	42	23	16	263	0.70	0.0971
4	Los Castanos t	0584965; 4111975	TMS	200	50	39	15	343	0.83	0.0971
4	Mine valley	0590297; 4113911	TMS	200	62	36	28	471	1.00	0.0971
4	Los Alias	0581409; 4111344	TMS	200	45	33	23	366	0.86	0.0971
4	Los Alias	0581418; 4111448	TMS	200	23	10	4	81	0.35	0.0971
C	Modern river	0592198; 4111513	TMS	18	80	45	28	287	1.13	0.0971

Appendix 5

Calculation data for cosmogenic exposure dating

(Chapter 7)

A5.1: Data table for cosmogenic exposure dating

Sample name	UTM	Elevation	Elv/ pressure	Depth	+/-	Density	Shield- ing	Erosion rate	[Be-10]	+/-	Be AMS	[Al-26]	sigma ²⁶ Al at/g	Al AMS
		(m)	flag	(cm)		(g cm-2)	Correc- tion	(cm yr- 1)	atoms g-1	atoms g-1	standard	0	0	standard
GS 0M	0575756 4109450	495	std	5	5	1.935	1	0	1.09E+ 06	3.15E+04	Nist_27900	5.98E+ 06	2.06E+0 5	Z92- 0222
GS 0.5M	0575756 4109450	495	std	50	10	1.935	1	0	8.87E+ 05	2.93E+04	Nist_27900	4.64E+ 06	1.58E+0 5	Z92- 0222
GS 1.0M	0575756 4109450	495	std	100	10	1.935	1	0	6.79E+ 05	2.13E+04	Nist_27900	3.46E+ 06	1.23E+0 5	Z92- 0222
GS 1.5M	0575756 4109450	495	std	150	10	1.935	1	0	5.74E+ 05	1.86E+04	Nist_27900	2.72E+ 06	9.67E+0 4	Z92- 0222
GS 2.0M	0575756 4109450	495	std	200	10	1.935	1	0	4.21E+ 05	1.39E+04	Nist_27900	2.22E+ 06	7.60E+0 4	Z92- 0222
GTB 0M	0577312 4109292	454	std	5	5	1.935	1	0	9.621E +05	3.115E+04	Nist_27900			Z92- 0222
GTB 0.5M	0577312 4109292	454	std	50	10	1.935	1	0	6.855E +05	2.382E+04	Nist_27900			Z92- 0222
GTB 1.0M	0577312 4109292	454	std	100	10	1.935	1	0	4.257E +05	1.468E+04	Nist_27900			Z92- 0222
GTB 1.5M	0577312 4109292	454	std	150	10	1.935	1	0	3.482E +05	1.142E+04	Nist_27900			Z92- 0222
GTB 2.0M	0577312 4109292	454	std	200	10	1.935	1	0	3.096E +05	1.078E+04	Nist_27900			Z92- 0222

Sample name	UTM	Elevation	Elv/ pressure	Depth	+/-	Density	Shield- ing	Erosion rate	[Be-10]	+/-	Be AMS	at ²⁶ Al/g	sigma ²⁶ Al at/g	Al AMS
		(m)	flag	(cm)		(g cm-2)	correcti on	(cm yr-1)	atoms g-1	atoms g-1	standard	0	0	standard
G30M	0575574: 4111057	480	std	5	5	1.935	1	0	4.725E +05	1.483E +04	Nist_27900			Z92- 0222
G30.5 M	0575574: 4111057	480	std	50	10	1.935	1	0	2.529E +05	8.902E +03	Nist_27900			Z92- 0222
G31.0 M	0575574: 4111057	480	std	100	10	1.935	1	0	1.545E +05	5.434E +03	Nist_27900			Z92- 0222
G31.5 M	0575574: 4111057	480	std	150	10	1.935	1	0	9.671E +04	3.359E +03	Nist_27900			Z92- 0222
G32M	0575574: 4111057	480	std	200	10	1.935	1	0	6.685E +04	2.462E +03	Nist_27900			Z92- 0222
MTC 0.0	0581425; 4106200	380	std	5	5	1.935	1	0	7.229E +05	1.856E +04	Nist_27900	4.32E+0 6	2.79E+05	Z92- 0222
MTC 0.5	0581425; 4106200	380	std	50	10	1.935	1	0	5.110E +05	1.333E +04	Nist_27900	2.81E+0 6	1.94E+05	Z92- 0222
MTC 1.0	0581425; 4106200	380	std	100	10	1.935	1	0	1.030E +06	3.130E +04	Nist_27900	5.40E+0 6	4.47E+05	Z92- 0222
MTC 1.5	0581425; 4106200	380	std	150	10	1.935	1	0	5.094E +05	1.305E +04	Nist_27900	2.50E+0 6	1.58E+05	Z92- 0222
MTC 2.0	0581425; 4106200	380	std	200	10	1.935	1	0	2.923E +05	6.640E +03	Nist_27900	1.59E+0 6	7.63E+04	Z92- 0222

Sample name	UTM	Elevation	Elv/pressure	Depth	+/-	Density	Shielding	Erosion rate	[Be-10]	+/-	Be AMS	at ²⁶ Al/g	sigma ²⁶ Al at/g	Al AMS
		(m)	flag	(cm)		(g cm ⁻²)	correction	(cm yr ⁻¹)	atoms g ⁻¹	atoms g ⁻¹	standard	0	0	standard
TBP00	0583950: 4095100	230	std	5	5	1.935	1	0	2.089E+05	7.071E+03	Nist_27900	2.18E+06	9.17E+04	Z92-0222
TBP05	0583950: 4095100	230	std	50	10	1.935	1	0	1.678E+05	5.945E+03	Nist_27900	1.46E+06	6.97E+04	Z92-0222
TBP10	0583950: 4095100	230	std	100	10	1.935	1	0	2.089E+05	7.071E+03	Nist_27900	1.76E+06	7.62E+04	Z92-0222
TBP15	0583950: 4095100	230	std	150	10	1.935	1	0	1.678E+05	5.945E+03	Nist_27900	9.44E+05	3.97E+04	Z92-0222
TBP20	0583950: 4095100	230	std	200	10	1.935	1	0	1.777E+05	6.312E+03	Nist_27900	1.12E+06	4.76E+04	Z92-0222
TCF0M	0578475: 4105825	453	std	5	5	1.935	1	0	5.78E+05	1.86E+04	Nist_27900	3.50E+06	1.32E+05	Z92-0222
TCF0.5M	0578475: 4105825	453	std	50	10	1.935	1	0	3.82E+05	1.26E+04	Nist_27900	2.41E+06	9.29E+04	Z92-0222
TCF1.0M	0578475: 4105825	453	std	100	10	1.935	1	0	3.92E+05	1.28E+04	Nist_27900	2.43E+06	8.48E+04	Z92-0222
TCF1.5M	0578475: 4105825	453	std	150	10	1.935	1	0	3.62E+05	1.26E+04	Nist_27900	2.19E+06	7.85E+04	Z92-0222
TCF2.0M	0578475: 4105825	453	std	200	10	1.935	1	0	3.42E+05	1.17E+04	Nist_27900			Z92-0222

Sample name	UTM	Elevation	Elv/pressure	Depth	+/-	Density	Shielding	Erosion rate	[Be-10]	+/-	Be AMS	at ²⁶ Al/g	sigma ²⁶ Al at/g	Al AMS
		(m)	flag	(cm)		(g cm ⁻²)	correction	(cm yr ⁻¹)	atoms g ⁻¹	atoms g ⁻¹	standard	0	0	standard
CB00	0575600 4108254	479	std	5	5	1.935	1	0	9.157E+05	3.220E+04	Nist_27900	5.11E+06	2.08E+05	Z92-0222
CB05	0575600 4108254	479	std	50	10	1.935	1	0	6.206E+05	2.182E+04	Nist_27900	3.29E+06	1.40E+05	Z92-0222
CB10	0575600 4108254	479	std	100	10	1.935	1	0	3.105E+05	1.026E+04	Nist_27900	1.55E+06	6.43E+04	Z92-0222
CB15	0575600 4108254	479	std	150	10	1.935	1	0	3.378E+05	1.181E+04	Nist_27900	1.62E+06	6.07E+04	Z92-0222
CB20	0575600 4108254	479	std	200	10	1.935	1	0	3.091E+05	1.084E+04	Nist_27900	1.55E+06	6.16E+04	Z92-0222

Appendix 6

Tectonic uplift calculations

(Chapter 8)

A6.1: Uplift calculations

Rate 1	Time gap	Cal space	Graph	Rate 2	Time gap	Cal space	Graph	Rate 3	Time gap	Cal space	Graph
0.08 m ka ⁻¹	1.2 Ma	96 m	114.64	0.07 ka ⁻¹	1.2 Ma	84 m	100.31	0.16 m ka ⁻¹	1.2 Ma	192 m	228.84
0.08 m ka ⁻¹	134 ka	10.72 m	18.64	0.07 ka ⁻¹	134 ka	9.38 m	16.31	0.16 m ka ⁻¹	134 ka	21 m	36.84
0.08 m ka ⁻¹	51 ka	4.08 m	7.92	0.07 ka ⁻¹	51 ka	3.57 m	6.93	0.16 m ka ⁻¹	51 ka	8.16 m	15.84
0.08 m ka ⁻¹	48 ka	3.84 m	3.84	0.07 ka ⁻¹	48 ka	3.36 m	3.36	0.16 m ka ⁻¹	48 ka	7.68 m	7.68
	Total	114.64			Total	100.31			Total	228.84	

Terrace level	Age	Time gap	Spacing	Uplift rate
A	264 ka	1.2 Ma	20	0.02 m ka ⁻¹
B	130 ka	134 ka	28	0.21 m ka ⁻¹
C	79 ka	51 ka	20	0.40 m ka ⁻¹
D	31 ka	48 ka	34	0.71 m ka ⁻¹

Rate 1	Time gap	Cal space	Graph	Rate 2	Time gap	Cal space	Graph	Rate 3	Time gap	Cal space	Graph
0.08 m ka ⁻¹	1.2 Ma	96 m	117.12	0.07 ka ⁻¹	1.2 Ma	84 m	102.48	0.16 m ka ⁻¹	1.2 Ma	192 m	233.8
0.08 m ka ⁻¹	134 ka	10.72 m	21.12	0.07 ka ⁻¹	134 ka	9.38 m	18.48	0.16 m ka ⁻¹	134 ka	21 m	41.8
0.08 m ka ⁻¹	51 ka	4.08 m	10.4	0.07 ka ⁻¹	51 ka	3.57 m	9.1	0.16 m ka ⁻¹	51 ka	8.16 m	20.8
0.08 m ka ⁻¹	48 ka	3.84 m	6.32	0.07 ka ⁻¹	48 ka	3.36 m	5.53	0.16 m ka ⁻¹	48 ka	7.68 m	12.64
0.08 m ka ⁻¹	31 ka	2.48 m	3.84	0.07 ka ⁻¹	31 ka	2.17 m	3.36	0.16 m ka ⁻¹	31 ka	4.96 m	7.68
	Total	117.12			Total	102.48			Total	233.8	

Terrace Level	Age	Time gap	Spacing	Uplift rate
1	264 ka	1.2 Ma	0	< 0.01 m ka ⁻¹
2	130 ka	134 ka	29	0.22 m ka ⁻¹
3	79 ka	51 ka	20	0.40 m ka ⁻¹
4	31 ka	48 ka	8	0.18 m ka ⁻¹
Modern river	0	31 ka	4	0.14 m ka ⁻¹

